An Analytical Investigation of Transverse Joints in Precast-Panel Bridge-Deck Replacement Systems

by

Brian Mark Rhett

A Thesis submitted to the Graduate Faculty of
Auburn University
in partial fulfillment of the
requirements for the Degree of
Master of Science

Auburn, Alabama
December 8, 2012

Approved by

Robert Barnes, Chair, Associate Professor of Civil Engineering
Anton K. Schindler, Professor Civil Engineering
Hassan Abbas, Assistant Professor of Civil Engineering

Abstract

In recent years precast bridge deck panels have offered a solution for rapid bridge deck rehabilitation by minimizing traffic interruption and accelerating construction. Cracking and early deterioration of the connections between these joints is commonplace, and as more rapid rehabilitation is needed in an ever busier world, the demand for more efficient and effective deck replacement connections has arisen.

In an effort to implement a rapid rehabilitation system, the Alabama Department of Transportation commissioned an investigation of these systems. In order to select a system that minimized traffic interruption, an extensive study on rehabilitation systems was conducted, with a focus on eliminating timely post-tensioning from precast deck systems. To assess the feasibility of such a system three separate bridges—one simply supported and two continuously supported—were modeled using a finite-element bridge analysis program. The effects that transverse joints would experience under HS-20 fatigue loading were determined. Based on this modeling and the review of previous studies, guidelines for the future testing and implementation of a transverse joint connection between bridge deck panels are given.

Through researching previous studies and finite-element modeling, it was determined that the best transverse connection would be a looped-bar joint for locations experiencing negative flexural stresses or an unreinforced shear key or a looped-bar joint for joints under positive flexure. Under negative bending, it was determined that the top fiber of the joint needed to withstand a tensile stress of at least 256 psi. In the positive bending scenario, the model

generated tensile stresses of 226 psi in the bottom fiber of the transverse joint. Based on these results laboratory testing is recommended that assesses the fatigue life and performance of joints under a conservative stress of 300 psi.

Table of Contents

List of Tables

List of Figures

List of Abbreviations

AASHTO……..American Association of State Highway and Transportation Officials

ALDOT…….Alabama Department of Transpiration

ASTM……...…American Society for Testing and Materials

DOT(s)……..Department(s) of Transportation

FHWA……...Federal Highway Administration

PCI……Precast/Prestressed Concrete Institute

NCHRP…….National Cooperative Highway Research Program

CHAPTER 1: INTRODUCTION

1.1 Introduction

With roughly 80,000 bridges in the United States being rated as structurally deficient, a key issue facing transportation officials today is the rehabilitation of such bridges (FHWA 2007). The Alabama Department of Transportation (ALDOT) maintains over 3 miles, or 600,000 ft^2, of bridge deck near downtown Birmingham with considerable deck deterioration and cracking. Crowded thoroughfares and roadways such as these have generated great demands for unobtrusive construction techniques that minimize traffic congestion and detours. For the rehabilitation of bridge decks, it is apparent that rapid bridge construction techniques provide a solution to minimize traffic interruptions and meet public demands.

There are numerous types of rapid bridge-deck replacement options, and they all provide a new riding surface within a fraction of the time that it would take to conventionally replace a deficient bridge deck. The process is fairly simple: a precast deck panel is formed and cured away from the construction site, and while the units are being installed, they are typically joined with a grouting material between panel joints (Figure 1.1). This off-site fabrication minimizes curing times to that of the cast-in-place grouting materials, which in turn allows bridge construction to be completed with minimal closures or, in many cases, only partial bridge closures.

Despite these benefits, a main issue deterring transportation agencies from using these rapid bridge-deck replacement options is the service life of the joints. Many of these deck panel connections, especially the transverse joints, have a history of early deterioration and cracking problems (Biswas et al. 1986; Issa et al. 1995). More elaborate reinforcement methods and improvements to the cold transverse joint have been made in recent years; however, these

options tend to complicate construction and can further extend a bridge's closure time. Additionally, agencies are further pushing for replacement methods that can be used in bridges with more demanding loading and service requirements (Issa et al. 1995a).

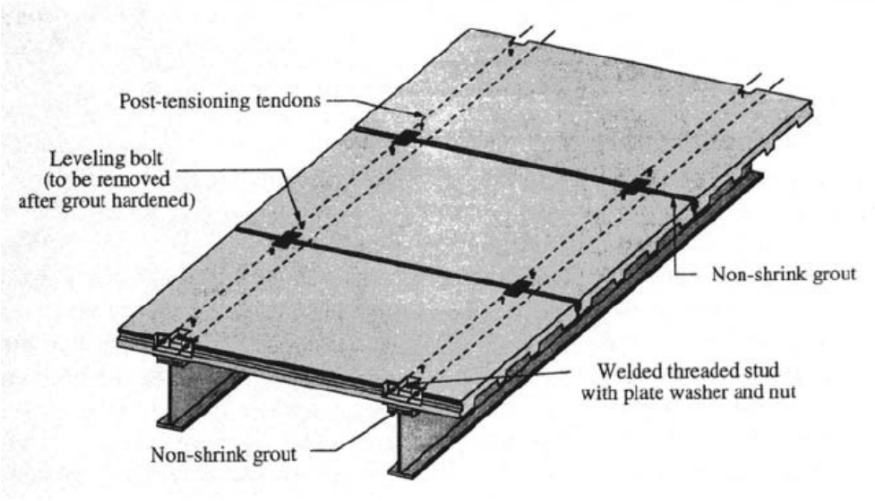

Figure 1.1: Typical Deck Panel with Grouted Transverse Joints (Yamane et al. 1998)

When considering the use of precast panels for high-volume bridges, ALDOT decided to first test the system on bridges with lower traffic volumes. They elected two sister bridges located near Collinsville, Alabama in order to verify the systems effectiveness and assess any issues. Additionally, ALDOT set parameters that the deck panels should meet. ALDOT required that the transverse deck system connection

- Be suited for rapid deck replacement
- Be a proven concept
- Avoid the use of longitudinal post-tensioning
- Provide adequate durability and fatigue life
- Avoid the use of an overlay

By following these directives, effort was devoted to two deck replacement options: exodermic fully precast and full-depth precast concrete panels (Figures 1.2 and 1.3). Both of these panel systems meet the listed requirements above, and they both have a variety of transverse panel joint connection options.

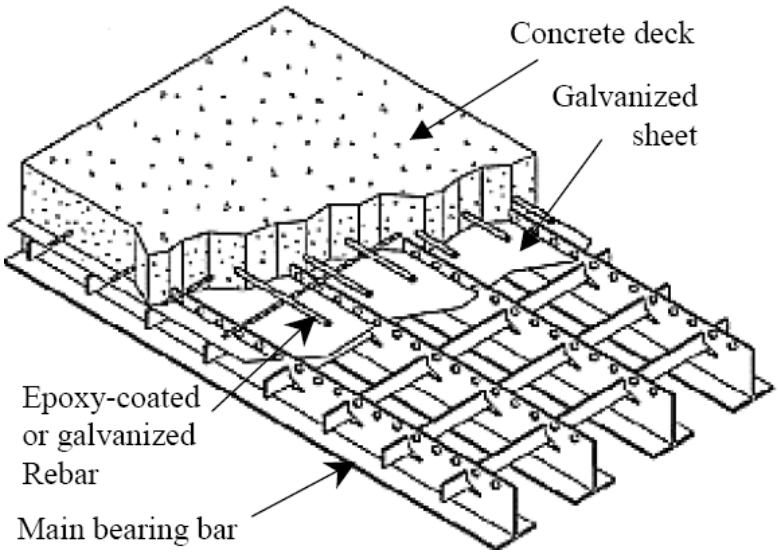

Figure 1.2: Revised Exodermic Bridge Deck System (EBDI 2010)

Figure 1.3: Typical Full-Depth Precast Panel (Culmo 2000)

Clearly, the use of a rapid replacement system is a complex and technical issue that requires careful consideration to assess practicality in construction, acceptable serviceability, and minimization of traffic interruption.

1.2 Objective and Scope

The primary objective of this research was to investigate the feasibility and recommend testing procedures for the laboratory assessment of transverse connection types for precast decks. Through the use of computer modeling and by researching previous studies, testing criteria were developed to assess the durability, performance, and serviceability of a transverse-joint connection type over the expected life of the deck system.

Both exodermic and full-depth precast panels offer a variety of connection options. After researching and assessing these connections, three main transverse joint connections were found to meet ALDOT requirements: a standard female-to-female joint, an alternating looped-bar joint, and the reinforced joint based on NCHRP Report 584 (2008). These joints have diverse performance histories, some offer sacrifices in construction speed for better durability, while others are more proprietary and do not have a clear in-field performance record. However each of these joints offer a potential solution to the transverse connection issues, as each has the durability and effective constructability that is vital in rapid deck replacement systems.

In order to accurately assess these joints for in-field performance, the Collinsville simple-span bridges were modeled using a finite-element program. From this analysis, the stresses and other key force effects that the deck and the joint might experience were established. Additionally two standard drawings for continuous-span bridges were obtained from ALDOT and modeled to establish what this system might experience in negative flexure. The worst-case truck loading scenarios were established based on AASHTO LRFD, and these stresses were recorded and used to create testing criteria for transverse joints.

1.3 Organization of Thesis

The first phase of this project, which is documented in Chapter 2, involved a thorough investigation of the deck replacement options, including an investigation of some transverse connection methods and available rapid redecking panels. The performance of these systems in representative projects and also recommended improvements and design concerns were all researched to form conclusions regarding each system's capacity for constructability and serviceability. Prior methods of laboratory testing for these various joints were also documented in order to recommend appropriate testing procedures.

The second part of this study involved a finite-element analysis of the bridge itself. Using SAP2000, the widened Collinsville bridges and two other ALDOT bridges were modeled to determine the effects the joints will likely experience. Chapter 3 outlines the modeling setup and methodology, while Chapter 4 presents the modeling results.

As a result of this research, Chapter 5 presents testing procedures and criteria that are recommended for future laboratory assessment of the transverse joining methods for precast deck panels. Various testing systems, their rationale, and general testing procedures are presented.

Finally, Chapter 6 summarizes conclusions and recommendation for the whole of this research project.

CHAPTER 2: RAPID DECK REPLACEMENT SYSTEMS, CONNECTIONS, AND PREVIOUS RESEARCH

2.1 Introduction

This chapter is divided into three major sections: the first is an overview of the various rapid deck replacement systems, the second explores the various transverse deck joint options, and the third summarizes past transverse deck joint testing, modeling, and research. In the first two sections a detailed description of either the deck system or joint will be given. These descriptions include the history, implementation, and past performance of the deck system or joint, with the third section providing an overview of relevant testing previously conducted on the transverse joints. The information gained from previous research and performance helped guide the modeling process described in this report.

2.2 Rapid Deck Replacement Systems

The advantages of minimizing traffic disruption by implementing a rapid bridge-deck replacement have prompted many transportation agencies to fund studies and further research in hopes of devising more efficient and pragmatic systems. The two rapid deck replacement systems under consideration by the Alabama Department of Transportation are full-depth precast concrete panels and exodermic panels. Their performance, excluding joint connections, is discussed in the following sections.

2.2.1 Full-Depth Precast Concrete Panels

2.2.1.1 Introduction and History

Full-depth precast concrete panel systems have seen a dramatic increase in usage since the early 1970's (Yousif 1998). In this type of system, virtually the entire bridge deck can be cast off-site, minimizing in-field casting to the connection of slabs and closures. These advantages

have spurred an increase in full-depth precast panel research beginning with an investigation of feasibility and performance in 1975 (Kluge et al.). In the 1980's, the PCI Bridge Committee conducted two separate surveys to confirm the growth and analyze the different construction methods for this system (PCI 1987); these results later became the first recommended practice for precast panel construction (PCI 1988). In 1998, ASTM introduced a standard for the laboratory testing of bridge decks, which gave guidelines for the testing of bridge deck modules (ASTM D6275 1998). Although this standard was withdrawn in 2004, many designers are still using the withdrawn standard as a guideline for precast panel design, as commonly recognized bridge standards include little information relevant to these types of deck panels (Higgins 2010). AASHTO LRFD section 9.7.5 (2008) briefly discusses full-depth panels but gives no guidelines on connectors or grouting.

New standards and practices for the design and testing of full-depth precast concrete panels continue to be developed; however, the vast majority of these recommend longitudinal post-tensioning, which is not congruent with the stated directives of this research study listed in Section 1.1.

2.2.1.2 Implementation and Performance

The most widely implemented precast deck panel system is full-depth precast panel rehabilitation. These panels have been successfully used in a variety of bridge types including bridges with skewed, superelevated, and crowned profiles as well as bridges with different substructures (Issa et al. 1995a).

Issa et al. (1995) conducted a survey of the different rapid construction techniques used in the United States and Canada, finding that 13 of the 51 DOTs surveyed reported using full-depth precast concrete panels (Issa et al. 1995a). It was found that the majority of these

departments had designed their own precast panels producing many varieties of joint designs. From these designs, Issa et al. concluded that an effective deck panel system included an efficient construction sequence, transverse prestressing, longitudinal post-tensioning, an appropriate connection between the slab and supporting system, and the appropriate grouting of panel to panel joints (Issa et al. 1995b). Issa et al. (1998) later conducted a quantitative study to determine the amount of post-tensioning needed for adequate performance in full-depth precast bridges. They concluded that a minimum average compressive stress of 200 psi from longitudinal post-tensioning was required for simple span bridges, while continuous span bridges required 450 psi at interior supports (negative moment regions) and 200 psi at the bridge's midspan. These recommended prestress amounts have since been standard in many precast panel bridge designs.

2.2.2 Exodermic Fully Precast Panels

2.2.2.1 Introduction and History

An "exodermic", or composite unfilled steel grid deck, comprises a thin reinforced concrete slab made composite with a steel grid that remains void of concrete in construction as depicted in Figure 2.1 (EBDI 2011). This design utilizes the compressive strength of concrete while minimizing weight, as the tensile region of the slab is comprised of the unfilled steel grid. Developed in the early 1980's, this rapid deck replacement option builds on the durable record of steel grids, while introducing the economy of concrete to make a lighter deck when compared to full-depth concrete decks. The first project using exodermic panels was the 1984 widening of the Driscoll Bridge in New Jersey (Bettigole 1997). Earlier projects were cast-in-place, and exodermic decks were later modified from this original design to include a simpler shear transfer mechanism for a more efficient installation and for improved performance of the deck system.

More prominent examples of exodermic decks include the 1998 rehabilitation of New York's Tappan Zee Bridge, which has become a major project in assessing the performance and validity exodermic deck systems (Caltrans 2003). Although this system is said to perform similar to full-depth precast concrete panels, no research has been conducted to assess exodermic transverse joint connection behavior compared to similar connections on full-depth concrete specimens.

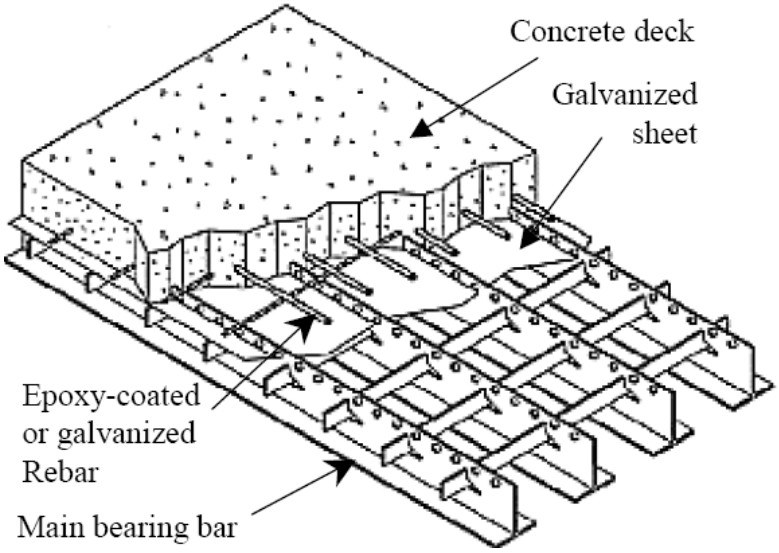

Figure 2.1: Revised Exodermic Bridge Deck System (EBDI 2011)

2.2.2.2 Implementation and Performance

Exodermic deck units have the option of being fully precast or cast-in-place, however only precast exodermic decks are relevant to this study. A precast exodermic deck behaves similar to a full-depth precast concrete panel in installation with the main exception being the connection of the exodermic panels to the girders. A main advantage for exodermic installation is that the typical weight of these panels ranges from 44 to 84 psf, which represent weight reductions up to 60 percent when compared to other deck rehabilitation systems (Bettigole 1997). This weight reduction is significant in that it allows an increase in the load capacity of

the bridge and can also help bring an aging bridge substructure into compliance with design code provisions. A typical exodermic unit ranges from 6.5 to 10 inches in thickness, and these units are typically 6 to 10 ft long with some of the longest panels spanning over 18 ft (EBDI 2010).

An early project using exodermic decks was the rehabilitation of the Russell Road Bridge in New York. Like most of the earlier exodermic projects, this bridge's deck was replaced with a cast-in-place exodermic deck system, which performed well and was comparable to full-depth cast-in-place concrete panels in both performance and installation (Darlow et al. 1989). A precast system was implemented in 1998 on the east deck truss of the cantilever Tappan Zee Bridge in New York (Caltrans 2003), and a later study conducted by Caltrans (2003) concluded that the exodermic decks offered all the same advantages of typical precast panels: they permit rapid construction, are lighter, are easy to install and maintain, and permit partial bridge closures .

Since the Tappan Zee rehabilitation, exodermic usage began to spread more rapidly out of the New England region. Florida and many Midwestern states like Wisconsin have rehabilitated bridges with this system, and the majority has performed adequately to date (WDOT 2010). Exodermic deck application has been used in many different bridge types ranging from cantilever to bascule bridges. The most common problems experienced are deck panel connection deterioration and concrete shrinkage cracking, often seen when high performance concrete is used in the panel (Kaczinski 2010). Additionally, some structural cracking has been noted, usually occurring in negative moment regions where no additional reinforcement was included in the upper concrete section (Kaczinski 2010). Overall the exodermic system has performed comparable to full-depth precast concrete panels (Caltrans 2003), especially in terms of transverse joint connection issues; however, there are no comparative studies assessing the performance of exodermic transverse joints against full-depth precast joints. Figure 2.2 shows an

EBDI recommended transverse joint section, and given the complexity of this configuration when compared to full-depth precast transverse joints, an assessment between this system and an equivalent full-depth precast system should be made.

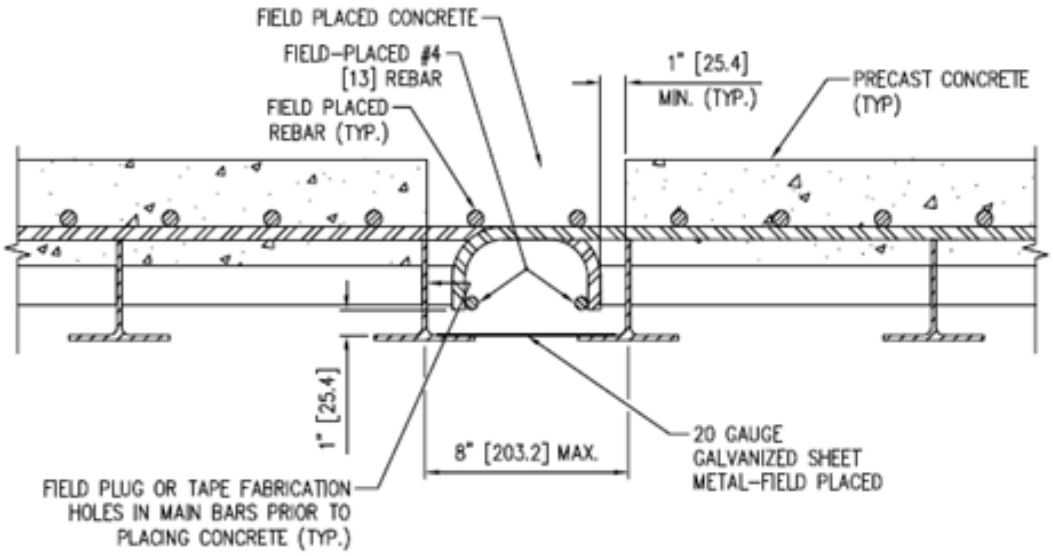

Figure 2.2: Typical Section at Panel Splice (EBDI 1011)

2.3 Comparison of Transverse Connections

Individual deck panels can be connected longitudinally (with joint running parallel to the girders, the length of the bridge) or transversely (with joint running across the width of the bridge as shown in Figure 2.3). These connections can be made through closure pours, mechanical connections, or a variety of other options. Joints are designed to protect the connecting panels from relative vertical movement and transfer vehicular loads to the next panel smoothly. Some of the first research conducted on precast deck panel connections was conducted by Biswas et al. (1984), and since then there has been a consistent problem with the construction and performance of these joints. Issa et al. (1995a.) determined from a nationwide

survey that one of the major issues deterring DOTs from using rapid bridge deck rehabilitation was cracking and early deterioration of the connecting joints. Since their report, much effort has been made toward finding better connections that can meet acceptable standards of constructability and serviceability. While advancements have been made, most previous research focuses solely on positive bending in simply supported bridges; little research has been done to compare the performance of different transverse joints experiencing negative flexure.

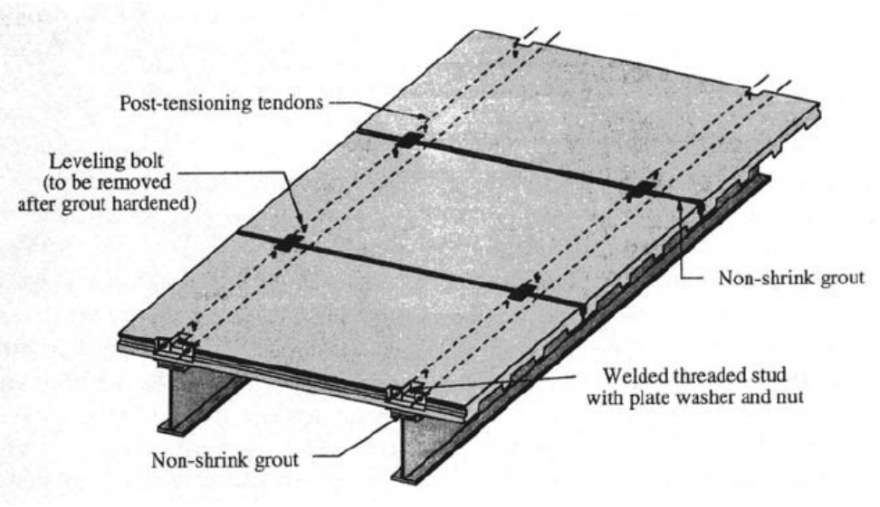

Figure 2.3: Typical Deck Panel with Grouted Transverse Joints (Yamane et al. 1998)

2.3.1 Shear Key Transverse Joint

Shear keys are typically unreinforced joints that connect two panels together. As shown in Figure 2.4, male-to-female joints, usually involve a male end that mates with another female end to form a connection, which is epoxied closed. These joints are known to experience extreme stress concentrations and can be difficult to mate during construction (Issa et al. 1995b) Furthermore, male-to-female joints require that panels be slid together making an issue as to the connection of the deck panel to the girder. For these reasons, and a poor performance record

when compared to female-to-female joints (Sullivan 2007), male-to-female joints are no longer commonly used.

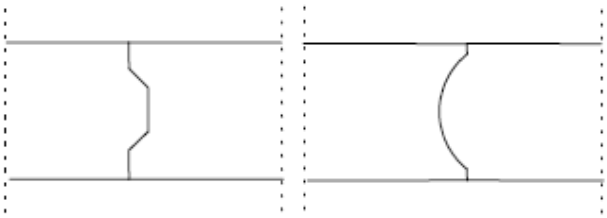

Figure 2.4: Various Male-to-Female Shear Keys (Swenty 2009)

Female-to-female shear keys are currently the most commonly used unreinforced joint for transverse connections, based on their performance and ease of installation. A female-to-female joint involves two matching female joints that have a grouted gap in between them that creates a cold joint connection as indicated in Figure 2.4. This grout pocket prevents the high stress concentrations that male-to-female joints experience, and this pocket should be grouted with a high-strength, non-shrink grout (Yousif 1998). There are many variations including unreinforced, welded, and post-tensioned connections. Unreinforced connections are fairly common, but they have an unclear performance record, as some of these joints have been known to crack, leak, and have difficulties with the spalling of concrete (Issa et al. 1995b) However, these problems continue to be reduced due to better grouting materials and improved construction standards (Culmo 2003; Swenty 2009). Increased attention paid to the joint and panel interface, such as sand blasting, has also greatly reduced debonding cracking and other joint failures (Issa et al. 2003). Various forms of welded connections have been developed, and the typical design usually involves a plate anchored into each side of the shear key. Once the panels are placed, a joining rod is welded on both sides to join the two separate plates to the rod, thus completing the welded connection so that grout can used to fill the joint. This joint has been known to experience similar issues as unreinforced shear key joints, in that cracking and leaking

were found to be common (Issa et al. 1995b). An example of a welded connection successfully used on an I-84 bridge by the Utah Department of Transportation can be seen in Figure 2.6 (Porter 2009).

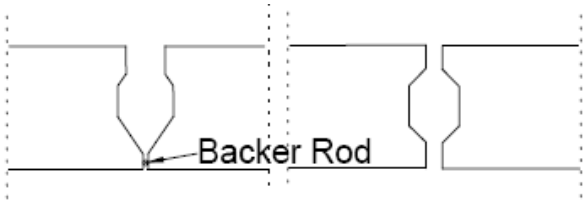

Figure 2.5: Typical Female-to-Female Shear Keys (Swenty 2009)

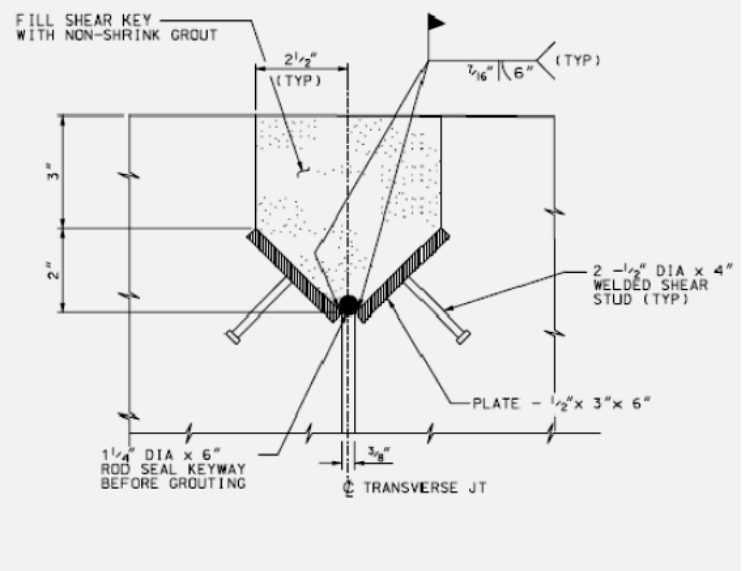

Figure 2.6: UDOT Standard Connection (Utah Department of Transportation 2008)

The most proven transverse shear key is the female-to-female longitudinally post-tensioned joint. By post-tensioning a joint, the joint's connection becomes tighter, and this post-tensioning force helps maintain joint compression and prevents cracking in both the joint and the deck panel, thus improving the overall behavior of the deck panel system (Issa et al. 2000). Through post-tensioning, deck compression can be maintained through a bridge's entire service life, and thus mitigate cracks and the infiltration of corrosive materials (Swartz 2008). Although

the nationwide survey conducted by Issa et al. did find some issues of cracking and leaking, these problems were attributed to poor construction practices and proprietary grouting materials (1995a). Issa et al. (2000) later noted that “the biggest cause of any adverse effects (for bridge decks) was the lack of post-tensioning in the longitudinal direction of the structure to secure the tightness of the joints." Originally, Issa et al. (1995b.) recommended a minimum of 150 psi of longitudinal post-tensioning to be applied to simply supported bridges while roughly 300 psi should be applied to continuous span bridges. Since Issa et al.’s survey (1995b.), much testing and observation has been conducted to determine adequate longitudinal post-tensioning levels. Ranging from finite-element modeling to full-scale bridge specimens and in-field data, the majority of these findings determined that approximately 200 psi of post-tensioning is required for simple span bridges while 300 psi or more is required for continuous span bridges. A summary of these recommended stresses and the type of research conducted can be seen in Table 2.1.

Table 2.1: Initial Joint Concrete Post-Tensioning Stress Level Recommendations for Precast Deck Panels

Bridge Type	Stress Level	Notes	Reference
Continuous Span*	340 psi	Representative bridge	(Swenty 2009)
Simple Span*	200 psi		(Bowers 2007), (Sullivan 2007)
Continuous (2 Span)	500 psi	Prototype bridge	(Issa et al. 2007)
Simple/Continuous*	150 psi/ 300 psi	After losses	(Issa 2002)
Continuous (2 Span models)	208 psi & 308 psi		(Issa et al. 2000)
1 Span FEM model*	200 psi	Did not include losses	(Issa et al. 1998)
3 Span FEM model*	450 psi		
18 Simple Spans	~150 psi	Bridges that performed well over time	(Issa et al. 1995b.)
1 Continuous Span	300 psi		
Continuous (2 Span models)*	290 psi		(Shim and Chang 2002)
All Spans	200 psi	After losses	(Precast/Prestressed 2002)
2 Simple Spans	200 psi		(Babaei et al. 2001)
3 Bridges	250 psi		(Culmo 2000)
Simple Span	200 psi		(Yamane et al. 1998)
Continuous Span	200-800 psi	Based on study	

*Modeled with Finite-Element Program

2.3.2 Reinforcing Bar Joints

Reinforcing bar joints are typically female-to-female shear keys that are simply spaced farther apart to allow the development of reinforcing bars within the grouted joint as shown in Figure 2.7. They are rarely post-tensioned and therefore crack when loaded in a continuous composite deck (Swenty 2009). The main issue observed with reinforced joints has been durability, especially in the earlier projects from the 1970's (Biswas 1974). Durability simply refers to a joint's capacity to handle repetitive truck loadings without inappropriate degradation. This degradation can be caused by the truck itself, or by subsequent issues, such as infiltration, due to cracking induced from the truck's loading. Issa et al. (1995b.) confirmed again that durability was a major issue in joints without post-tensioning, by investigating the in-field performance of numerous joints.

The most commonly used reinforced joint in practice is the looped joint. They can either be connected in place by tying rebar loops between panels (Figure 2.7) or they can alternate in an offset splice configuration (Figure 2.8). The Ministry of Transportation in Ontario Canada has devised a connection similar to both Figures 2.7 and 2.8. They conducted a number of scaled tests to verify these joints; however, the results only confirmed that these joints perform satisfactorily under positive flexural stresses (Au et al. 2008). Swenty (2009) conducted tests on a looped-bar connection joint and found that it performed satisfactory under the design life specified by the Virginia DOT; however, he did note that the post-tensioned female-to-female key he tested performed much better. He observed that reinforcing bar joints inevitably experience leakage due to noteworthy cracking (Swenty 2009). Furthermore, research at the University of Tennessee investigated alternating looped-bar joints using 4 deck panel specimens and determined that, under both positive and negative bending moments, this type of joint does

provide a viable connection option (Zhu 2010). However, some cracking did occur in these joints, and the University of Tennessee joint was not assessed for infiltration of foreign materials.

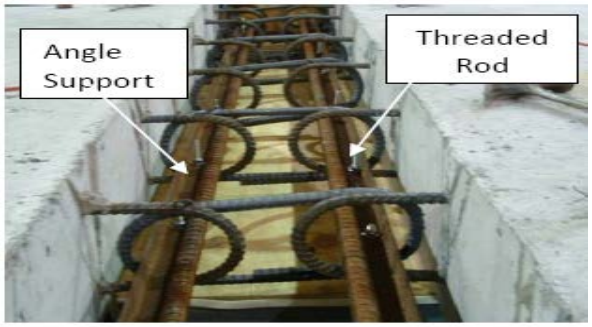

Figure 2.7: A Typical Reinforcing Bar Joint before Grouting (Swenty 2009)

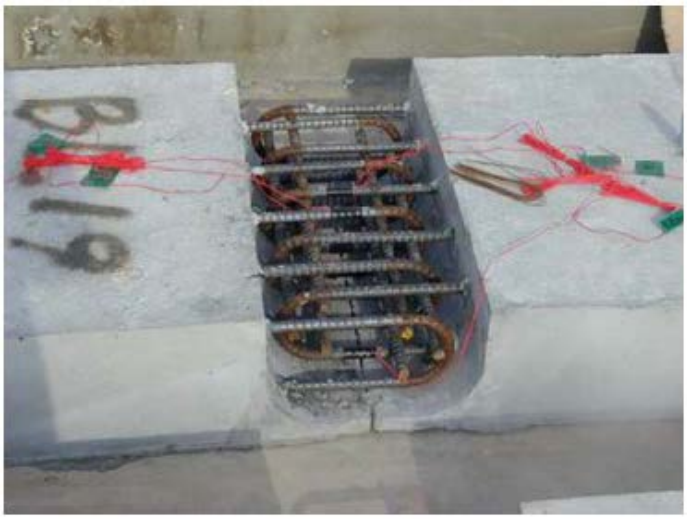

Figure 2.8: Alternating Looped-Bar Joint (Ryu 2007)

A proprietary reinforcing bar joint system was proposed by Badie et al.(2006)and was published by NCHRP in 2008 (Badie et al. 2008). A diagram of the NCHRP joint is shown in Figure 2.9. They developed a connection system for full-depth precast concrete bridge deck panels that did not require the use of an overlay or post-tensioning. This system involves elongated joint HSS tubing cast near the joint. The HSS tube has a cut slot that allows a rebar section to be dropped in the tube thus creating a spliced connection when the joint and tubes are

grouted. The joints developed were found to not leak water or crack after being tested in high fatigue cyclic tests (Badie et al. 2006). In addition the NCHRP Report 584 joint is fairly simple to construct, especially when compared to looped rebar joints, which can be tedious to connect.

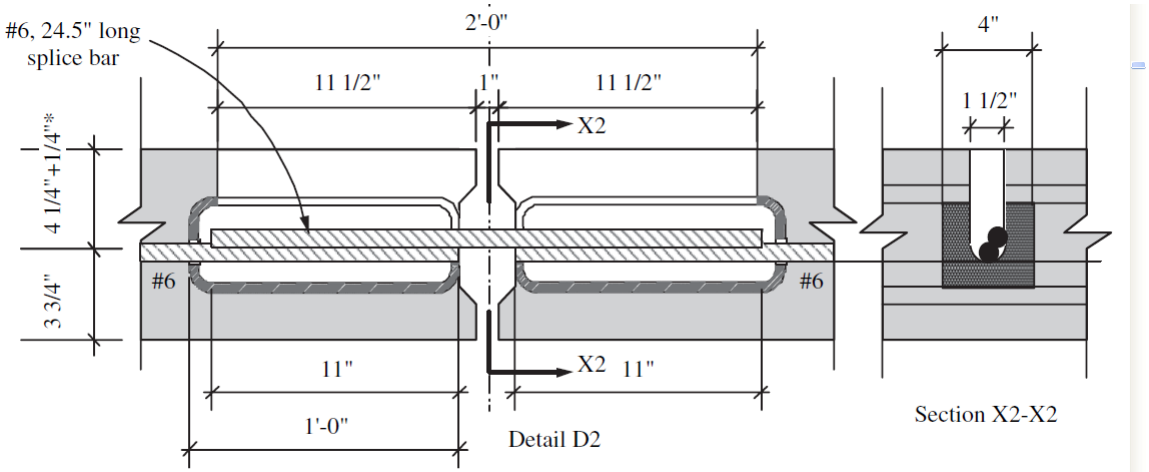

Figure 2.9: Embedded Reinforcing Bar Joint (Badie et al. 2006)

Other reinforced joints designed through various combinations of the female-to-female shear keys and reinforcing bar joints have been developed in past years and have been implemented somewhat effectively; however, these systems remain proprietary and are limited in wide usage based on constructability issues (Versace 2004). The main challenges in reinforcing bar joints is finding a design that can be installed easily and quickly while still providing adequate reinforcement and performance. While better joint connections are being developed, Reinforcing bar joints will continue to be unreliable until a joint can provide consistent long-term performance (Swenty 2009).

2.4 Experimental Testing of Transverse Joints

Transverse joints are primarily subjected to two types of forces: a vertical shear force and a bending moment (Badie et al. 2006). The shear force acts vertically to break the bond between

the grout and the panel joint, while the moment places two portions of the joint in compression or tension, depending on the positive or negative flexure. Many tests have been devised to assess these joints over the years, with some testing a connection's shear, moment, or axial capacities, while other attempt to mimic traffic loading. These tests are tailored to the specific purpose of each investigation; there is not an official recognized standard to validate the methodologies utilized. This section summarizes the progression and current practice for experimental testing of transverse joints, with more attention given to the few studies that analyzed joints without post-tensioning under negative flexure.

Some of the earlier tests assessing transverse deck panel connections have assessed a connection under one force effect, instead of a combination of forces as seen in actual truck loading. Pure shear testing is one such a test. A typical way to accomplish this test is through connecting two 'L'-shaped specimens and joining these sections with a shear key as seen in Figure 2.10a. The specimen is then loaded on the top and/or bottom to determine the maximum pure shear capacity of the joint. In order to further assess a joint's performance a tensile test and a flexural test are usually conducted as seen in Figures 2.10b and 2.10c, respectively. For tensile tests two slabs are connected using the desired joint and then pulled apart until failure. The flexural test involves applying a moment to the joint, without any shear, thus determining a joint's behavior in bending. These methods have typically been used to assess grouts, although many researchers have used them to also assess the performance of a particular joint (Backhoum 1991; Gulyas 1995; Issa et al. 2003). These tests are effective in the determination of a joint's capacities; however common problems for transverse joints have historically involved fatigue performance and infiltration of water and other foreign materials (Issa et al. 1995a). Due to this

fatigue issue, many researchers have used more comprehensive tests to validate deck connections.

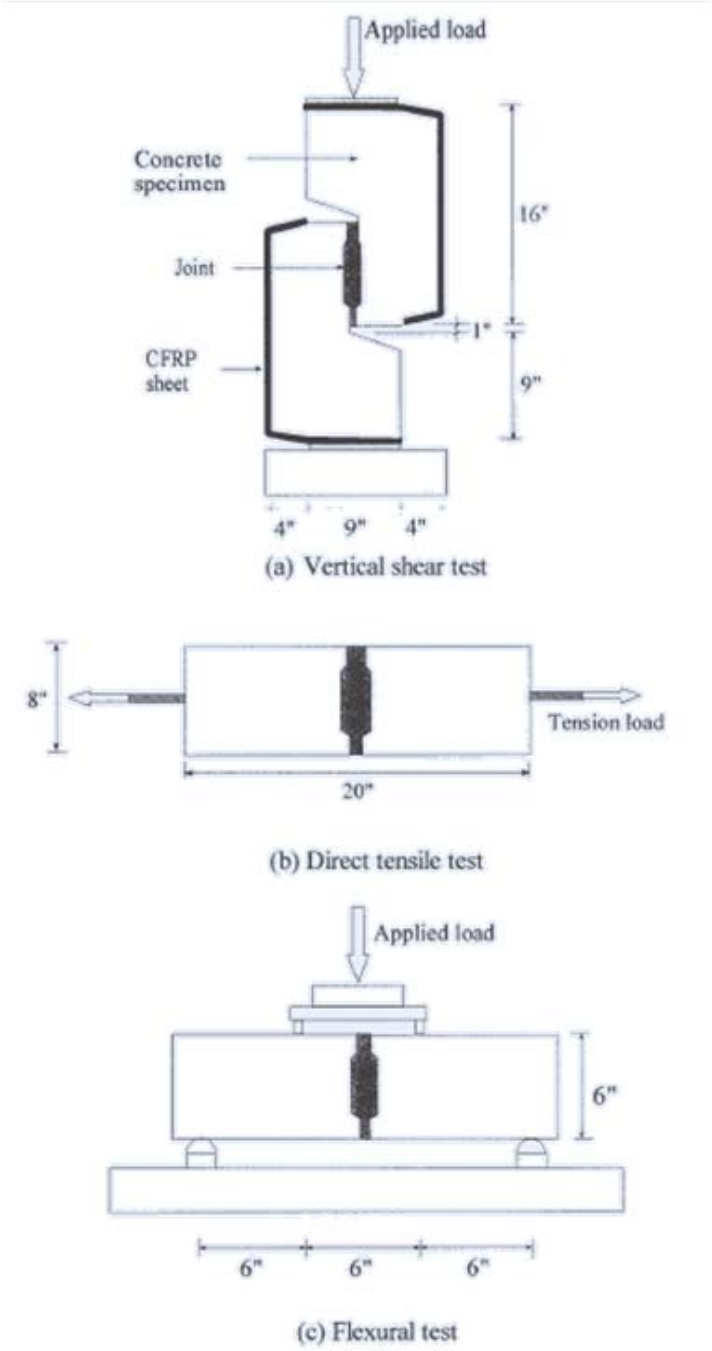

Figure 2.10: Typical Shear Key Tests (Issa 2003)

Badie et al. (2006) tested a full scale bridge model to assess the performance of the reinforced joint proposed by NCHRP Report 584. By using one axle load of a HS-20 design truck, they applied a positive moment and simultaneous shear to the joint, which experienced this fatigue-level loading for 2,000,000 cycles. Badie et al. (2006) observed no separation between the grout and the vertical surface of the joint, nor was there any tensile cracking on the bottom surface of the joint. Overall this joint performed satisfactorily, and is recommended for use in simply supported structures.

Some more recent research on reinforcing bar joint systems has shown promise for designers. Swenty (2009) conducted research at Virginia Polytechnic Institute comparing various types of joints including two different reinforcing bar joints. Swenty's approach to testing involved a scaled laboratory bridge based on an existing bridge in Southwest Virginia. This continuous bridge was built with transverse joints located directly above the piers of the structure. Under traffic loading, this location produced negative bending behavior in the joints. The resulting tensile stresses have long been known to be detrimental to these joints, so three standard joint systems were devised to assess which joints could perform adequately. Figure 2.11 shows the joints tested: an embedded rebar joint similar to NCHRP 584, a looped reinforcing bar joint, and two post-tensioned female-to-female shear keys. As can be seen in Figure 2.12, Swenty (2009) placed the transverse joints in pure negative flexure. Steel girders were utilized, as previous research indicated that steel girders provide the worst-case situation for deck panel joints (Bowers 2007). The joints were designed to withstand the factored design moments from service loads. Stress levels were calculated using finite-element analysis, and they were designed to be the same as the stress level produced from loading the real bridge. The test consisted of 1,000,000 cycles of fatigue loading, and at various points during these cycles,

loading was stopped in order to conduct ponding tests for leakage. A HS-20 truck loading was used for practicality, although it was found that the HL-93 loading, a combination of the HS-20 truck and lane loading produced slightly higher stresses (Swenty 2009).

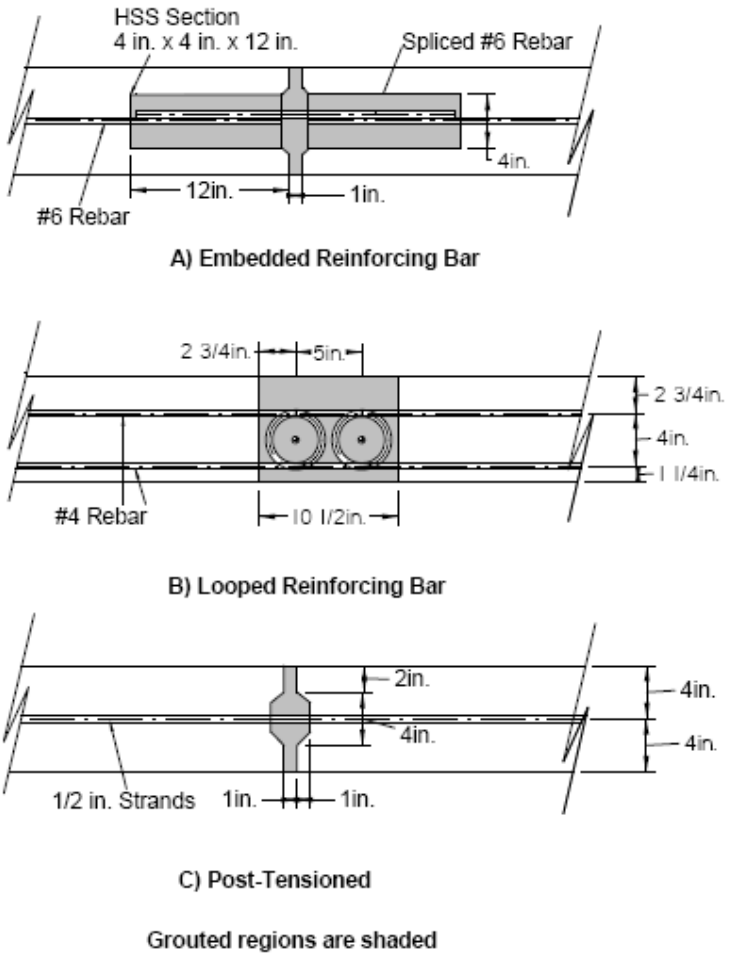

Figure 2.11: Joints Tested by M. Swenty (2009)

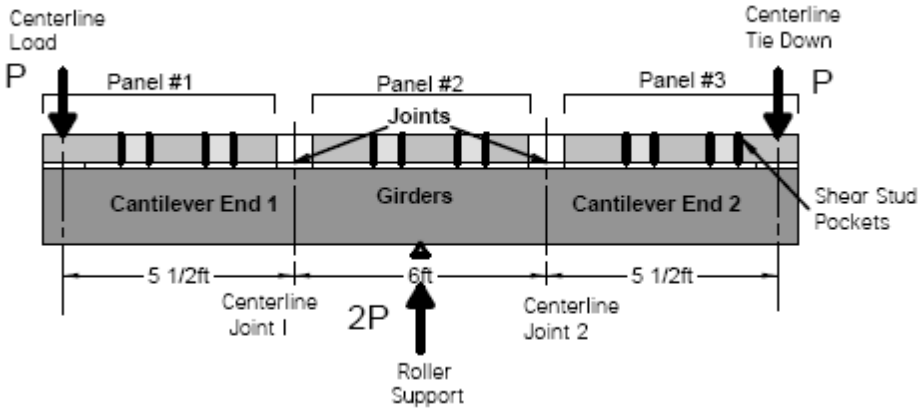

Figure 2.12: Negative Bending Testing Setup (Swenty 2009)

Overall, Swenty's (2009) study found that the two post-tensioned joints performed the best. The 340 psi post-tensioned joint experienced the smallest cracking and no leakage, while the 167 psi post-tensioned joint experienced the second largest cracking with no leakage. The looped-bar joint experienced the second smallest cracking, however when simultaneously loaded and tested with water ponding, 75 percent of the joint leaked water. The only joint to perform unacceptably was the embedded rebar joint, based on NCHRP 584, with large cracking and full leakage. Swenty noted that all joints, except the 340 psi post-tensioned joint, experienced acceptable but immediate cracking under top-fiber tensile loading from negative bending (Swenty 2009). He also observed that shrinkage cracking between the concrete and grout interface of the joint will occur if no surface preparation is used, regardless of the joint. In conclusion, Swenty's (2009) testing found that if longitudinal post-tensioning on a female-to-female shear key is not an option, a looped-bar joint (Figure 2.11b) would perform satisfactory.

Researchers at the University of Tennessee conducted another study on negative flexure in reinforced looped-bar transverse joints (Chapman 2010). By testing four separate reinforced looped-bar joints with varying development lengths and spacings, Chapman was able to confirm that some looped-bar joints can perform successfully under negative flexure. Figure 2.13 shows

the testing setup utilized. Related testing of the pure tensile capacity under fatigue loading showed promising results for this looped-bar joint (Zhu 2010).

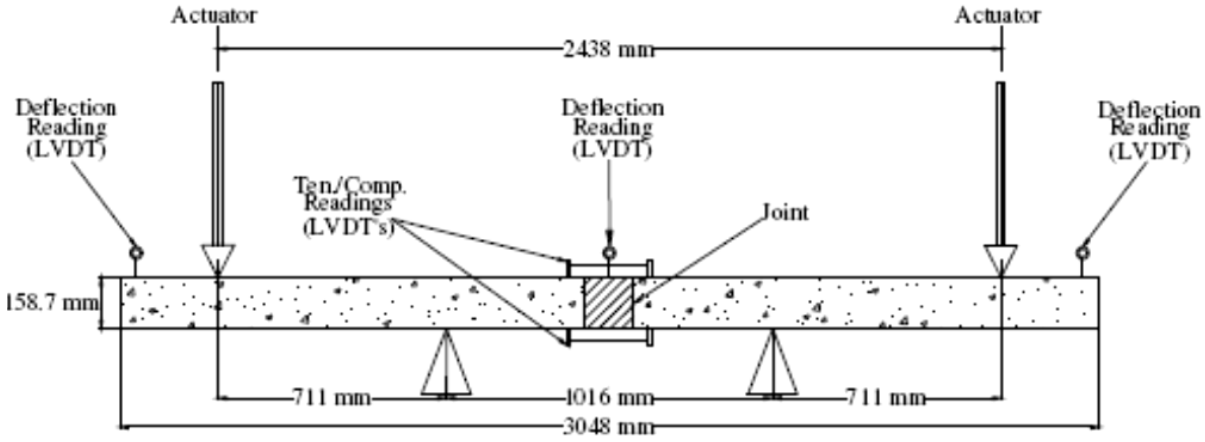

Figure 2.13: Negative Flexural Testing conducted by Chapman (2010)

Transverse joint tests range from simple shear push-off tests and pure-flexural tests to scale-model bridges with joints experiencing both shear and moment simultaneously. Although extensive testing of transverse joints has been conducted over the years, there are few tests that address negative bending nor are there many tests addressing shear and moment simultaneously applied to a joint. Tests are generally conducted on full-depth precast panels, without any testing exodermic deck connections' behavior. Although the in-service behavior of exodermic deck panels has been consistent with full-depth precast panels (Kaczinski 2010), the lack of studies comparing these deck connections' behaviors is noteworthy.

Table 2.2 shows a summary of relevant testing with general notes on how the test was conducted. All of the panels tested were full-depth precast concrete panels, and it can be seen from the table that the vast majority are post-tensioned female-to-female transverse joints. Hardly any of these tests assess different types of joints under the same loading scenarios; most previous tests were conducted to determine the adequacy of a certain joint.

Table 2.2: Tests Analyzing Full-Depth Precast Concrete Deck Panel Transverse Joints

SOURCE	DECK PANEL	JOINT(S)	TEST	LOADING			PONDING TEST
				Loading	Load (kips)	Fatigue Cycles	
(Roberts 2009)	Post-tensioned	Female-to-Female, curved bolt (2)	Negative moment with shear	HS-20 (axle)	40	N/A	N/A
(Swenty 2009)	Prestressed, post-tensioned	Female-to-female (4), reinforced (2)	Negative moment with shear	HS-20 (axle)	75.5	1,000,000	Interval and Continuous
(Sullivan 2007)	Prestressed, post-tensioned	Female-to-female (2), male-to-female (2)	Positive Moment with/without shear	HS-20 (wheel)	37.33	2,000,000*	Interval
(Olivia 2007)	Prestressed, post-tensioned	Female-to-female (2)	Positive moment with shear	HS-20 (axle)	40.4	2,000,000	N/A
(Issa et al. 2007)	Prestressed, post-tensioned	Female-to-female (2)	Positive/negative moment with shear	HS-20 (2 axles)	92	N/A	N/A
(Badie et al. 2006)	Prestressed	Spliced Joints (2)	Positive moment with shear	HS-20 (axle)	42.56	2,000,000*	Continuous
(Shim 2001)	Prestressed, post-tensioned	Female-to-female (2)	Positive moment with shear	HS-25 (wheel)	28.1	2,000,000	N/A
(Yamane et al. 1998)	Varying Depth; prestressed, post-tensioned	Female-to-female (2)	Positive moment with shear	HS-25 (wheel)	25	2,000,000	Continuous
***Referenced ASTM D6275 as utilized standard**							

2.5 Summary and Conclusions

Rapid bridge-deck replacement options are a feasible and effective means of rehabilitating bridges quickly and with minimal disruption of traffic. One of the key issues impeding the implementation of this system is finding an inter-panel connection system that can be installed quickly with sufficient durability and thus adequate service life. There is an abundance of research pertaining to certain areas of this research, however some newer transverse joints and aspects of certain panel systems have been largely avoided and need validation. Based on in-field performance and laboratory testing, the panel-to-panel joints should:

- Have testing focusing on fatigue life, as the failure of most joints in service and in laboratory testing was primarily due to cracking caused by cyclic, fatigue loading. Under the design-life fatigue testing, be designed for no cracking or only minute cracking that allows minimal infiltration of water.
- Be sanded after production and filled with non-shrink grout to minimize shrinkage cracking and debonding at the joint-panel interface (Issa et al. 2003).
- Have no cracks under repeated service loads and no water leakage (Issa 1995a); however, with no longitudinal post-tensioning, cracking and leakage will likely occur.
- Although it does not satisfy ALDOT requirements, previous performance has shown that joints should preferably be longitudinally post-tensioned, as it is the most effective way to maintain transverse joint compression, despite its prolonging of construction time.
- Be a post-tensioned or looped-bar joint, if it is expected to experience negative flexure, as these are the only joints that have consistently performed well in tension loading.

- For positive flexure, some unreinforced shear keys have shown promise based on laboratory testing. An unreinforced shear key, the NCHRP system, looped-bar joint, or a post-tensioned joint all have several studies suggesting they could be applied to simply supported bridges.
- As there is no previous research comparing exodermic-panel transverse joints to full-depth precast transverse joints, testing should be conducted to compare the behavior between the two deck panel systems' transverse joint systems. This testing should assess identical joints under the same conditions in each panel system.

In regard to the selection of a precast deck panel, exodermic and full-depth precast systems behavior proved similar based on in-field data. Both are effective in minimizing the disruption of traffic and both are proven methods backed by years of satisfactory in-field performance. The main advantage of exodermic panels is that they can offer a 40-60 percent weight savings over full-depth precast. The main issues of selecting one of these precast systems is cost, weight savings, and considerations as to whether the transverse joint between the systems will behave the same for both full-depth precast and exodermic panels.

CHAPTER 3: MODELING OF THREE ALDOT BRIDGES

3.1 Introduction

The modeling process of the three Alabama Department of Transportation bridges is discussed in this chapter. One of these bridges was selected as it is simply supported bridge that is going to be rehabilitated in the near future. The other two bridges were chosen based on standard bridge designs circa the mid 1950's; these continuous-span, steel-girder bridges were selected because they are expected to generate the greatest demand on transverse joints among bridges that are potential candidates for deck replacement.

3.2 Description of Bridges

The Collinsville Bridge is two sister bridges running alongside one another on I-59 in Collinsville, Alabama and crossing over State Road 68. This bridge was used as the pilot field study to better understand the feasibility and performance of the previously mentioned rapid deck replacement systems. The two sister bridges each consist of simply supported spans of approximately 56 ft. The existing deck is 33 ft 2 in. wide supported by four W36x150 steel girders; however, since the bridge is going to be widened for the rapid rehabilitation study, the widened 46 ft 9 in. deck was used in the modeling process with six W36x150 steel girders with cover plates. A typical cross-section of the deck for all three bridges can be seen in Figure 3.1.

The second bridge modeled was a standard bridge type used ALDOT. Standard bridge type B2807 consists of a three-span (60-80-60 ft) continuous bridge with a superstructure design almost identical to that of the Collinsville Bridge. This continuous span bridge has a two-lane design width that is anticipated to be widened if selected for rapid bridge deck rehabilitation, and therefore the bridge deck model was widened to accommodate three lanes supported by six girders.

The final bridge modeled was a three span, 80-100-80 ft continuous span bridge design from ALDOT standard drawing B2806. This bridge utilizes larger steel sections than the other two bridges, with four W36x194 girders with cover plates. Like the other two bridges selected for modeling, the width of the deck has been increased to accommodate current AASHTO standards for three lanes of traffic, under six steel girders. The plans for the simple span Collinsville Bridge and the 60-80-60 ft and 80-100-80 ft continuously supported bridges can be seen in Appendix C.

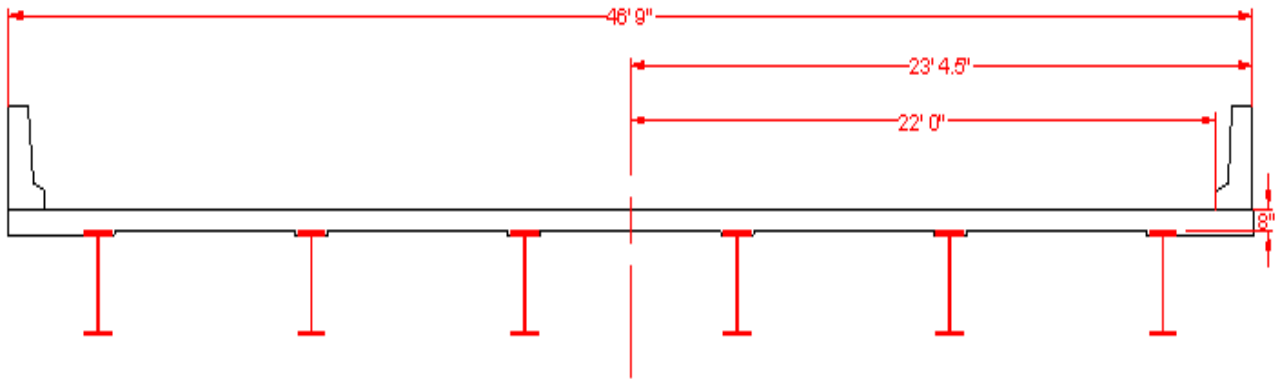

Figure 3.1: Typical Transverse Cross Section of Bridges

3.3 Modeling

The three bridges were modeled using the finite-element program SAP2000 (Computer and Structures, Inc. 2011). More specifically, the SAP2000 Bridge Modeler Wizard was used to model the bridge. The following is a basic overview of the modeling process including choices made about model discretization and the type of SAP structural model. This modeling process follows AASHTO LRFD (2007) specifications for refined methods of analysis, using an isotropic plate model for the deck and following the requirements for beam-slab bridges

(AASHTO 4.6.3). The SAP2000 program utilized linear-elastic analysis in the calculation of results.

First, layout lines were used as the reference lines to define the horizontal and vertical alignment of the bridges. Once the general shape of the structure was established, the deck sections were then modeled to replicate the superstructure of the bridge. The deck, haunches, and steel girders with cover plates were modeled according to design specifications, while the guardrails were excluded, as they were deemed unnecessary for these analysis purposes. The existing steel yield strength of 33 ksi was used in modeling the girders, while the concrete deck's properties were modeled based on expected values for the replacement deck. The concrete's compressive strength was set at 4 ksi with a 3,600 ksi modulus of elasticity. The girders were not modeled using area objects, but instead remained full girder solid objects in order to generate more accurate results in the deck elements. The final steps involved assembling the bridge object. The spans were defined, and then deck sections, diaphragms, abutments, and bents were assigned to their appropriate locations in the spans. Support conditions were then assigned to behave as the actual bridges were designed. For the simply supported bridge, a pinned support condition on the south end, with a roller support at the opposite end. Based from the ALDOT design, the continuous bridge had the two interior bents pinned against lateral movement, with the support conditions at the abutments being rollers.

The final step in completing the bridge model was the selection of the type of structural model. Initially a spine model was chosen to verify the overall behavior of the bridge to calculated results. A spine model takes the superstructure and models it as frame elements, thus performing a simple, nearly 2-dimensional analysis of the superstructure. As spine model results matched expected behavior, a more complex and thorough modeling process was chosen for the

deck analysis. An area object model was chosen for analysis purposes, as this form of model provides a better representation of 3-dimensional behavior and also more accurately accounts for loading eccentricities. Area object modeling provides the most detailed response results for the deck by using shell elements for the girders and deck. The discretization of the deck spans and other elements was chosen to maintain a square element area shape, in order to satisfy aspect ratio limits specified in AASHTO 4.6.3.1.

3.4 Loading

After the bridges were modeled the next step in the analytical process involved the vehicular loading of the structure. All of the various lane loading scenarios were defined in accordance with AASHTO design lane and lane loading criteria. Having determined fatigue as the controlling criteria of transverse joint design, the loading was done in accordance to AASHTO 3.6.1.4 Fatigue Load.

Figure 3.2 shows this loading; the spacing from the center axle to the rear axle of the HS20 truck is set at 14 ft for fatigue loading. One fatigue design truck was used to investigate the worst possible loading of the deck area objects.

All analysis was conducted without the use of dynamic load allowance (IM) per AASHTO LRFD 3.6.2 and also without the application of multiple presence factors (m), Section 3.1.1.2. Dynamic load allowance is meant to account for wheel load impact from moving vehicles, and although the modeler used did not account for wheel load impact, it was determined to apply this factor to the modeled output results. Essentially, all model-produced stresses unless otherwise listed should be increased by 15 percent for fatigue and fracture limit states and by 33 percent for all other limit states.

At first influence-based analysis was used to determine the maximum stresses in the deck. This analysis automatically generates worst-case loading scenarios by determining the greatest effect a truck loading can generate within a specified area or lane. By selecting three lanes, this analysis loads each lane individually, then loads all lanes, and then omits each lane from loading in order to establish what the number of trucks and what position of each truck causes a critical loading. A minimum of one and maximum of three trucks were used to load the bridge, and the loading areas (lanes) were established based on engineering judgment and trial and error. Through this analysis, the worst-case effects for each deck element were established thus creating an influence surface that showed the minimum and maximum response quantities for each deck element and girder in the structure. By generating a contour graph showing the largest compressive and tensile forces that could be experienced in the deck, the highest magnitude stresses were located, and thus the critical transverse deck sections for both positive and negative flexural stresses were located for each of the bridges.

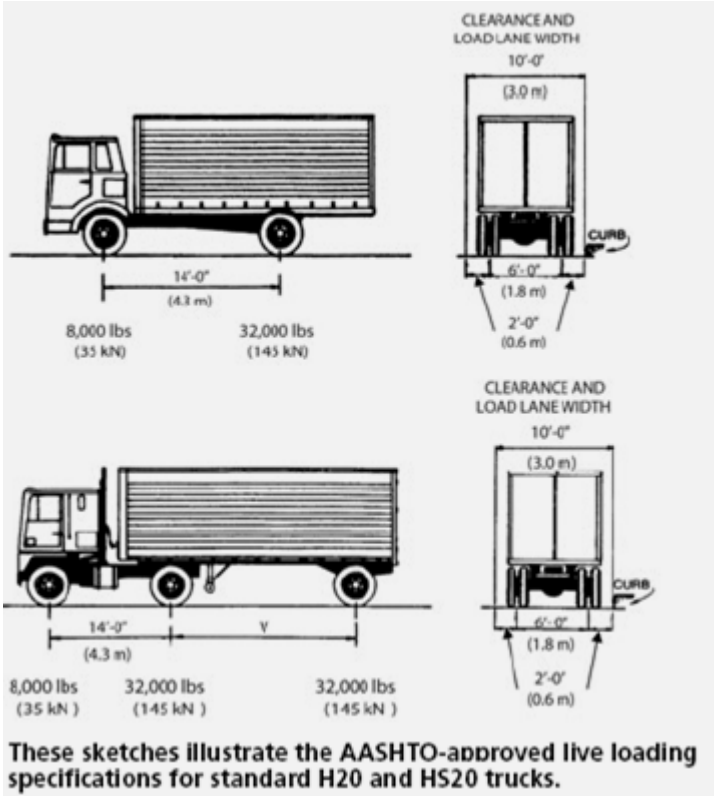

Figure 3.2: AASHTO Truck Loading Scenarios (AASHTO 2007)

In order to verify this influenced-based analysis as well as the model itself, the model-calculated girder moments were compared to girder-line analysis results, based on the approximate method of analysis for beam-slab bridges, AASHTO LRFD section 4.6.2.2. The girder-line analysis simply assumes that vertical traffic loads are applied to one girder, thus giving the total moment that a load will apply to the bridge. By summing the model-generated moments for each girder, the total moment that the bridge experiences in modeling can be established. This model-generated moment can then be compared to the girder-line analysis moment in order to ensure that the model-generated moments are reasonable. As shown in Table 3.1, the girder-line analysis moments were found to be virtually the same as those moments

generated from the model with less than a one percent difference for three different loading scenarios.

Table 3.1: Comparison of Moments

Girder	3 Trucks M (k-ft)	2 Trucks M (k-ft)	1 Truck M (k-ft)
West Exterior	26.9	3.5	-6.1
Interior	78.7	35.1	10.1
Interior	178.9	83.5	32.4
Interior	305.2	193.0	75.2
Interior	357.7	333.3	186.3
East Exterior	354.1	372.4	314.7
Model Moments Summed:	1301.5	1020.8	612.6
Girder-Line Moments per AASHTO LRFD:	1306.4	1024.6	614.8

The next validation step involved calculating deck stresses from the girder-line analysis and model-generated moments. Assuming plane sections remain plane, linear-elastic material behavior, and composite action between the girder and the deck, a section modulus was calculated for the interior deck/girder section and for the exterior deck/girder section. The deck stresses were then calculated by dividing the girder-line and model-generated moments by the section modulus. Figure 3.3 shows the results. The x-axis represents a transverse cross section of the bridge at midspan with transverse position 0 (TP-0) being the center of the bridge and positions -24 (TP-24-) and 24 (TP-24) being the transverse edges of the bridge roadway. The orange dotted line represents model-generated stresses from influenced-based analysis, while the flat bar lines represent the uniformly distributed stresses calculated from both model-generated girder moments and girder-line analysis moments. These stresses in the top fiber of the deck due to girder-line and model-generated moments were assumed to be uniformly distributed across the effective flange width of the girder. From this figure it can be seen that the model-generated stresses coincide with the AASHTO girder-line analysis calculated stresses; the discrepancy

between the two is mostly due to localized forces acting in the deck between the girders. Overall, the girder-line analysis results indicate that the model-generated stresses are reasonable.

After having located the critical transverse cross section(s) in each bridge, a step-by-step analysis was conducted to determine the locations of the trucks causing the maximum stresses in the deck. A step-by-step analysis involves specifying a truck to cross the bridge at a certain transverse point, and with a certain number of discretization points. Choosing a discretization of every 3 inches, this process essentially moved the fatigue truck across the bridge, recording element data for the entire bridge every 3 inches that the truck progressed. Having determined a critical longitudinal location, the transverse location of the truck needed to be determined. In order to determine this transverse location for an extreme loading scenario, the fatigue truck was run across the bridge repeatedly, each time moving transversely by 1 ft. Figure 3.4 and 3.5 illustrate the transverse movement of the truck from position TR-0 to TR-18.

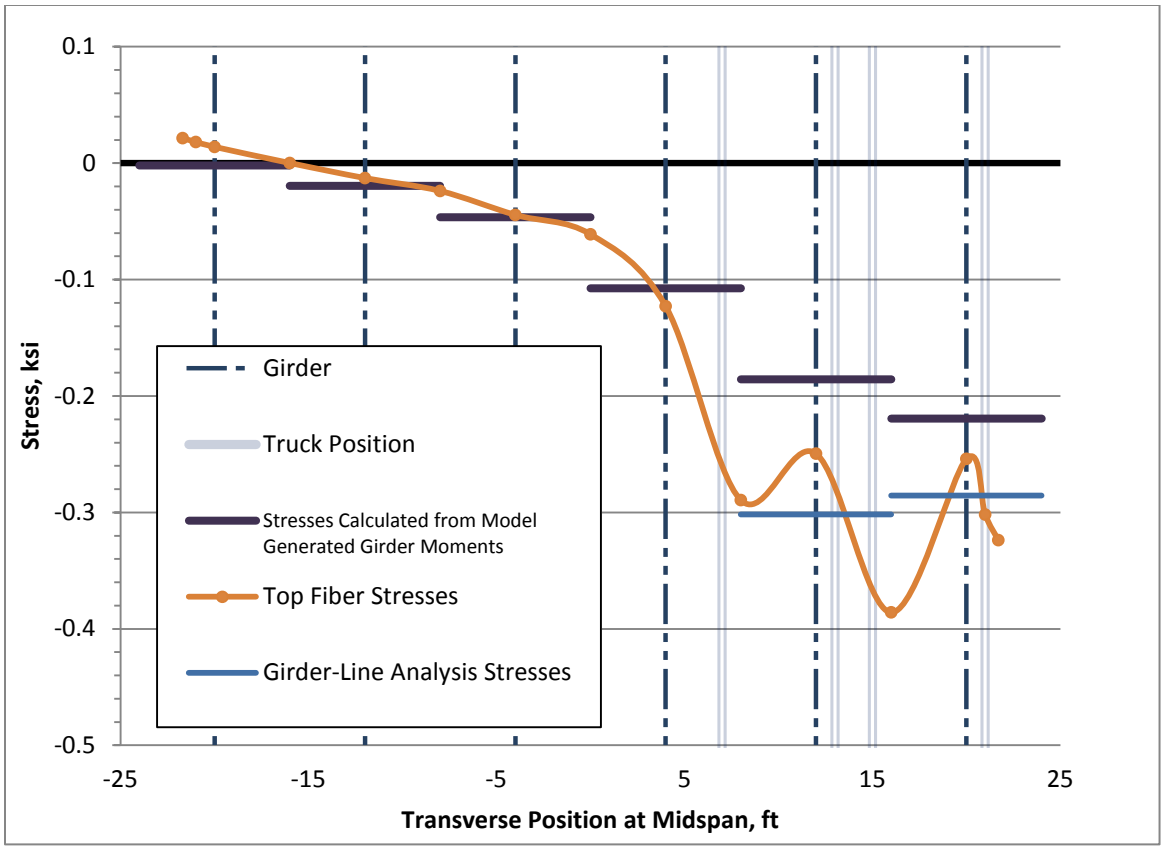

Figure 3.3: Top Fiber Stress Comparisons at Midspan (Simple Span Bridge)

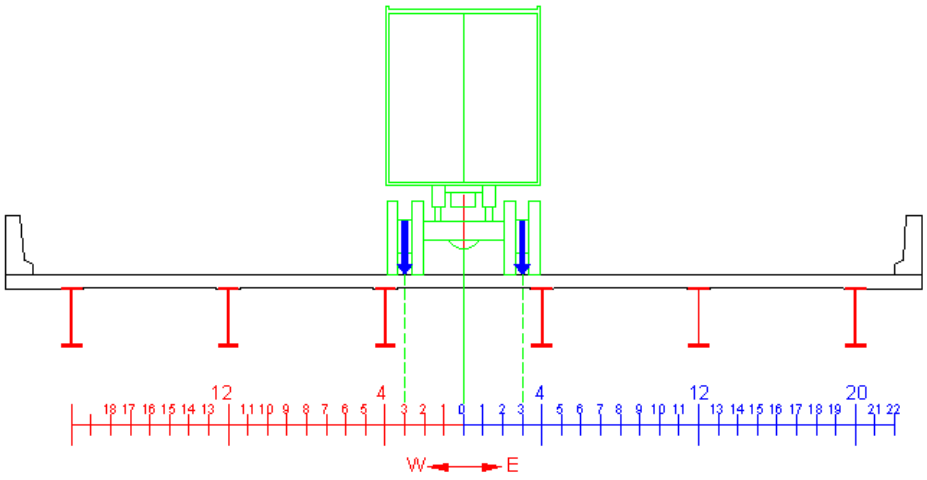

Figure 3.4: Transverse Truck Position 0 (TR-0)

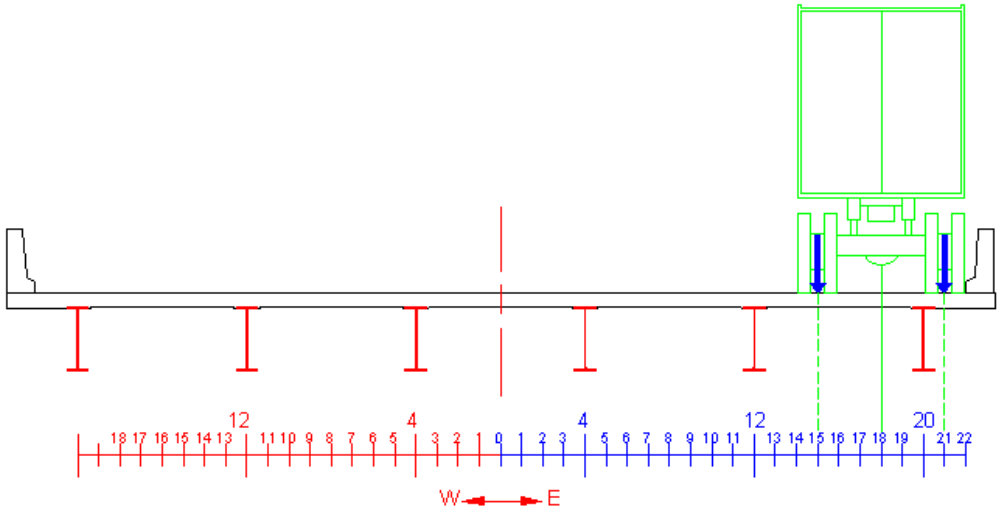

Figure 3.5: Transverse Truck Position 18 (TR-18)

Starting at position TR-0 (Figure 3.4) the center of the truck is located at the center of the bridge, with the left and right set of the wheels located 3-feet offset from position TR-0. The truck is moved from position TR-0 to TR-1, then to TR-2, and so on until the truck reaches the extreme allowable position TR-18, which places the exterior wheel load one foot away from the edge of the curb (Figure 3.5). In each transverse position, the truck is run along the length of the bridge and then data are compared to determine the extreme case loading scenario for both longitudinal and transverse loading. There are two worst-case loadings for causing tensile stresses in the deck in each of the continuously supported bridges: a top-fiber, negative-moment extreme case; and a bottom-fiber, positive-moment extreme case. Both cases are extreme as they test the tensile capacity of the joint; top fiber stresses refer to the extreme top fiber of the joint, while bottom fiber stresses refer to the extreme bottom fiber of the joint. The compressive forces were found to be well within normal service-load capacities. It must be noted that as these bridges are all transversely symmetrical, the transverse truck position movement was only

conducted for one half of the transverse deck section, and data will be reported for loading the transverse eastern portion of the bridge (Figure 3.6).

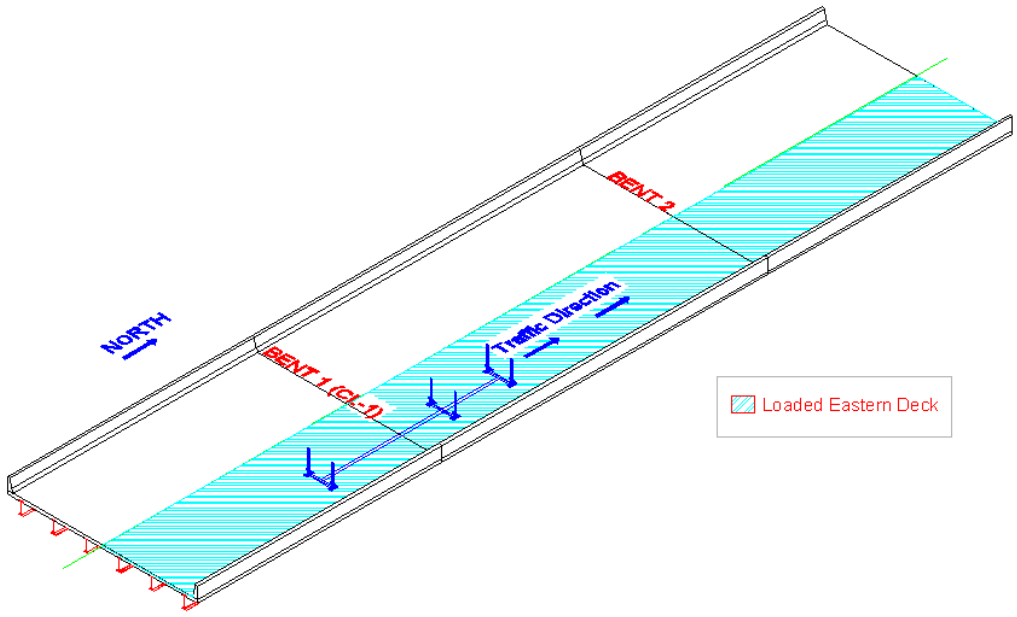

Figure 3.6: Loading of Bridge and Direction of Traffic

After determining the extreme tensile effects for top and bottom fibers, a step-by-step analysis was used to determine shear effects. The trucks were located at the worst-case position previously found for bending stress, and shear was recorded at those critical deck locations. Additionally, the model also analyzed the truck's passing of the bridge to find the largest magnitude shear force that occurs in critical location CL-1 and CL-2. The results from these stress and shear modeling processes are discussed in further detail in the following chapter.

CHAPTER 4: MODELING RESULTS AND DISCUSSION

4.1 Organization of Results

The results from the modeling of three bridges are discussed in this section, with attention being given to extreme case scenarios. The stresses and shears are expected to represent the modeled load effects that a transverse joint would experience, and therefore these forces should be considered in the testing and selection of a transverse joint connection.

4.2 Results from 60-80-60 ft ALDOT Continuous Span Bridge

As a continuous span bridge is subject to both positive and negative bending moment, there are multiple extreme loading scenarios for the 80-60-80 ft bridge. The results from the positive bending worst case scenario will be discussed first, followed by the negative bending extreme loading results, and finally the shear loading results will be shown.

4.2.1 Extreme Positive-Flexure Stress

Using a step-by-step analysis, the AASHTO HS-20 fatigue design truck was run along the length bridge in all transverse truck positions TR-0 through TR-18 (Figure 3.4 and 3.6). The critical location for positive-flexure stresses (across a transverse joint) was already known from influence-based analysis; it occurs approximately 5 feet past the first interior bent and is referred to as CL-2 for convenience. Figure 4.1 illustrates this critical transverse location. Having located CL-2, a graph of each transverse position was made to determine the longitudinal extreme case truck position. For TR-13, the extreme positive-flexure stress occurred when the front 8 kip axle of the truck was positioned 19 ft 3 in. past the first bent with the trailing 32 kip axles located 5 ft 3 in. past the bent and 24 ft 9 in. before the bent. Figure 4.2 shows the effect, at CL-2, of the truck as it moved across the bridge. By locating the peak top fiber stress, the critical longitudinal

truck position was located, as shown in Figure 4.3. This longitudinal position resulted in extreme joint stresses for all transverse positions TR-0 through TR-18.

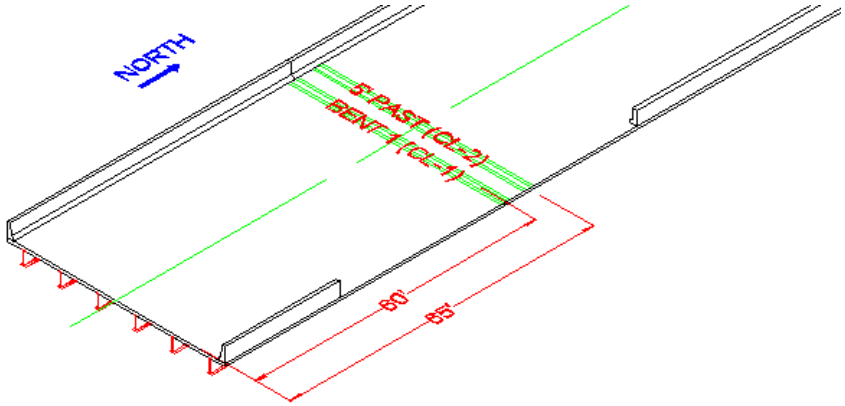

Figure 4.1: Critical Locations for 60-80-60 Continuous Bridge

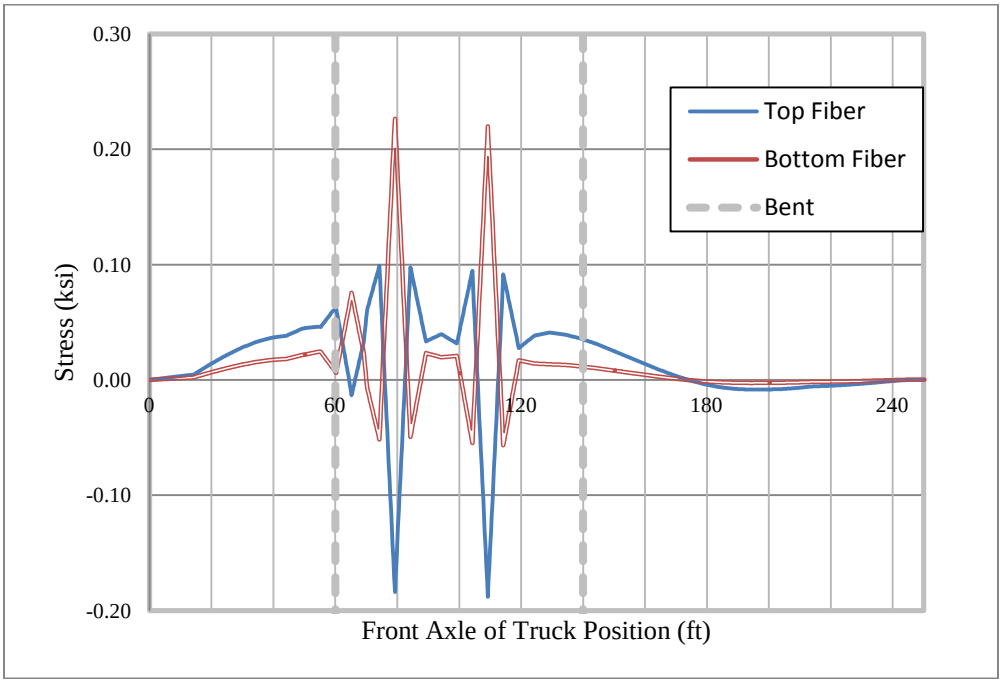

Figure 4.2: Longitudinal Plot of the Effects of TR-13 on CL-2 (60-80-60 Bridge)

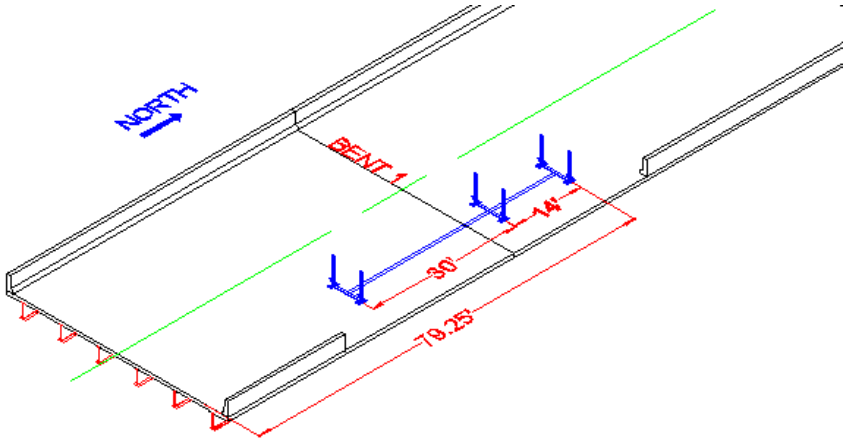

Figure 4.3: Longitudinal Position of Truck for Extreme Positive-Flexure Stresses (60-80-60 Bridge)

From this extreme positive-flexure stress loading, Figure 4.4 summarizes the values generated by the SAP2000 model. This graph represents the greatest stresses normal to a transverse deck joint for each transverse truck position at the critical longitudinal location. It can be seen from Figure 4.4 that the higher stresses are reached when the truck is positioned at transverse positions TR-3, 5, 11, and 13. These loadings are seen in black in the figure, and they represent trucks having either their left or right side wheels located on the deck exactly between two lines of girders (Figure 4.5). Conversely, the smallest stresses occur when half of the truck loading was located directly above a girder, as seen in truck positions TR-1, 7, 9, 15, and 17. Figure 4.6 illustrates this loading of the girder. It can be seen from Figure 4.4 that the stresses in the panels showed a decreasing trend, as truck tires were moved from the middle between girders to on top of the girders. Furthermore, stresses increased as the truck position was moved into the extreme transverse position at the edge of the bridge roadway. These results show that the extreme case for positive-flexure stress across a transverse joint occurs when a set of wheel loads is placed midway between girder lines.

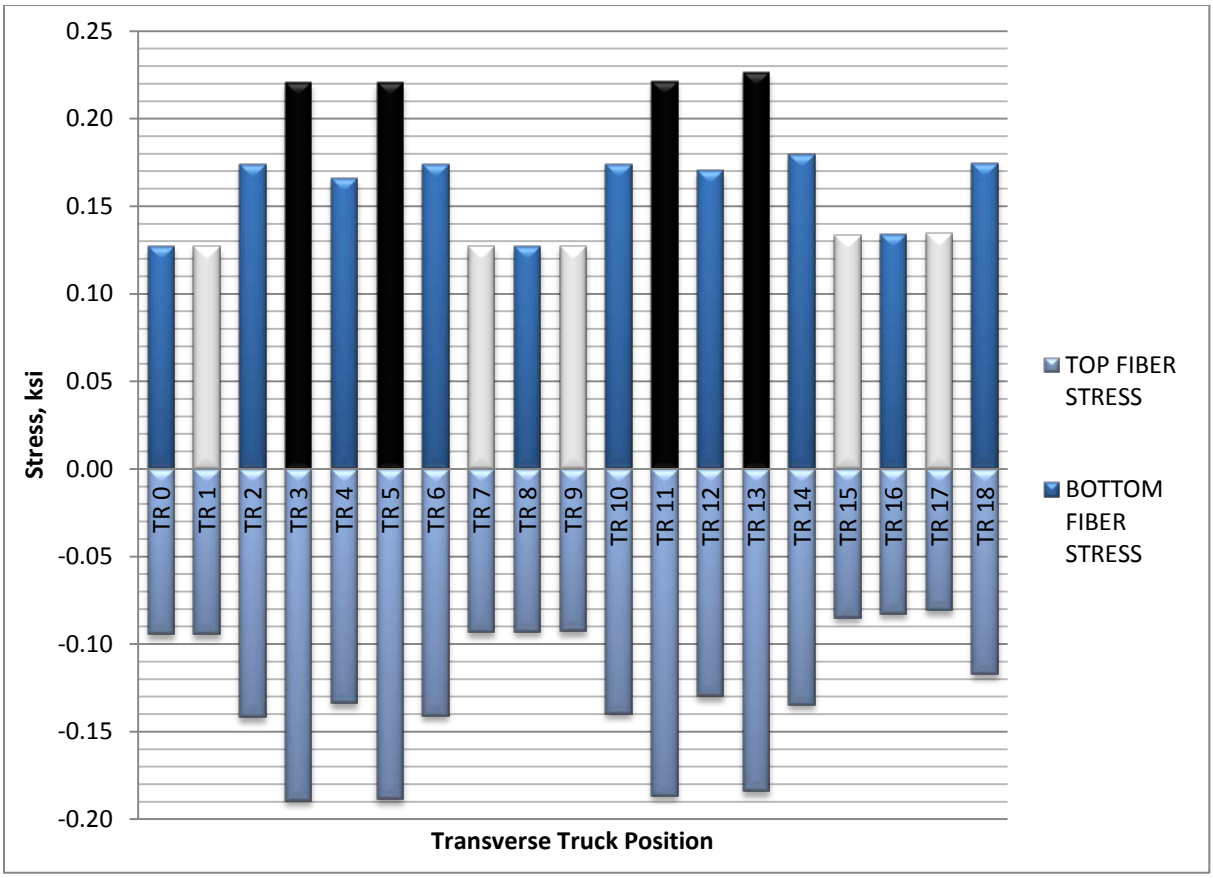

Figure 4.4: Maximum Stresses per Transverse Position due to Positive Flexure (60-80-60 Bridge)

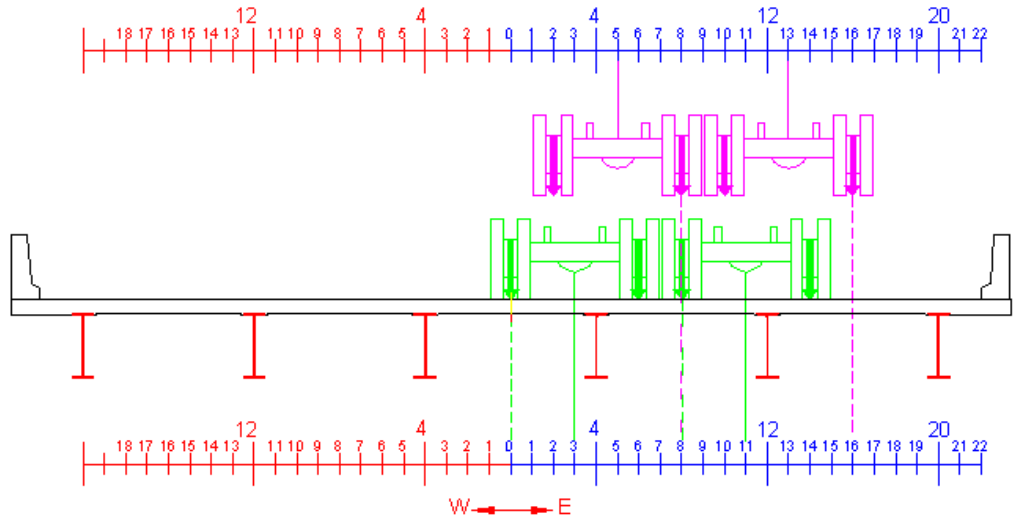

Figure 4.5:Transverse Truck Positions TR-3, 5, 11, and 13 Loading the Exact Middle Between Girders

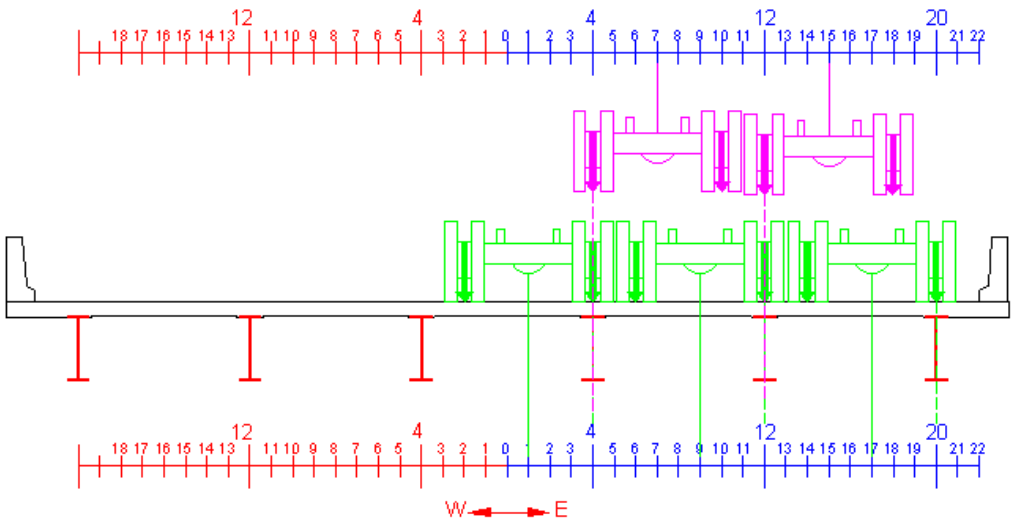

Figure 4.6: Transverse Truck Positions TR-1, 7, 9, 15, and 17 Loading the Girders

Table 4.1 shows the values generated during this extreme positive-flexure stress scenario graphed in Figure 4.4. These values do not include dynamic load allowance and are simply the effects of the design fatigue truck on the bridge deck. Furthermore, this table shows the truck loading scenario, bottom and top fiber stresses, the transverse location of the critical stress, and the modulus of rupture. The modulus of rupture (MR) was calculated using $MR = 7.5\sqrt{f'c}$, with the compressive strength of concrete being 4000 psi. The transverse location column is based off the scale seen in Figure 4.6, and it can be seen from this column that all the critical locations for each deck panel fall exactly between girders at transverse positions 0, 8, and 16. This signifies that the highest bottom fiber tensile stresses occur in the portion of the deck that is transversely centered between girders. Consistent with expected positive flexural behavior, the bottom fiber of the deck is in tension while the top fiber remains in compression under these maximum stress cases.

Table 4.1: Stresses at CL-2 due to Positive-Flexure Truck Loading (60-80-60 Bridge)

Truck Transverse Position (ft)	Transverse Location of Critical Stress (ft)	Stress, Bottom Fiber (ksi)	Stress, Top Fiber (ksi)
TR 0	0	0.128	-0.094
TR 1	0	0.127	-0.094
TR 2	0	0.174	-0.142
TR 3	0	0.221	-0.189
TR 4	8	0.166	-0.134
TR 5	8	0.221	-0.189
TR 6	8	0.174	-0.141
TR 7	8	0.127	-0.093
TR 8	8	0.128	-0.093
TR 9	8	0.128	-0.093
TR 10	8	0.174	-0.140
TR 11	8	0.221	-0.187
TR 12	16	0.171	-0.130
TR 13	16	0.226	-0.184
TR 14	16	0.18	-0.134
TR 15	16	0.133	-0.085
TR 16	16	0.134	-0.083
TR 17	16	0.134	-0.081
TR 18	16	0.175	-0.117
Extreme Tensile-Stress Case:	**16**	**0.226**	**-0.184**

After determining the stresses in Table 4.1, they were compared to the modulus of rupture. It must be noted that the modulus of rupture is not representative of any joint's capacity; the modulus is simply a benchmark with which the tensile stresses can be referenced. The extreme fatigue stress found at TR-13 was only 0.226 ksi, less than half of the modulus of rupture, which showed significant capacity in the joints to handle fatigue loading. Graphs of the full transverse cross section at Critical Location 2 can be seen in Figure 4.7, Figure 4.8, and Figure 4.9. These figures illustrate the maximum tensile stress that occurs in the deck between

girders, and they also show how the force effects due to truck loading are largely localized at the location of the wheels. The localized high stresses normal to a transverse deck joint from truck loading dissipate significantly after the deck panel crosses over a girder support.

Figure 4.7: Deck Stresses due to TR-13 at Critical Location 2 (60-80-60 Bridge)

Figure 4.8:Deck Stresses due to TR-11 at Critical Location 2 (60-80-60 Bridge)

Figure 4.9: Deck Stresses due to TR-0 at Critical Location 2 (60-80-60 Bridge)

To further assess the extreme effects for the deck panels, other truck scenarios were analyzed and then compared to the worst case stress of 0.226 ksi from the fatigue design truck. As stated in AASHTO LRFD (2007) Article 3.6.2.2, a dynamic load allowance of 1.15 should be multiplied by this fatigue stress, making the fatigue design stress 0.260 ksi. When analyzing the bridge under AASHTO limit states other than fatigue, different dynamic load allowances must be included and a multiple presence factor should be applied to determine maximum stresses. Further modeling included adding multiple trucks in critical configurations and also changing the truck's rear axle spacing from 30 ft to 14 ft. Scenarios involving one, two, and three trucks were conducted. The single truck analysis validated the fatigue loading scenarios as the critical loading occurred over transverse truck position 13. After numerous analyses, the worst-case conditions for multiple truck loadings was found to occur when the trucks were positioned as close to the eastern edge as permissible. Table 4.2 shows the modeled extreme service load values that can be expected to be experienced in the deck. By multiplying the truck effects by the appropriate AASHTO multiple presence factor and the 1.33 dynamic load allowance, this table shows the results of loading the bridge with a service load. The extreme effect of 0.361 ksi occurred due to single fatigue truck loading.

Table 4.2: Extreme Service Load Stresses at CL-2

Truck Transverse Position (ft)	Rear Axle Spacing (ft)	Multiple Presence Factor, m	Dynamic Load Allowance, IM	Transverse Location of Critical Stress (ft)	Stress, Top Fiber (including m & IM) (ksi)
TR 13	30	1.20	1.33	16	0.361
TR 13	14	1.20	1.33	16	0.354
TR 7 & 17	30	1.00	1.33	16	0.190
TR 7 & 17	14	1.00	1.33	16	0.176
TR (-1),7, & 17	30	0.85	1.33	16	0.162
TR (-1),7, & 17	14	0.85	1.33	16	0.150
Extreme Case:		TR-13 @ 30ft		16	0.361

4.2.2 Extreme Negative-Flexure Stress Case

As with the extreme positive-flexure stress investigation, the AASHTO HS-20 fatigue design truck was run along the bridge length in all transverse positions TR-0 through TR-18. A plot of the reaction at the critical location as these trucks crossed the bridge showed the critical locations for each transverse truck position.

Figure 4.11 shows this type of plot for transverse truck position TR-13. The controlling negative-flexure stress scenario occurred when the front 8 kip axle of the truck was positioned 29 ft 3 in. past the first bent with the trailing 32 kip axles located 15 ft 3 in. past the bent and 14 ft 9 in. before the bent (Figure 4.10). This longitudinal truck location was the extreme case position of the truck for all transverse positions TR-0 through TR-18, causing the largest tensile forces in the top fiber of the deck at the first bent. This tensile stress is largely consistent with the maximum girder-line negative moment stresses that would be expected over the bent. This critical location at the first bent, seen in Figure 4.1, will be referred to as CL-1.

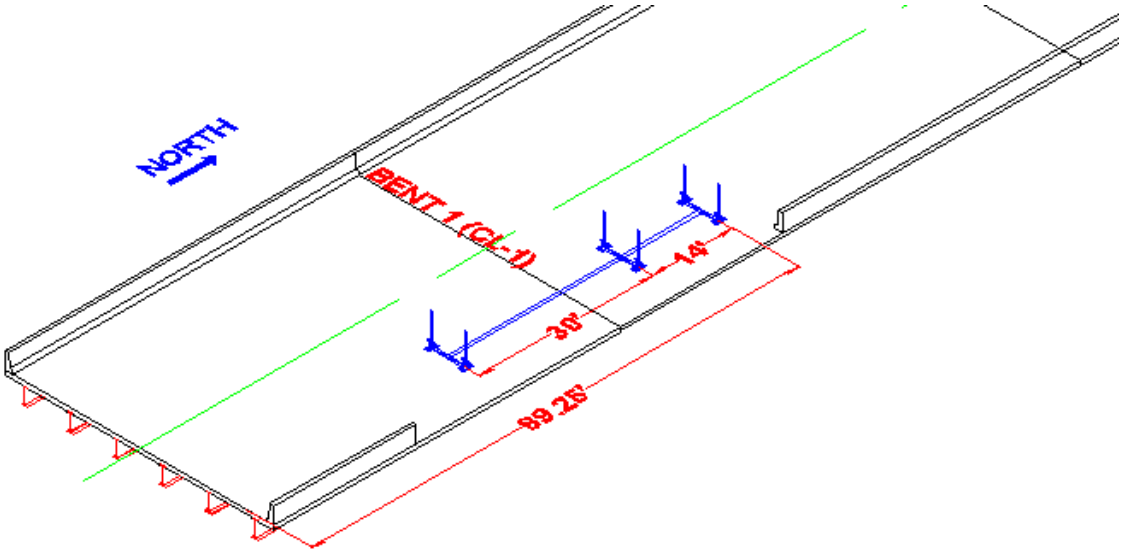

Figure 4.10:Longitudinal Position of Truck for Extreme Negative-Flexure Stresses (60-80-60 Bridge)

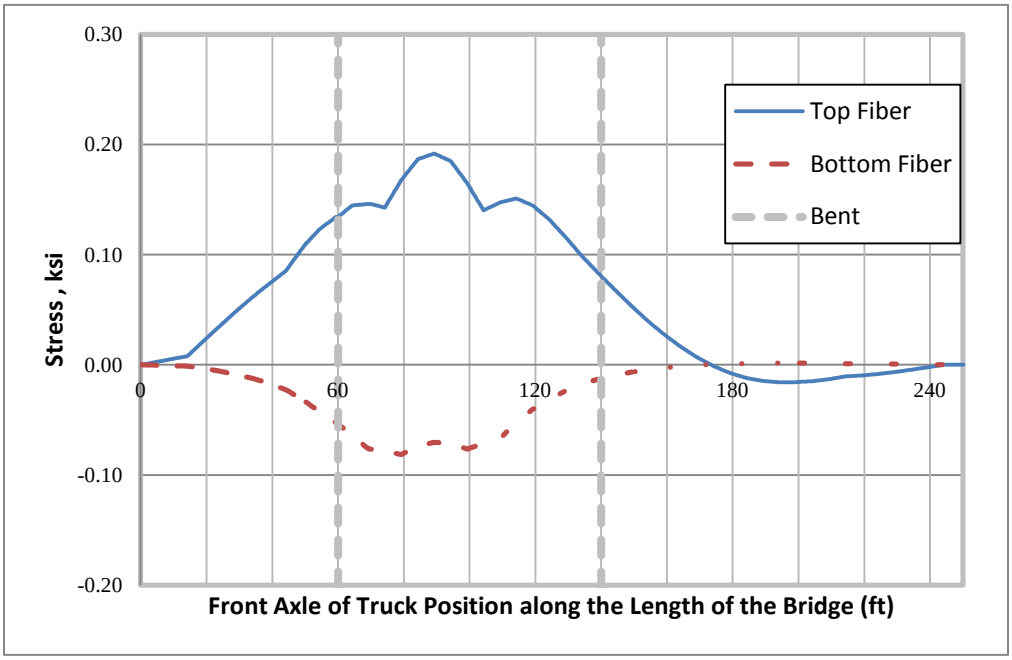

Figure 4.11: Longitudinal Plot of the Effects of TR-13 on CL-1 (60-80-60 Bridge)

The maximum tensile stresses found for each transverse truck position can be seen in Figure 4.12 and Table 4.3. As the trucks moved towards the outer eastern edge of the bridge, top

fiber tensile stresses increased. The general trend followed the same pattern as for the extreme positive-flexure stress case; truck positions centered directly over or within a foot of the girder created the highest interior deck stresses. Correspondingly, stresses were lowest at TR-0 and TR-8, as the trucks were centered over the midpoint between the girders, thus placing their tires near portions of the panel directly above the girders. The difference between this case and the positive-flexure stress scenario is that these transverse truck positions caused higher tensile stresses in the deck directly above the girder, as opposed to in between girders. This is because the deck is acting as a tension flange for composite girder bending at these locations. The negative-flexure stresses in the deck were critical at these above girder locations. Another difference in the extreme negative-flexure stress case was that the edge of the deck experienced the highest tensile stresses, with tensile stresses growing rapidly as the truck was moved to the exterior most position TR-18.

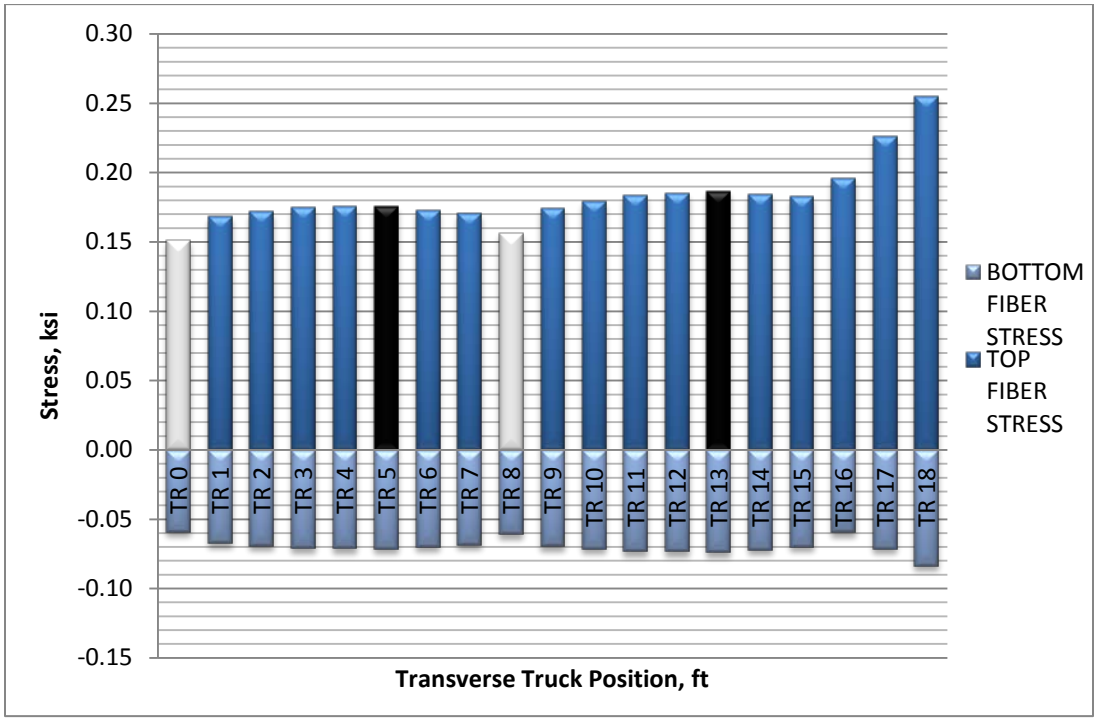

Figure 4.12: Maximum Stresses per Transverse Position due to Negative Flexure (60-80-60 Bridge)

Table 4.3: Stresses at CL-1 due to Negative-Flexure Truck Loading (60-80-60 Bridge)

Truck Transverse Position (ft)	Transverse Location of Critical Stress (ft)	Stress, Top Fiber (ksi)	Stress, Bottom Fiber (ksi)
TR 0	4	0.151	-0.059
TR 1	4	0.168	-0.067
TR 2	4	0.172	-0.069
TR 3	4	0.175	-0.071
TR 4	4	0.175	-0.071
TR 5	4	0.176	-0.071
TR 6	4	0.173	-0.070
TR 7	4	0.171	-0.068
TR 8	12	0.157	-0.061
TR 9	12	0.175	-0.069
TR 10	12	0.179	-0.071
TR 11	12	0.184	-0.073
TR 12	12	0.185	-0.073
TR 13	12	0.187	-0.074
TR 14	12	0.185	-0.072
TR 15	12	0.183	-0.070
TR 16	20	0.196	-0.059
TR 17	20	0.226	-0.071
TR 18	20	0.255	-0.084
Extreme Tensile-Stress Case:	**20**	**0.255**	**-0.084**

Overall these stresses are well below the 0.474 ksi modulus of rupture. Even when the AASHTO dynamic load allowance of 1.15 is included, a maximum fatigue stress of only 0.293 ksi occurs. As with the extreme positive-flexure stress scenario, multiple trucks were run at various spacings to determine the worst tensile stresses at CL-1 for service loading. Appropriate AASHTO multiple presence factors and dynamic load allowances were applied for service loading; Table 4.4 shows these results. Truck critical transverse loading positions were the same as in the positive-flexure stress case for both truck loading scenarios involving two or three trucks; however, the worst case scenario for a single truck occurred at TR-18, not TR-13. The

maximum tensile stress from these extreme negative-flexure stress cases was found to be 0.407 ksi due to truck loading TR-18, about 13 percent greater than the critical stress from the positive-flexure stress cases.

Table 4.4: Negative-Flexure Service Load Stresses at CL-1

Truck Transverse Position (ft)	Rear Axle Spacing (ft)	Multiple Presence Factor, m	Dynamic Load Allowance, IM	Transverse Location of Critical Stress (ft)	Stress, Top Fiber (including m & IM) (ksi)
TR 18	30	1.20	1.33	20	0.407
TR 18	14	1.20	1.33	20	0.402
TR 7 & 17	30	1.00	1.33	20	0.398
TR 7 & 17	14	1.00	1.33	20	0.389
TR (-1),7, & 17	30	0.85	1.33	20	0.338
TR (-1),7, & 17	14	0.85	1.33	20	0.331
Extreme Case:		TR-18 @ 30ft		20	0.407

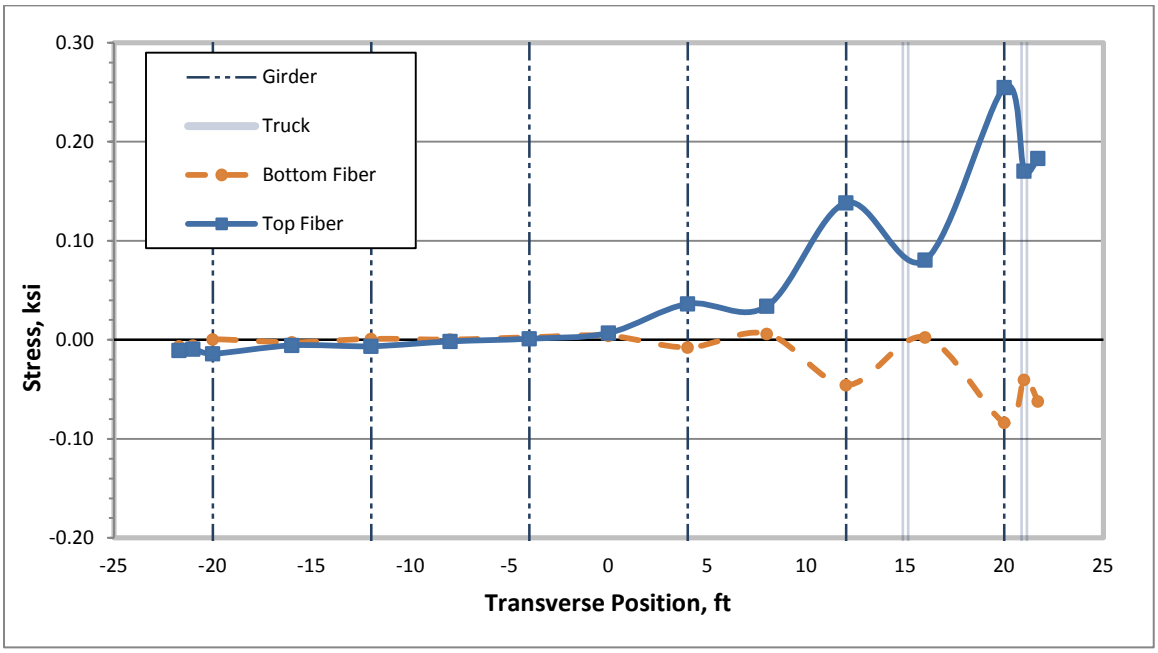

Figure 4.13: Deck Stresses due to TR-18 at Critical Location 1 (60-80-60 Bridge)

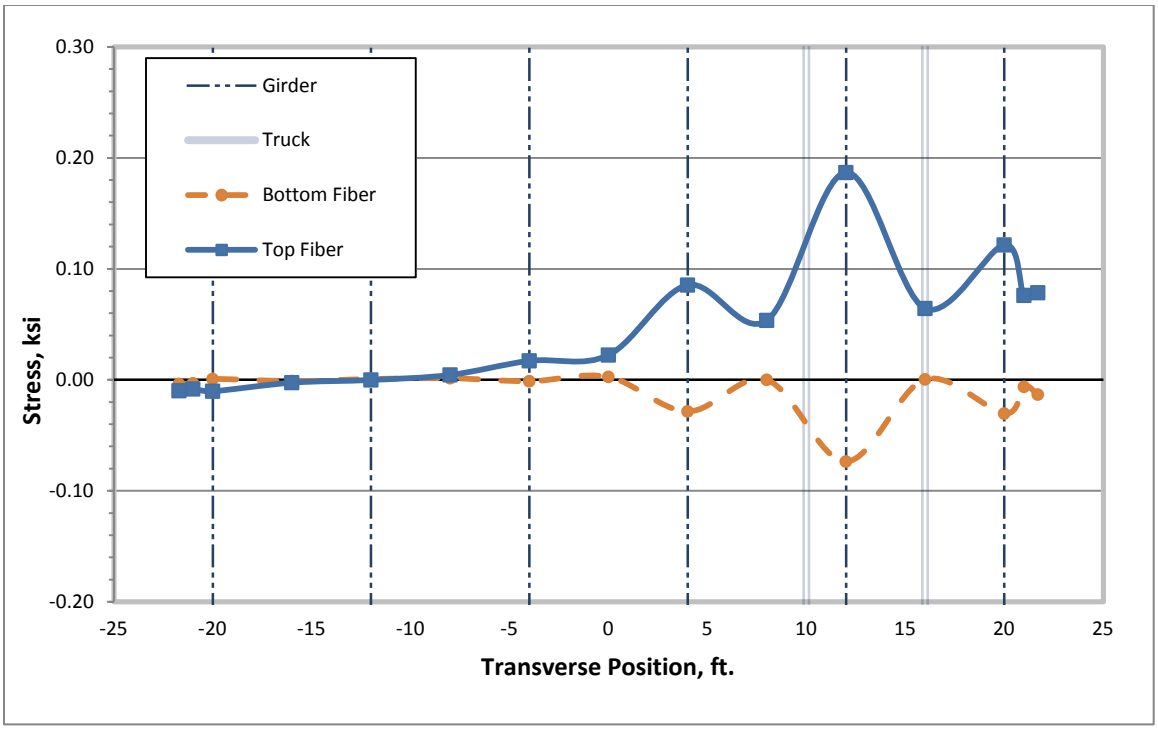

Figure 4.14: Deck Stresses due to TR-13 at Critical Location 1 (60-80-60 Bridge)

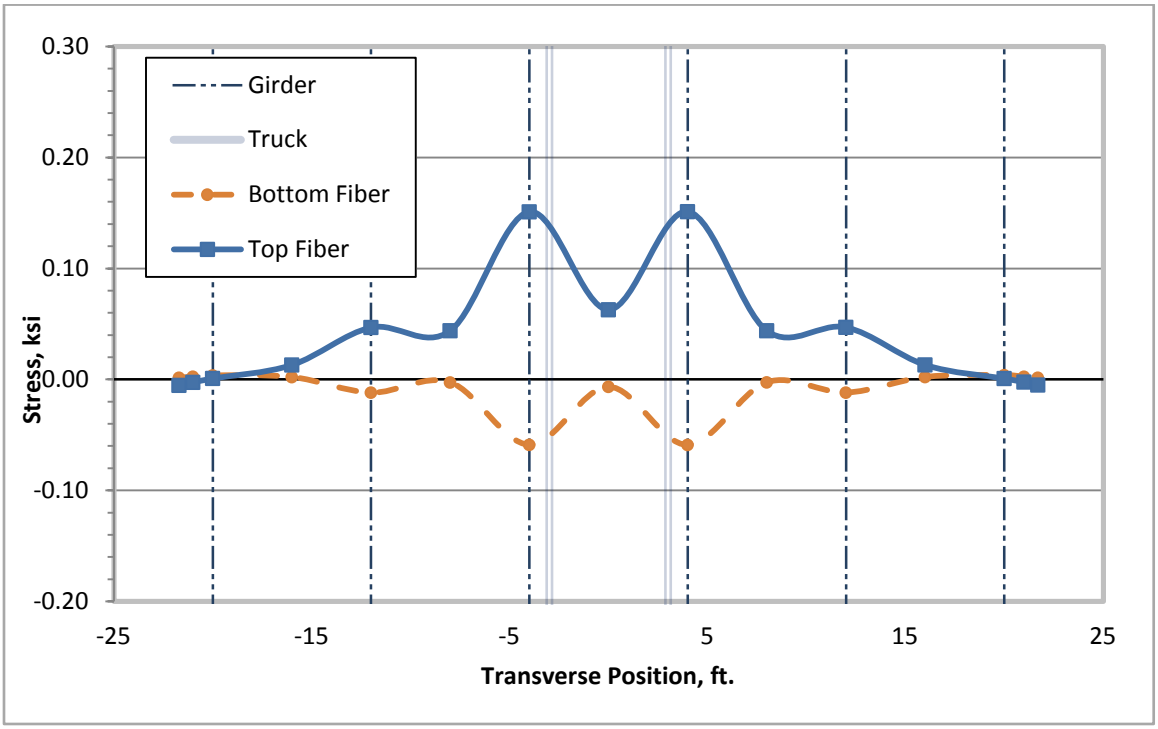

Figure 4.15: Deck Stresses due to TR-0 at Critical Location 1 (60-80-60 Bridge)

4.2.3 Shear Evaluation at CL-1 and CL-2

This section addresses the vertical shear forces that occur at the critical locations for both positive- and negative-flexure stresses. For the positive-flexural stress scenario, at CL-2, Figure 4.16 shows the stresses occurring just before (south of the cross section) and just after (north of the cross section) the transverse cross-section at CL-2. These stresses occur when a fatigue truck is loaded at the exact same longitudinal position that causes the extreme positive-flexure stress; this is not the extreme case for shear force. A longitudinal plot of the shear forces that occur at the critical deck transverse location, located at transverse position 16, can be seen in Figure 4.17. This graph represents the critical truck, TR-13, passing across the bridge, and shows the shear force effects that truck causes in the deck at transverse position 16, longitudinal position CL-2. The critical location of the front axle of the TR-13 is at position 79.25 ft, which is coincidentally a peak shear value, close to the maximum shear value. Figure 4.16 shows that the peak shear force per unit width is -0.634 kips/ft before and 0.728 kips/ft after CL-2. Having an 8 in. thick deck, these unit shear forces cause average shear stresses over the uncracked deck cross section of approximately 7–8 psi. Using ACI 318-08 Section 22.5.4, this shear force can be related to the nominal shear strength of the concrete. Shown below, Equation 4.1 can be used to determine this relationship. By applying the appropriate 0.55 strength reduction factor, using an 8 in. thick deck, 1 ft unit width, and a concrete strength of 4000 psi, the nominal shear strength can be found to be approximately 4.45 kips/ft. The 0.728 kips/ft shear force per unit width is thus approximately 15 percent of the design shear strength of monolithic unreinforced concrete. Thus, the shear stresses do not appear to be critical relative to the flexural stresses. These shear stresses are relatively small because the composite deck transfers the majority of the truck-induced vertical forces directly into the supporting girders, rather than through shearing of the joints.

$$\emptyset V_n = \emptyset \frac{4}{3} \sqrt{f'c} \cdot bh \quad \text{(Eq. 4.1)}$$

For the extreme negative-flexure stress cases, transverse deck position 12 was chosen over TP-20, despite TP-20 having the highest stresses due to worst-case fatigue loading. Deck position TP-12 was chosen as it did have a localized critical fatigue stresses, and therefore TP-12 was deemed a representative joint location for this shear analysis. The critical negative-flexural stress location in the deck was at TP-12. This critical flexural stress occurred as a truck was positioned at transverse truck position 13 and longitudinally located 89 ft 3 in. north of the first, southern abutment. As can be seen in the longitudinal plot of shear (Figure 4.19), a maximum shear does not occur at this point. When taking a look at the cross section at CL-1 (Figure 4.18), the shear can be seen to be somewhat less than the shears from the positive-flexural stress case. This is most likely due to the girders being located directly below transverse deck position 12. Figure 4.18 shows that the shear force per unit width occurring at TR-12 are 0.439 and -.479 kips/ft before and after the joint, respectively.

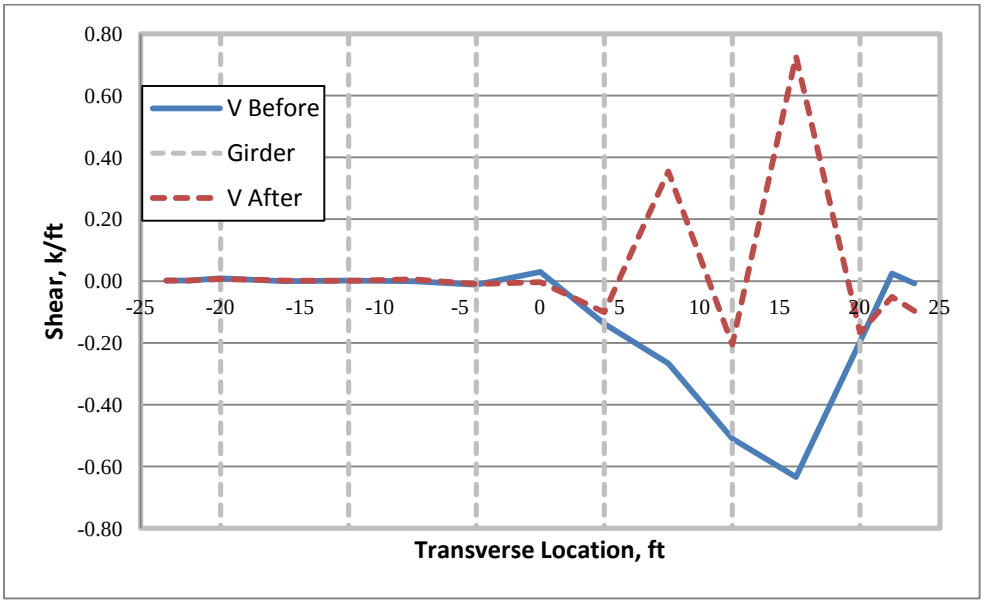

Figure 4.16: Shear experienced at Transverse Cross-Section CL-2 (60-80-60 Bridge)

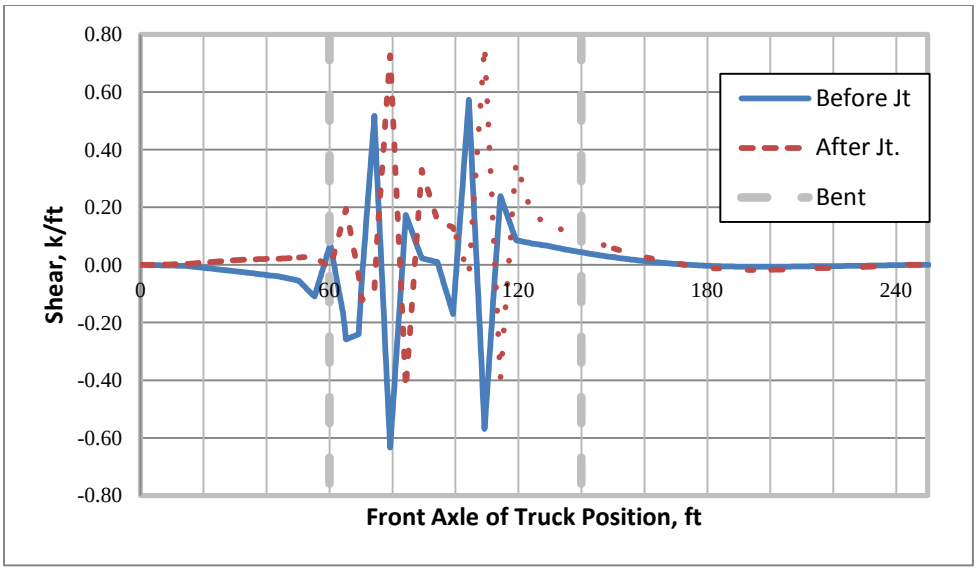

Figure 4.17: Longitudinal Plot of Shear Experienced at Transverse Position 16 as TR-13 passes (CL-2)

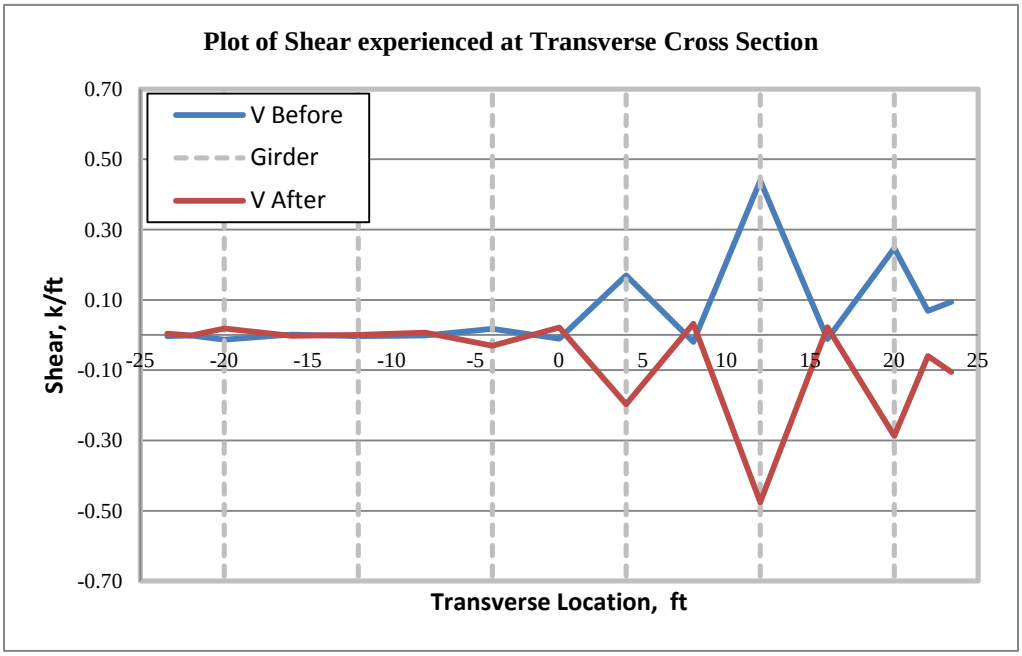

Figure 4.18: Shear experienced at Transverse Cross-Section CL-1 (60-80-60 Bridge)

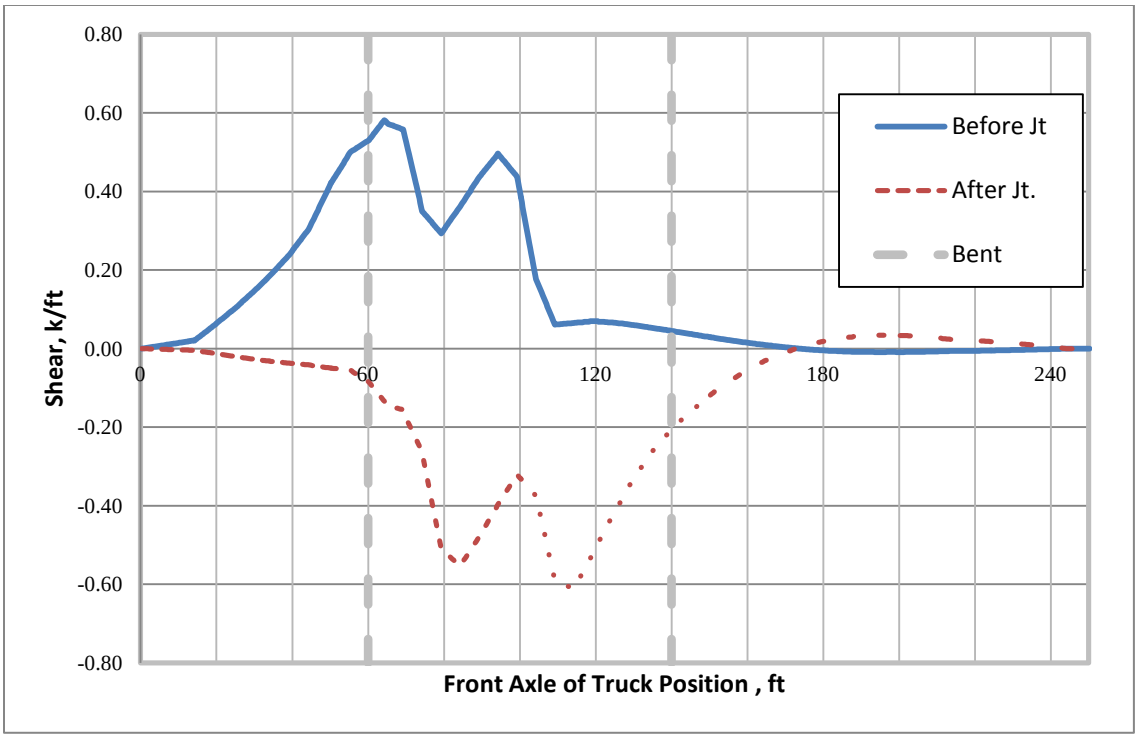

Figure 4.19: Longitudinal Plot of Shear Experienced at Transverse Position 12 as TR-13 passes (CL-1)

The significance of this shear behavior is best shown through combining a longitudinal plot of unit shear force with a longitudinal plot of bending moment. Through this combination, the forces that the deck experiences at positions CL-1 and CL-2 during each truck passage can be better understood. By juxtaposing the negative moment and shear at position CL-1, Figure 4.20 shows a crude interpretation of the shear and moment cycle that this transverse cross section experiences with every truck passage. The bending moment increases parabolically to a peak, while the shear increases somewhat linearly, and, at the peak bending moment, the shear reverses and then decreases while the moment reduces to zero. For the positive moment loading at CL-2, Figure 4.21 shows a much different relation between shear and moment, which shows sharp loading and unloading of both forces effects.

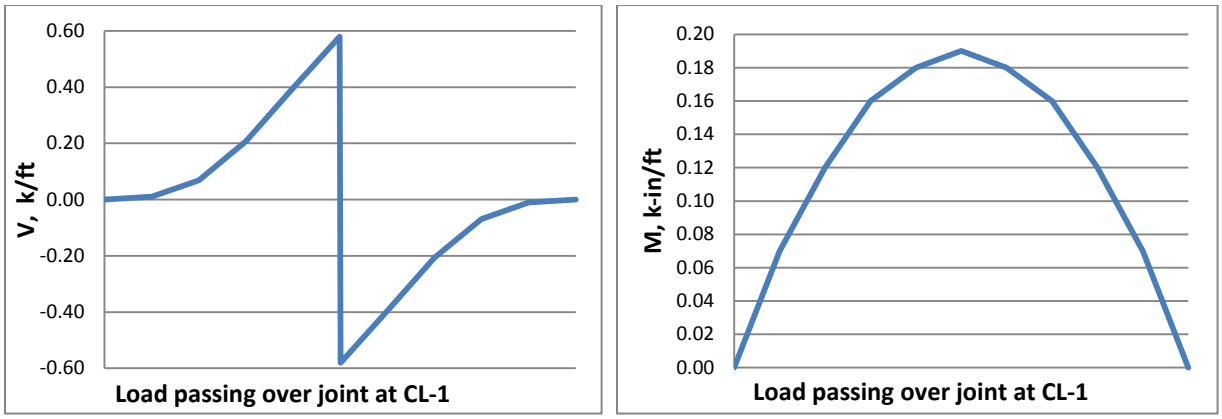

(a) Shear (b) Moment

Figure 4.20: Moment and Shear Diagrams for CL-1

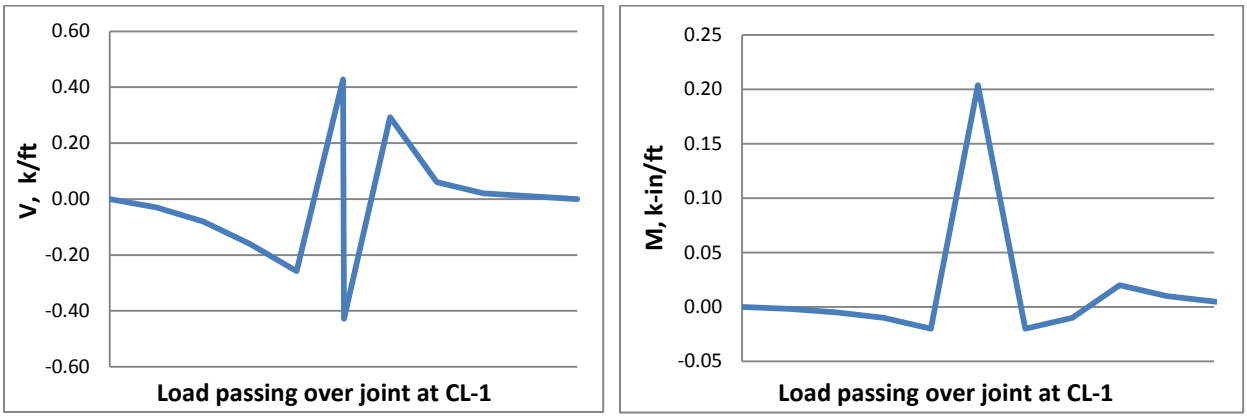

(a) Shear (b) Moment

Figure 4.21: Moment and Shear Diagrams for CL-2

4.3 Results from 80-100-80 ft ALDOT Continuous Span Bridge

As with the 60-80-60 continuous span bridge, the 80-100-80 has multiple extreme loading scenarios. These data coincide with the 60-80-60 bridge's data and give a perspective as to the effect of span length on the deck stresses. The results from the positive bending extreme case scenario will be discussed first, followed by the negative bending extreme loading results.

4.3.1 Extreme Positive-Flexure Stress Case

Using the same analysis process from the 60-80-60 bridge, fatigue trucks were run from positions TR-0 through TR-18. The critical location for positive-flexure stress occurred 5 feet past the bent and will be referred to as CL-2. For all transverse truck positions, the extreme positive-flexure stress occurred when the front 8 kip axle of the truck was positioned 19 ft 3 in. past the first bent with the trailing 32 kip axles located 5 ft 3 in. past the bent and 24 ft 9 in. before the bent. When referenced from the first bent, this truck location is identical to the truck locations for the 60-80-60 bridge.

From this positive-flexure loading, Figure 4.22 and Table 4.5 summarize the values generated by the SAP2000 model. This graph represents the highest possible stresses in the deck for each transverse truck position at the critical longitudinal location. These stresses behave nearly the same as the 60-80-60 bridge except that the critical stress point in the deck is at position 8 for truck loading at TR-3, instead of at position 0, as seen underlined in Table 4.5. In general truck locations loading the center of a deck between girders cause the highest stresses, and overall the stresses from this case are only slightly less than the 60-80-60 bridge, most likely attributed to the larger girders used in this 80-100-80 bridge. A transverse plot of the truck loading at TR-13 is also shown in Figure 4.23 to further illustrate the related behavior between the two continuous span bridges.

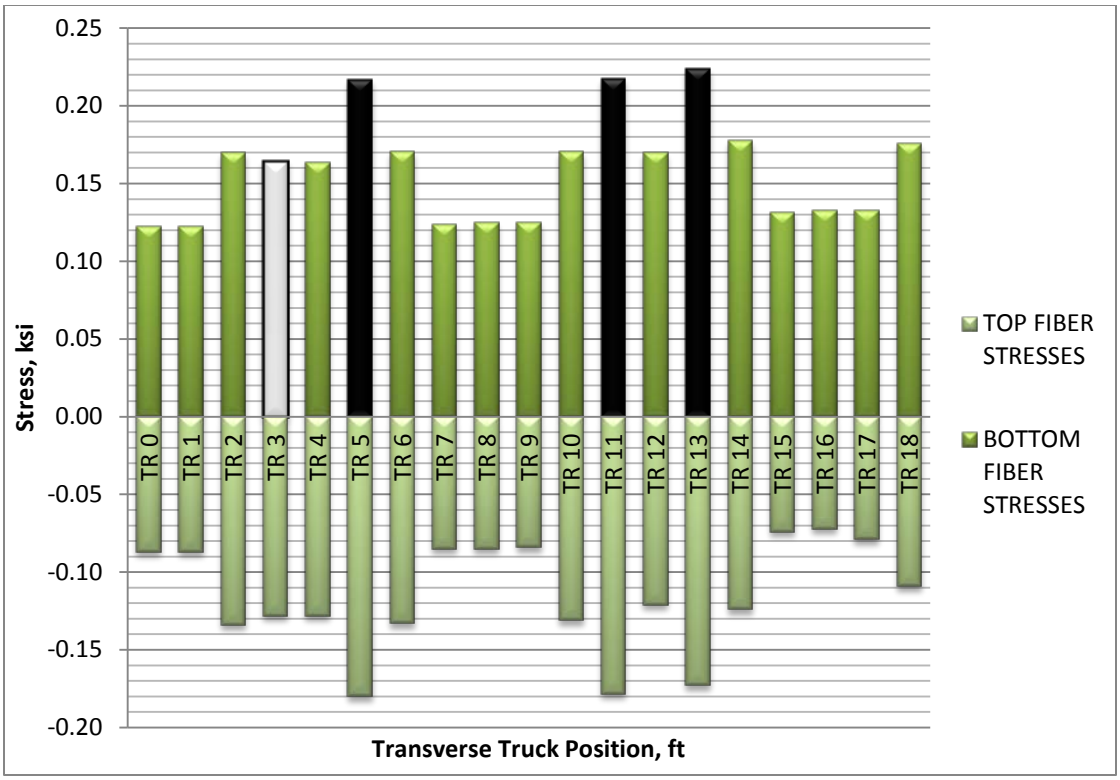

Figure 4.22: Maximum Stresses per Transverse Position due to Positive Flexure (80-100-80 Bridge)

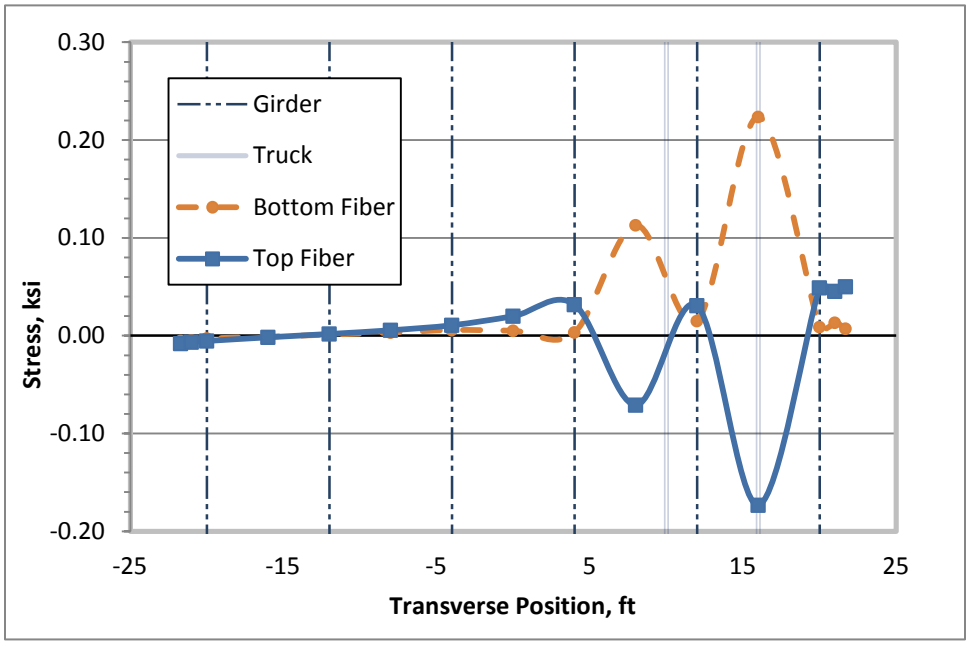

Figure 4.23: Deck Stresses due to TR-13 at Critical Location 2 (80-100-80 Bridge)

Table 4.5: Stresses at CL-2 due to Positive-Flexure Truck Loading (80-100-80 Bridge)

Truck Transverse Position (ft)	Transverse Location of Critical Stress (ft)	Stress, Bottom Fiber (ksi)	Stress, Top Fiber (ksi)
TR 0	0	0.123	-0.087
TR 1	0	0.123	-0.087
TR 2	0	0.170	-0.134
TR 3	8	0.164	-0.128
TR 4	8	0.164	-0.128
TR 5	8	0.217	-0.180
TR 6	8	0.171	-0.133
TR 7	8	0.124	-0.085
TR 8	8	0.125	-0.085
TR 9	8	0.125	-0.084
TR 10	8	0.171	-0.131
TR 11	8	0.218	-0.178
TR 12	16	0.170	-0.121
TR 13	16	0.224	-0.173
TR 14	16	0.178	-0.124
TR 15	16	0.132	-0.074
TR 16	16	0.133	-0.072
TR 17	16	0.133	-0.079
TR 18	16	0.176	-0.109
Extreme Tensile-Stress Case:	**16**	**0.224**	**-0.173**

4.3.2 Extreme Negative-Flexure Stress Case

The extreme negative-flexure stress case had consistent behavior with the data from the 60-80-60 bridge. The controlling negative-flexure stress truck placement occurred when the front 8 kip axle of the truck was positioned 29 ft 3 in. past the first bent with the trailing 32 kip axles located 15 ft 3 in. past the bent and 14 ft 9 in. before the bent. This truck location caused critical

effects at the first bent, CL-1. Figure 4.24 and Table 4.6 summarizes the values generated by the SAP2000 model.

Behavior coincided with that of the 60-80-60 bridge, as truck locations that loaded the center between girders causing higher deck stresses. Additionally, as the truck moved towards the eastern edge, stress values increased greatly. The maximum stress 0.223 ksi was well below the modulus of rupture, 0.474 ksi. As with the positive-flexure stress case, negative-flexure stresses were also slightly less than the 60-80-60 bridge. Shear effects were the same magnitude as the for the positive-flexure stress case; however less shear force occurred in the critical negative-flexure stress joint as this joint is located above the bent and directly on top of a girder. Transverse plots of each truck position for both positive- and negative-flexural stress can be seen in Appendix B.

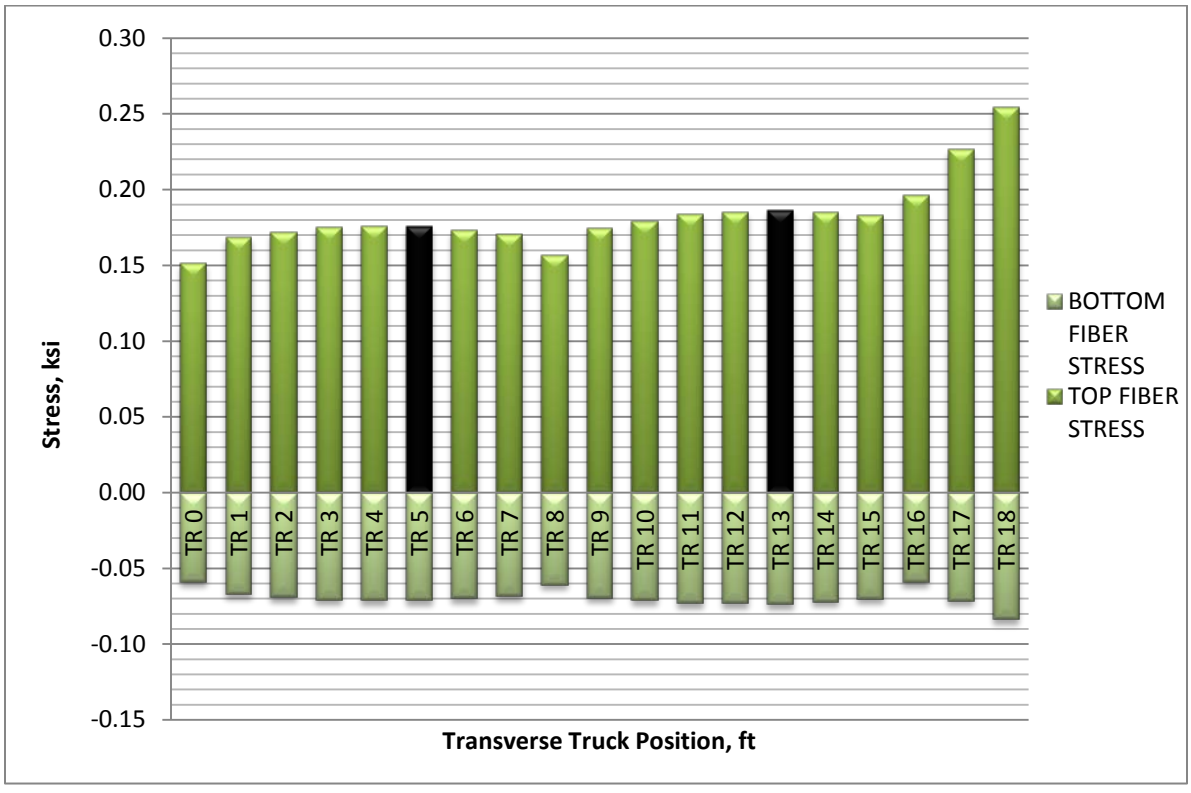

Figure 4.24: Maximum Stresses per Transverse Position due to Negative Flexure (80-100-80 Bridge)

Table 4.6: Stresses at CL-1 due to Negative-Flexure Truck Loading (80-100-80 Bridge)

Truck Transverse Position	Transverse Location of Critical Stress	Stress, Top Fiber	Stress, Bottom Fiber
(ft)	(ft)	(ksi)	(ksi)
TR 0	4	0.132	-0.037
TR 1	4	0.147	-0.043
TR 2	4	0.150	-0.044
TR 3	4	0.154	-0.045
TR 4	4	0.154	-0.045
TR 5	4	0.154	-0.045
TR 6	4	0.152	-0.045
TR 7	4	0.150	-0.044
TR 8	12	0.139	-0.038
TR 9	12	0.155	-0.044
TR 10	12	0.159	-0.045
TR 11	12	0.164	-0.046
TR 12	12	0.165	-0.046
TR 13	12	0.166	-0.045
TR 14	12	0.164	-0.044
TR 15	12	0.147	-0.027
TR 16	20	0.173	-0.030
TR 17	20	0.199	-0.037
TR 18	20	0.223	-0.045
Extreme Tensile-Stress Case:	**20**	**0.223**	**-0.045**

4.4 Results from Collinsville Bridge (Simple Span)

The simple span bridge has only one extreme loading scenario for positive-flexure stresses. This data coincides with the continuously supported bridges' positive-flexure stress behavior data and demonstrates the behavior expected to occur in the Collinsville Bridge.

4.4.1 Extreme Positive-Flexure Stress Case

Fatigue trucks were run across the structure in all transverse positions, causing a critical location for stress at the midspan of the bridge, CL-1. For all transverse truck positions, the extreme positive-flexure stress occurred when the front 8 kip axle of the truck was positioned 43 ft north of the abutment with the trailing 32 kip axles located 29 ft past the bent and before the abutment. Essentially, this location loads the midspan of the bridge with a 32 kip axle. Figure 4.25 shows the bridge's dimensions and critical truck placement.

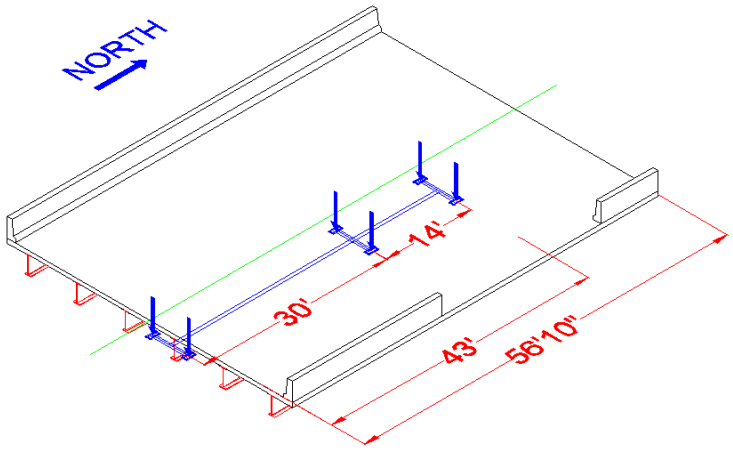

Figure 4.25: Simple Span Bridge Critical Truck Location

Figure 4.26 and Table 4.7 show the critical values from the step-by-step analysis. For the most part, the tensile stresses can be seen to be significantly less than the tensile stresses from the two continuously supported bridges, however the critical stress of 0.209 ksi is still close to the maximum tensile value of 0.226 ksi, from the 60-80-60 bridge. Additionally, the compressive top fiber stresses ranged from 40 to 65 percent greater than those from the continuously supported bridges; however these compressive stresses are well under the service-load compressive capacity of the concrete, and are most likely higher as the critical tensile location

for the Collinsville Bridge coincides with the critical compressive location. The critical truck location is located at TR-3, which is somewhat consistent with other data, as this position loads the center between two girders at position 0. Additionally, since the span of this bridge is only 56 ft 10 in., trucks with 14' rear axle spacing were run to determine the amount of stress increase expected. The results showed a negligible increase of less than 1 percent in most cases. It should also be noted that when this bridge is loaded on the eastern edge, a small tensile force is created on the other edge in the bottom and top fibers (Figures 4.27 and 4.28). This tensile stress is well below the modulus of rupture, but could pose durability issues in a joint. Furthermore, joint shear forces were of the same magnitude as for the positive-flexure stress case of the continuous span bridges, and well within limits.

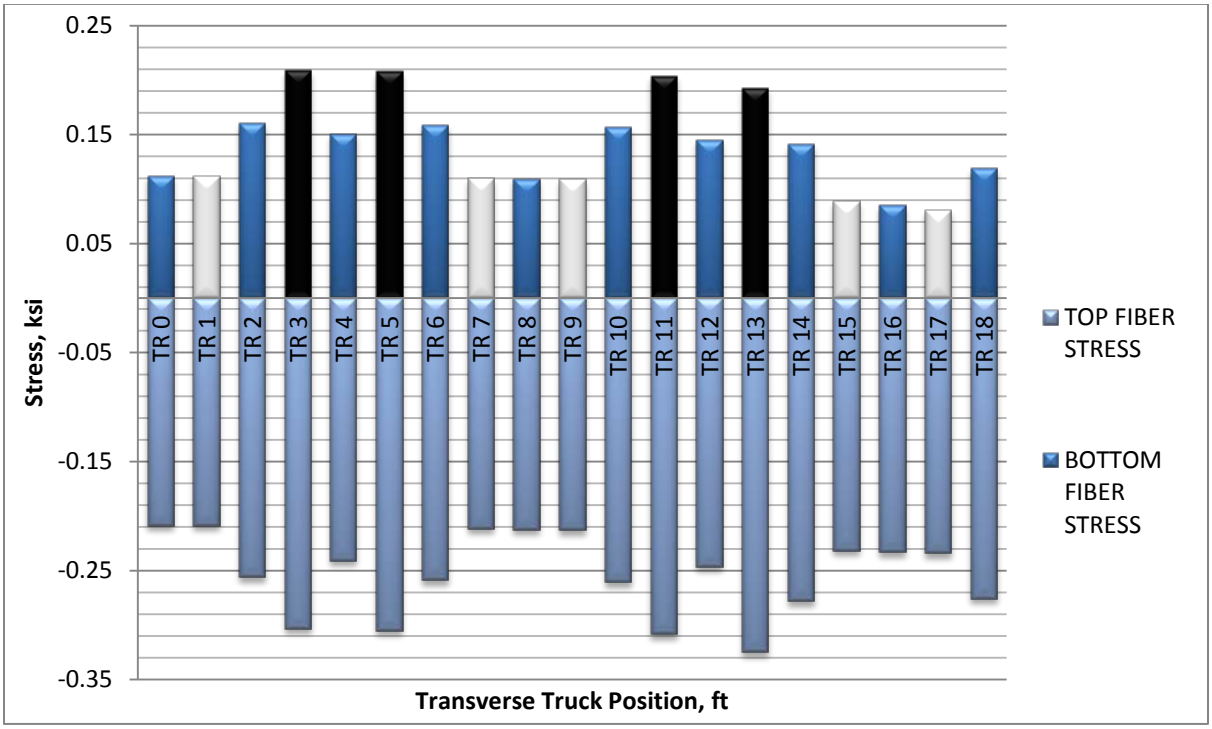

Figure 4.26: Maximum Stresses per Transverse Position due to Positive Flexure (Simple Span Bridge)

Table 4.7: Stresses at CL-1 due to Positive-Flexure Truck Loading (Simple Span Bridge)

Truck Transverse Position (ft)	Transverse Location of Critical Stress (ft)	Stress, Bottom Fiber (ksi)	Stress, Top Fiber (ksi)
TR 0	0	0.112	-0.209
TR 1	0	0.112	-0.209
TR 2	0	0.161	-0.256
TR 3	0	0.209	-0.303
TR 4	0	0.151	-0.241
TR 5	8	0.208	-0.305
TR 6	8	0.159	-0.259
TR 7	8	0.110	-0.212
TR 8	8	0.110	-0.212
TR 9	8	0.109	-0.213
TR 10	8	0.157	-0.261
TR 11	8	0.204	-0.308
TR 12	8	0.145	-0.247
TR 13	16	0.193	-0.325
TR 14	16	0.141	-0.278
TR 15	16	0.089	-0.232
TR 16	16	0.085	-0.233
TR 17	16	0.081	-0.234
TR 18	16	0.119	-0.276
Extreme Tensile-Stress Case:	**0**	**0.209**	**-0.303**

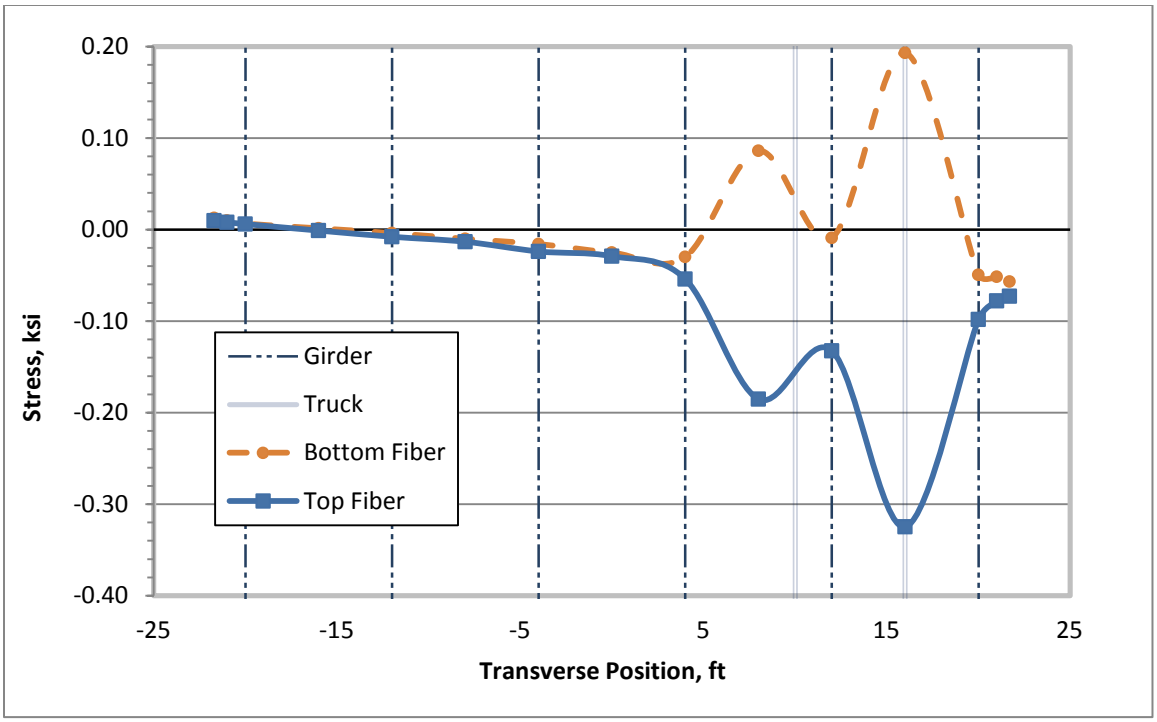

Figure 4.27: Deck Stresses due to TR-13 at Critical Location 1 (Simple Span Bridge)

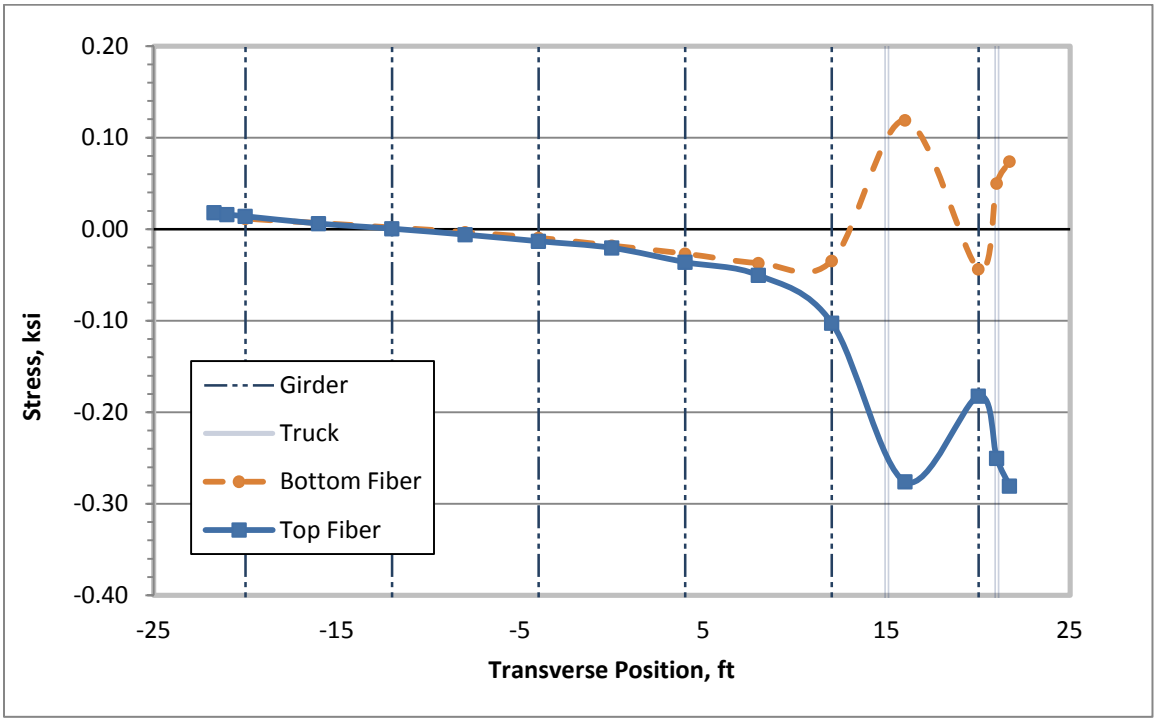

Figure 4.28: Deck Stresses due to TR-18 at Critical Location 1 (Simple Span Bridge)

4.5 Summary and Conclusions

The modeling of the two continuously supported bridges and the simply supported bridge gives better understanding of the behavior of bridge decks under truck loading. Through this modeling process several conclusions can be made as to the design and testing of transverse shear keys.

For all bridges

1. Loading of the deck on the transverse center between girder lines generally produces the largest tensile flexural stresses across transverse joints. These tensile stresses occur in the deck at that center point between girders if experiencing positive flexure. Under a negative flexure, the larger deck tensile stresses occur in the deck directly above the girder that is straddled by the truck. Without relation to the positive-flexure regions, negative-flexure regions experienced the largest tensile stresses as truck loadings were moved towards the edge of the bridge deck.
2. The loading causing the smallest flexural tensile and shear stresses for both positive and negative flexure occurred when a wheel loaded the deck exactly over a girder.
3. Trucks with the longest (30 ft) rear axle spacing caused the largest stresses in the deck. The simply supported bridge was an exception; it had nearly identical results from loading with the longest and shortest axle spacings.
4. There was little difference in both behavior and stresses in the two continuous span bridges. Based on the correlation between girder sizes and span, stresses from truck loads do not seem to increase dramatically as span changes, assuming girder design is adequate for the spans considered.

5. As the factored tensile stresses for both positive and negative flexure ranged from 0.293 to 0.260 ksi, it is recommended that any transverse joint be able to handle repeated loadings that induce a bending stress of at least 0.300 ksi (when computed on the basis of uncracked-section analysis).
6. In fatigue testing either of the positive- or negative-flexure scenarios, consideration should be given to the relation between the moment and shear that the deck section experiences under each truck passage. For the bottom fiber, a typical ratio for shear stress to flexural stress is 1:7. The top fiber has a ratio of 1:11 for shear stress to flexural stress.

CHAPTER 5: TRANSVERSE JOINT INVESTIGATION

5.1 Transverse Joint Selection

Based on previous research and performance of transverse joints, three transverse joint systems meet the criteria set by ALDOT for the Collinsville simply supported bridge. The NCHRP Project 584, female-to-female shear key, and reinforced looped-bar joints all have sufficient testing or in-field history to suggest that they could provide a durable and lasting connection for this rapid bridge deck replacement. However, when a joint experiences negative flexure, these options become even more limited. Testing conducted by Virginia Polytechnic Institute showed poor performance of the NCHRP reinforced joint design, with large deformations and cracking (Swenty 2009). Additionally, several tests have shown that without longitudinal post-tensioning, a female-to-female shear key cannot handle negative flexure (Issa et al. 2007; Swenty 2009). There are tests supporting the use of reinforced looped-bar joints for negative flexure, as well as several newer bridges showing adequate performance of this type of joint, at least for the early life of the bridge (Au et al. 2008; Swenty 2009).

When developing these tests it was important to consider that the goal was to test numerous types of joints. Testing which were relatively simple and cost-effective were needed, as the proposal includes testing three types of joints (NCHRP – 584, looped bar, and female-to-female) under six scenarios (positive and negative bending, shear reversal; with fatigue and monotonic-until-failure testing for all three). Additionally, a proposal to test each joint in both exodermic and full-depth precast concrete panels is included thus bringing the total number of panels to be constructed and tested to 38 panels. Simplistic testing that still provided representative data was a must.

This testing will illustrate the comparative behavior between different joints in different types of deck panels. Tests were devised to rigorously address the effects of bending and shear action. However, the stresses experienced in the joint are not completely representative of actual stresses experienced by the joints in a bridge; only primary one-way action is addressed. The stresses are a 2-dimensional representation used to simply the 3-dimensional effects that the joint might experience, and these 2-dimensional stresses are meant to provide a practical, cost-effective assessment of fatigue effects. A primary objective is to provide comparative results that can be used to evaluate each joint and panel's performance when compared to one another.

5.2 Testing

5.2.1 Introduction

In order to fully assess the available transverse joint options, testing should be conducted to evaluate the performance of each joint under expected conditions. As previous research has indicated, the primary cause of failures in these connection types is caused by fatigue from repeated load cycles (Issa et al. 1995a). Fatigue loading produces heavy cracking in the joints, which leads to infiltration and the degradation of the riding surface. For this reason, fatigue assessment should be a primary concern, followed by the joint's performance under critical static loading. Because the deck panels are typically designed for one-way flexure spanning between the girders, strength limit state loading is not critical unless the reinforcement (if any) crossing the transverse joints is used for the composite girder/slab negative-moment flexural capacity.

For these reasons, several tests were devised to assess a transverse joint's response to the critical stresses determined from the analysis reported in Chapter 4. Two flexural tests, one for positive bending and another for negative bending, are proposed to assess the joint's behavior under repeated shear and flexural loading cycles. Additionally, a third shear reversal test is

recommended to evaluate how the cyclic reversal of shear loading from passage of truck axle loads across the transverse joint affects a type of joint over numerous loadings.

Firstly, these tests are to be conducted with fatigue-level loadings; cyclic loading that replicate expected in-field conditions to assess the degradation resistance of the transverse joints. Additionally, monotonic tests to failure are proposed to determine the total strength of these joints in respect to expected loadings. This loading is done to establish whether there is a correlation between the static ultimate strength of a joint and its fatigue degradation resistance. The ultimate goal of this testing is to determine the most practical type of testing that should be performed to prequalify a type of transverse joint for use in rapid bridge construction. A summary of the critical loads, locations, stresses, and shear forces resulting from the analyses described in Chapter 4 can be seen in Table 5.1. As the critical stresses occurred in the 60-80-60 ft continuous bridge model, these values correspond to what that model experienced. Positive Bending stresses occurred due to positive flexure (M+) and shear, while M- represents negative-flexure stresses due negative moment and shear.

Table 5.1: Critical Stresses at Worst-Case Joint Locations for 60-80-60 ft Bridge

	Joint Location		Truck Position		Stress (ksi)		Shear (k/ft)	
Critical Stress	Longitudinal	Transverse	Transverse	Longitudinal (Front Axle)	Top Fiber	Bottom Fiber	Shear	Reversal
M+	Near Bent	TP-16 (Between GRDR)	TR-13	79.25'	-0.184	0.226	0.728	Yes (-0.425)
M-	At Bent	TP-12 (Over GRDR)	TR-13	91.5'	0.187	-0.074	-0.442	No
	At Bent	TP-20 (Over GRDR)	TR-18	91.5'	0.256	-0.084	-0.452	No

5.2.2 Positive Bending Test

In order to accurately account for the critical one-way stresses from bending, a positive bending test must reproduce the flexural stresses and shear that the joint experiences as a HS-20 truck passes over the critical location for a bridge. For this reason, it is suggested to test precast panel decks without girder support, as replicating the necessary shear and moment produced stresses within the joint would be difficult without a full-scale bridge model. By applying the load as shown in Figure 5.1, the joint experiences the appropriate flexural tensile stress and corresponding shear stress. However, due to the symmetry of the section, the elastic neutral axis will cause the critical bottom fiber tensile stresses to be the same magnitude as the top fiber compressive stresses. This does not replicate the computer analysis results seen in Table 5.1, but as transverse joints have shown large capacity and excellent behavior under compression (Issa et al. 1995), this inconsistency is acceptable.

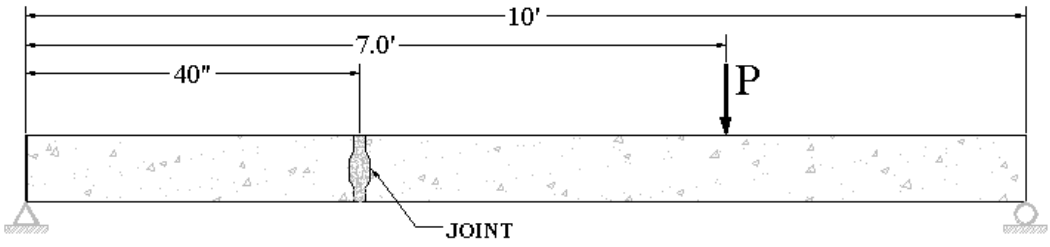

Figure 5.1: Positive Bending Test Setup

As seen in Figure 5.1, the joint is positioned at a 40 in. offset. This offset creates the appropriate ratio of shear and moment in the joint as the load is applied at position P. For testing purposes the 60-80-60 continuous bridge case was selected, as its deck experienced the highest stresses out of the three bridges modeled. However, as there is expected to be variance in these stresses due to different girder size to span ratios, it is proposed to conservatively increase the

critical tensile stress from 226 psi to 300 psi. Shear and flexural stresses from moment were then calculated and increased to be proportionally sized from 226 psi to the prescribed 300 psi, and the loading matrix given in Table 5.2 was created for various test panel joint widths.

Table 5.2: Positive Bending Loading Matrix

Panel Width (in.)	Total Peak Load, P (kips)	P per Panel Width (kips/ft)	Unit Joint Effects		
			Moment (kip-in/ft)	Shear (kips/ft)	Stress (ksi)
24	6.4				
48	12.8	3.2	38.4	0.960	0.300
96	25.6				

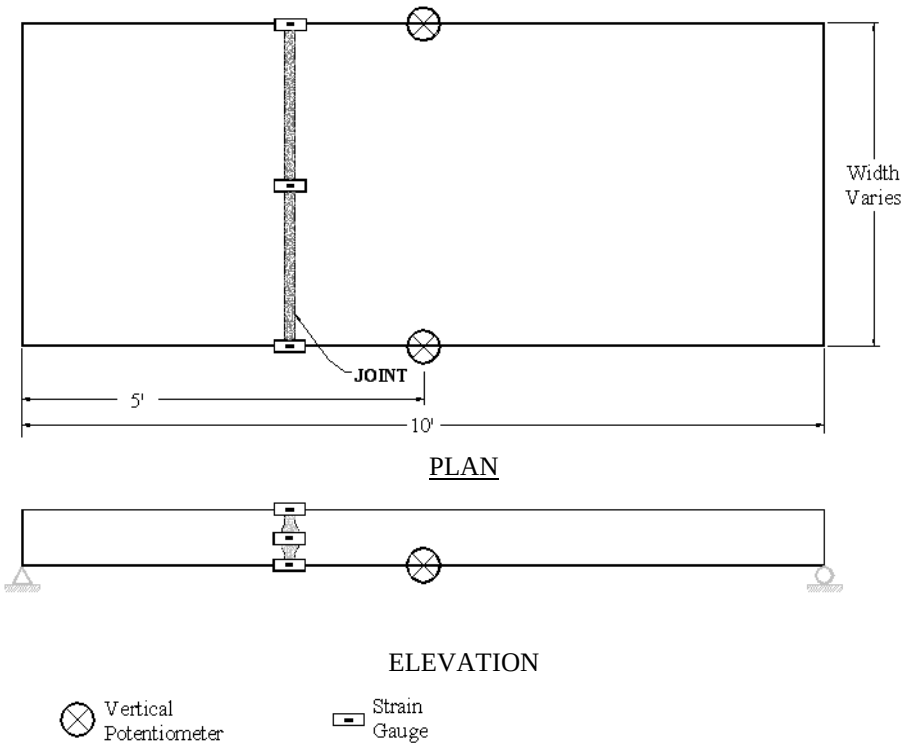

Figure 5.2: Strain Gauge Setup

Based on previous studies, fatigue testing for positive bending should be conducted for 2-million cycles. Though shear reversal is experienced by the actual joint, focus will be only on increasing the loading at point P from near 0 kips to a loading that gives 3.2 kips per foot of the joint specimen width. Shear reversal effects will be evaluated in the shear test. It is proposed to maintain a minimum load of 250 lbs per foot to ensure the stability of the testing setup. Loading from this minimum load to 3.2 kips/ft and back to the minimum load should be considered one complete cycle. At appropriate intervals the joint and the deck should be statically loaded to the 3.2 kips/ft and inspected for cracking; detailed notes and observations should be made. Additionally, water ponding tests are proposed at certain loading cycles to assess each joint's leakage and subsequent acceptability to infiltration. Water ponding generally consists of applying a 1.0 in. column of water over the joint for an hour to analyze leakage. Good joint behavior is considered little cracking, no visible water leakage, and a linear strain distribution through the depth of the joint (Swenty 2009). A proposed testing schedule is shown below in Table 5.3. Additionally, Figure 5.2 shows proposed strain gauge setup for the joint system. Again, during the analysis of this and the other tests, focus should be aimed at the comparative behavior of the joints.

Table 5.3: Testing Schedule

Loading Cycles	Ponding Test	Static Load Test/Inspection
0	x	x
1	x	x
1,000		x
5,000		x
10,000	x	x
20,000		x
30,000		x
40,000		x
50,000	x	x
100,000	x	x
200,000		x
300,000		x
400,000		x
500,000	x	x
600,000		x
700,000		x
800,000		x
900,000		x
1,000,000	x	x
1,250,000		x
1,500,000		x
1,750,000		x
2,000,000	x	x

Assuming the joint behaves adequately, upon the completion of the 2-million cycles it is proposed to test the panels monotonically to failure. The panel should be loaded at point P until the specimen refuses to resist additional load. Strains and crack widths, deflection values and other observations should be recorded at appropriate intervals as the loading increases in order to fully assess the joint's bending capacity. Furthermore, another specimen can be tested monotonically to failure without prior cyclic loading. These results can be compared to determine the 2-million fatigue cycle loads effect on the ultimate strength of the system.

Information may also be gained about whether short-term monotonic tests offer useful information about long-term, cyclic performance.

5.2.3 Negative Bending Test

The negative bending test was designed utilizing the same principles with which the positive bending test was designed. The critical tensile stresses from the 60-80-60 continuous bridge were used to determine loading, but the critical tensile stress was also conservatively increased to 300 psi from the analytically determined worst-case stress of 256 psi. Additionally, as these stresses occur over the bent (Table 5.1), the shear forces experience no reversal as the truck passed over the bridge; therefore this test accurately reproduces expected critical conditions. Figures 5.3 and 5.4 show the truck-induced shear forces and bending stresses experienced at transverse position 12 over the bent. Figure 5.5 shows the proposed loading and support configuration. By applying the load as shown, the joint experiences the appropriate ratio of moment-induced tensile stress to shear stress; however it may be an easier setup to turn the specimen and loading setup upside down. As with the positive bending test, compressive stresses are larger than indicated from the analysis, but testing tensile capacity remains the primary concern of these investigations.

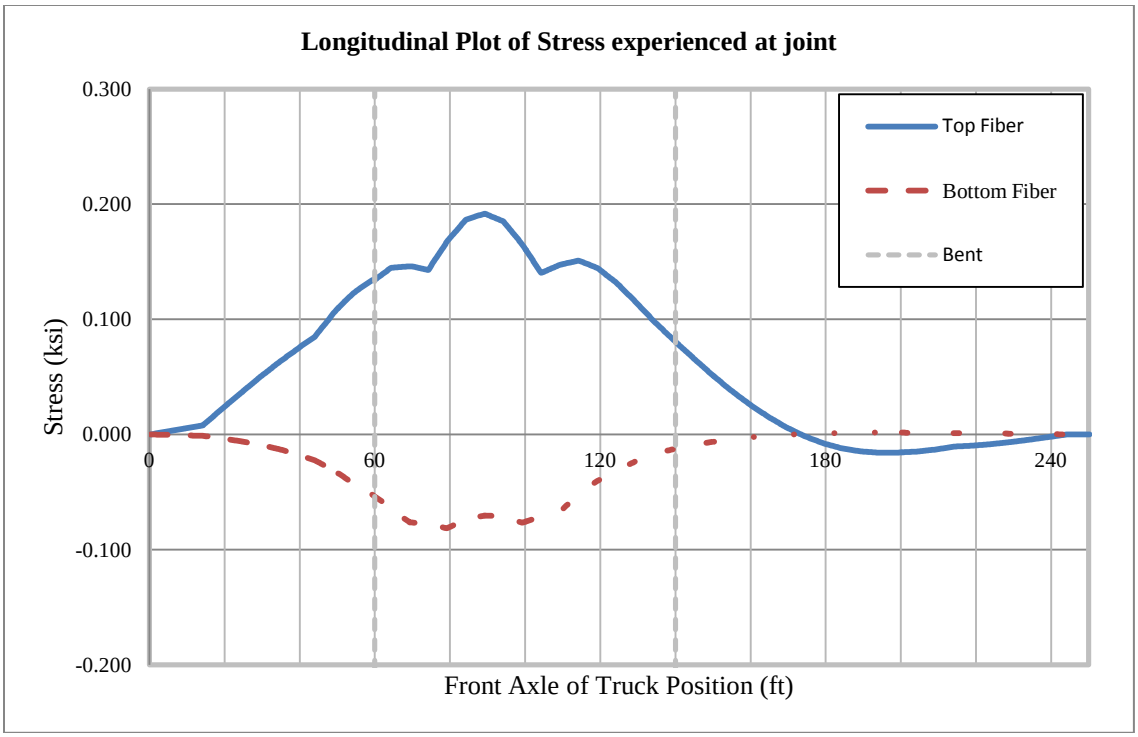

Figure 5.3: Stresses Experienced in Critical Joint as Truck Passes Over Bridge

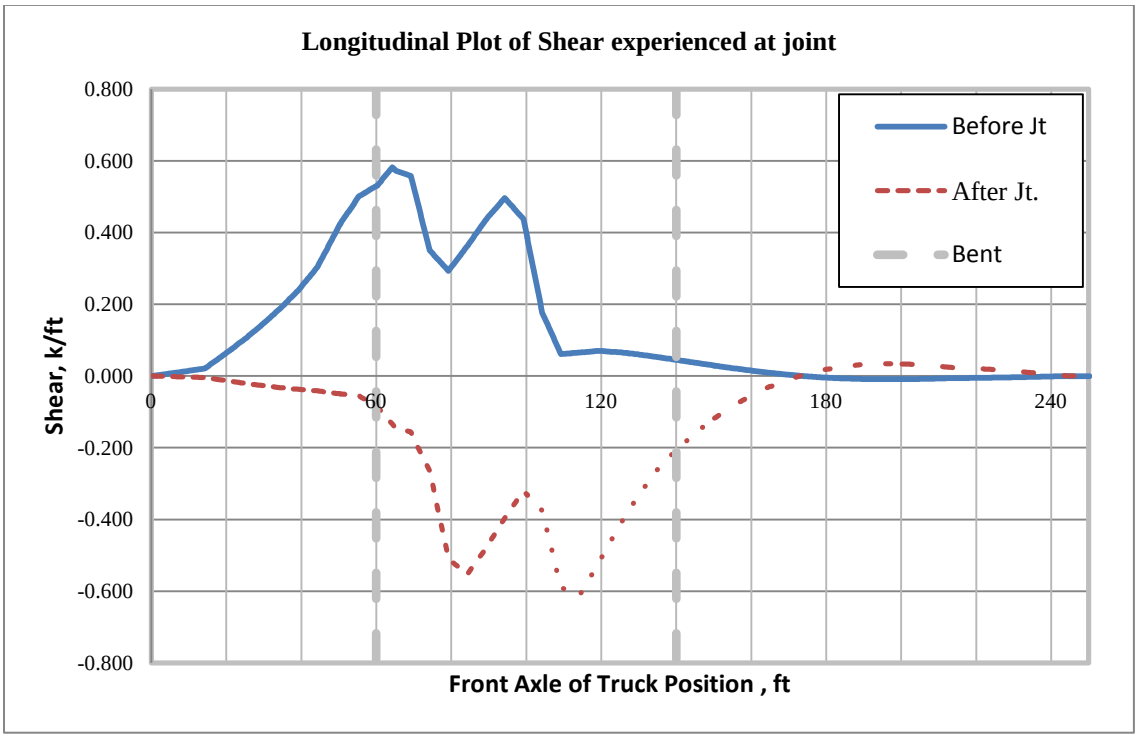

Figure 5.4: Shear Experienced at Critical Joint as Truck Passes Over Bridge

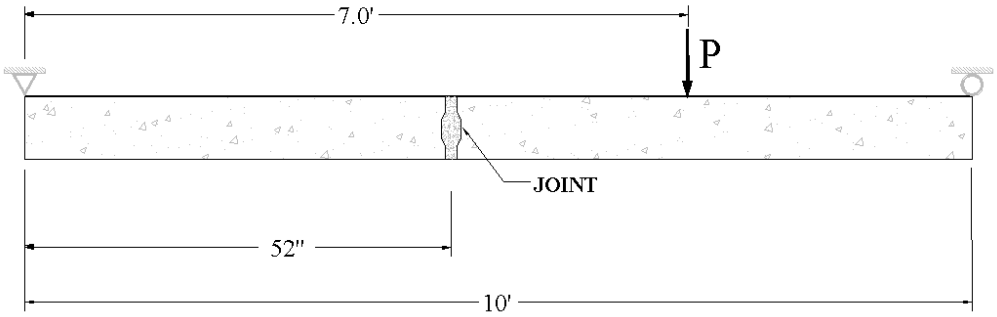

Figure 5.5: Negative Bending Test Setup

Table 5.4: Negative Bending Loading Matrix

Deck Width	Total Distributed Load, P	P per foot of width	At Joint		
			Moment	Shear	Stress
(in)	(kips)	(k/ft)	(k-in/ft)	(k/ft)	(ksi)
24	4.75				
48	9.50	2.37	38.4	0.710	0.300
96	19.00				

Figure 5.5 shows that the joint is positioned at a 52 in. offset in order to provide the appropriate ratio of shear and moment in the joint. In order to achieve a 300 psi stress, the loading matrix in Table 5.4 shows loadings for various deck section widths. Testing should be conducted in the same manner as with the positive bending test, with a 2-million cycle fatigue testing followed by a monolithic until failure test. Ponding and static load tests should be conducted in accordance to the positive bending proposed schedule (Table 5.3), and the deck will have the same strain gauge and potentiometer orientation as with the positive bending test (Figure 5.2). The main difference is that the loading at P will be decreased to 2.37 kips per foot of deck width. Again, good joint behavior is considered little cracking, no water leakage, and linear strain distribution through the depth of the joint.

5.2.4 Shear Reversal Test

The shear reversal experienced by the positive moment critical joint can be seen in Figure 5.6 below. Additionally the corresponding stresses experienced as the HS-20 truck passes the bridge can be seen in Figure 5.7. Based on the variations seen in these graphs, the shear reversal test was designed to produce similar shear loadings as well as the corresponding, simultaneously occurring tensile stresses.

Figure 5.6: Shear Experienced in Critical Joint as Truck Passes Over Bridge

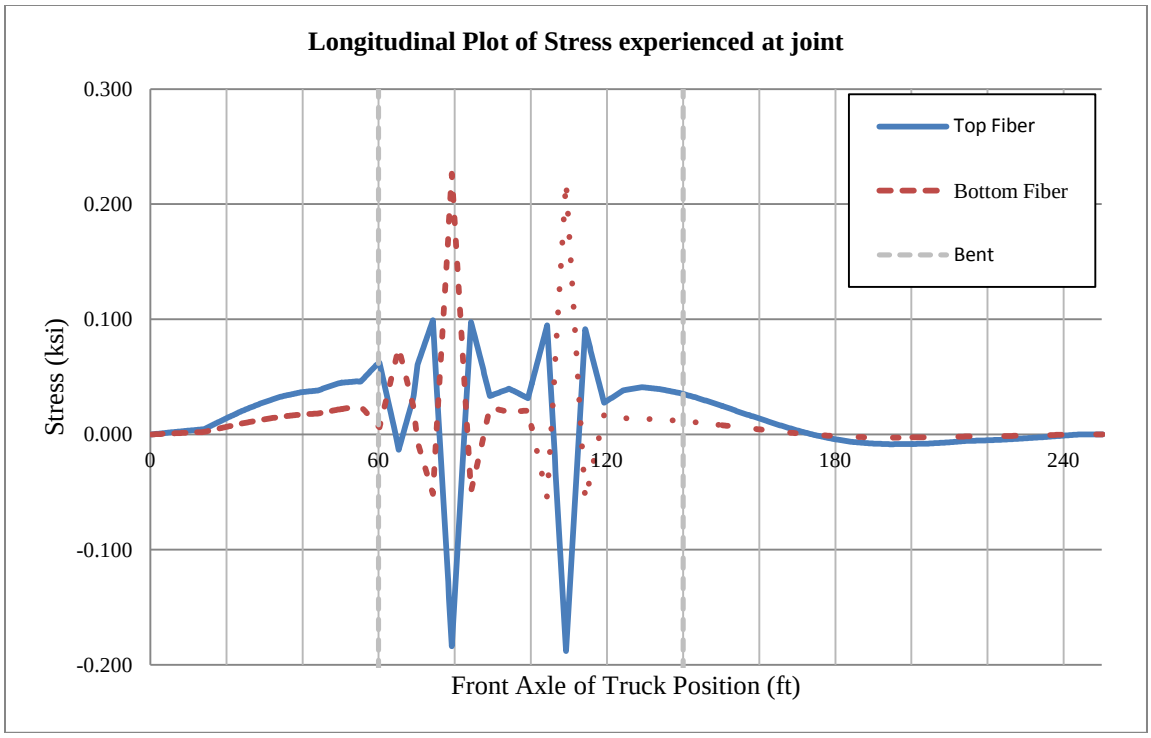

Figure 5.7: Stress Experienced in Critical Joint as Truck Passes Over Bridge

Table 5.5 summarizes the stresses in the critical joint from the computer analyses. As with the bending tests, the bottom fiber stress of 226 psi was increased to 300 psi. The top fiber critical tensile stress was increased proportionally from 99 psi to 130 psi; however, it was found that this did not produce a large enough negative shear. In order to ensure the maximum negative shear of 505 lb/ft was assessed, the shear reversal load was increased to -560 lb/ft thus creating a top fiber tensile load stress of 175 psi. Table 5.6 shows the appropriate loading for various deck widths. The discrepancy between 130 psi tensile stress in the top fiber and 175 psi is noteworthy and could result in quicker degradation of the joint.

Table 5.5: Critical Stresses and Shear at Worst-Case Joint Location for 60-80-60 ft Bridge

Critical Stress	Joint Location Longitudinal	Joint Location Transverse	Truck Position Transverse	Truck Position Longitudinal (Front Axle)	Stress (ksi) Top Fiber	Stress (ksi) Bottom Fiber	Shear (k/ft) Shear	Shear (k/ft) Reversal
V	Near Bent	TP-16 (Between GRDR)	TR-13	79.25'	-0.184	0.226	0.728	Yes (-0.425)
			TR-13	74.25'	0.099	-0.052	0.505	Yes (-0.646)

Table 5.6: Shear Test Loading Matrix

Deck Width (in)	Load Range, P (kips)	P per foot of width (k/ft)	At Joint Moment (k-in/ft)	At Joint Shear (k/ft)	At Joint Stress (ksi)
24	1.92 to -1.12	0.960 to -0.560	38.4 to -22.4	0.960 to -0.560	0.300 to -0.175
48	3.84 to -2.24				
96	7.68 to -4.48				

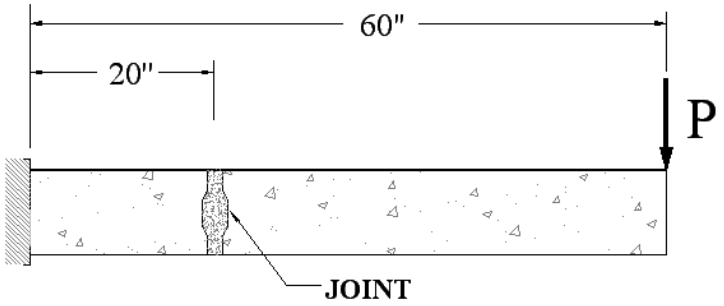

Figure 5.8 Shear Test Setup

Figure 5.8 shows a testing proposal for the shear reversal test. In the cantilever configuration, the joint experiences direct shear from the loading, and thus this system provides a simple, yet accurate way to reproduce model results in the testing joint. As with the bending

tests, testing with a 2-million cycle fatigue loading, followed by a monolithic until failure test should be conducted. A cycle should range with loading P from 0 lbs to 960 lbs, to -560 lbs, and back to 0 lbs to complete a cycle. Ponding and static load tests should be conducted in accordance to the positive bending test proposed schedule in Table 5.3. A proposed layout for gauges is shown in Figure 5.9. As with the other tests, good joint behavior is considered little cracking, no water leakage, and linear strain distribution through the depth of the joint.

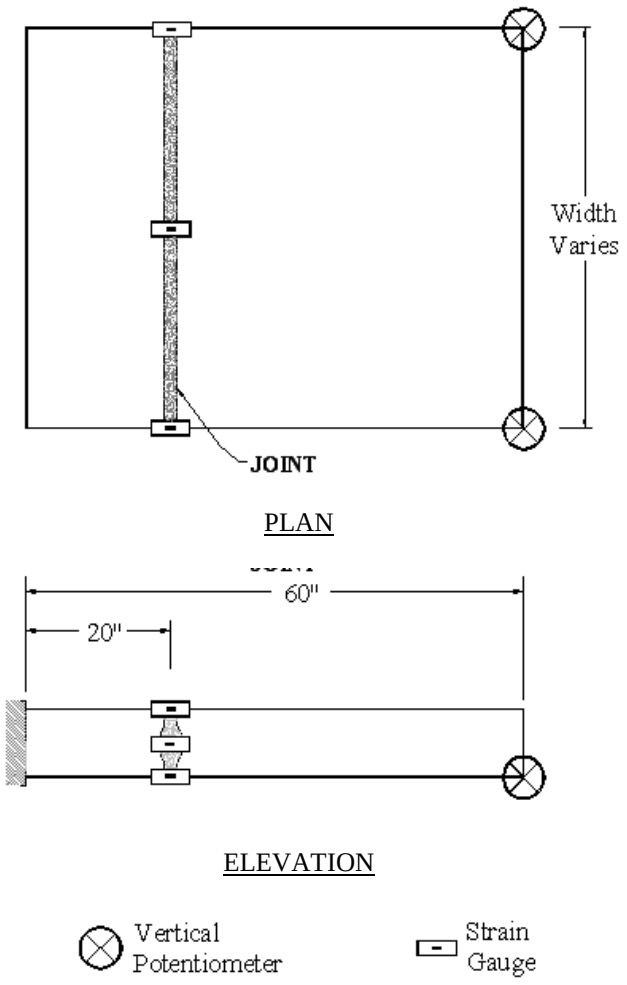

Figure 5.9: Strain Gauge Setup

CHAPTER 6: SUMMARY, CONCLUSION, AND RECOMMENDATIONS

6.1 Summary

The rapid rehabilitation of bridge decks continues to provide a way to restore reliable highway structures while minimizing traffic closures and congestion. For these systems to be effective, rehabilitation must be quick while having an adequate service life to prevent premature degradation. A critical component in both constructability and structural integrity is the transverse joint between deck panels.

This study consisted of an intensive review of rapid bridge deck replacement systems and their transverse joints. History, performances, advantages, and difficulties were all noted in order to make recommendations and suggestions for the implementation of an effective transverse joining system in Alabama. In addition, the Collinsville I-59 simply supported bridge and two continuously supported bridges were modeled using a finite-element analysis program to better understand the forces that a transverse joint would be likely to experience.

From this review and modeling, guidelines for the testing and selection of a transverse joint were made. In order to assess the selected joints, it is proposed to have three tests: positive and negative bending, and shear. These tests, described in Chapter 5, can accurately reproduce service loading stresses and determine the practicality of transverse joint options.

6.2 Conclusions from Research and Modeling

The conclusions and observations from the research and modeling of transverse joints are summarized as follows:

- A female-to-female shear key, NCHRP Report-584, or looped-bar joint are all suitable transverse joints in the simply supported bridge.
- A looped-bar joint or a longitudinally post-tensioned female-to-female shear key are recommended for use in bridges that experience negative flexure.
- The NCHRP system is largely proprietary; it should be tested extensively to further validate its performance.
- There is a lack of data comparing transverse joints in exodermic panels to those same joints in full-depth precast panels; all studies found were conducted on full-depth precast panels. Testing should be conducted for each joint in both a full-depth precast and exodermic panel.
- Joint failure induced from cyclic fatigue loading was the primary cause of failure in reviewed cases of laboratory testing and actual construction.
- Fatigue load modeling produced stresses 38 to 45 percent lower than cracking stress, while strength loading produced stresses 15 to 25 percent lower than the cracking stress of concrete.
- Maximum transverse joint flexural stresses were largely insensitive to the span length of the bridge.

6.3 Recommendations for Future Study

In this study, deck stresses from modeling were found to be within reason for transverse joints. Despite not analyzing actual transverse joints themselves, this research provides the parameters within which transverse joints should be tested. Future research to better assess which joints are suitable in rapid bridge deck replacement should be conducted in the following areas:

- Research should compare the performance of identical transverse joints cast in exodermic and full-depth precast panels to further validate exodermic panel performance.
- Future testing should consider the effects of shear reversal in combination with the implementation of flexural loading of a joint.
- Fatigue load testing with up to 2-million cycles should be conducted with water ponding and service load tests being done at several points during this cyclic loading.

REFERENCES

American Association of State Highway and Transportation Officials. 2007. AASHTO LRFD Bridge Design Specifications. 4th Edition. Washington, D.C.

ACI Committee 318. 2008. *Building Code Requirements for Structural Concrete and Commentary* (ACI 318-08). American Concrete Institute, Farmington Hills, MI.

American Society for Testing and Materials. 1998. ASTM Standard D6275-98: Standard Practice for Laboratory Testing of Bridge Decks.

Au, A., C. Lam, and B. Tharmabala. 2008. "Investigation of Prefabricated Bridges Using Reduced-Scale Models." *Journal of the Prestressed Concrete Institute* Nov.-Dec: 67-95.

Babei, K., A. Fouladagar, and R. Nicholson. 2001. "Nightime Bridge Deck Replacement with Full Depth Precast Concrete Panels at Route 7 over Route 50, Fairfax Country, Virginia." Paper presented at the 80th annual meeting of the Transportation Research Board 80th Annual Meeting, Washington, D.C.

Bakhoum, M. 1991. "Shear Behavior and Design of Joints in Precast Concrete Segmental Bridges." PhD thesis, Massachusetts Institute of Technology, Cambridge, MA.

Badie, S., M. Tadros, and A. Girgis. 2006. "Full-Depth, Precast-Concrete Bridge Deck Panel Systems." NCHRP, ed., National Research Council.

Badie, S., and Maher Tadros. 2008. Full-Depth Precast Concrete Bridge Deck Systems. National Cooperative Highway Research Program Report 584, Transportation Research Board of the National Academies, Washington, D.C.

Bettigole, N., and N. Robison. 1997. Bridge Decks: Design, Construction, Rehabilitation, Replacement. *ASCE Publications*.

Biswas, M. 1986. "Precast Bridge Deck Systems." *Journal of the Prestressed Concrete Institute* March-April: 40-94.

Biswas, M., J.E. Iffland , R.E. Schofield, and A.E. Gregory. 1974. "Innovations in construction and maintenance of transportation facilities: proceedings of the sixth summer meeting of the Highway Research Board in cooperation with the Washington State Department of Highways, August 6-8, 1973 Olympia." Washington. *Transportation Research Board, National Research Council*, Washington, 1974.

Bowers, S. 2007. "Recommendations for longitudinal post-tensioning in full-depth precast concrete bridge deck panels," M.S. thesis, Virginia Tech, Blacksburg, VA.

Brush, C. 2004. “Connection of Modular Steel Beam Precast Slab Units with Cast-in-Place Closure Pour Slabs.” M.S. thesis. Texas A&M University, College Station, TX.

CALTRANS. 2003. Lessons Learned from the Tappan Zee Bridge, New York. California Department of Transportation.

Chapman, C. 2010. “Behavior of Precast Bridge Deck Joints with Small Bend Diameter U-Bars.” M.S. thesis. University of Tennessee, Knoxville, TN.

Culmo, M. P. 2000. "Rapid Bridge Deck Replacement with Full-Depth Precast Concrete Slabs." *Transportation Research Record* No. 1712: 139-146.

Darlow, M., and N. Bettigole. 1989. “Instrumentation and Testing of Bridge Rehabilitated with Exodermic Deck.” *Journal of Structural Engineering, ASCE*: 2461-2480.

Exodermic Bridge Deck, Inc., 2011, “Exodermic Bridge Deck.” D.S. Brown Corporation. Accessed July 30. http://www.exodermic.com

Exodermic Bridge Deck, Inc. 1999. “Exodermic Bridge Deck Case Study - Tappan Zee Bridge,” Product Literature, Lakeville, CT.

Gulyas, R. J., G.J. Wirthlin., and J.T. Champa. 1995. “Evaluation of Keyway Grout Test Methods for Precast Concrete Bridges.” Jan.-Feb: 44-57.

Issa, M., A. Yousif, M. Issa, I. Kaspar, and S. Khayyat. 1995a. "Full Depth Precast and Precast, Prestressed Concrete Bridge Deck Panels.” *Journal of the Prestressed Concrete Institute Journal* Jan.-Feb: 59-80.

Issa, M., A. Yousif, M. Issa, I. Kaspar, and S. Khayyat. 1995b. "Field Performance of Full Depth Precast Concrete Panels in Bridge Deck Reconstruction." *Journal of the Prestressed Concrete Institute Journal* May-June: 82-108.

Issa, M., A. Yousif, and M. Issa. 1995c. "Construction Procedures for Rapid Replacement of Bridge Decks." *Concrete International* Feb: 49-52.

Issa, M., A. Yousif, M. Issa, I. Kaspar, and S. Khayyat. 1998. "Analysis of Full Depth Precast Concrete Bridge Deck Panels." *Journal of the Prestressed Concrete Institute Journal* Jan.-Feb: 74-85.

Issa, M., A. Yousif, and M. Issa. 2000. "Experimental Behavior of Full-Depth Precast Concrete Panels for Bridge Rehabilitation." *ACI Structural Journal* May-June: 397-407.

Issa, M.A., R. Anderson, T. Domagalski, and S. Khayyat. 2002. “Design Considerations of Full Depth Precast/Prestressed Concrete Bridge Deck Panels.” Proceedings of the 1st annual

Concrete Bridge Conference sponsored by FHWA and NCBC, and organized by PCI, October.

Issa, M., A. Yousif, M. Issa, I. Kaspar, and S. Khayyat. 2003. "Performance of Transverse Joint Grout Materials in Full-Depth Precast Concrete Bridge Deck Systems." *Journal of the Prestressed Concrete Institute Journal* July-Aug: 92-103.

Issa, M., R. Anderson, T. Domagalski, S. Asfour, and M. Islam. 2007. "Full-Scale Testing of Prefabricated Full-Depth Precast Concrete Bridge Deck Panel System." *ACI Structural Journal*, May-June: 324-332.

Kaczinski, M. 2010. The D.S. Brown Company. Phone Interview. July 17.

Markowski, S. 2005. "Experimental and Analytical Study of Full Depth Prestressed Precast Concrete Deck Panels for Highway Bridges," M.S. thesis. University of Wisconsin-Madison, Madison, WI.

Oliva, M., L. Bank, J. Russell, S. Markowski, G. Ehmke, and S. Chi. 2007. "Full Depth Precast Concrete Highway Bridge Decks." M.S. thesis. University of Wisconsin-Madison, Madison, WI.

Porter, S. 2009. "Laboratory Testing of Precast Bridge Deck Panel Transverse Connections for use in Accelerated Bridge Construction." M.S. thesis. Utah State University, Logan, Utah.

Precast/Prestressed Concrete Institute New England Region 2002. "Full Depth Precast Concrete Deck Slabs."

Roberts, K. 2009. "Performance of Transverse Post-Tensioned Joints Subjected to Negative Bending and Shear Stresses on Full Scale, Full Depth, Precast Concrete Bridge Deck System." M.S. thesis. Utah State University, Logan, Utah.

Ryu, H., Y. Kim, and S. Chang. 2007. "Experimental Study on Static and Fatigue Strength of Loop Joints." *Engineering Structures* Feb: 145-162.

Shim, C. S., and Chang, S. P. 2003."Cracking of Continuous Composite Beams with Precast Decks."*Journal of Constructional Steel Research* Feb: 201-214.

Sullivan, S. 2007. "Construction and Behavior of Precast Bridge Deck Panel Systems." PhD thesis. Virginia Tech, Blacksburg, VA.

Swartz, B. 2008. "Design Guide Development for Post-Tensioned Bridge Decks." *The Journal of the Post-Tensioning Institute*, Aug: 7-20.

Swenty, M. 2009. "The Investigation of Transverse Joints and Grouts on Full Depth Concrete Bridge Deck Panels." PhD thesis. Virginia Tech, Blacksburg, VA.

Utah Department of Transportation. 2008. "ABC standards, Full Depth Precast Concrete Deck Panel Standard Drawings" UDOT Structures Division, Salt Lake City, Utah. http://www.dot.state.ut.us/main/uconowner.gf?n=1966945409050115798

Versace, J.D., J.A. Ramirez. 2004. "Implementation of Full-Width Precast Bridge Deck Panels: A Synthesis Study." Purdue University, West Lafayette, Indiana.

Wisconsin Department of Transportation. 2010. “Exodermic Bridge Deck Performance Evaluation.” Report FEP-06-10, July.

Yamane, T., M. Tadros, S. Badie, and M. Baishya. 1998. "Full Depth Precast, Prestressed Concrete Bridge Deck System." *Journal of the Prestressed Concrete Institute Journal*, May-June: 50-66.

Yousif, A. “Experimental Behavior of Full Depth Precast Concrete Deck Panels for Bridge Reconstruction.” M.S. thesis. University of Illinois at Chicago, Chicago, Illinois. 1998.

APPENDIX A: Max Moment Comparisons

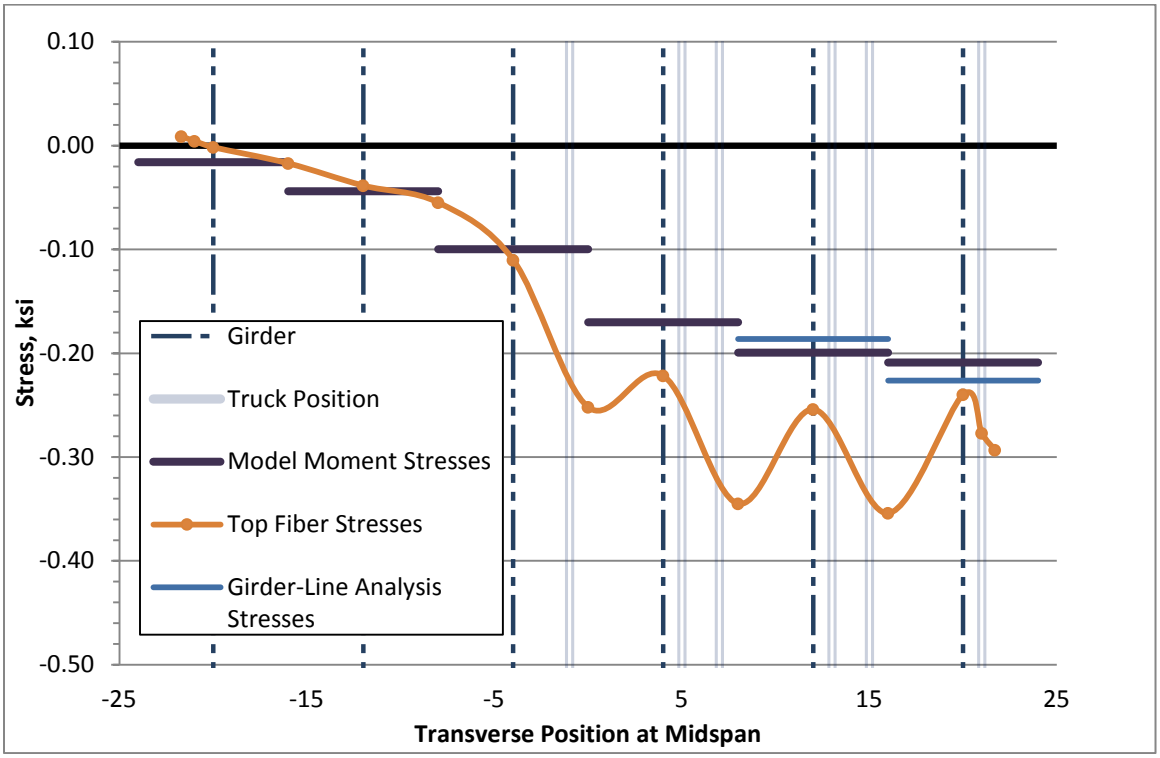

Figure A.1: Max Moment Comparisons for 3 Trucks Loading Simple Span Bridge

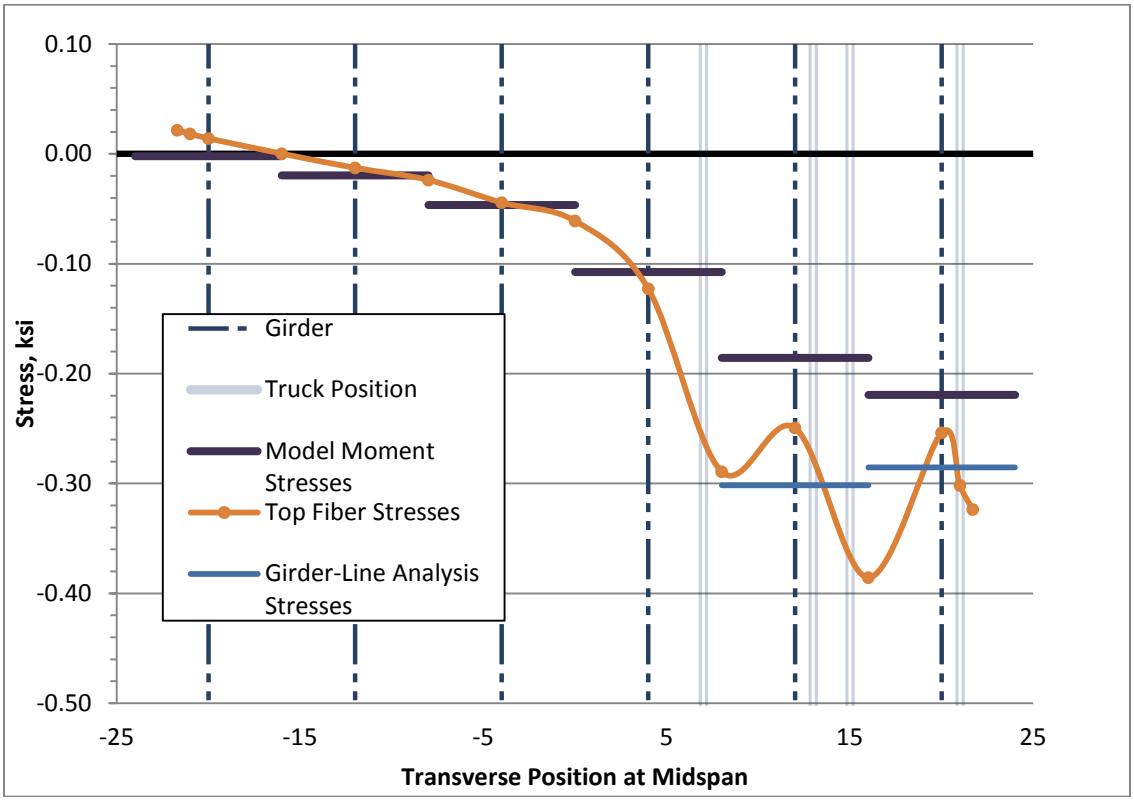

Figure A.2: Max Moment Comparisons for 2 Trucks Loading Simple Span Bridge

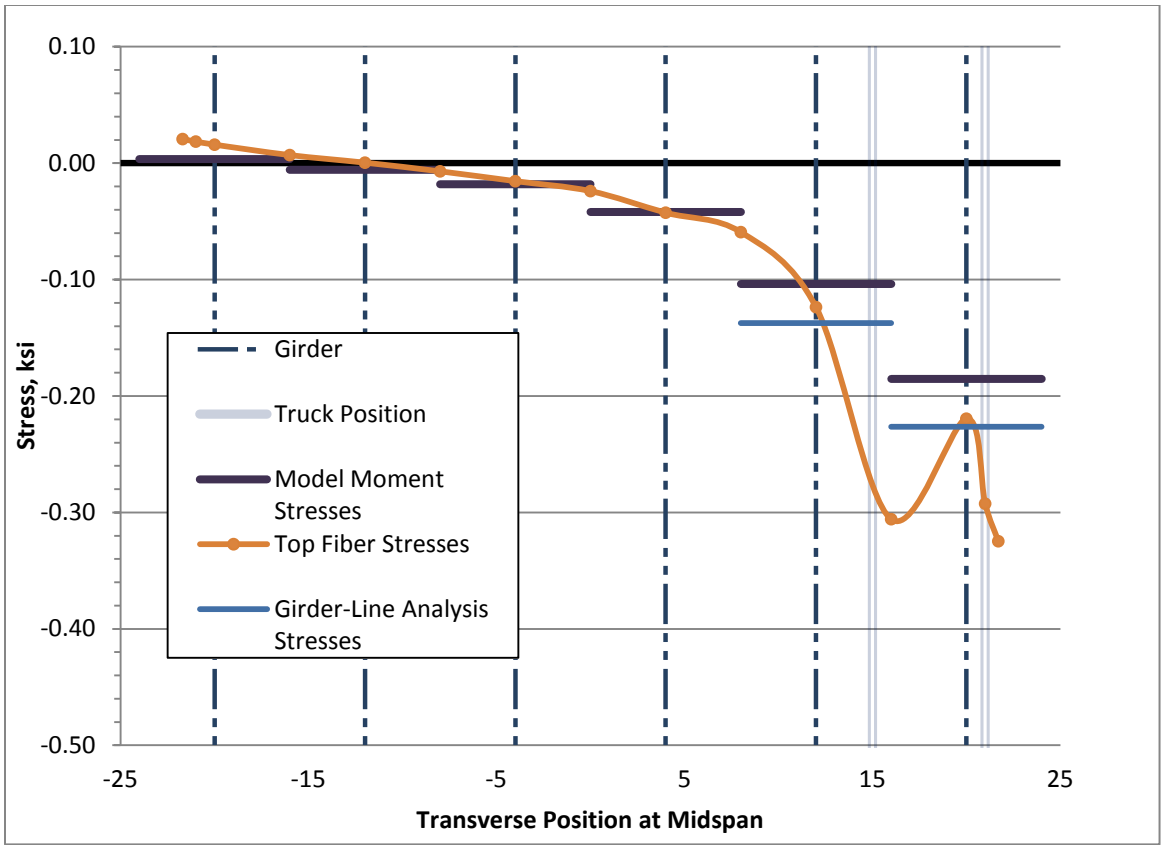

Figure A.3: Max Moment Comparisons for 1 Truck Loading Simple Span Bridge

APPENDIX B: Transverse Stress Plots

B.1 Transverse Stress Plots of Positive Moment Extreme Case for 60-80-60 Bridge

Figure B.1: Deck Stresses due to TR-0 at Critical Location 2 (60-80-60 Bridge)

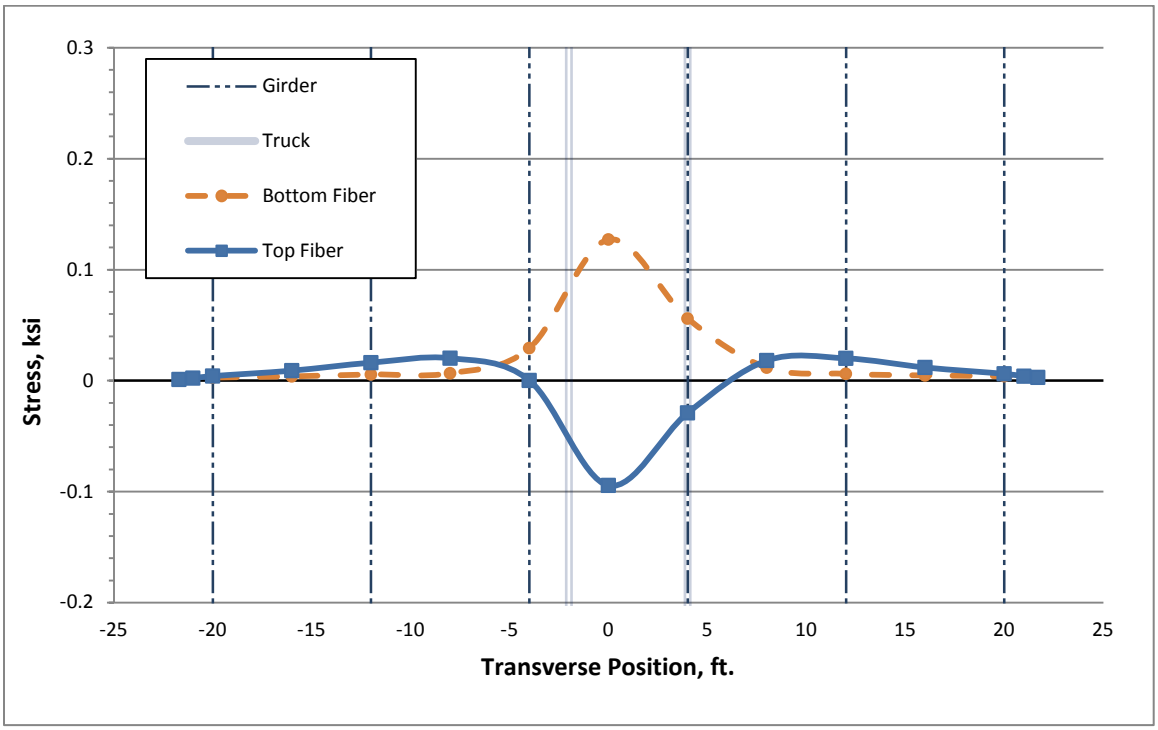

Figure B.2:Deck Stresses due to TR-1at Critical Location 2 (60-80-60 Bridge)

Figure B.3: Deck Stresses due to TR-2 at Critical Location 2 (60-80-60 Bridge)

Figure B.4: Deck Stresses due to TR-3 at Critical Location 2 (60-80-60 Bridge)

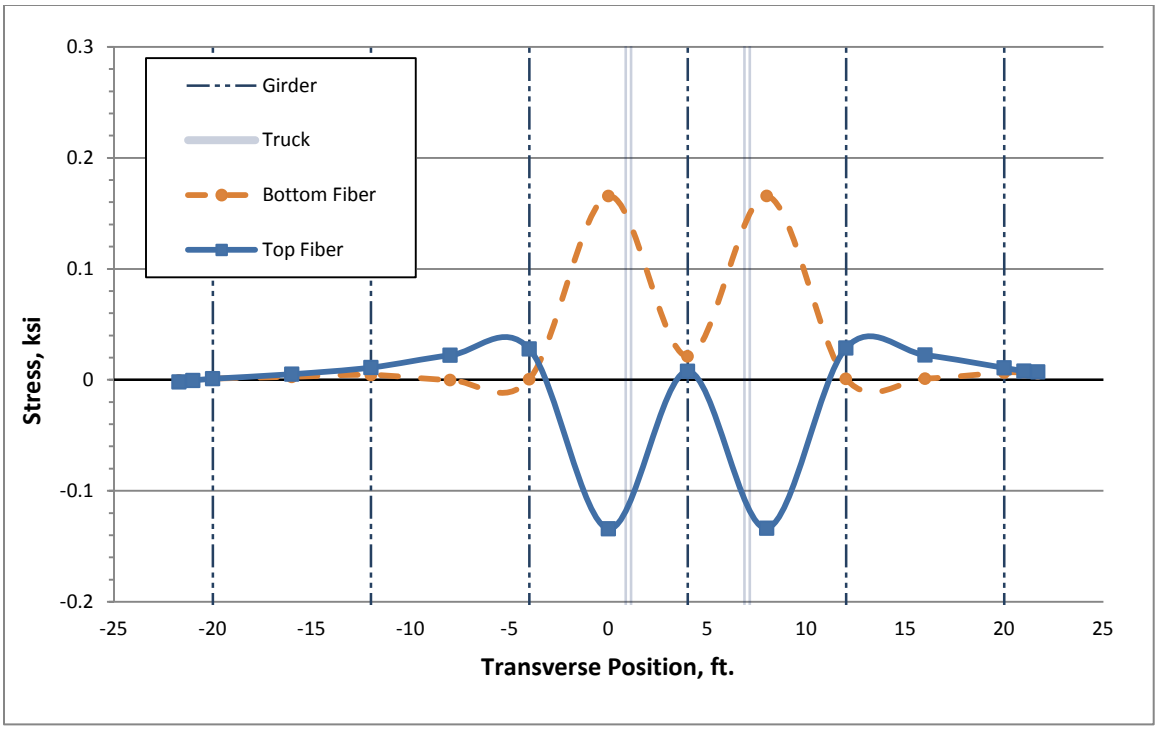

Figure B.5: Deck Stresses due to TR-4 at Critical Location 2 (60-80-60 Bridge)

Figure B.6: Deck Stresses due to TR-5 at Critical Location 2 (60-80-60 Bridge)

Figure B.7: Deck Stresses due to TR-6 at Critical Location 2 (60-80-60 Bridge)

Figure B.8: Deck Stresses due to TR-7 at Critical Location 2 (60-80-60 Bridge)

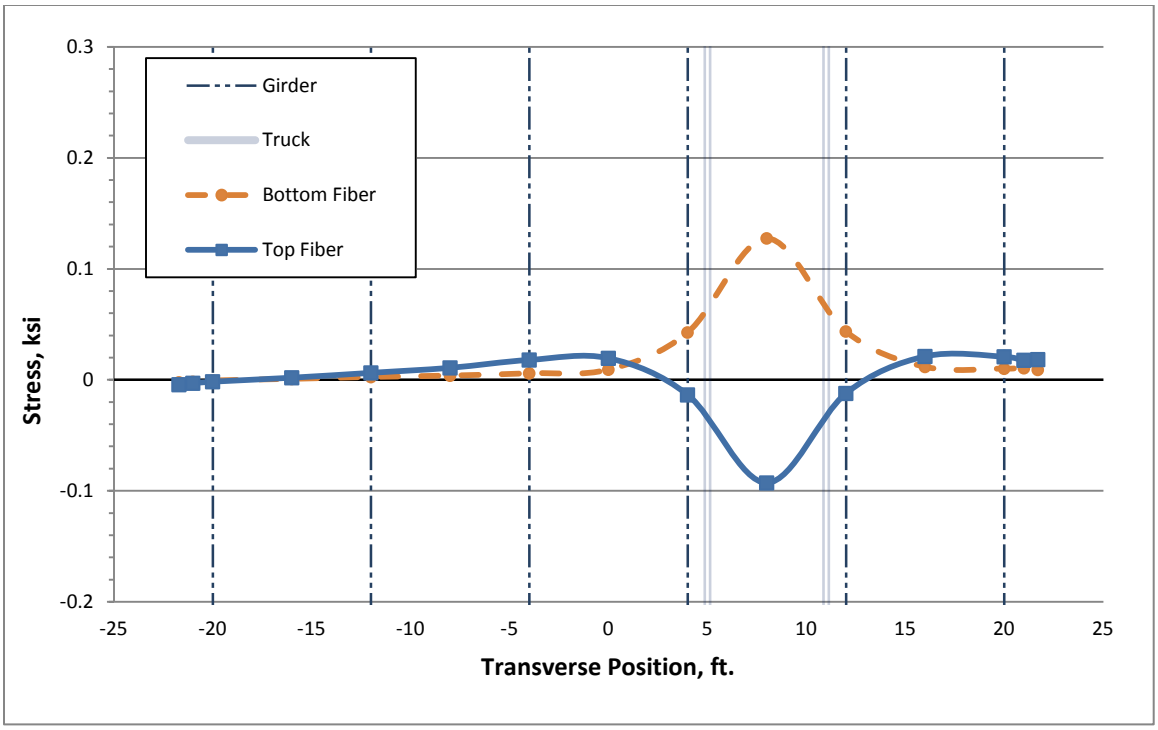

Figure B.9: Deck Stresses due to TR-8 at Critical Location 2 (60-80-60 Bridge)

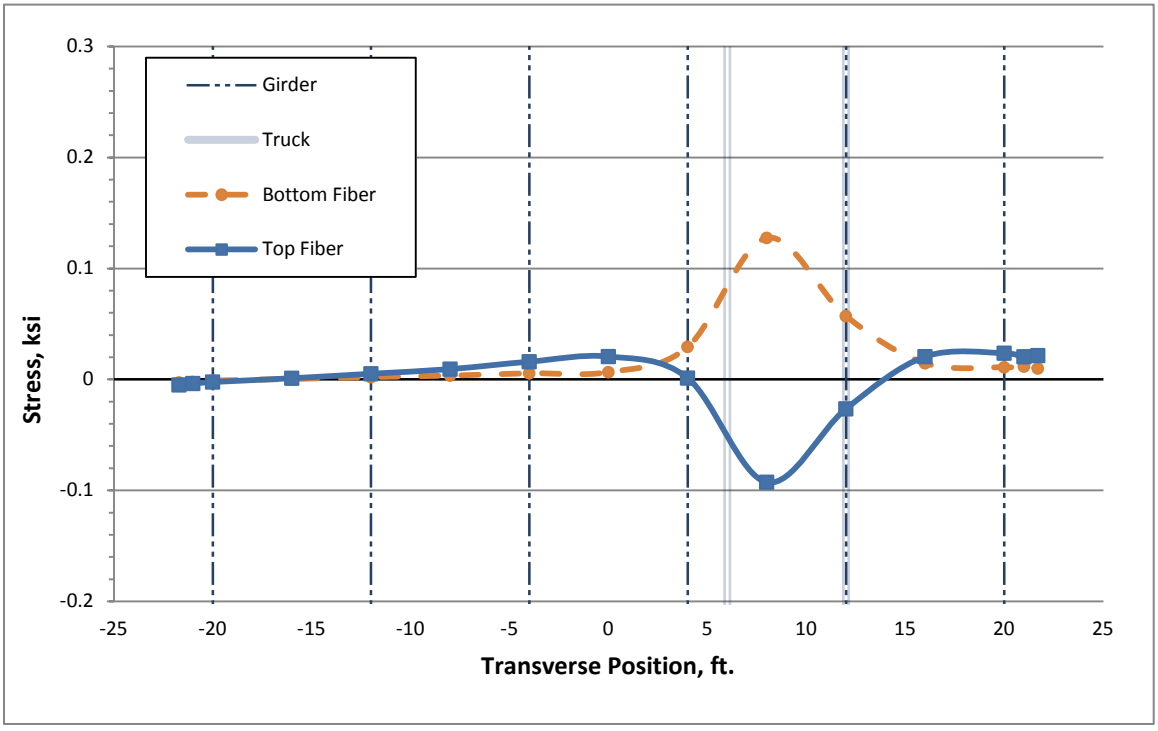

Figure B.10: Deck Stresses due to TR-9 at Critical Location 2 (60-80-60 Bridge)

Figure B.11: Deck Stresses due to TR-10 at Critical Location 2 (60-80-60 Bridge)

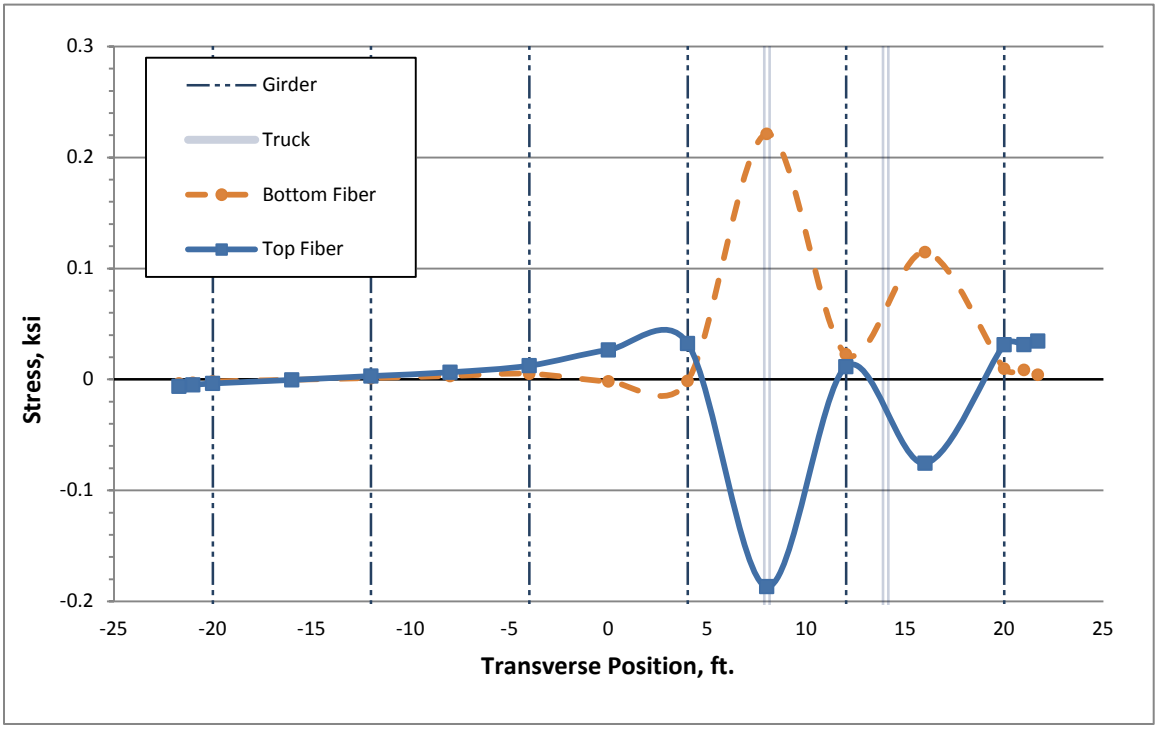

Figure B.12: Deck Stresses due to TR-11 at Critical Location 2 (60-80-60 Bridge)

Figure B.13: Deck Stresses due to TR-12 at Critical Location 2 (60-80-60 Bridge)

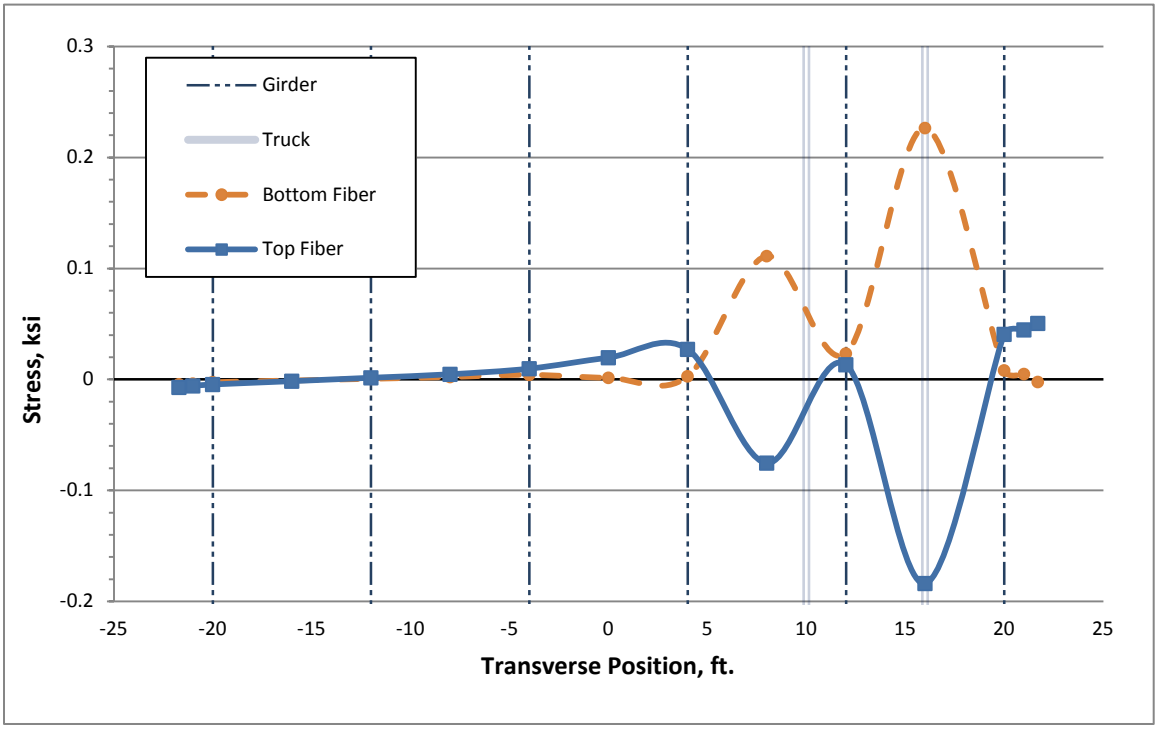

Figure B.14: Deck Stresses due to TR-13 at Critical Location 2 (60-80-60 Bridge)

Figure B.15: Deck Stresses due to TR-14 at Critical Location 2 (60-80-60 Bridge)

Figure B.16: Deck Stresses due to TR-15 at Critical Location 2 (60-80-60 Bridge)

Figure B.17: Deck Stresses due to TR-16 at Critical Location 2 (60-80-60 Bridge)

Figure B.18: Deck Stresses due to TR-17 at Critical Location 2 (60-80-60 Bridge)

Figure B.19: Deck Stresses due to TR-18 at Critical Location 2 (60-80-60 Bridge)

B.2 Transverse Stress Plots for Positive-Flexure Extreme Case for 60-80-60 Bridge

Figure B.20: Deck Stresses due to TR-0 at Critical Location 1 (60-80-60 Bridge)

Figure B.21:Deck Stresses due to TR-1at Critical Location 1 (60-80-60 Bridge)

Figure B.22: Deck Stresses due to TR-2 at Critical Location 1 (60-80-60 Bridge)

Figure B.23: Deck Stresses due to TR-3 at Critical Location 1 (60-80-60 Bridge)

Figure B.24: Deck Stresses due to TR-4 at Critical Location 1 (60-80-60 Bridge)

Figure B.25: Deck Stresses due to TR-5 at Critical Location 1 (60-80-60 Bridge)

Figure B.26: Deck Stresses due to TR-6 at Critical Location 1 (60-80-60 Bridge)

Figure B.27: Deck Stresses due to TR-7 at Critical Location 1 (60-80-60 Bridge)

Figure B.28: Deck Stresses due to TR-8 at Critical Location 1 (60-80-60 Bridge)

Figure B.29: Deck Stresses due to TR-9 at Critical Location 1 (60-80-60 Bridge)

Figure B.30: Deck Stresses due to TR-10 at Critical Location 1 (60-80-60 Bridge)

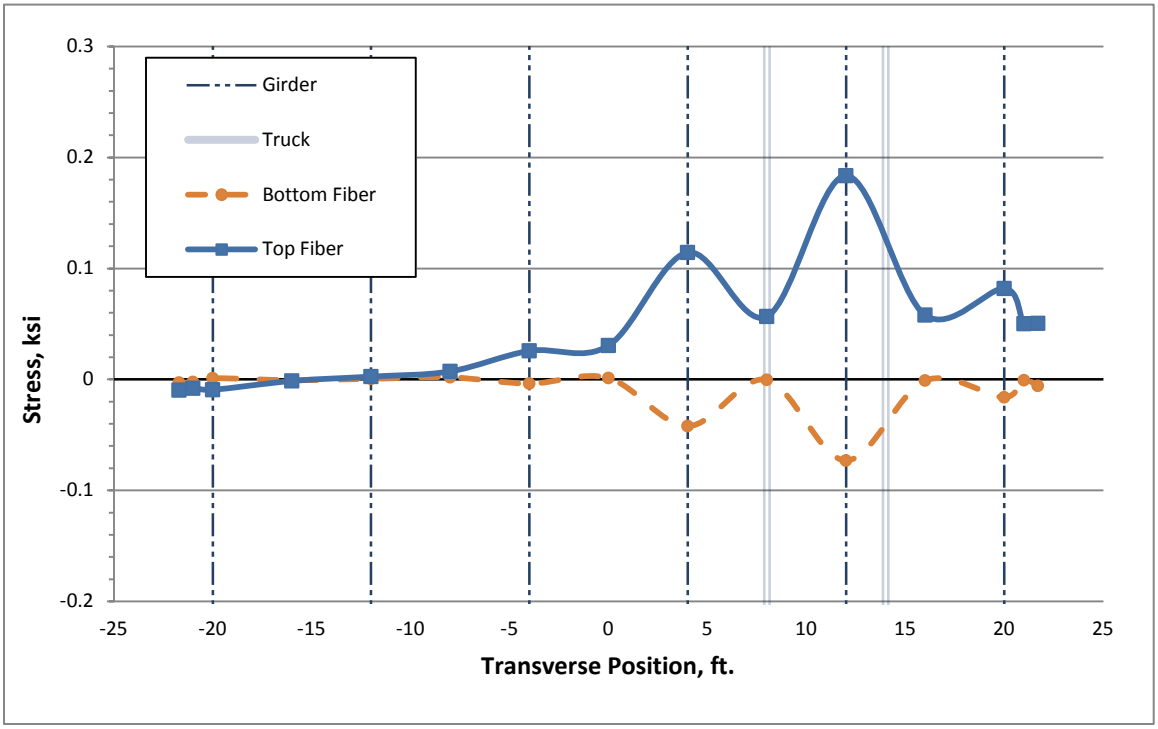

Figure B.31: Deck Stresses due to TR-11 at Critical Location 1 (60-80-60 Bridge)

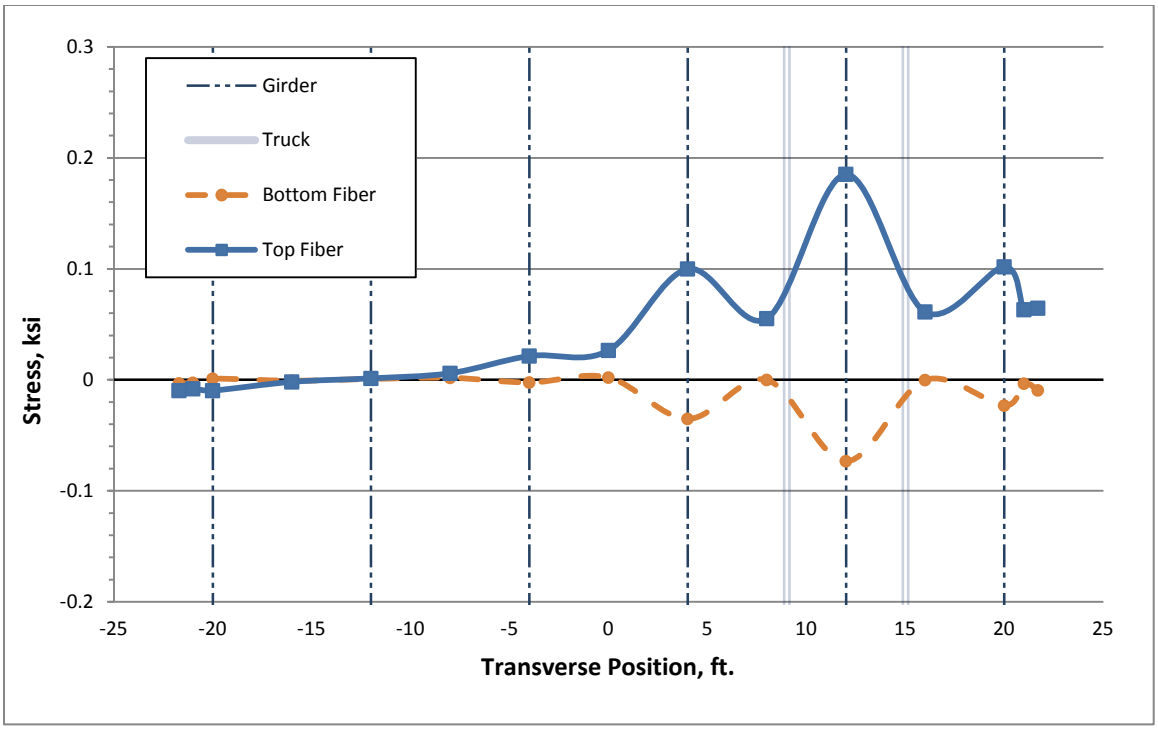

Figure B.32: Deck Stresses due to TR-12 at Critical Location 1 (60-80-60 Bridge)

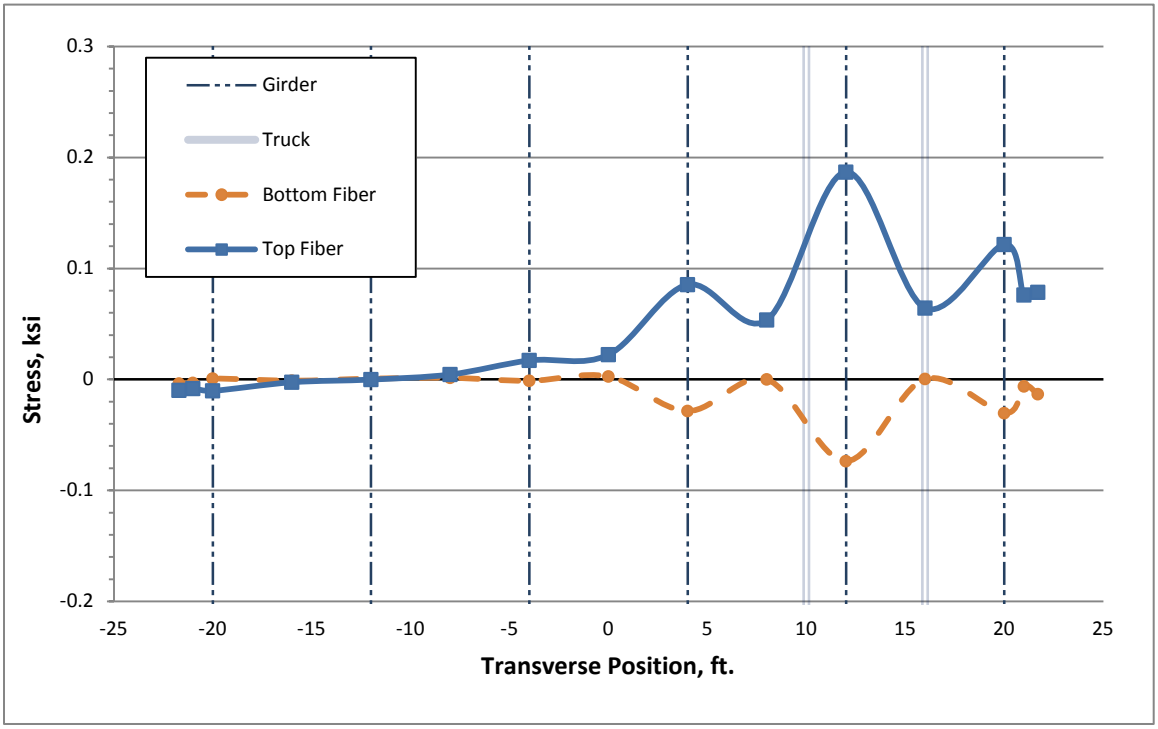

Figure B.33: Deck Stresses due to TR-13 at Critical Location 1 (60-80-60 Bridge)

Figure B.34: Deck Stresses due to TR-14 at Critical Location 1 (60-80-60 Bridge)

Figure B.35: Deck Stresses due to TR-15 at Critical Location 1 (60-80-60 Bridge)

Figure B.36: Deck Stresses due to TR-16 at Critical Location 1 (60-80-60 Bridge)

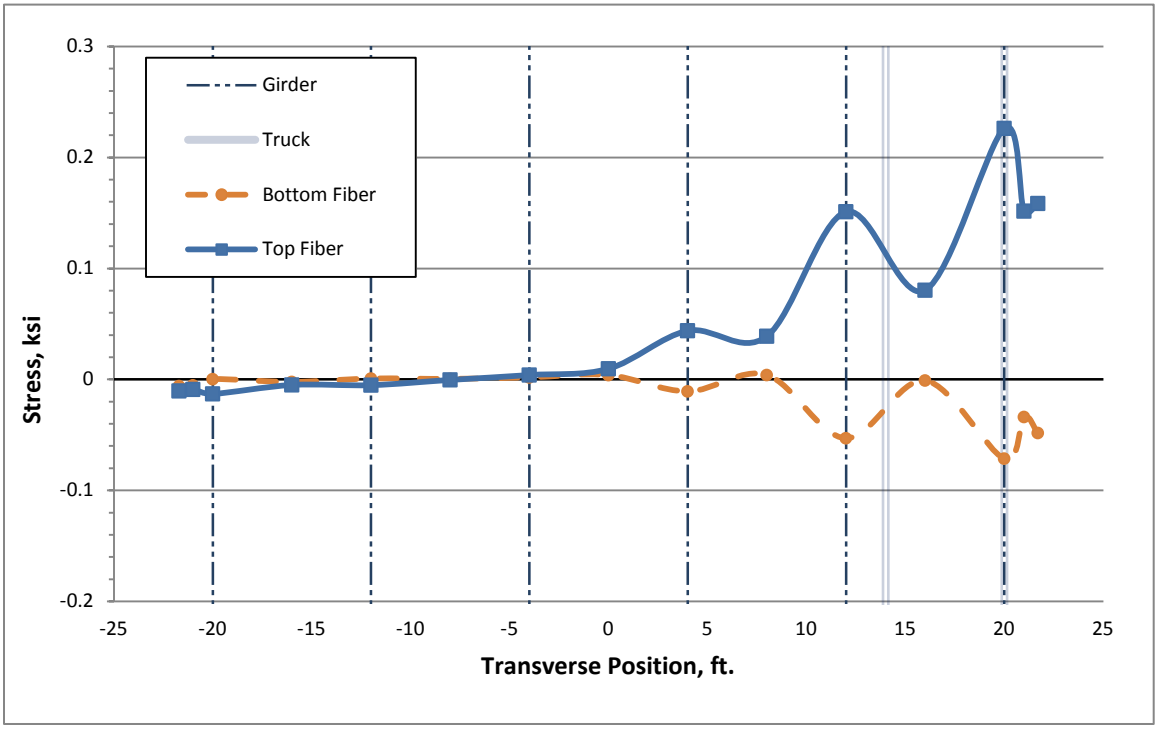

Figure B.37: Deck Stresses due to TR-17 at Critical Location 1 (60-80-60 Bridge)

Figure B.38: Deck Stresses due to TR-18 at Critical Location 1 (60-80-60 Bridge)

B.3 Transverse Stress Plots for Positive-Flexure Extreme Case for 80-100-80 Bridge

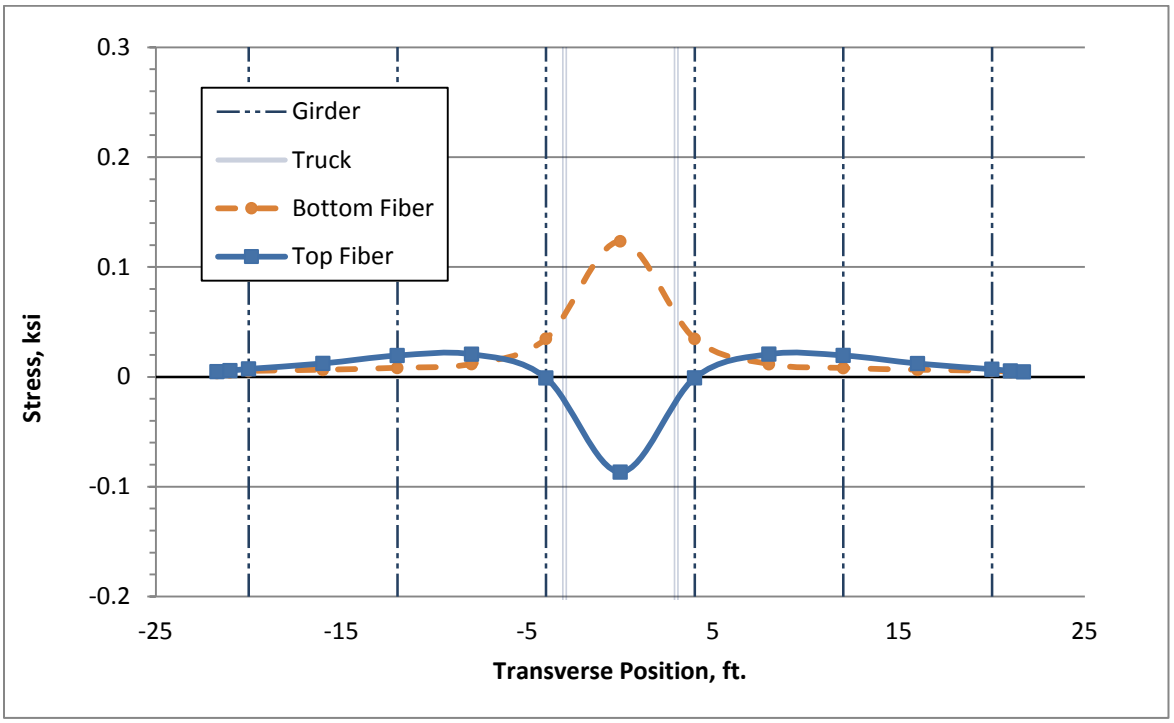

Figure B.39: Deck Stresses due to TR-0 at Critical Location 2 (80-100-80 Bridge)

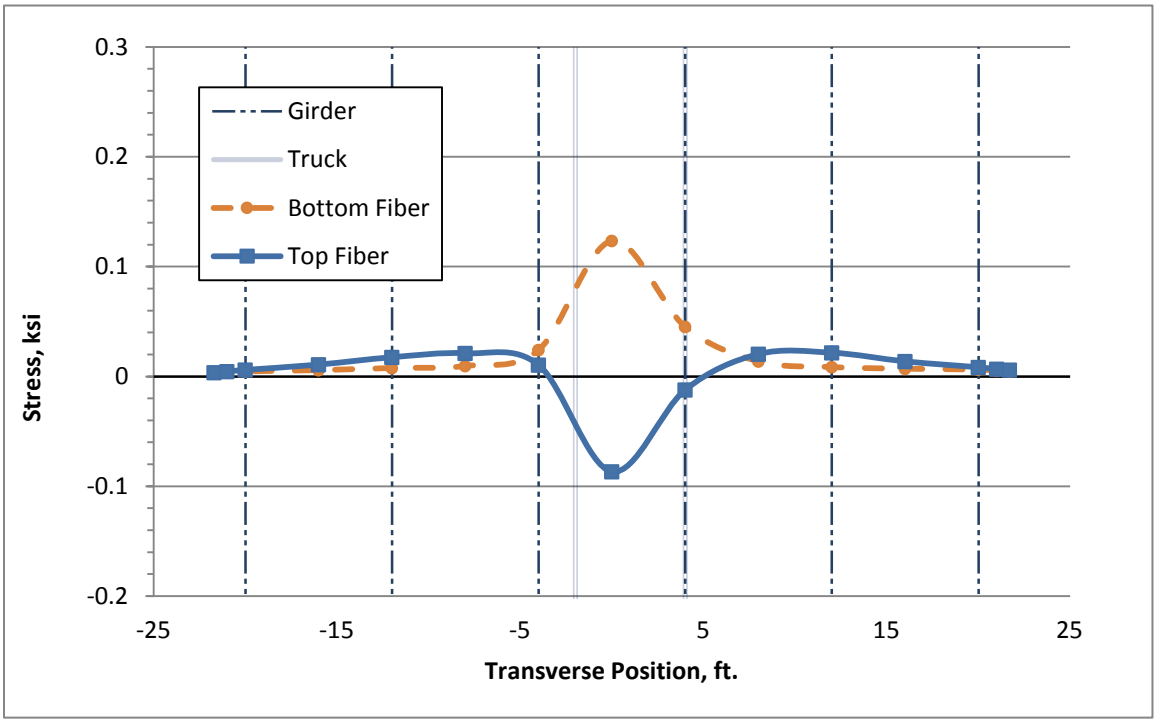

Figure B.40:Deck Stresses due to TR-1at Critical Location 2 (80-100-80 Bridge)

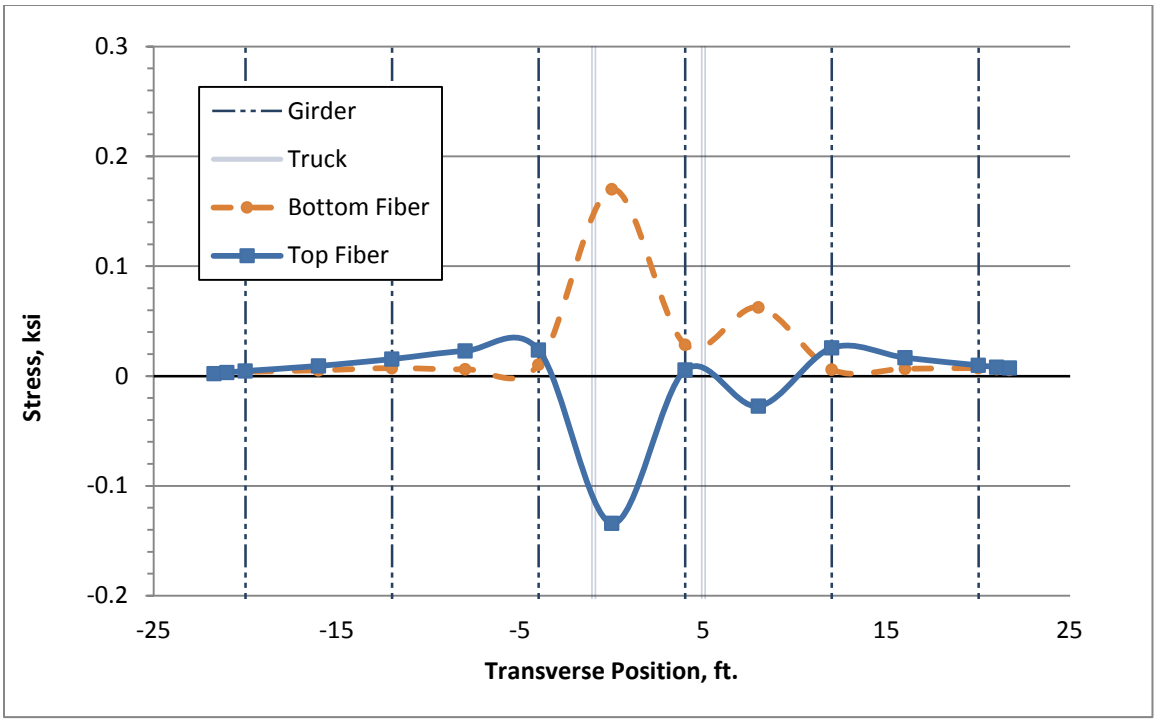

Figure B.41: Deck Stresses due to TR-2 at Critical Location 2 (80-100-80 Bridge)

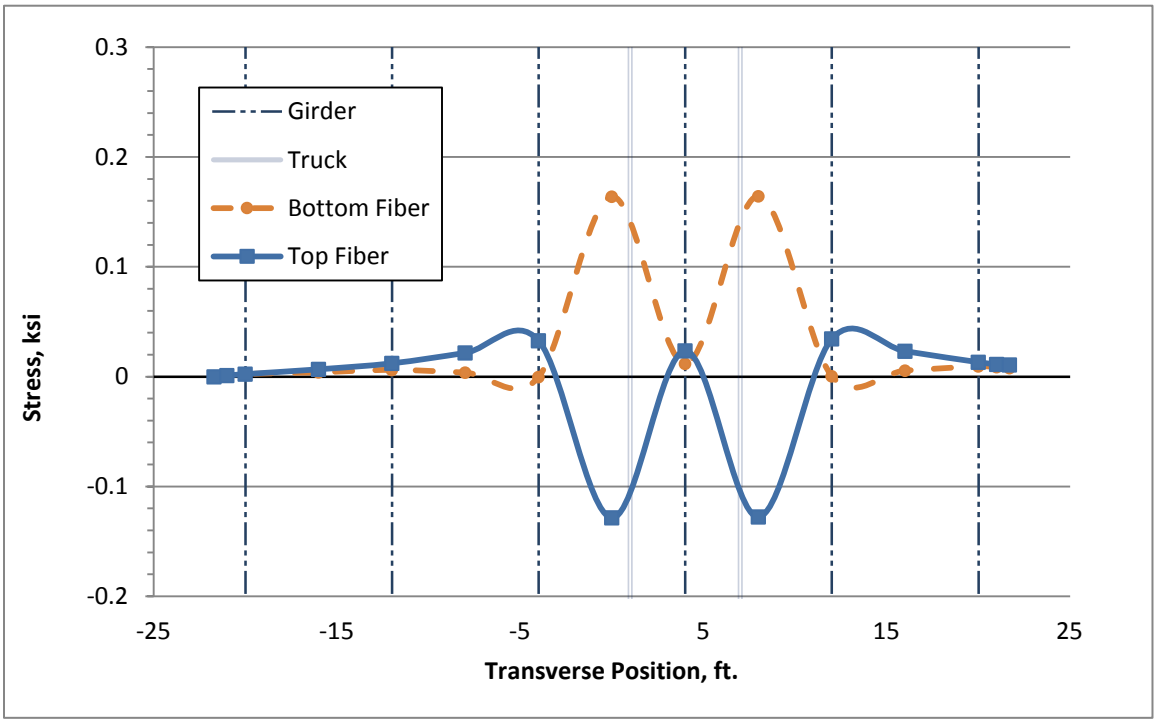

Figure B.42: Deck Stresses due to TR-3 at Critical Location 2 (80-100-80 Bridge)

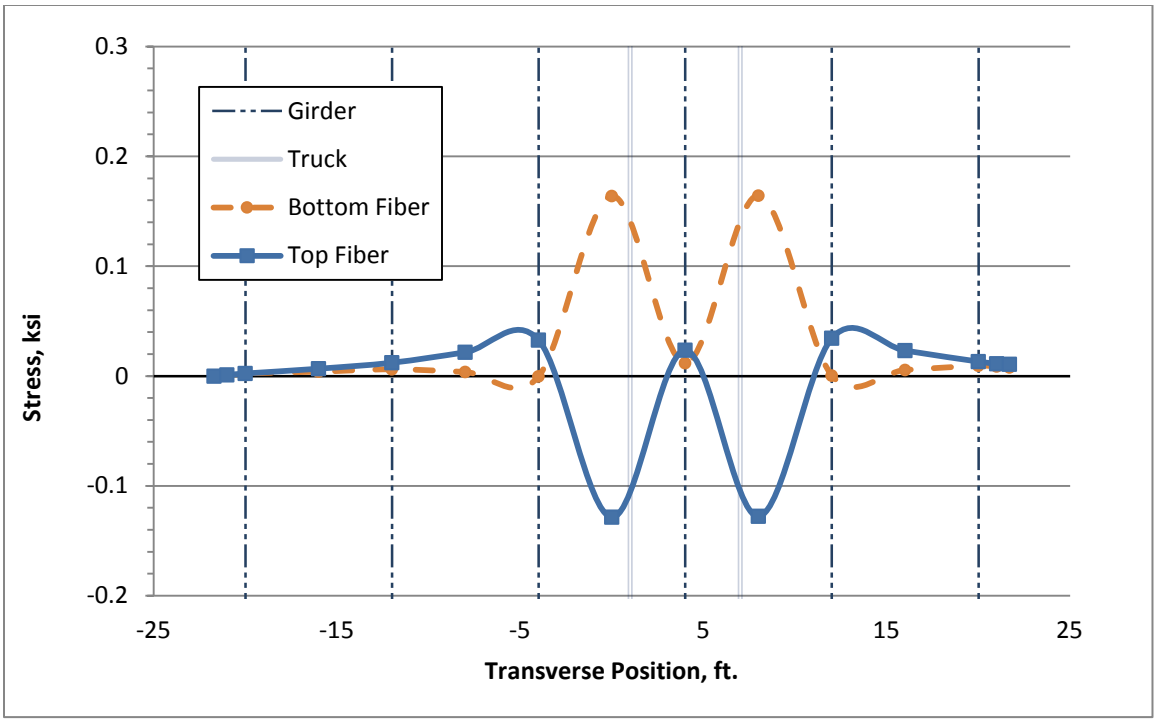

Figure B.43: Deck Stresses due to TR-4 at Critical Location 2 (80-100-80 Bridge)

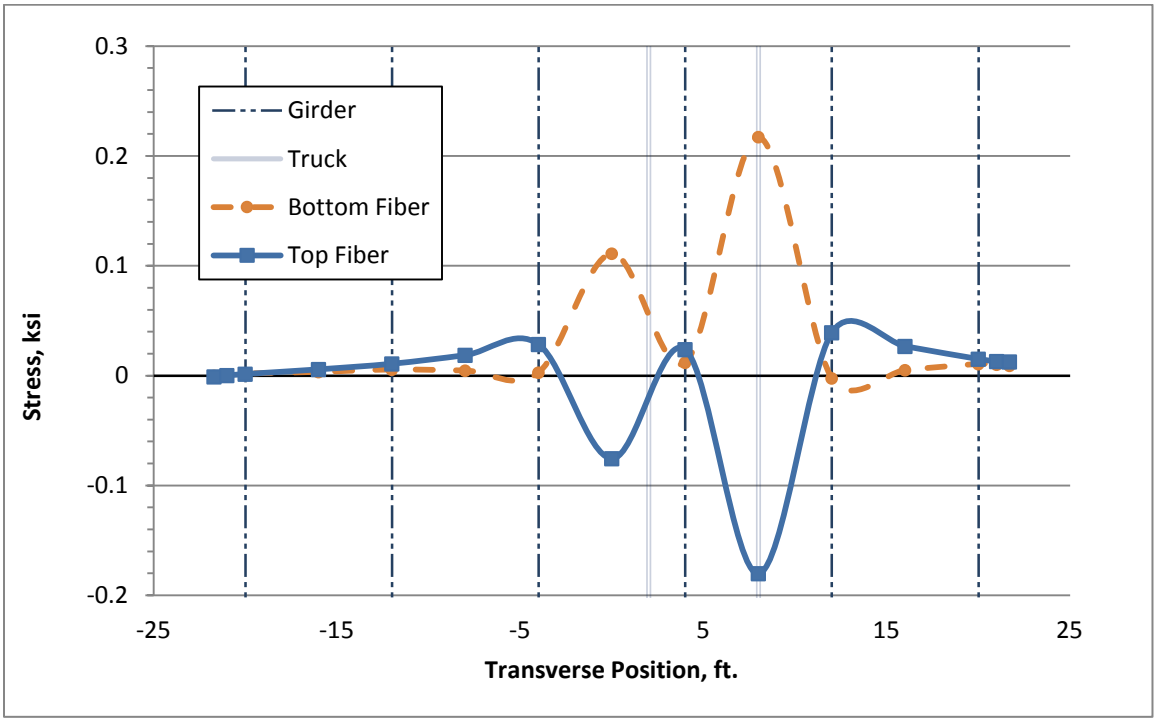

Figure B.44: Deck Stresses due to TR-5 at Critical Location 2 (80-100-80 Bridge)

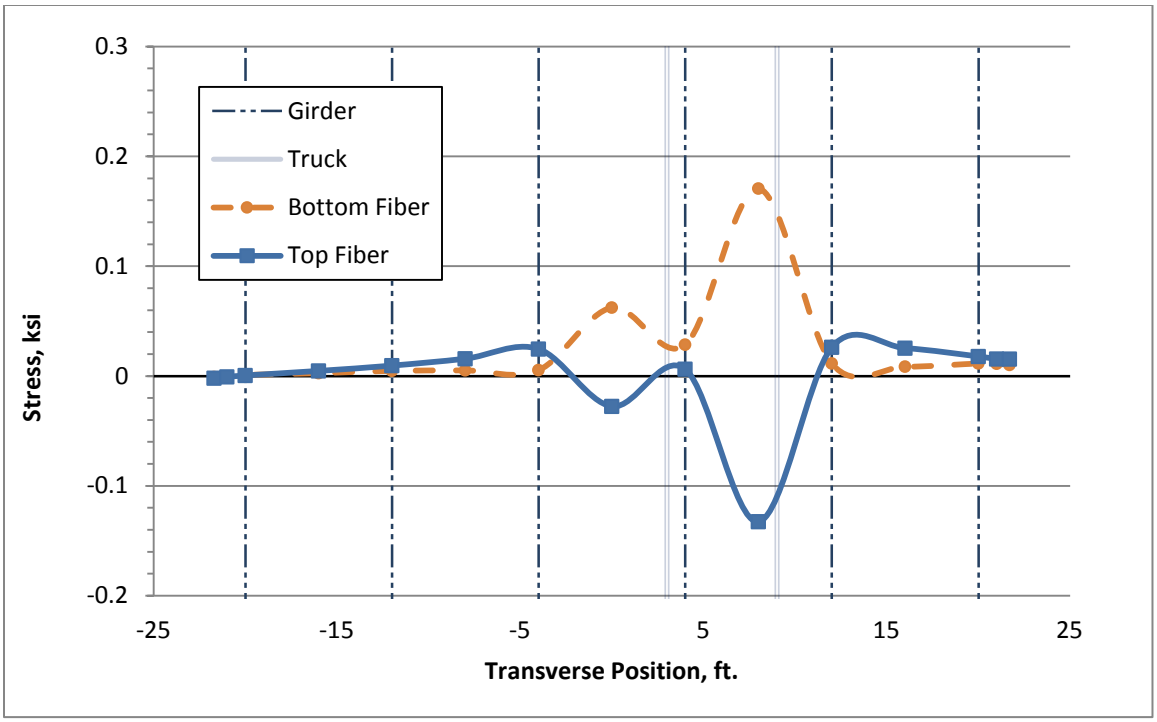

Figure B.45: Deck Stresses due to TR-6 at Critical Location 2 (80-100-80 Bridge)

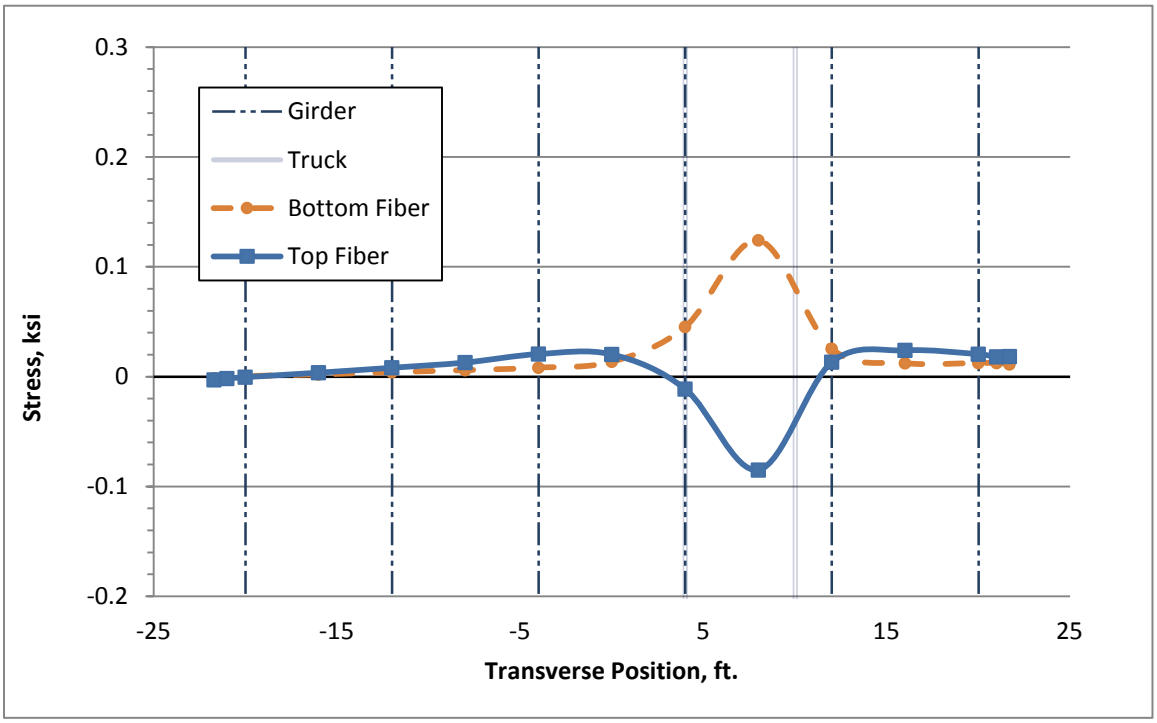

Figure B.46: Deck Stresses due to TR-7 at Critical Location 2 (80-100-80 Bridge)

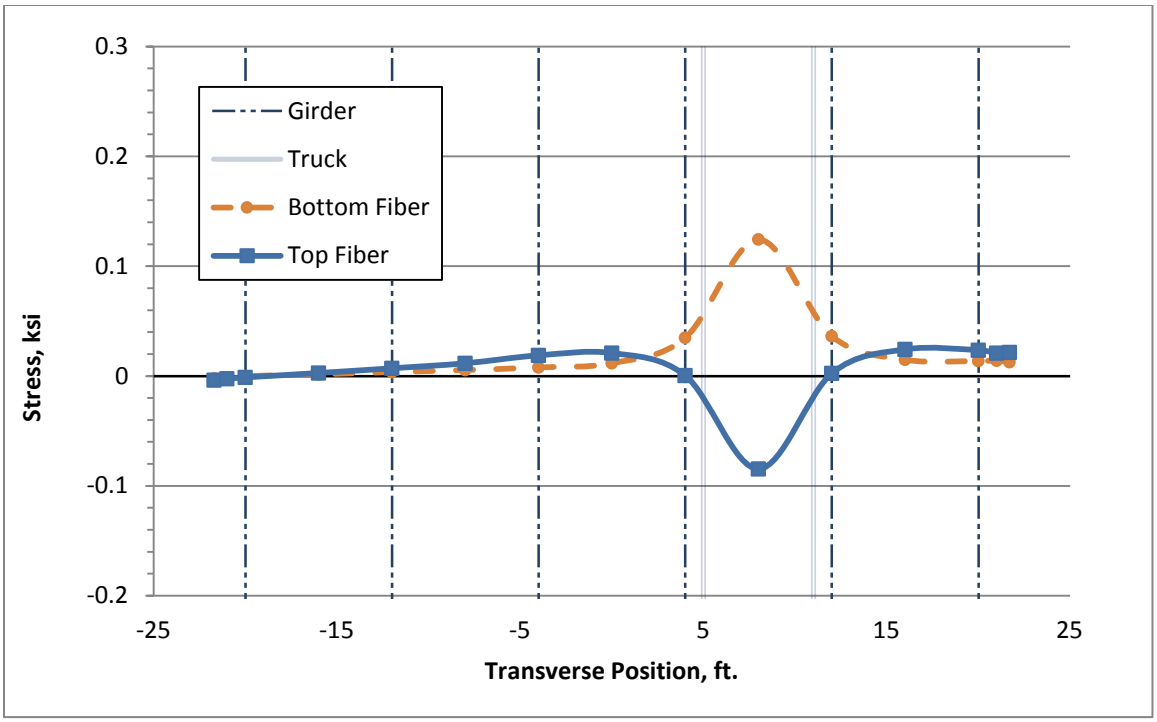

Figure B.47: Deck Stresses due to TR-8 at Critical Location 2 (80-100-80 Bridge)

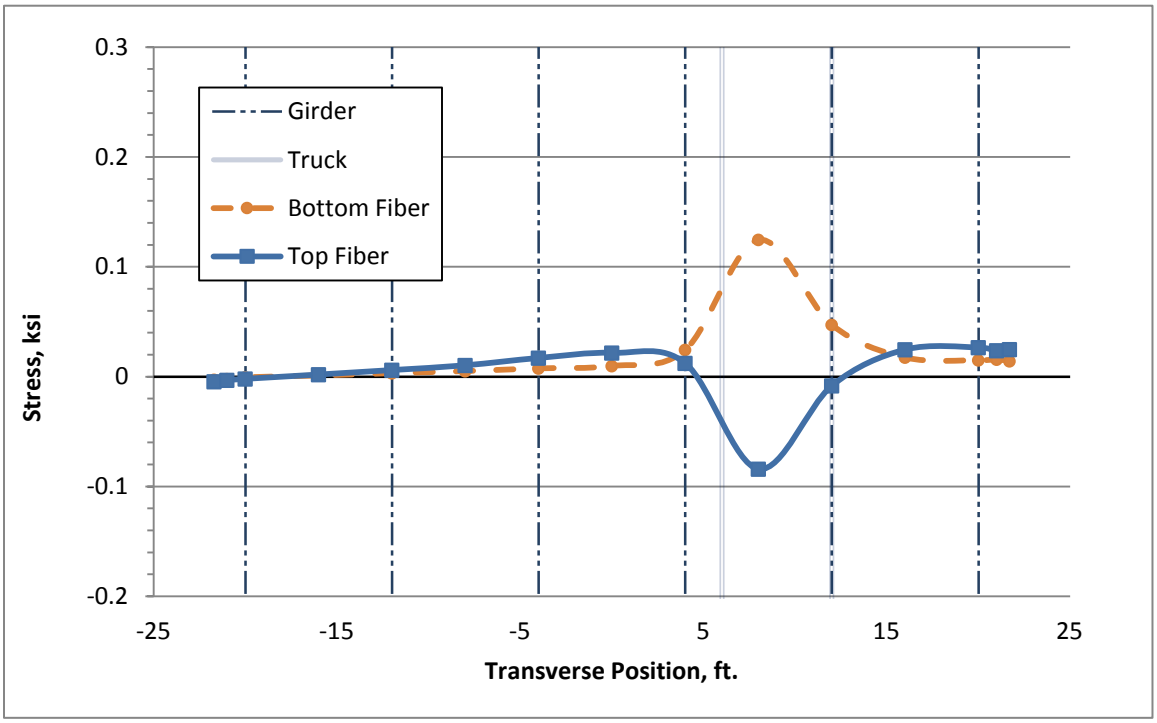

Figure B.48: Deck Stresses due to TR-9 at Critical Location 2 (80-100-80 Bridge)

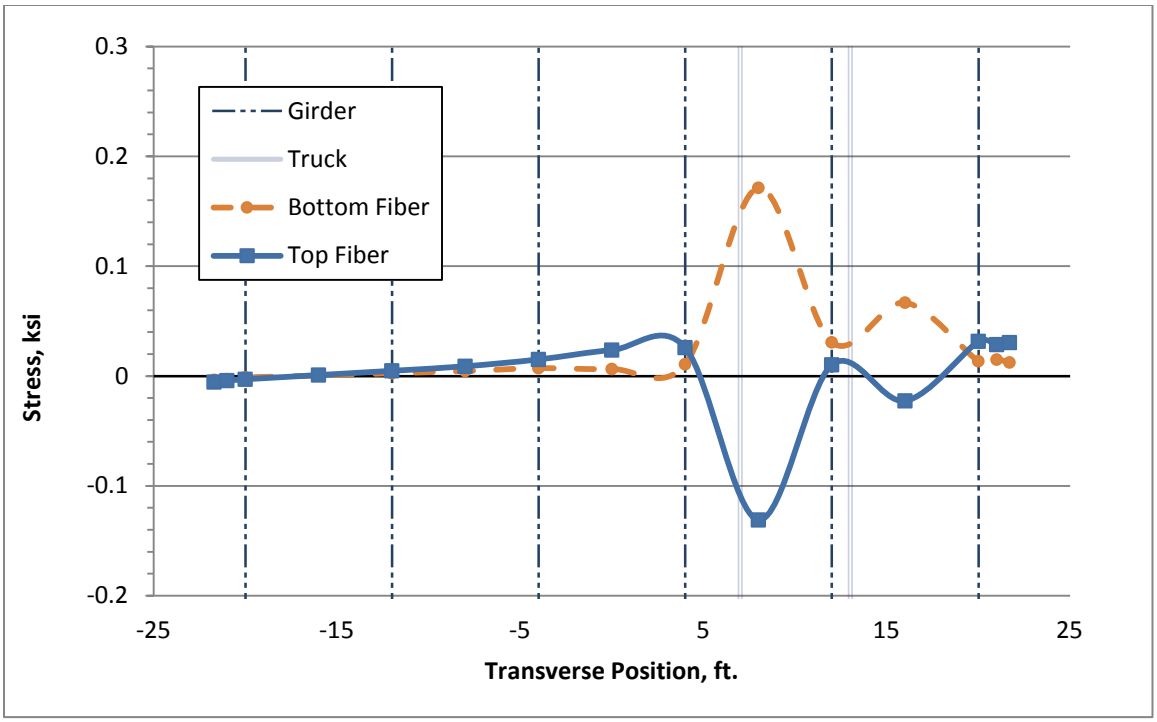

Figure B.49: Deck Stresses due to TR-10 at Critical Location 2 (80-100-80 Bridge)

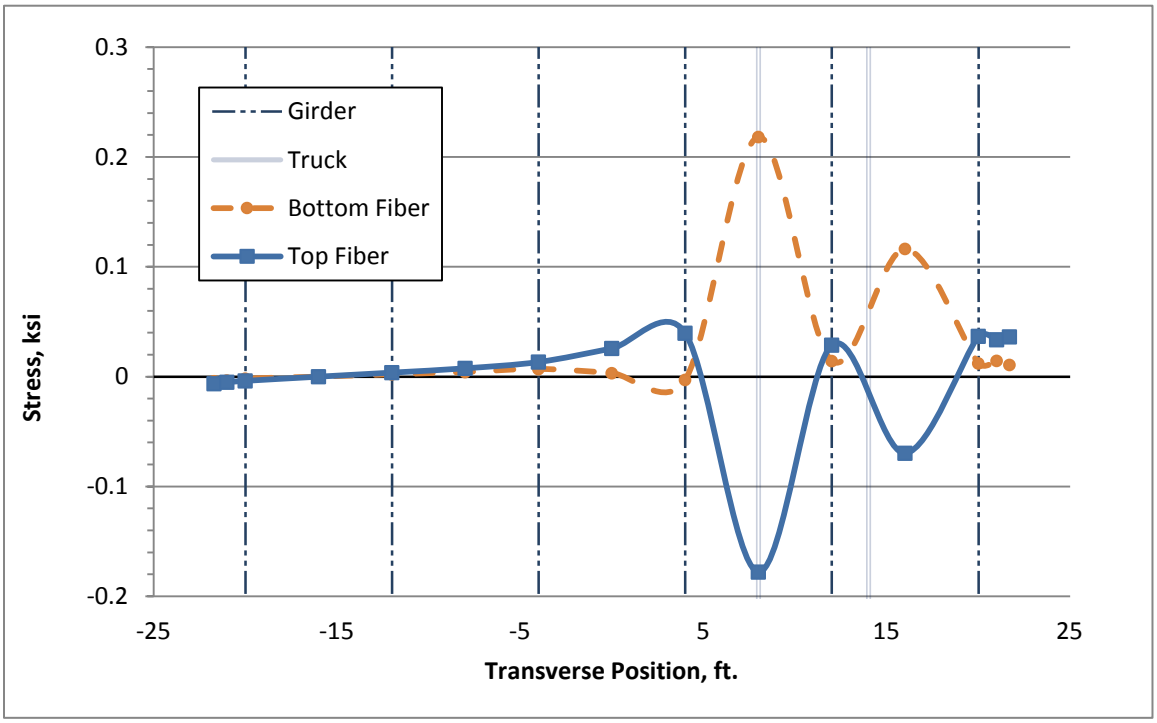

Figure B.50: Deck Stresses due to TR-11 at Critical Location 2 (80-100-80 Bridge)

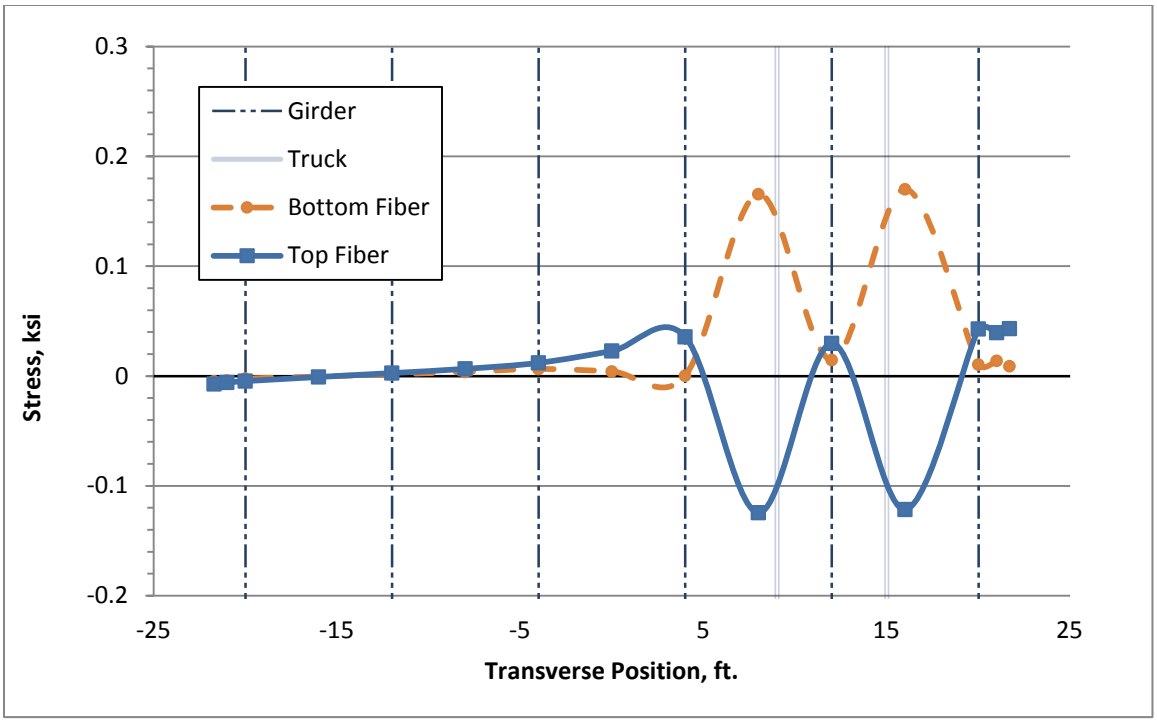

Figure B.51: Deck Stresses due to TR-12 at Critical Location 2 (80-100-80 Bridge)

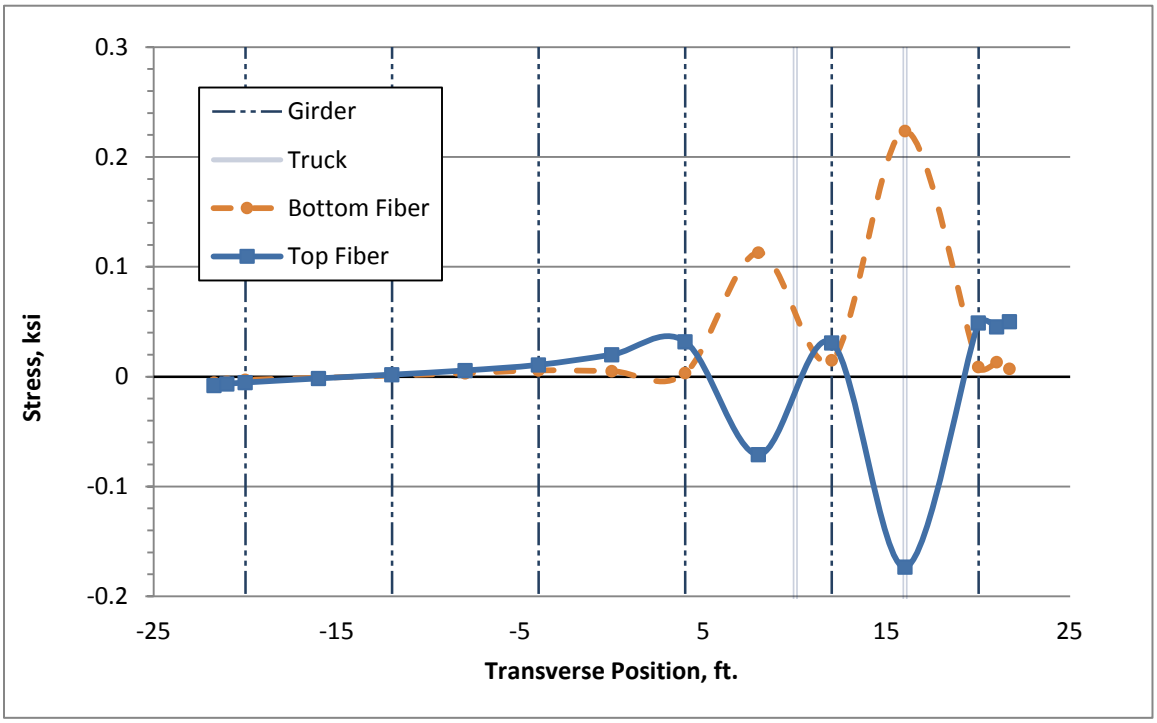

Figure B.52: Deck Stresses due to TR-13 at Critical Location 2 (80-100-80 Bridge)

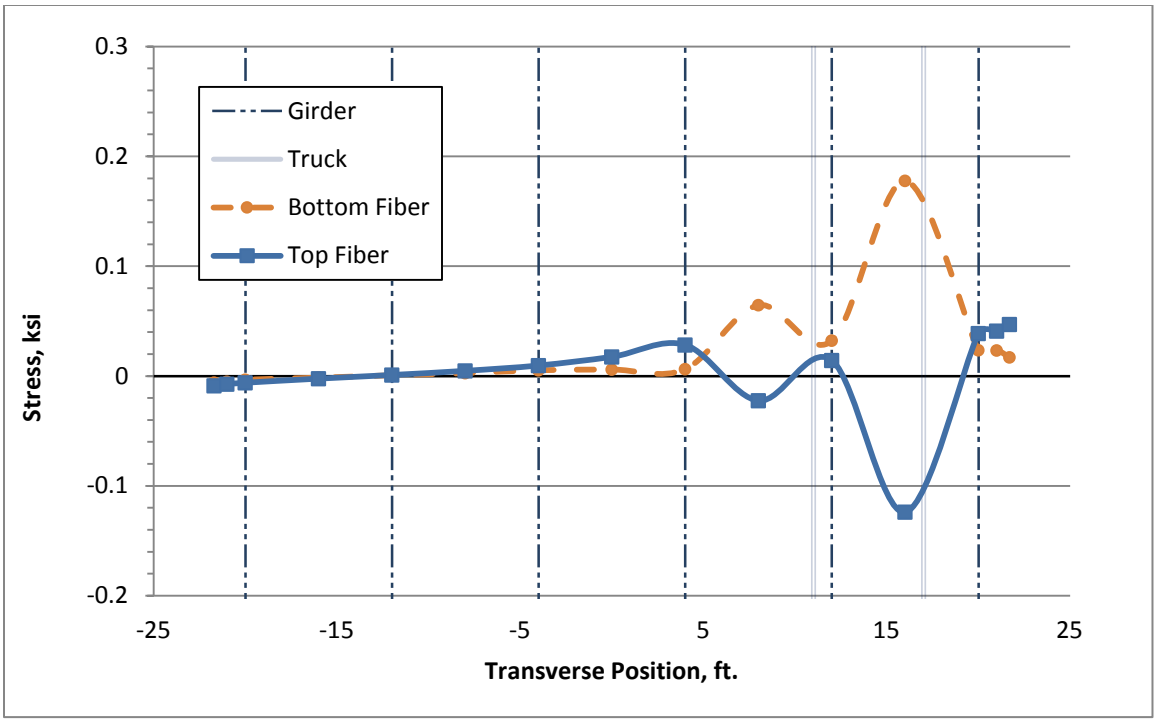

Figure B.53: Deck Stresses due to TR-14 at Critical Location 2 (80-100-80 Bridge)

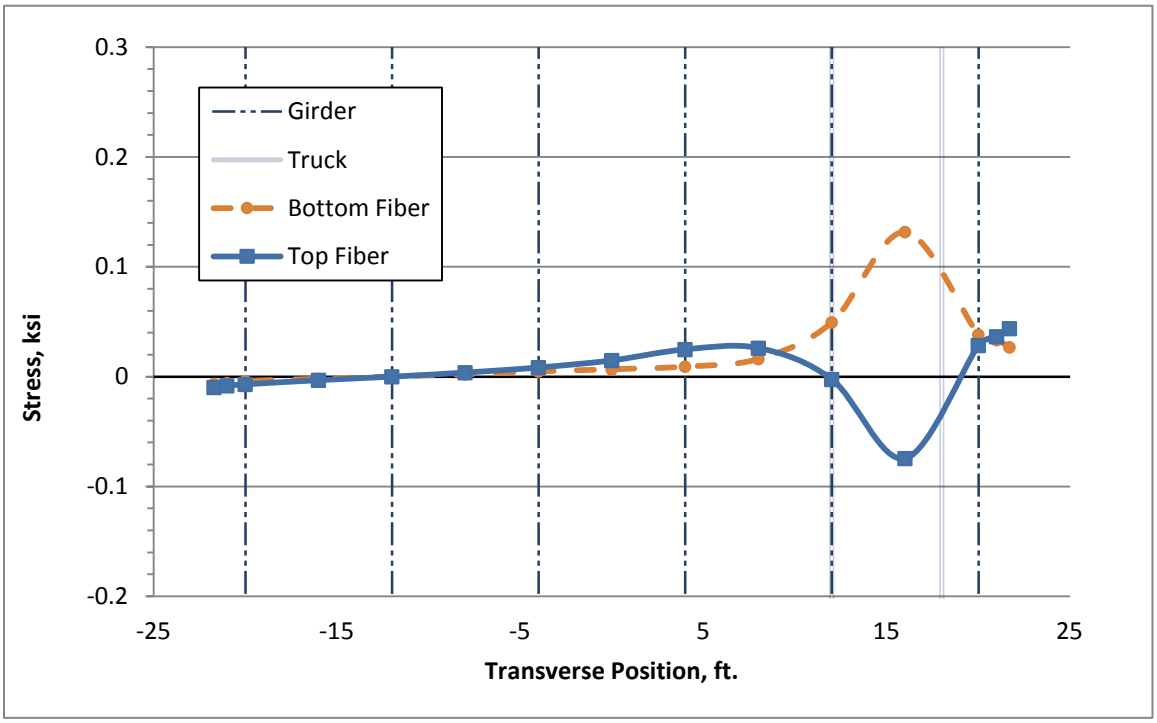

Figure B.54: Deck Stresses due to TR-15 at Critical Location 2 (80-100-80 Bridge)

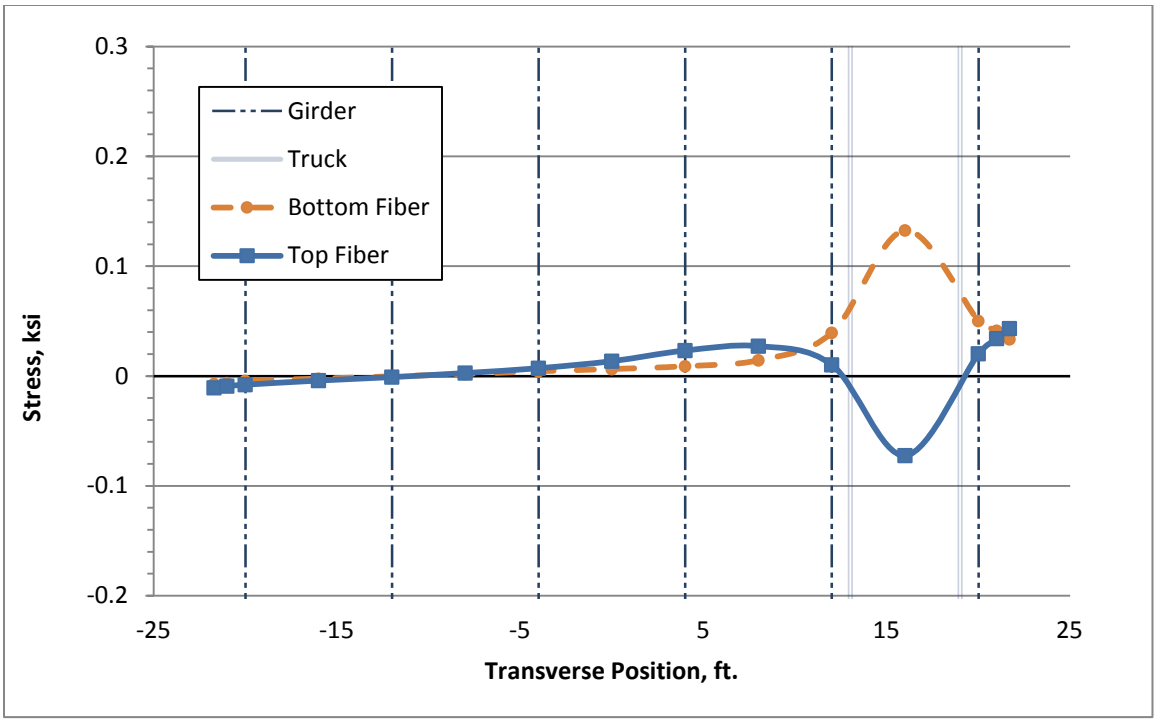

Figure B.55: Deck Stresses due to TR-16 at Critical Location 2 (80-100-80 Bridge)

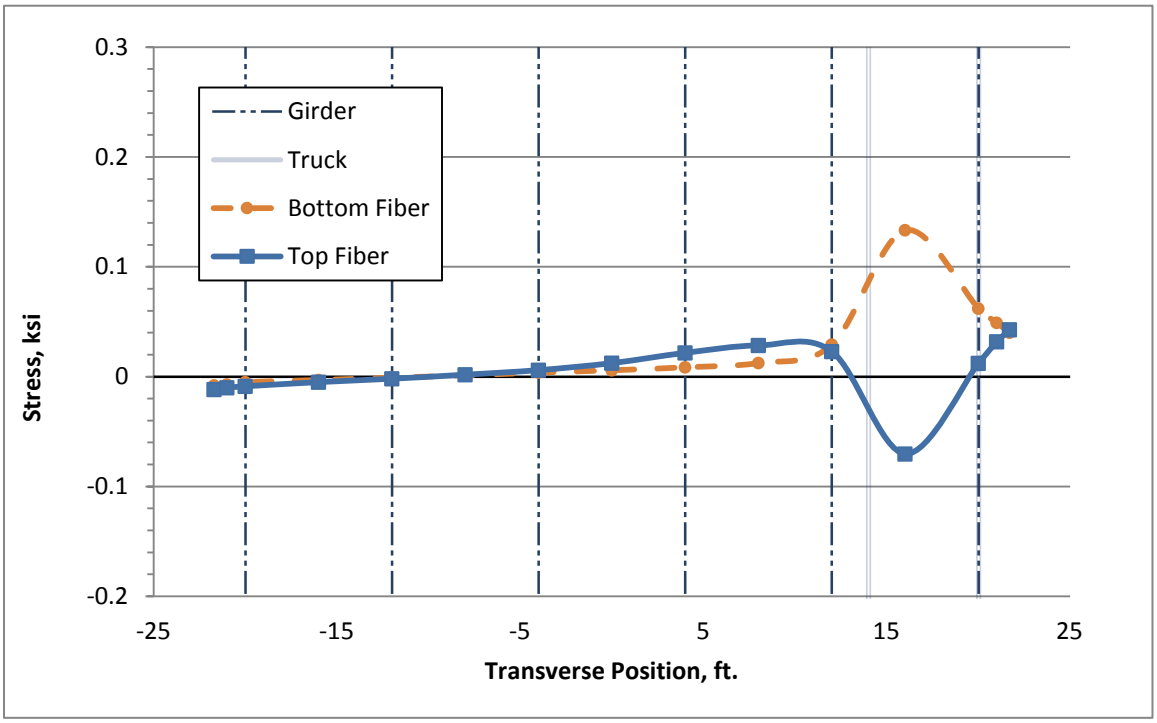

Figure B.56: Deck Stresses due to TR-17 at Critical Location 2 (80-100-80 Bridge)

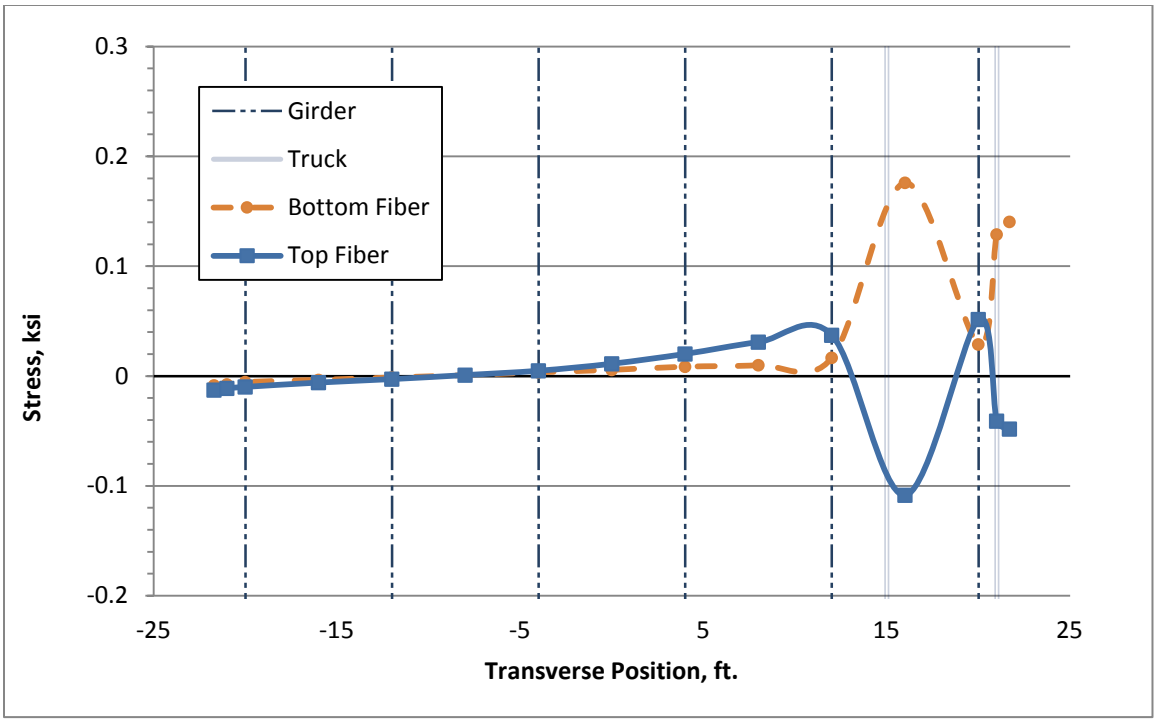

Figure B.57: Deck Stresses due to TR-18 at Critical Location 2 (80-100-80 Bridge)

A.1 Transverse Stress Plots of Negative Moment Extreme Case for 80-100-80 Bridge

Figure B.58: Deck Stresses due to TR-0 at Critical Location 1 (80-100-80 Bridge)

Figure B.59:Deck Stresses due to TR-1at Critical Location 1 (80-100-80 Bridge)

Figure B.60: Deck Stresses due to TR-2 at Critical Location 1 (80-100-80 Bridge)

Figure B.61: Deck Stresses due to TR-3 at Critical Location 1 (80-100-80 Bridge)

Figure B.62: Deck Stresses due to TR-4 at Critical Location 1 (80-100-80 Bridge)

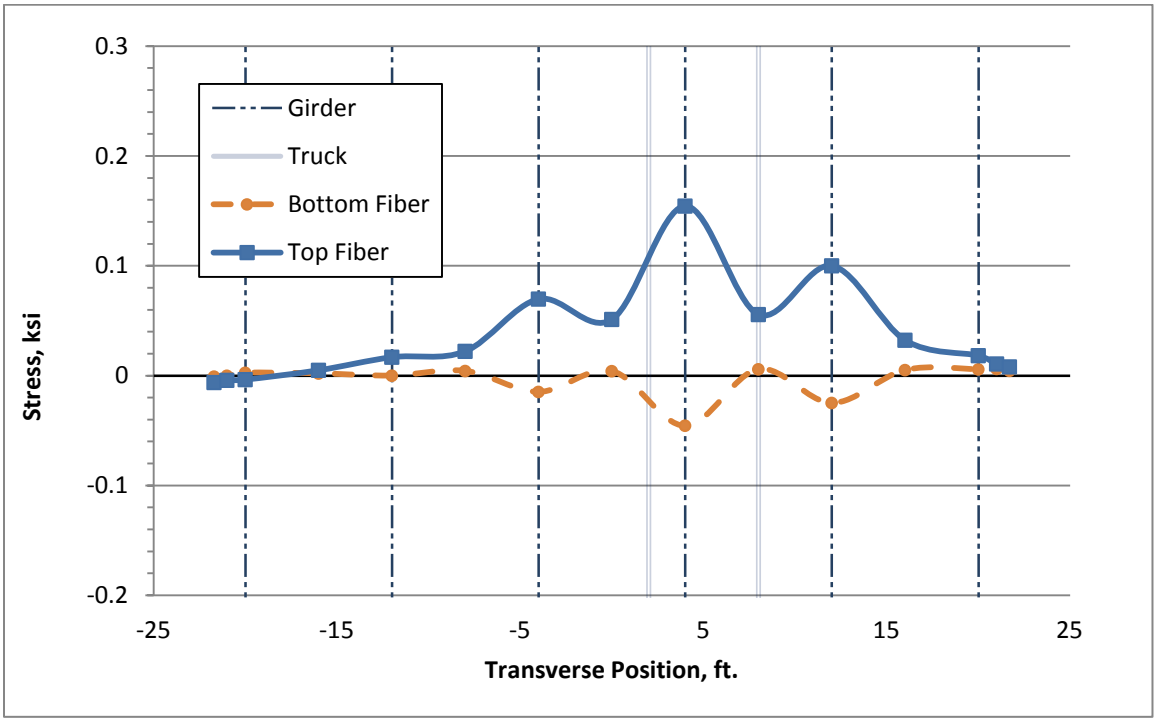

Figure B.63: Deck Stresses due to TR-5 at Critical Location 1 (80-100-80 Bridge)

Figure B.64: Deck Stresses due to TR-6 at Critical Location 1 (80-100-80 Bridge)

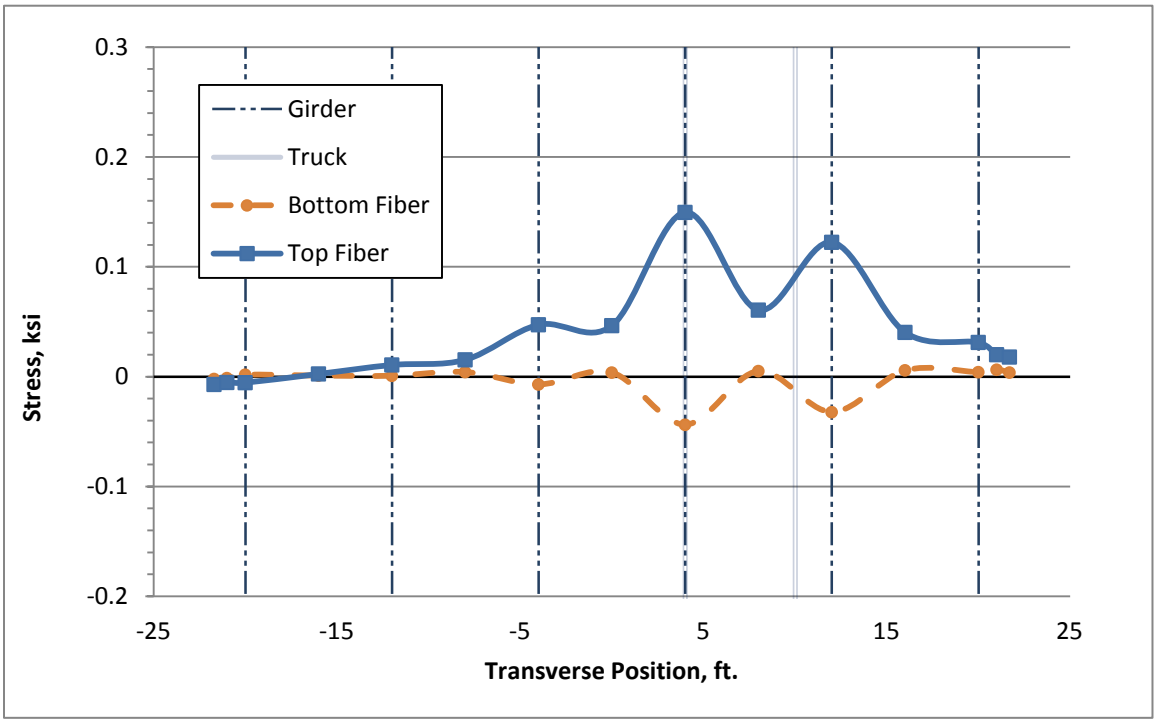

Figure B.65: Deck Stresses due to TR-7 at Critical Location 1 (80-100-80 Bridge)

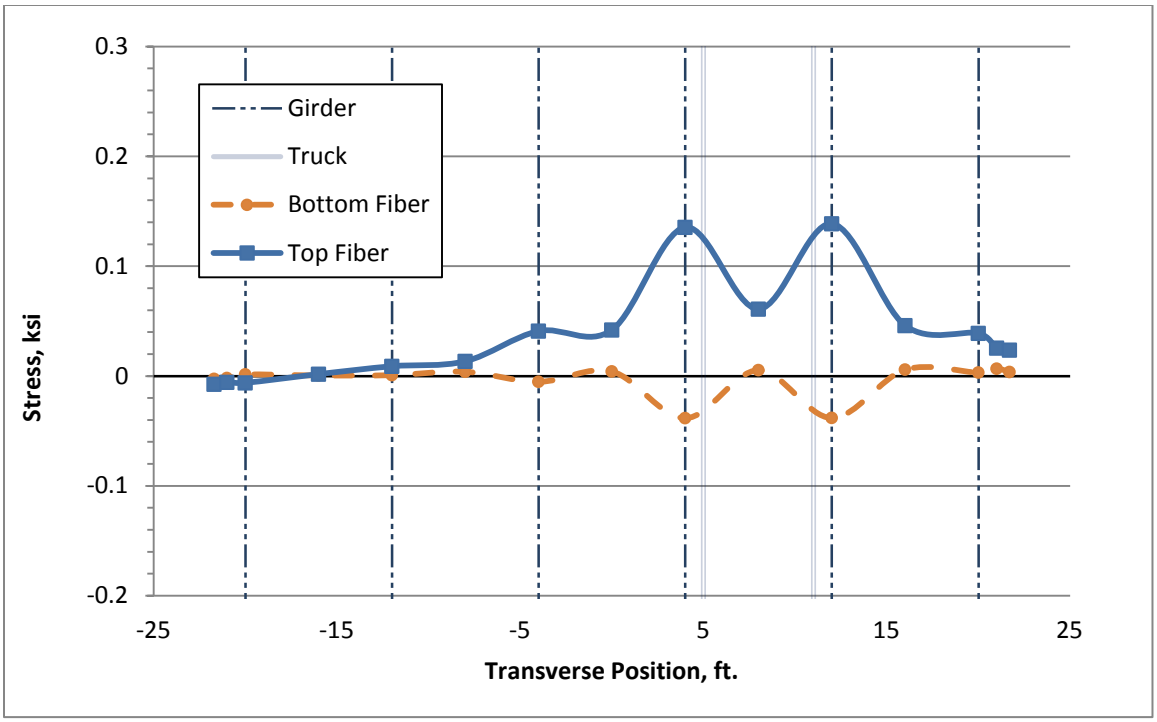

Figure B.66: Deck Stresses due to TR-8 at Critical Location 1 (80-100-80 Bridge)

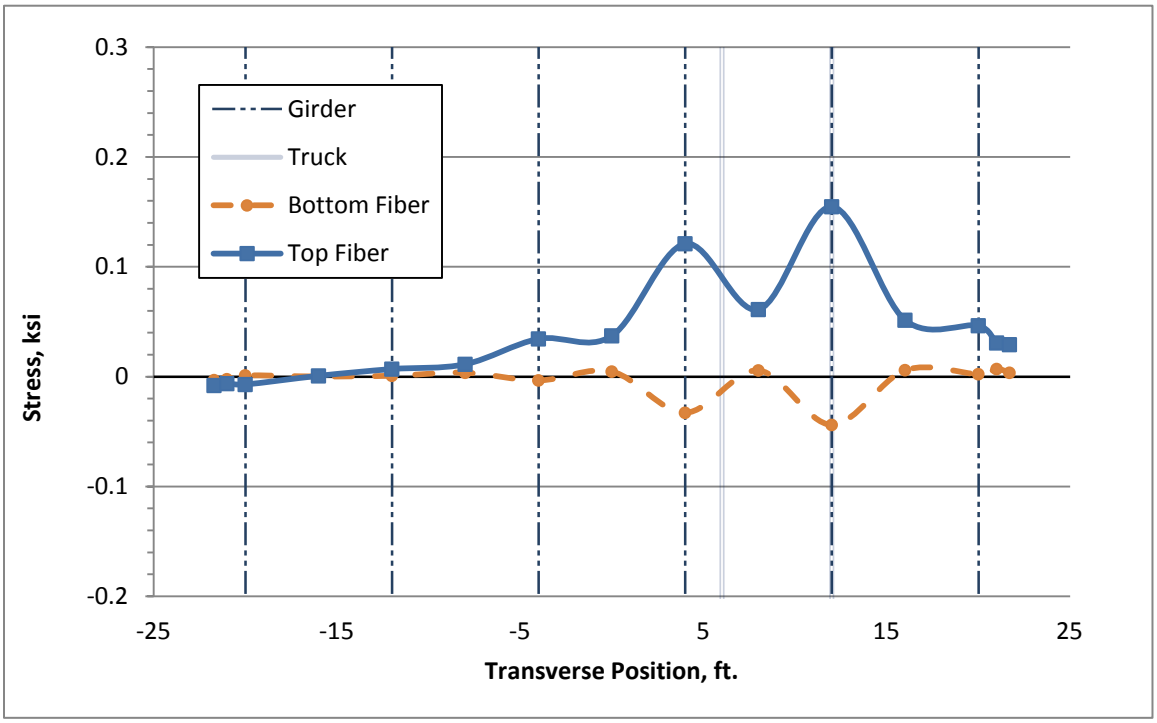

Figure B.67: Deck Stresses due to TR-9 at Critical Location 1 (80-100-80 Bridge)

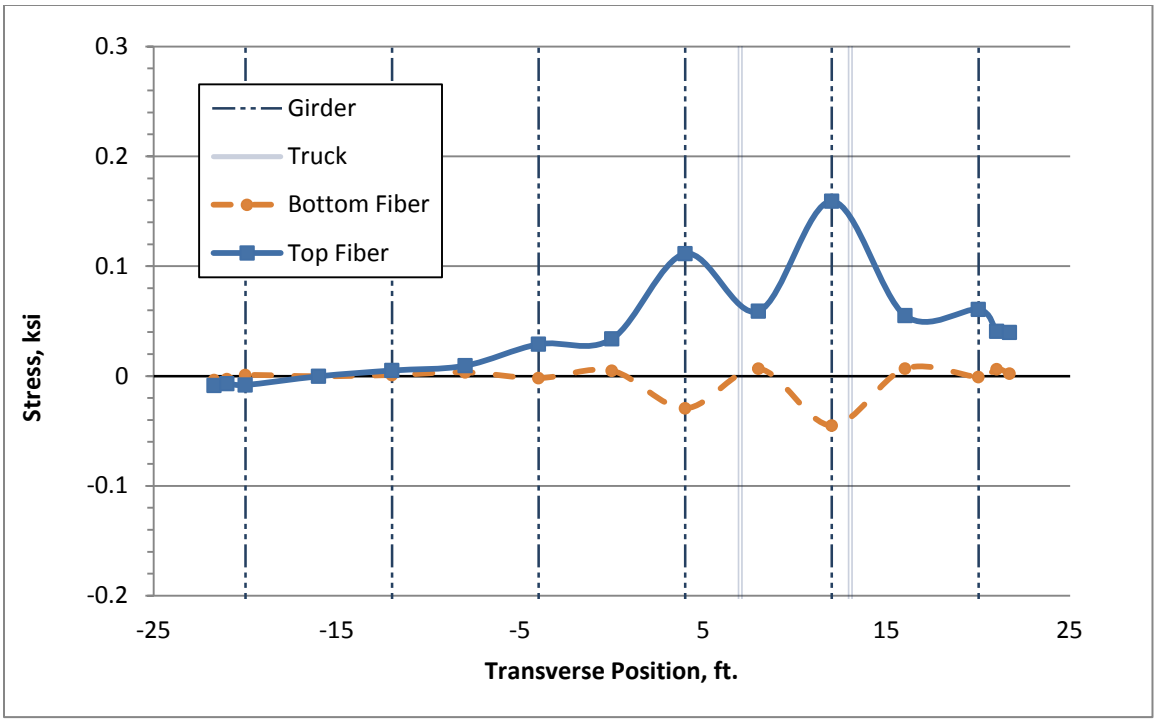

Figure B.68: Deck Stresses due to TR-10 at Critical Location 1 (80-100-80 Bridge)

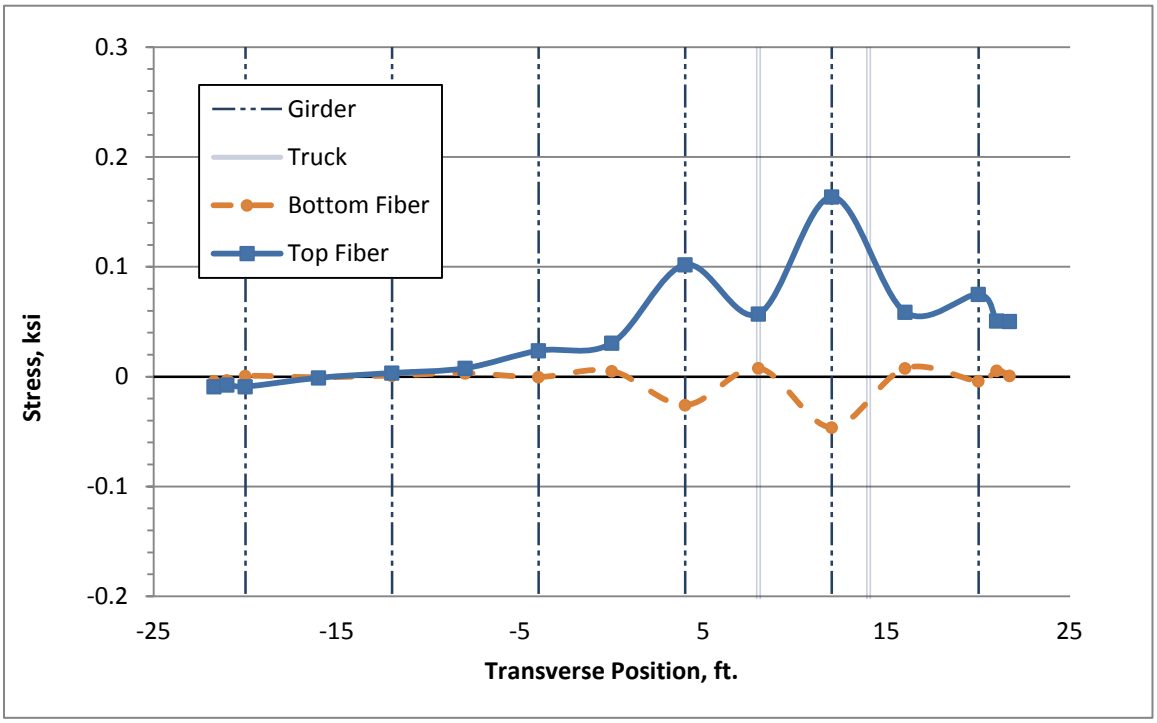

Figure B.69: Deck Stresses due to TR-11 at Critical Location 1 (80-100-80 Bridge)

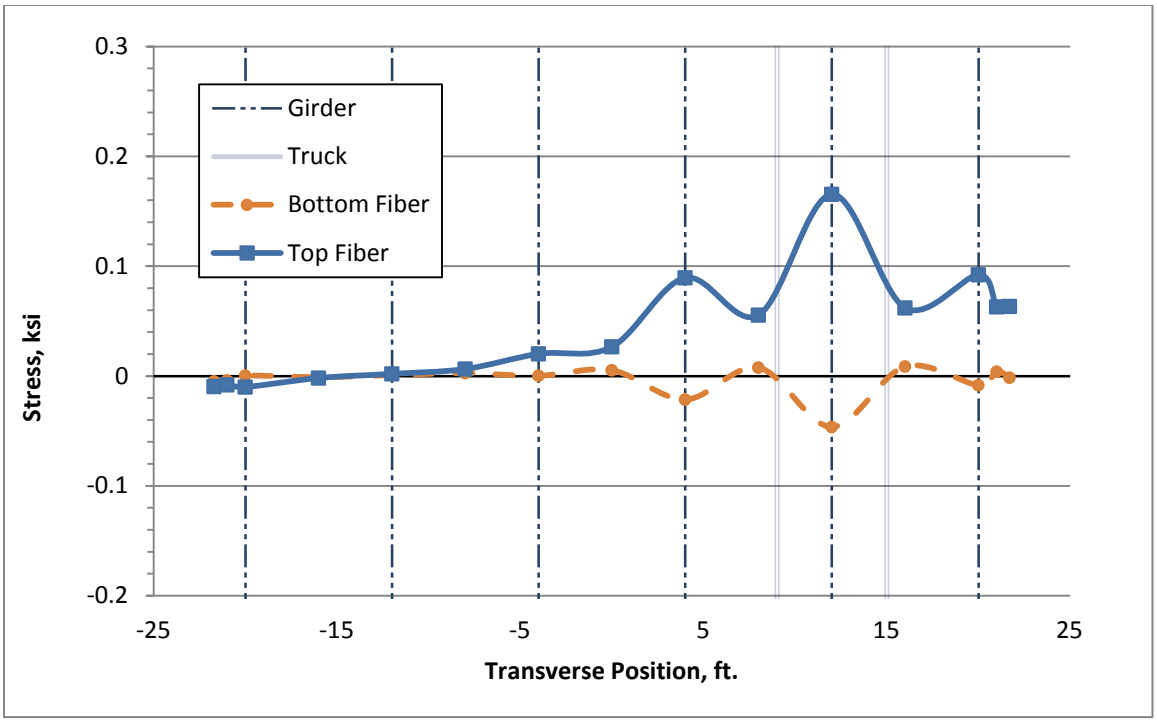

Figure B.70: Deck Stresses due to TR-12 at Critical Location 1 (80-100-80 Bridge)

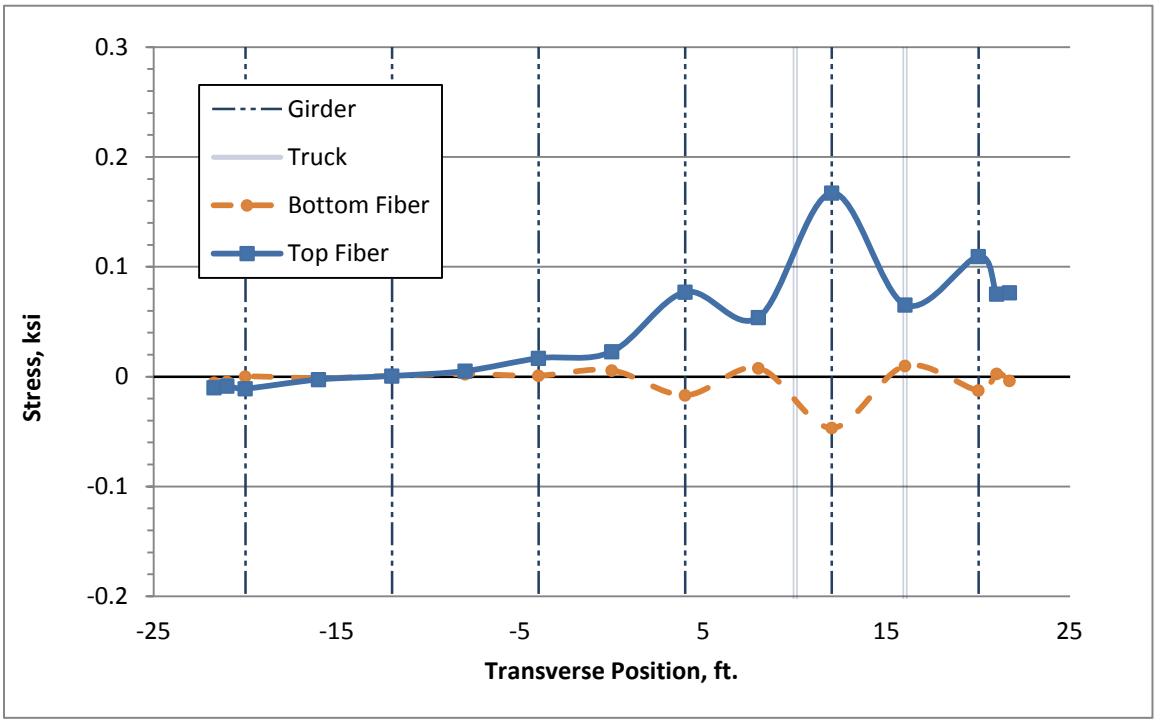

Figure B.71: Deck Stresses due to TR-13 at Critical Location 1 (80-100-80 Bridge)

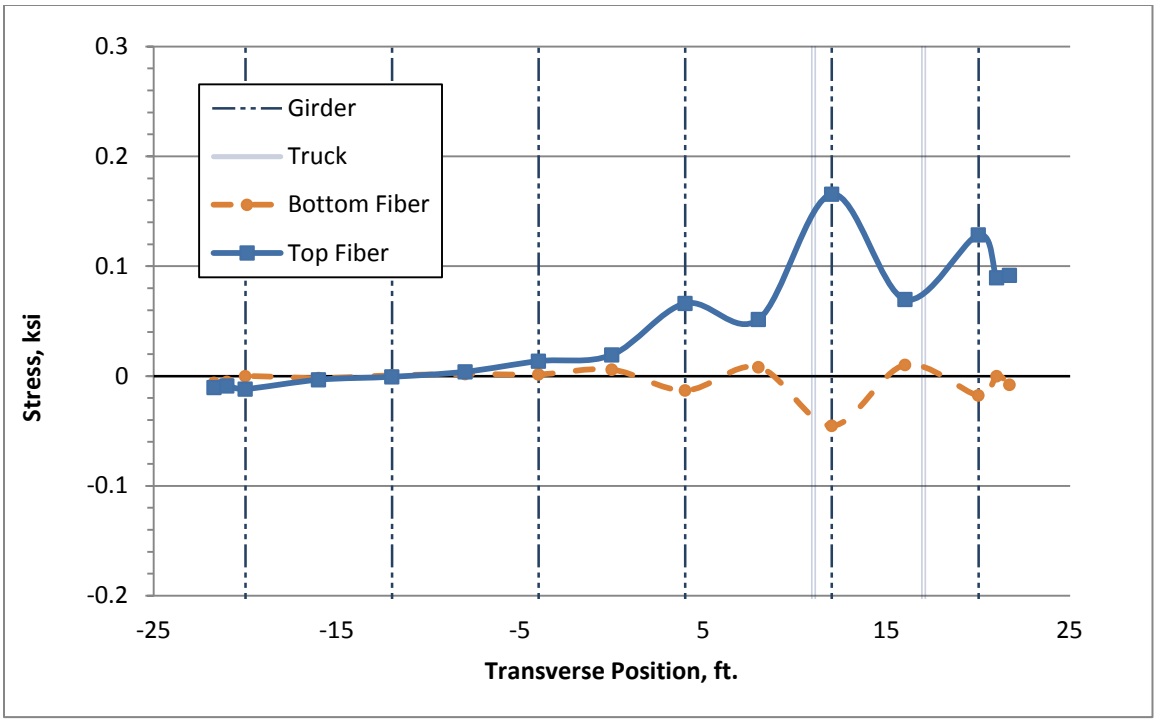

Figure B.72: Deck Stresses due to TR-14 at Critical Location 1 (80-100-80 Bridge)

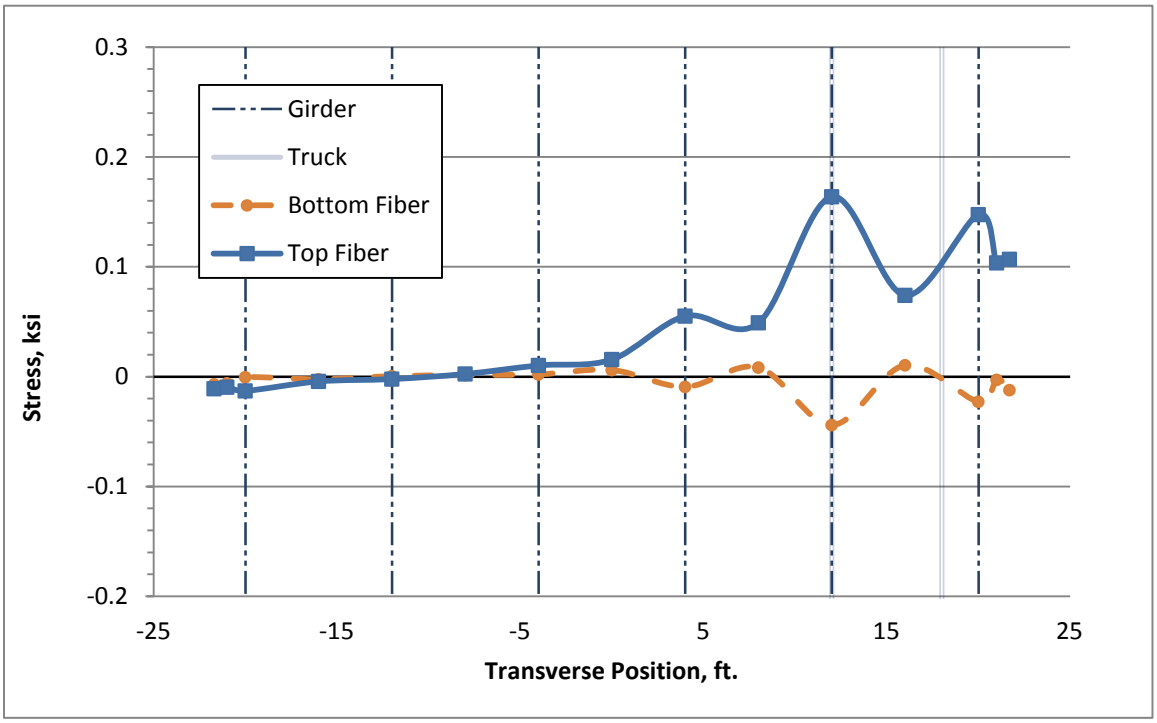

Figure B.73: Deck Stresses due to TR-15 at Critical Location 1 (80-100-80 Bridge)

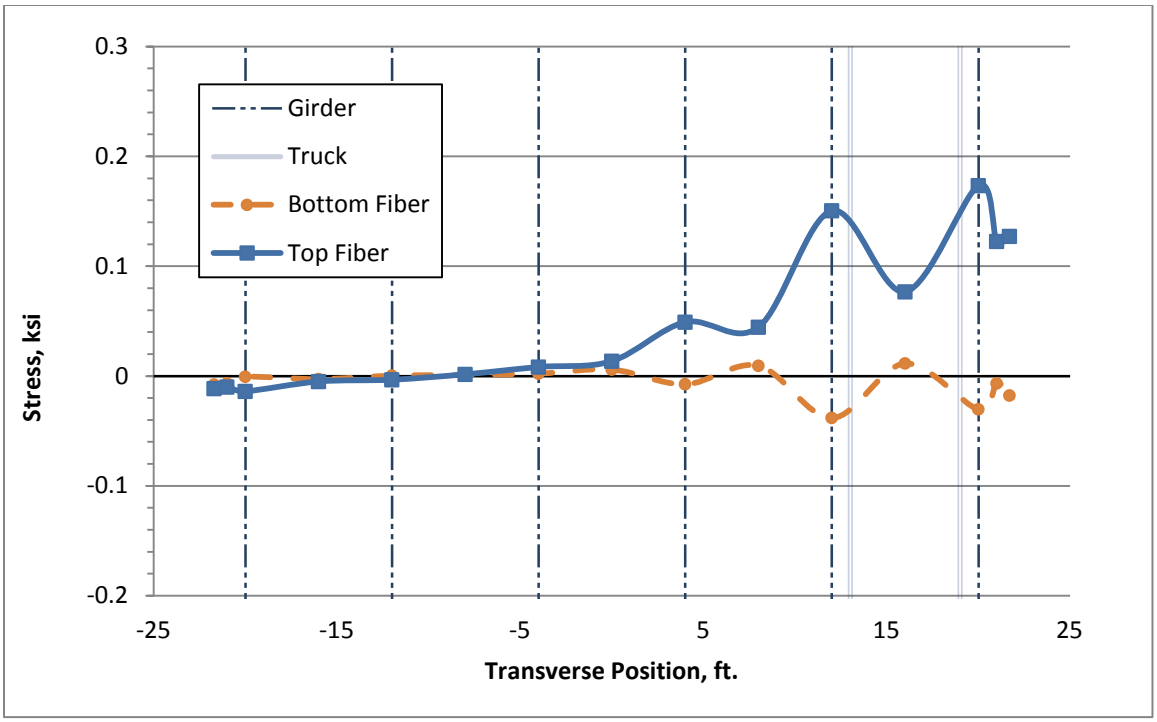

Figure B.74: Deck Stresses due to TR-16 at Critical Location 1 (80-100-80 Bridge)

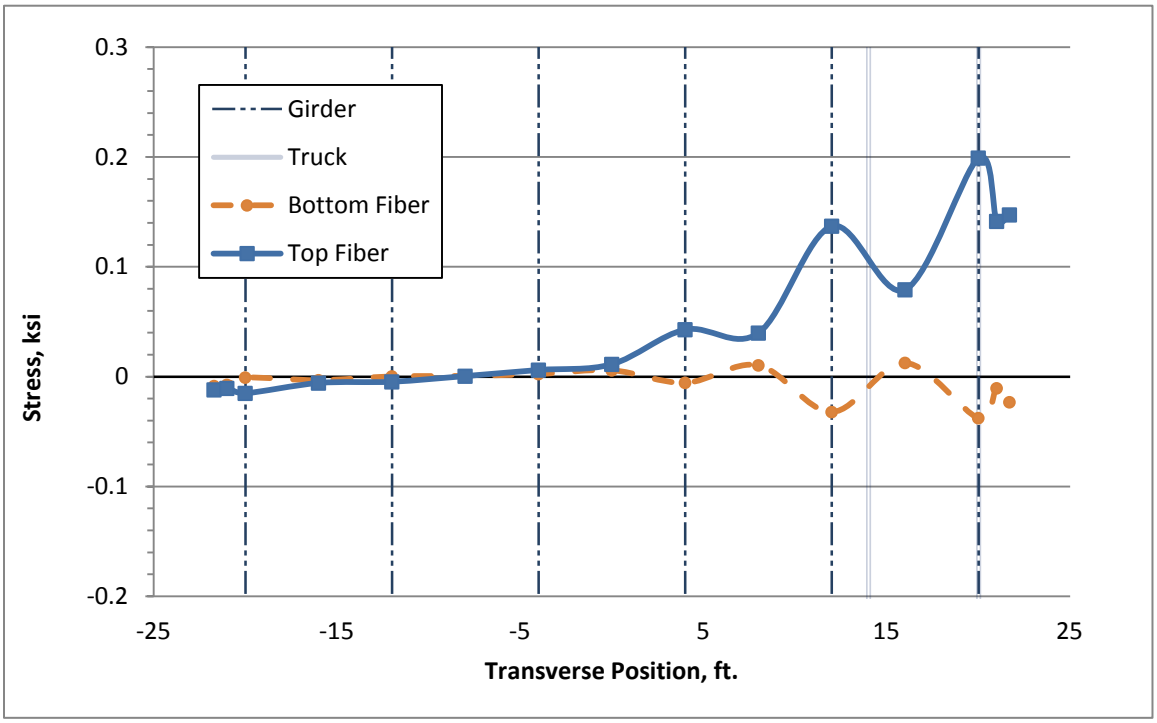

Figure B.75: Deck Stresses due to TR-17 at Critical Location 1 (80-100-80 Bridge)

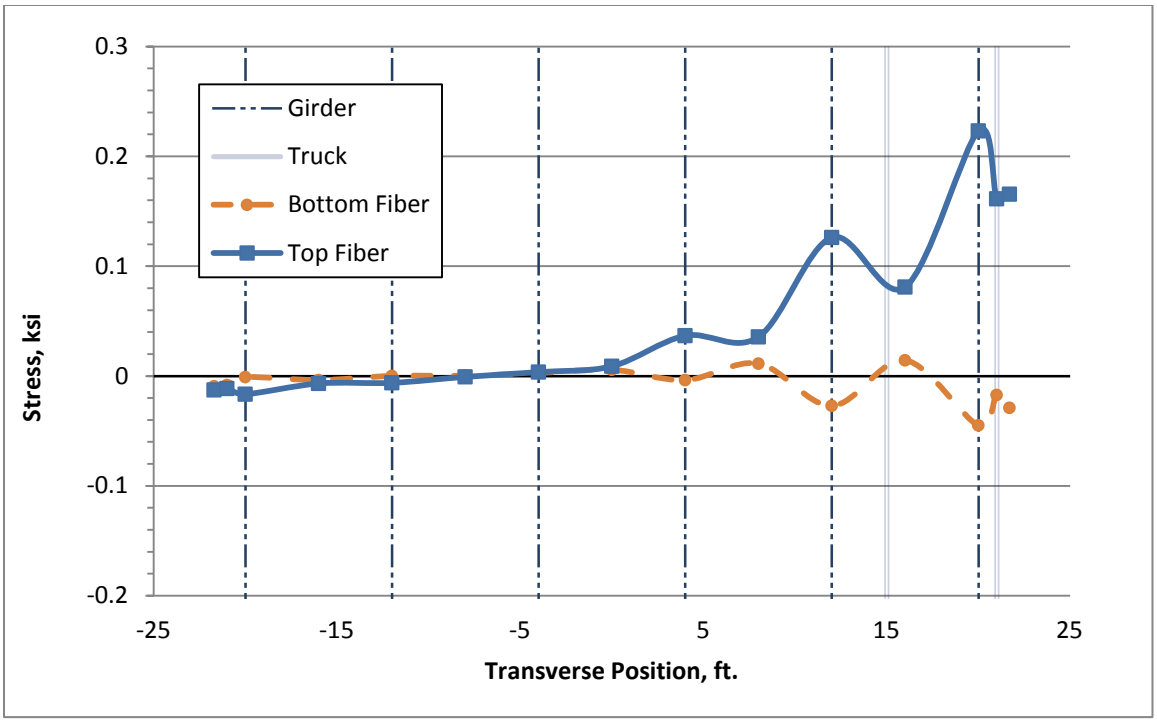

Figure B.76: Deck Stresses due to TR-18 at Critical Location 1 (80-100-80 Bridge)

A.2 Transverse Stress Plots for Positive-Flexure Extreme Case for Simple Span Bridge

Figure B.77: Deck Stresses due to TR-0 at Critical Location 1(Simple Span Bridge)

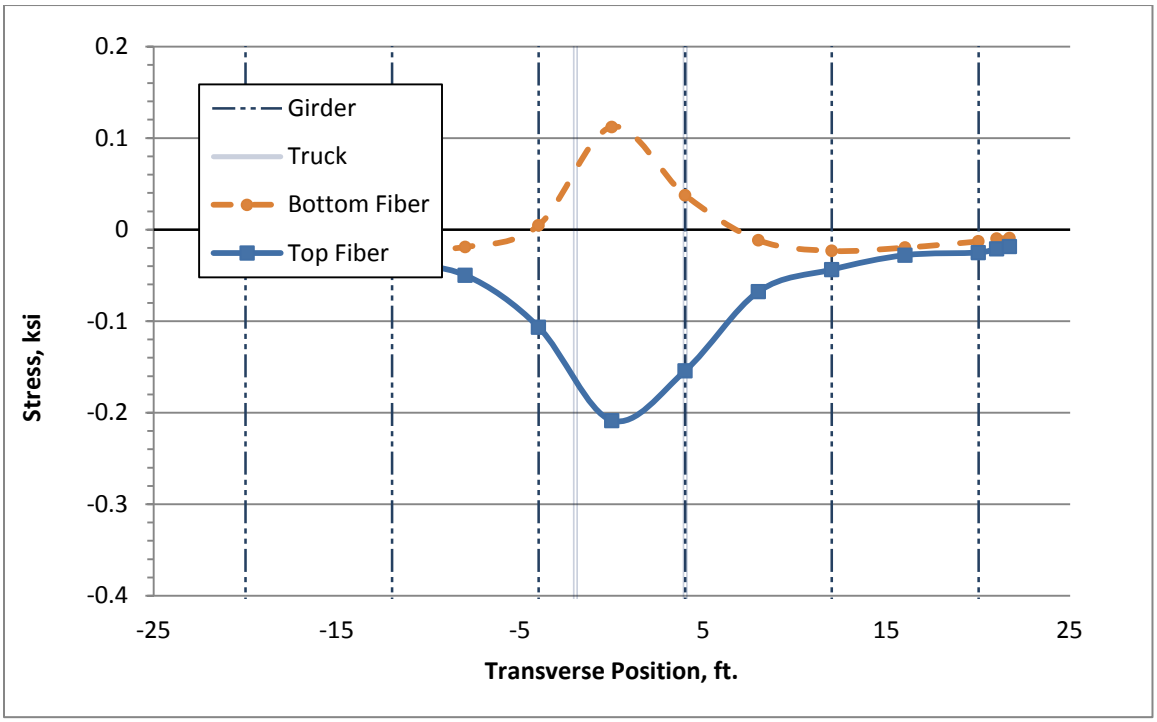

Figure B.78: Deck Stresses due to TR-1at Critical Location 1(Simple Span Bridge)

Figure B.79: Deck Stresses due to TR-2 at Critical Location 1 (Simple Span Bridge)

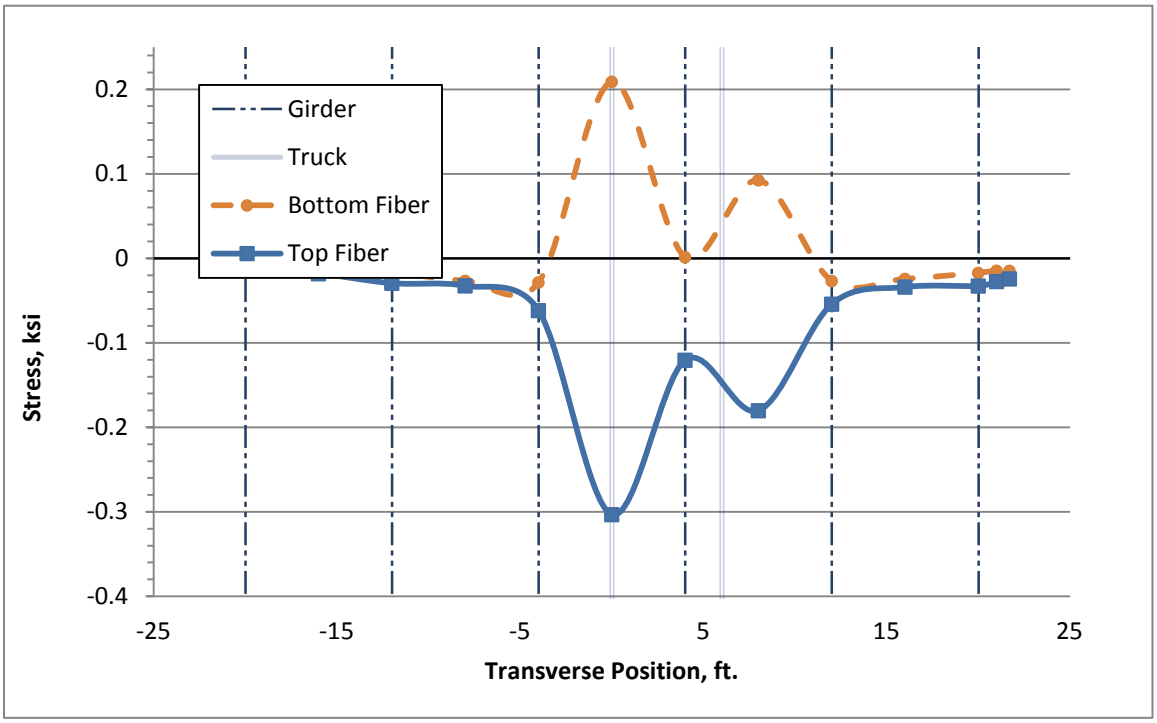

Figure B.80: Deck Stresses due to TR-3 at Critical Location 1 (Simple Span Bridge)

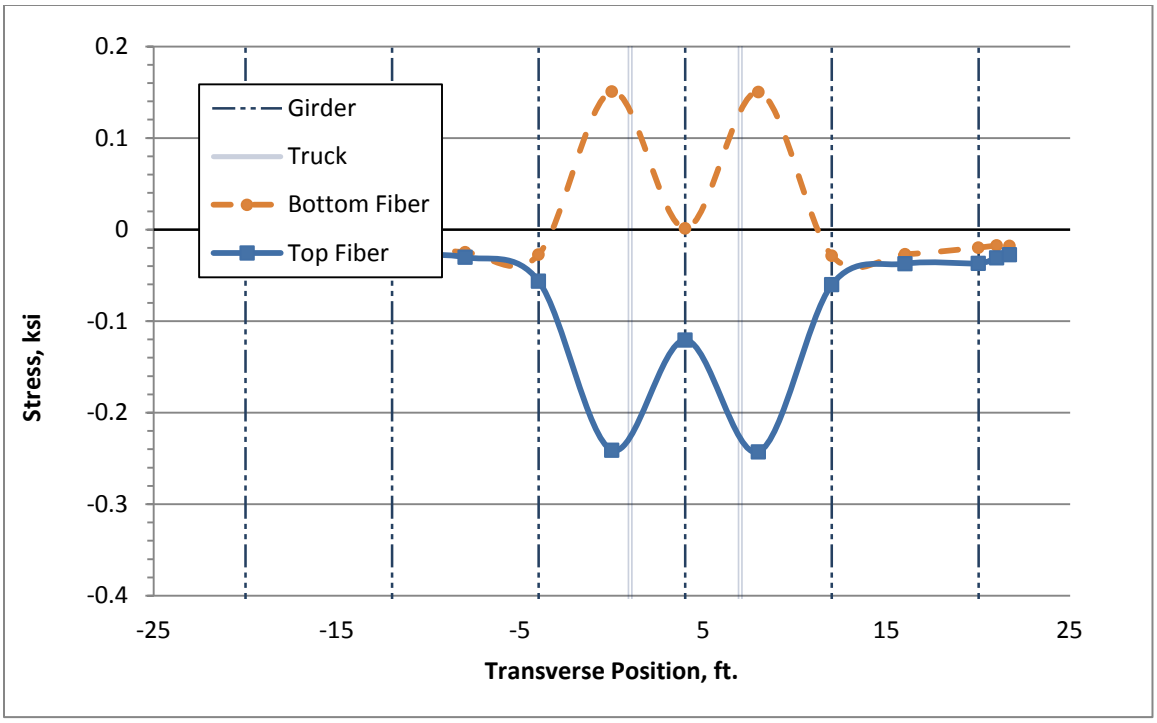

Figure B.81: Deck Stresses due to TR-4 at Critical Location 1 (Simple Span Bridge)

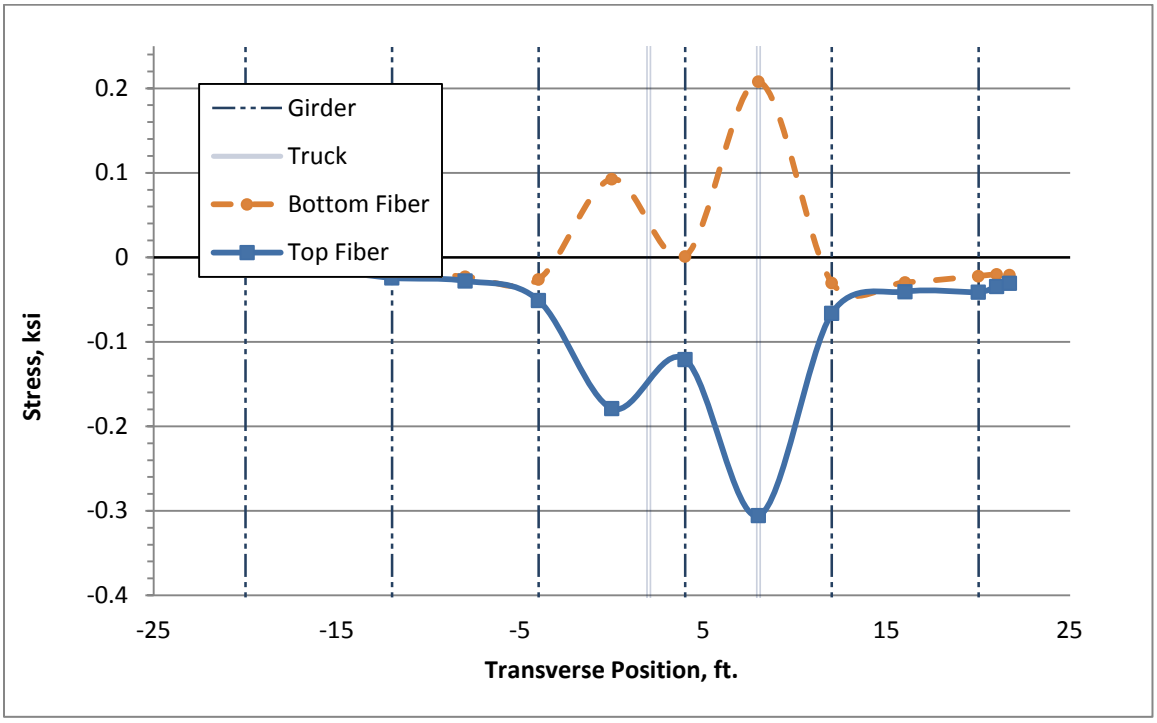

Figure B.82: Deck Stresses due to TR-5 at Critical Location 1 (Simple Span Bridge)

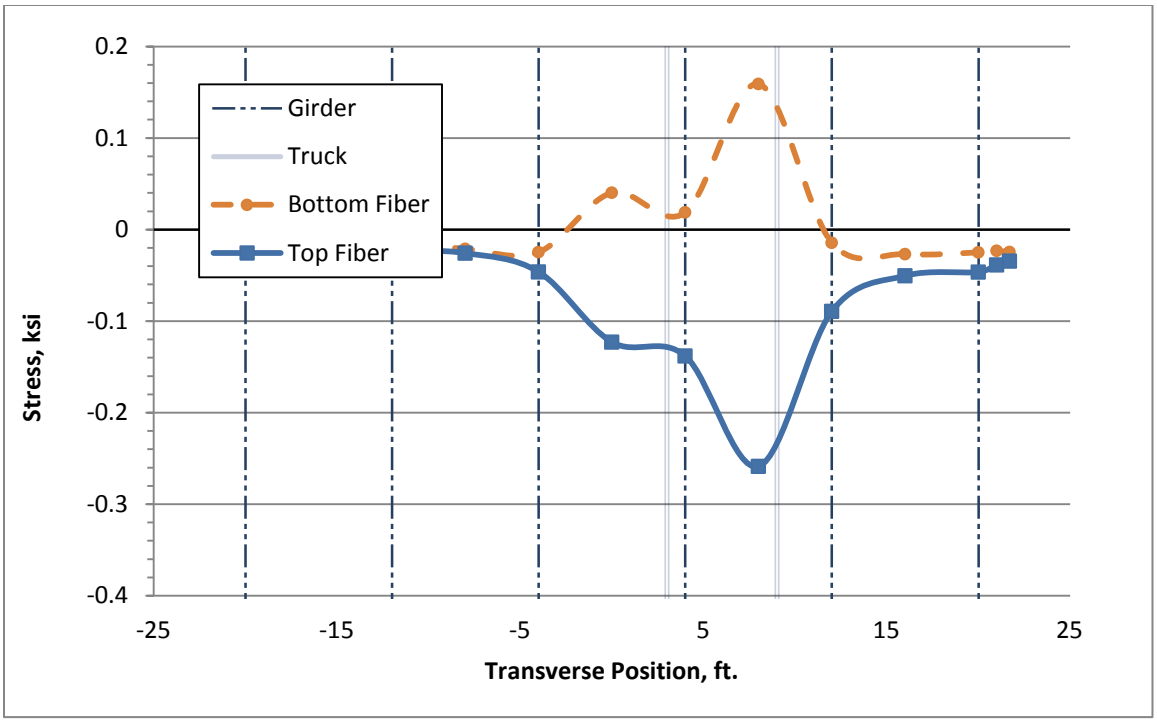

Figure B.83: Deck Stresses due to TR-6 at Critical Location 1 (Simple Span Bridge)

Figure B.84: Deck Stresses due to TR-7 at Critical Location 1 (Simple Span Bridge)

Figure B.85: Deck Stresses due to TR-8 at Critical Location 1 (Simple Span Bridge)

Figure B.86: Deck Stresses due to TR-9 at Critical Location 1 (Simple Span Bridge)

Figure B.87: Deck Stresses due to TR-10 at Critical Location 1 (Simple Span Bridge)

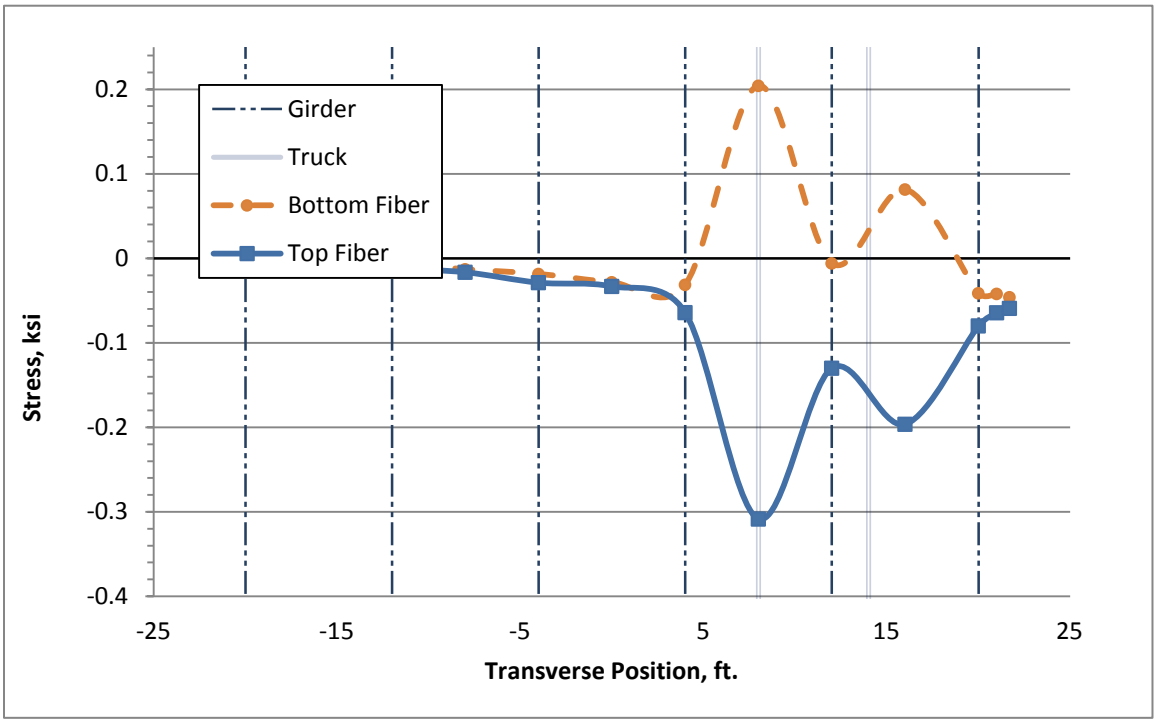

Figure B.88: Deck Stresses due to TR-11 at Critical Location 1 (Simple Span Bridge)

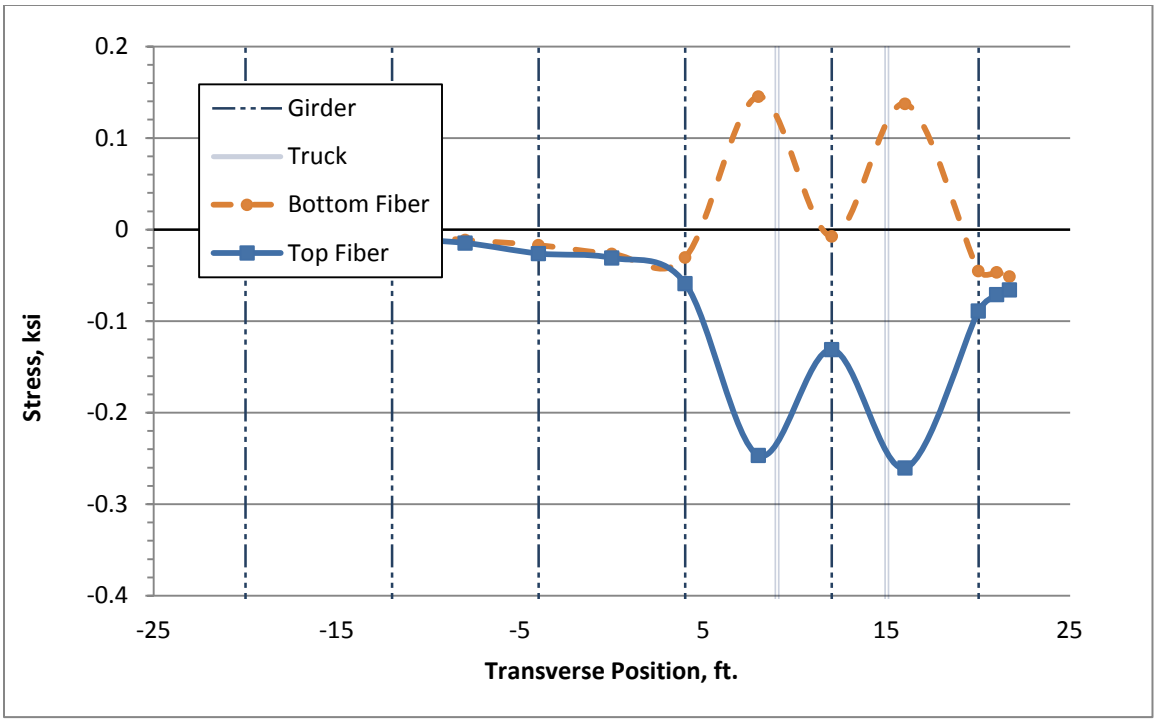

Figure B.89: Deck Stresses due to TR-12 at Critical Location 1 (Simple Span Bridge)

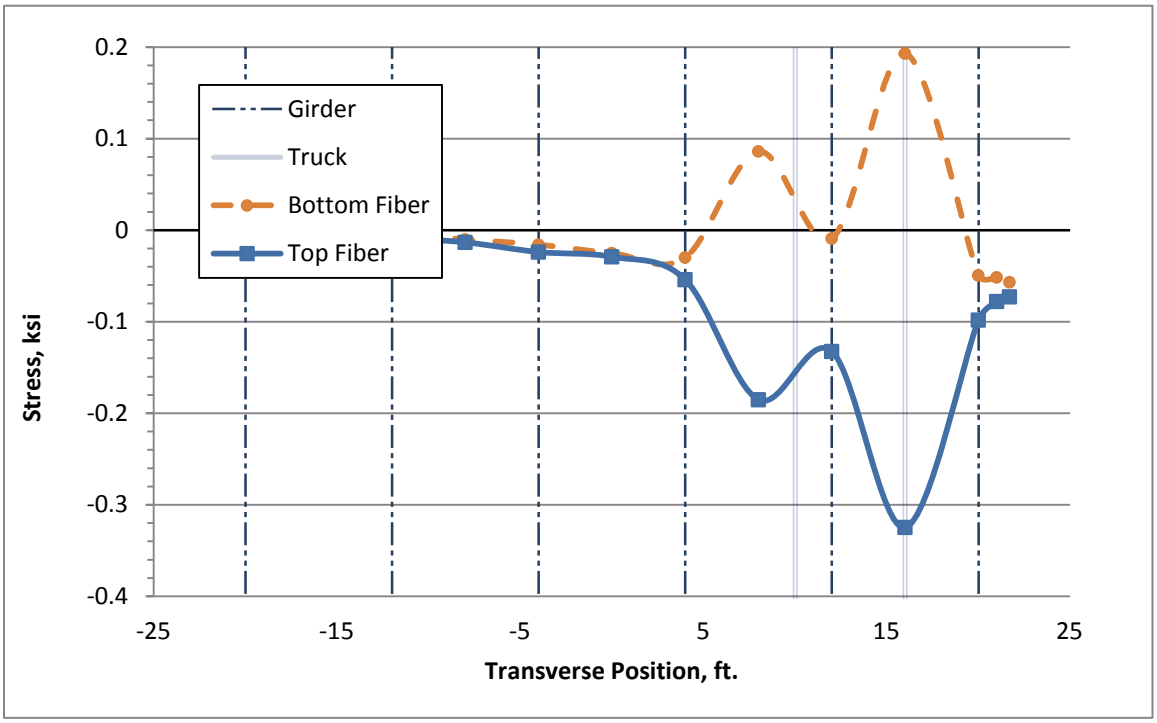

Figure B.90: Deck Stresses due to TR-13 at Critical Location 1 (Simple Span Bridge)

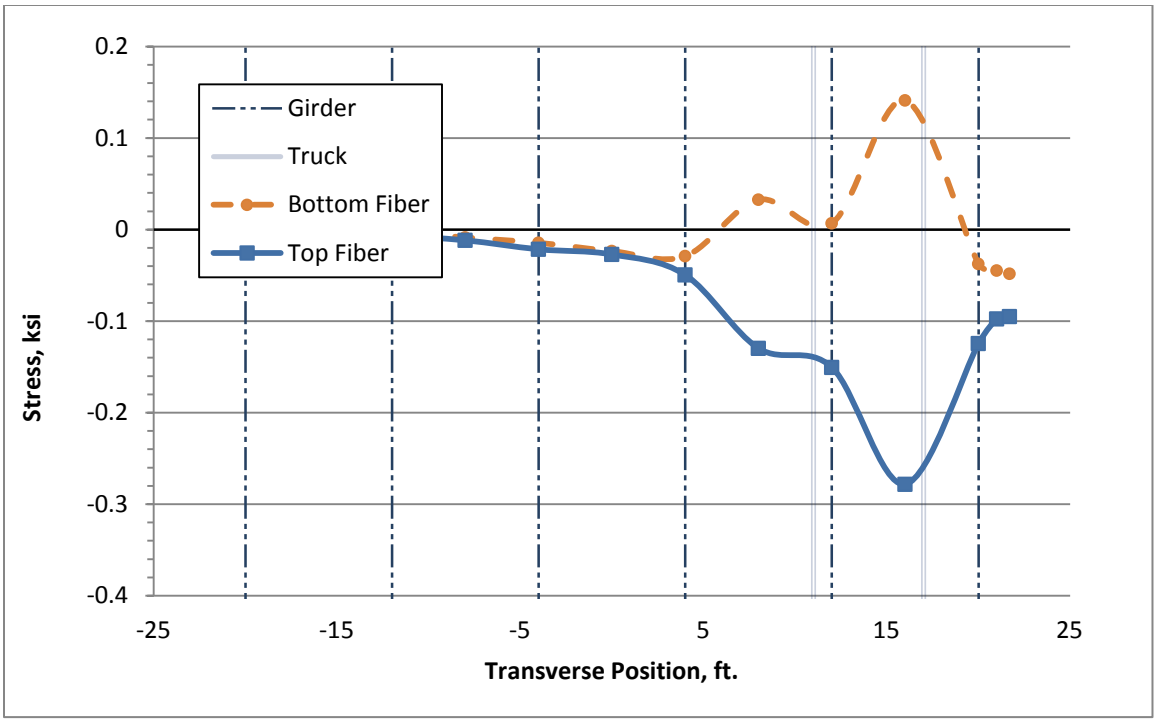

Figure B.91: Deck Stresses due to TR-14 at Critical Location 1 (Simple Span Bridge)

Figure B.92: Deck Stresses due to TR-15 at Critical Location 1 (Simple Span Bridge)

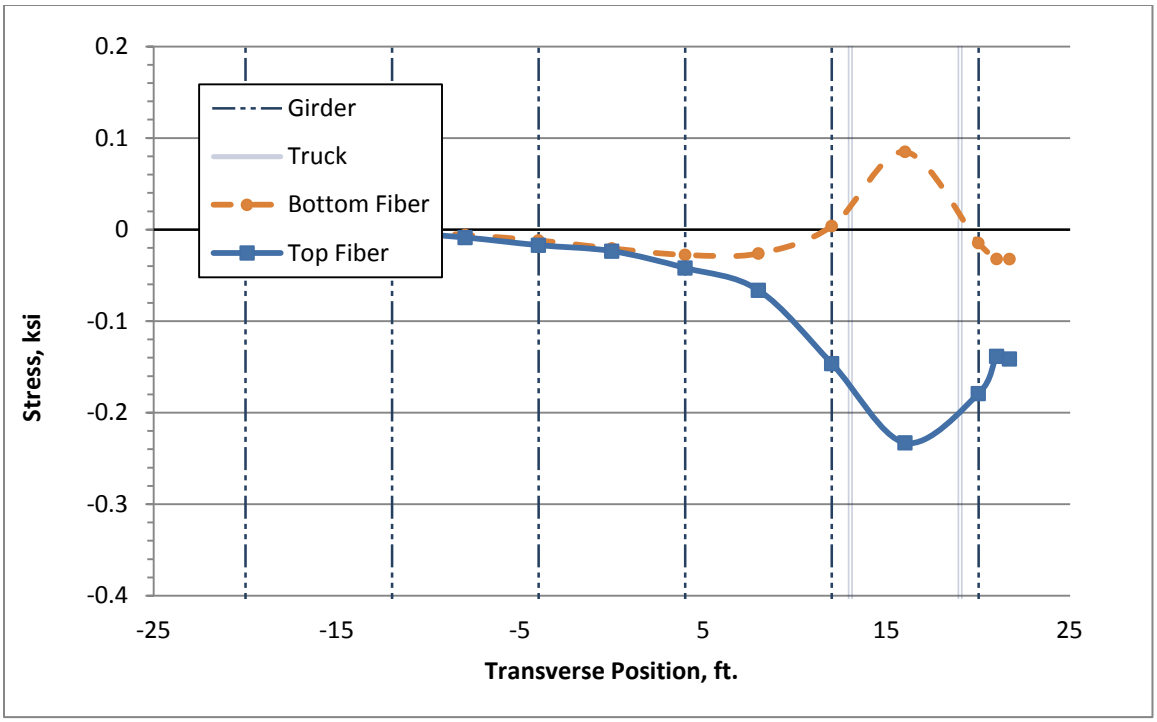

Figure B.93: Deck Stresses due to TR-16 at Critical Location 1 (Simple Span Bridge)

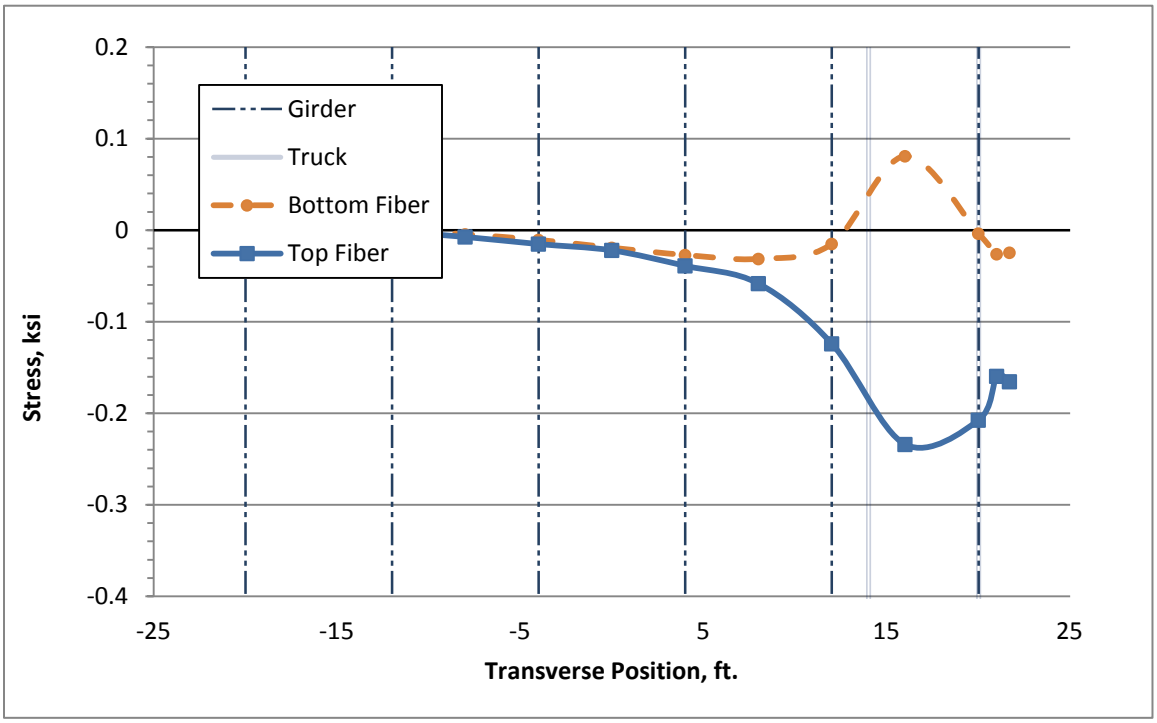

Figure B.94: Deck Stresses due to TR-17 at Critical Location 1 (Simple Span Bridge)

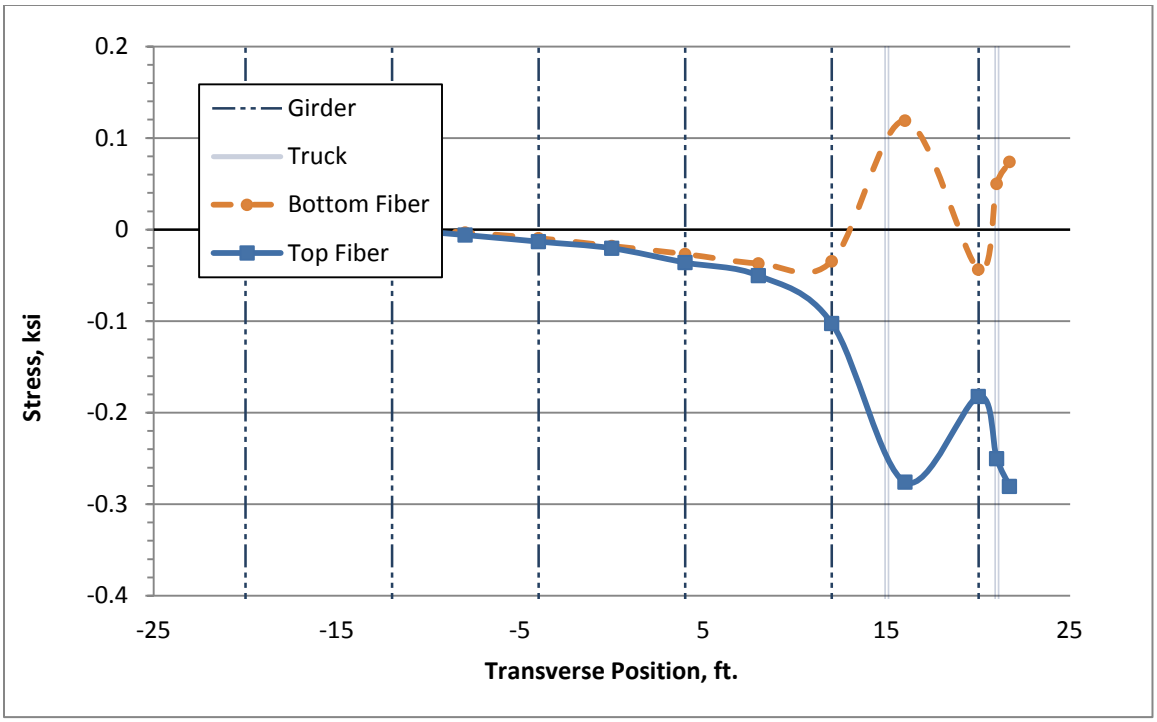

Figure B.95: Deck Stresses due to TR-18 at Critical Location 1 (Simple Span Bridge)

APPENDIX C:

Bridge Plan

FED. RD. DIV. NO.	STATE	PROJ. NO.	FISCAL YEAR	SHEET NO.	TOTAL SHEETS
3	ALA.	I-59-2(21) Map "C"	1961	72	86

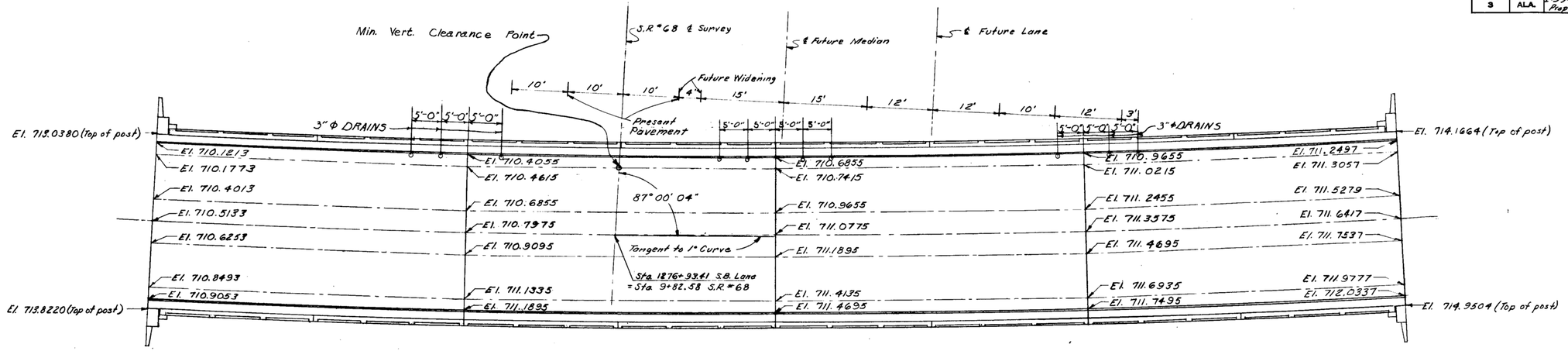

PLAN
SOUTHBOUND LANE

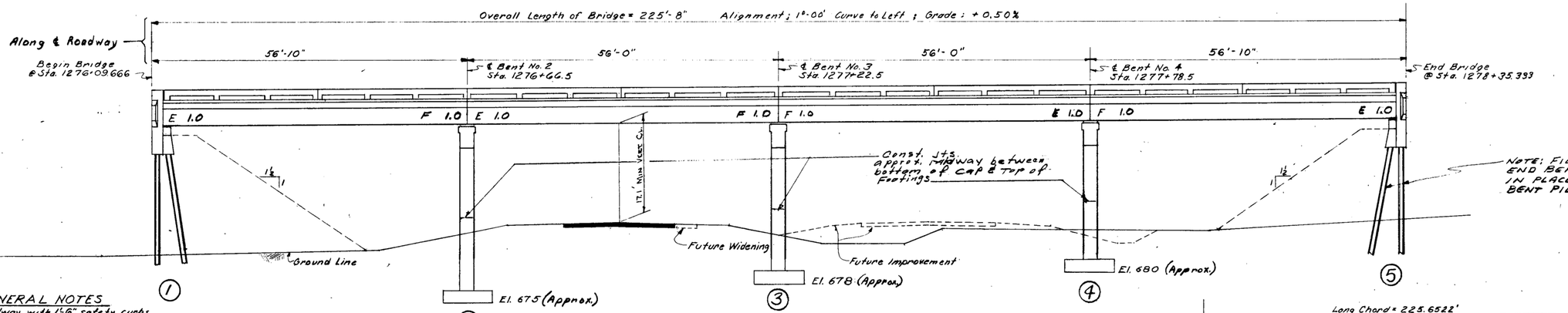

GENERAL NOTES

Roadway: 28'-0" Roadway with 1'-6" safety curbs

(1)
(2) H 20:S16-44 & Alt. Loading PPM 20-4 Dated 8-10-56
(3)
(4)
(5)
(7)
(9)
(10)
(11) Abuts. 15 Tons
(13)
(21)
(28)

HORIZONTAL CURVE DATA
SOUTHBOUND LANE

P.I. STA. 1272+76.75
Δ = 17°22' 00"
D = 1° 00' 00"
R = 3729.38
T = 818.04
L = 1736.67
E = 66.43
Sε = .028 ft./ft.

ELEVATION
SOUTHBOUND LANE

ESTIMATED QUANTITIES

S.B. Lane	N.B. Lane	Total	ITEM
370.0	370.0	740.0	Cu. Yds. Unclassified Bridge Excavation
345.0	345.0	690.0	Cu. Yds. Bridge Concrete, Class "A"
1	1	2	Each Steel Test Piles (10" BP @ 42")
5	5	10	Each Steel Pile Splices
800	800	1600	Lin. Ft. Steel Piling (10" BP @ 42")
85975	85975	171950	Lbs. Steel Reinforcement
166800	166800	336600	Lbs. Structural Steel
1	1	2	Each Loading Tests
1*	1*	2*	Sets of Self Lubricating Bronze Plates

*Note: 1 Set Brg. Pls. = 32 Pcs

REQUIRED

S.B. Lane	N.B. Lane	Total	ITEM
2	2	4	56'-10" R.C. & Steel Beam End Spans -- Br. Sheet No. Z5
2	2	4	56'-0" R.C. & Steel Beam Int. Spans -- Br. Sheet No. Z5
2	2	4	R.C. & Steel Pile Abutments ---------- Std. Dwg. No. 1 PA-2805 & Br. Sheet No. Z6
3	3	6	R.C. Int. Bents (Spread Footings) -- Std. Dwg. No. 1 CB-2800 & Br. Sheet No. Z6
		1	Set General Notes ---------- Std. Dwg. No. GN-1
		1	Set Brg. Pl. Details ---------- Std. Dwg. No. I-100*
		1	Miscellaneous Standard Details -- Std. Dwg. No. I-111

CONCRETE SUMMARY

SB Lane	NB Lane	Total	ITEM
180.0	180.0	360.0	Cu. Yds. Superstructure
115.0	115.0	230.0	Cu. Yds. Substructure (Less Footings)
50.0	50.0	100.0	Cu. Yds. Footings
345.0	345.0	690.0	Cu. Yds. Total

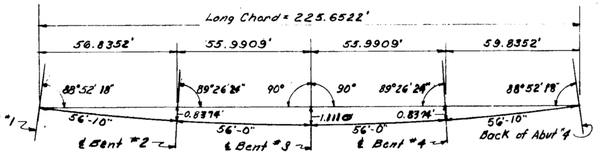

℄ of Bents & Back of Abuts. are on Radial Lines

BRIDGE LAYOUT SKETCH - SOUTHBOUND & NORTHBOUND LANE ON 1° 00' CURVE

BRIDGE SHEET NO. 23 OF 30

REVISIONS
(1) Foundation pile Note. 7-26-61

STATE OF ALABAMA
HIGHWAY DEPARTMENT

PROJECT NO. I-59-2-(21) 197
OVERPASS FOR S.R. NO. 68
AT STATION 1276+93.41
ETOWAH CO. LINE TO S.R. NO. 68
DEKALB CO. ALA.

GENERAL PLAN & ELEVATION - S'BOUND LANE

APPROVED: [signature] CHIEF BRIDGE DESIGN ENGINEER
[signature] BRIDGE ENGINEER

SCALE:	DESIGNED:	DRAWN: GAW	TRACED:	CHECKED: J.F.A-4-18-61	QUANTITIES COMP. MCM-Ray CKD. WEH	DATE
1"=10'-0"						

FED. RD. DIV. NO.	STATE	PROJ. NO.	FISCAL YEAR	SHEET NO.	TOTAL SHEETS
3	ALA.	I-59-3(20) Prop. 2"	1961	73	86

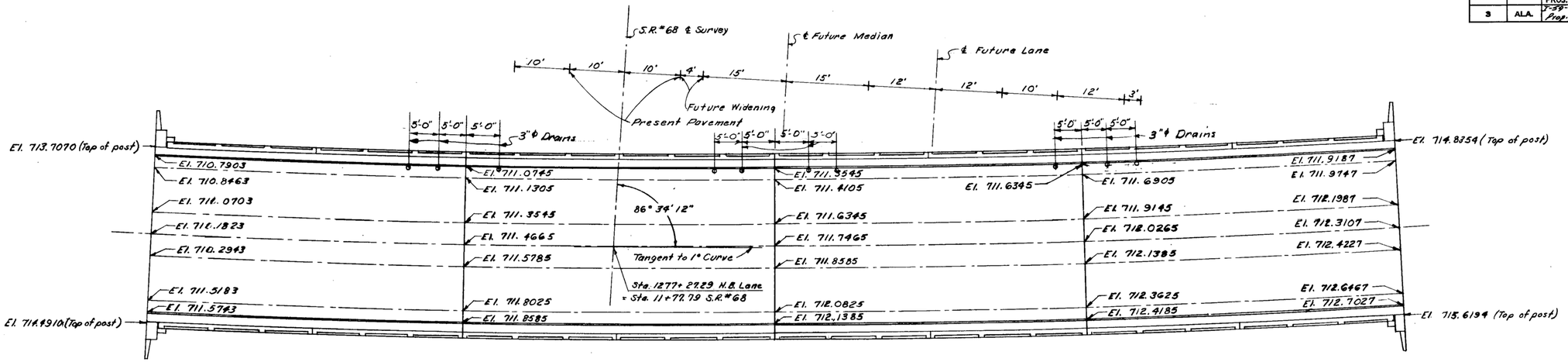

PLAN
NORTHBOUND LANE

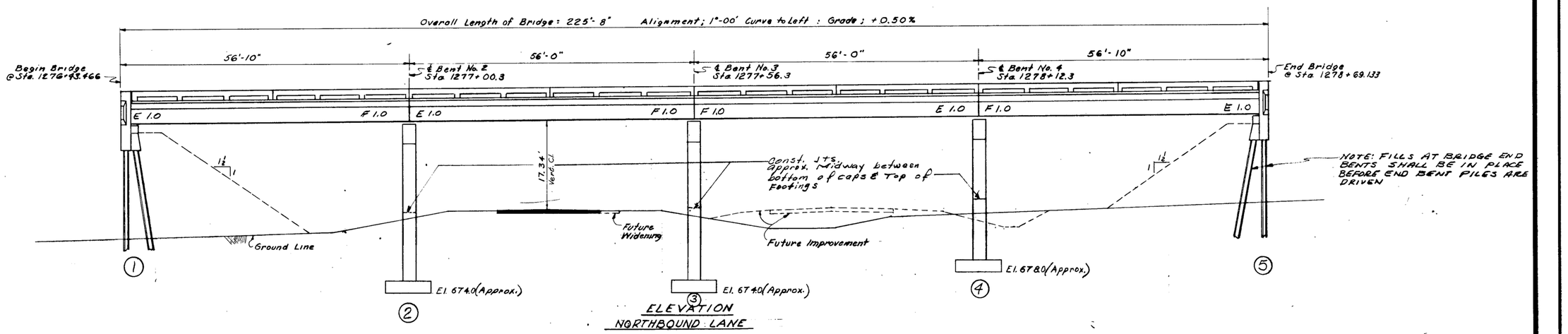

ELEVATION
NORTHBOUND LANE

Note: Foundation piles, if required, will be paid for at price bid per linear Ft. steel piling (10" BP42)

Note: For General Notes, Bridge Layout Sketch and Estimated Quantities, See On Sheet No. 2.3

HORIZONTAL CURVE DATA
NORTHBOUND LANE

PI. Sta. 1277 + 34.85
Δ = 17°48'20" Lt.
D = 1°00'00"
R = 5729.58
T = 897.51
L = 1780.56'
E = 69.87
SE = 0.028 ft/ft.

BRIDGE SHEET NO. 2.2 OF 30

REVISIONS
① Foundation pile Note 7-28-61. T.L.A.

STATE OF ALABAMA
HIGHWAY DEPARTMENT

PROJECT NO. I-59-2-(21)197
OVERPASS FOR S.R. NO. 68
AT STA. 1277+27.29
ETOWAH CO. LINE TO S.R. NO. 88
DEKALB CO ALA.

GENERAL PLAN & ELEVATION - N'BOUND LANE

APPROVED:
CHIEF BRIDGE DESIGN ENGINEER
BRIDGE ENGINEER

SCALE: 1"=10'-0"
DESIGNED:
DRAWN: GAW
TRACED:
CHECKED: J.F.A-4-19-61
QUANTITIES
DATE

909015

FED. RD. DIV. NO.	STATE	PROJ. NO.	FISCAL YEAR	SHEET NO.	TOTAL SHEETS
3	ALA.	I-59-2(21) Prog. "C"	1961	74	86

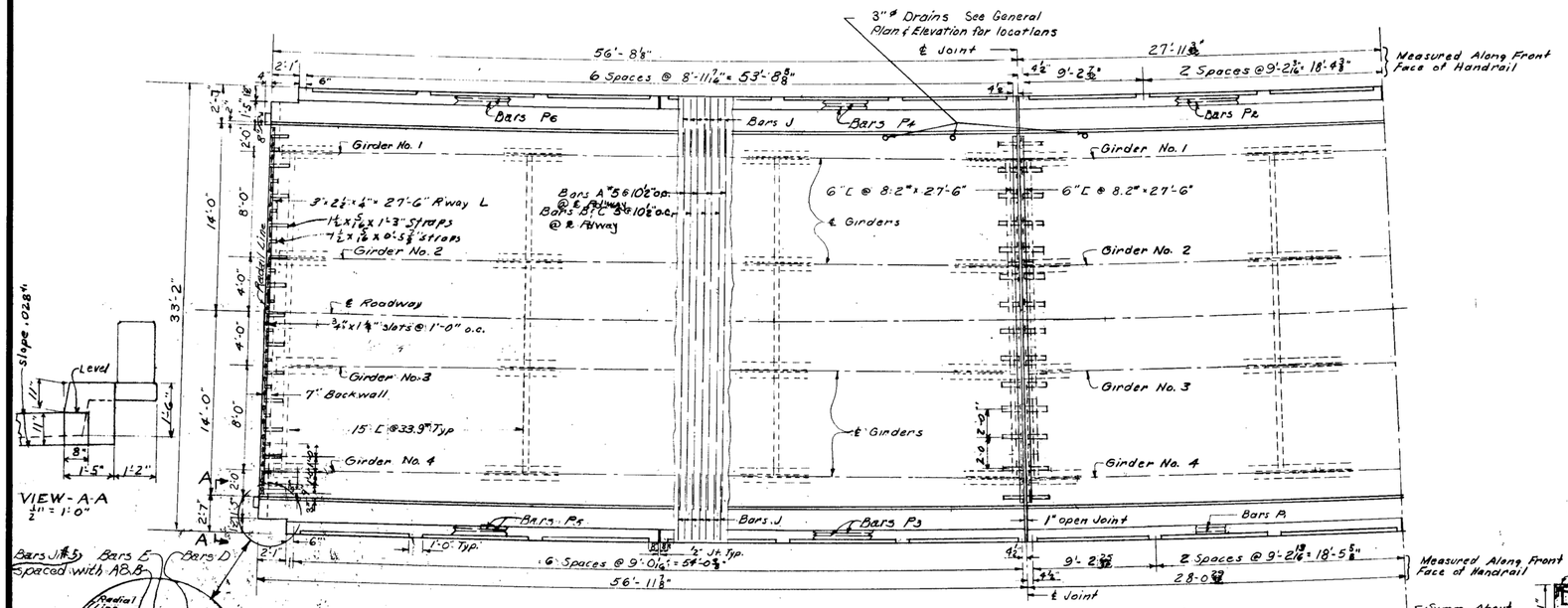

SHEAR DEVELOPER DETAILS

Granular or Solid Flux-Filled Studs (or approved equal) Shall Be Used As Shear Connectors. Studs Shall Be Automatically End Welded to Steel Beams. Welded Base of Studs Should Be of Least ⅞" Diameter and Are to Be Welded on Centers as Indicated on This Drawing. All Stud Welds Shall be Made in Accordance With Recomendations of The Manufacturer.

ALTERNATE SHEAR DEVELOPER: For Each Line of ¾" ϕ Studs the Fabricator May Substitute one 4" L @ 9.25# x 0'-6" Welded all round With ¼" Fillet Weld. Toe of Flange Shall be Turned Toward ℄ of Span. For The Purpose of Payment, the Weight of Structural Steel in Shear Developers Shall be Based on the Weight of ¾" ϕ Studs (calculated at .625 lbs. per Stud) Whether Studs or Channels are Used. This Weight will be Included in And Paid For as Lbs. Structural Steel.

ESTIMATED QUANTITIES

ITEM	END SPAN	INT. SPAN
Cu. Yds. Class A. Concrete	42.8	42.2
Lbs. Reinforcement Steel	11,700	11530
Lbs. Structural Steel	39900	40000
GIRDER LENGTHS		

	GIR. NO 1	GIR. NO. 2	GIR. NO 3	GIR. NO 4
END SPAN *	56.7197	56.7931	56.8724	56.9518
INT. SPAN ▲	55.8823	55.9607	56.0389	56.1171

* Measured From Back of Abut. to ℄ Joint
▲ Measured From ℄ Joint To ℄ Joint

BRIDGE SHEET NO. 25 OF 30

REVISIONS
COVER PL CHANGED FROM 11"x⅛" TO 10" x ⅛" — FILL PL CHANGED TO SAME 9/15/61 — AMERICAN BR. CO.
BARS T REV. JD 11-10-61

STATE OF ALABAMA
HIGHWAY DEPARTMENT

PROJECT NO. I-59-2(21)197
OVERPASS FOR S.R. NO. 68
AT STA. 1276+93.41 & STA. 1277+27.25
ETOWAH CO. LINE TO S.R. NO. 68
DEKALB CO. ALA.

SPECIAL DETAILS - 56' "I" BEAM SPAN

APPROVED: J.H. Chambers
CHIEF BRIDGE DESIGN ENGINEER
BRIDGE ENGINEER

SCALE: AS SHOWN
DESIGNED:
DRAWN: GAW
TRACED:
CHECKED: J.F.A. 8-19-61
QUANTITIES COMP.: GAW CHK'D: WCB
DATE

7 1015

FED. RD. DIV. NO.	STATE	PROJ. NO.	FISCAL YEAR	SHEET NO.	TOTAL SHEETS
3	ALA.	I-59-2(21) Proj. "C"	1961	75	86

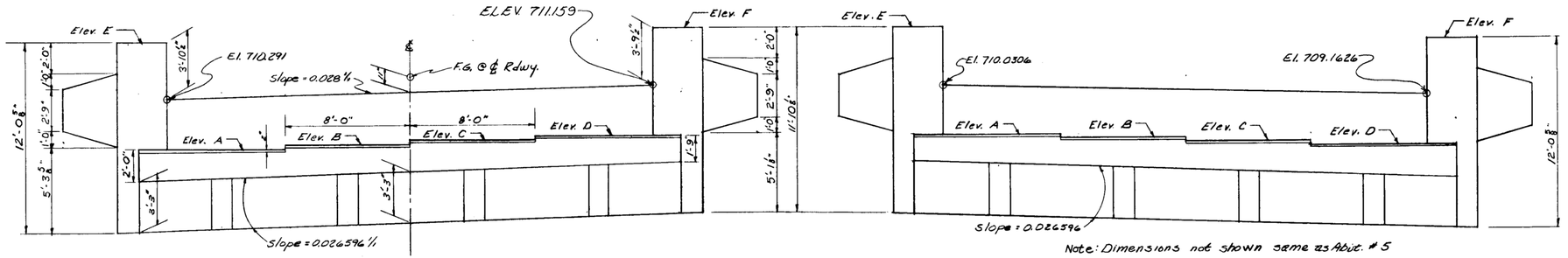

ELEVATION - ABUTMENT NO. 5

Note: Dimensions not shown same as Abut. # 5

ELEVATION - ABUTMENT NO. 1

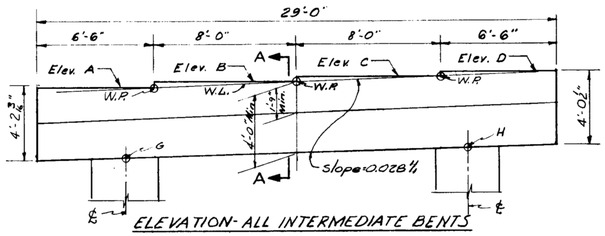

ELEVATION - ALL INTERMEDIATE BENTS
Looking Ahead

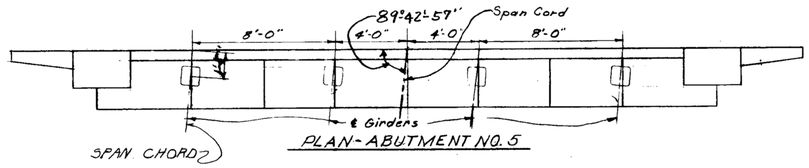

PLAN - ABUTMENT NO. 5

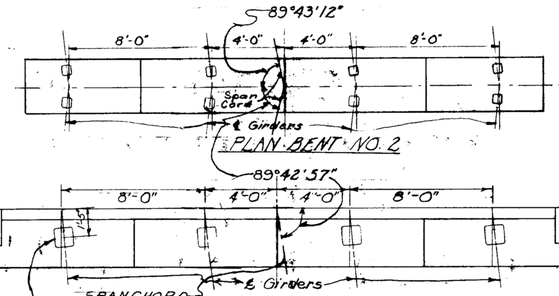

PLAN - BENT NO. 2

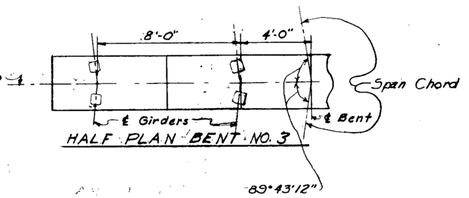

HALF PLAN BENT NO. 3

PLAN - ABUTMENT NO. 1

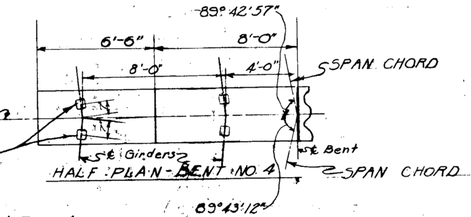

HALF PLAN BENT NO. 4

TABLE of ELEVATIONS - SOUTHBOUND LANE					
ELEV.	ABUT No.1	BENT No. 2	Bent No. 3	BENT No. 4	ABUT No. 5
A	706.9460	706.5582	706.8382	707.1182	707.4024
B	706.7220	706.7822	707.0622	707.3422	707.6264
C	706.4980	707.0062	707.2862	707.5662	707.8504
D	706.2740	707.2302	707.5102	707.7902	708.0744
E	713.8220				714.1664
F	713.0380				714.9504
G		702.5162	702.7962	703.0762	
H		703.0482	703.3282	703.6082	

TABLE of ELEVATIONS - NORTHBOUND LANE					
ELEV.	ABUT No. 1	BENT No. 2	BENT No. 3	BENT No. 4	ABUT No5
A	707.6150	707.2272	707.5072	707.7872	708.0714
B	707.3910	707.4512	707.7312	708.0112	708.2954
C	707.1670	707.6752	707.9552	708.2352	708.5194
D	706.9430	707.8992	708.1792	708.4592	708.7434
E	714.4910				714.8358
F	713.7070				715.6194
G		708.1852	708.4652	708.7452	
H		708.7172	708.9972	709.2772	

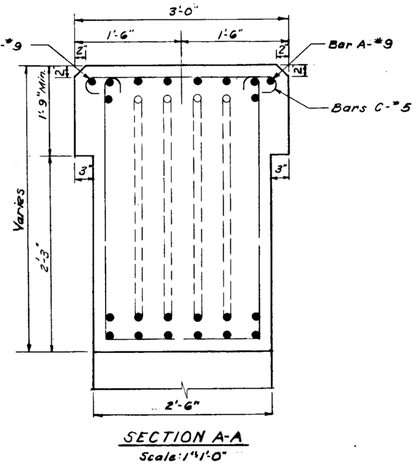

SECTION A-A
Scale: 1"=1'-0"

Note: For Details and Reinf. not shown on Abutments see Std. Dwg. NO. I.PA-2805
For Details and Reinf. not shown on int. bents see Std. Dwg. NO. ICB-2800

℄ set ¾" in conc. Block out if desired: Typical all grds. on both Abuts. (See Std. Dwg. I-100

℄ set ¾" in conc. Block out if desired. Typical all grds, all int. bents. See Std. I-100

BRIDGE SHEET NO. 26 OF 30

REVISIONS

STATE OF ALABAMA
HIGHWAY DEPARTMENT

PROJECT NO. I-59-2(21) 197
OVERPASS FOR S.R. NO. 68
AT STA. 1276+93.41 & STA. 1277+27.29
ETOWAH CO. LINE TO S.R. NO. 68
DEKALB CO. ALA.

SPECIAL DETAILS

APPROVED: M.M. Chambers
CHIEF BRIDGE DESIGN ENGINEER
BRIDGE ENGINEER

SCALE: 1"=1'-0" UNLESS SHOWN

DESIGNED:
DRAWN: GAW
TRACED:
CHECKED: JFA 4-19-61

QUANTITIES

DATE: 2-23-61

M & T F-1 (2)

C/L Ft. Survey T. STA. 12+66

Elevation of Hub 680.3

680.3	to	679.0	Med. dry brown silt
679.0	"	676.0	Stiff brown silty clay w/ a few
"		"	boulders
676.0	"	670.1	Stiff brown silty clay w/ chert
670.1	"	664.0	Med. gray shaley limestone
"		"	
"		"	
"		"	

C/L Ft. Survey T. STA. 13+00

Elevation of Hub 679.3

679.3	to	679.0	Med. dry brown silt
679.0	"	673.0	Very stiff moist brown
"		"	silty clay
673.0	"	669.6	Stiff damp gray brown silty
"		"	cherty clay
669.6	"	664.0	Med. gray shaley limestone
"		"	
"		"	

C/L Ft. Survey T. STA. 13+34

Elevation of Hub 680.6

680.6	to	679.0	Med. moist brown silt
679.0	"	674.0	Very stiff moist brown silty clay
674.0	"	670.3	Stiff damp brown silty clay
670.3	"	664.5	Med. gray shaley limestone
"		"	
"		"	
"		"	

M & T F-1 (3)

C/L Ft. L4 (SB) T. STA. 1278+35

Elevation of Hub 689.8

689.8	to	688.0	Med. brown silt (moist)
688.0	"	685.0	Very stiff brown moist very
"		"	silty clay
685.0	"	680.8	Hard brown silty clay
680.8	"	-	Rock
"		"	
"		"	
"		"	

C/L Ft. L4 (SB) T. STA. 1277+78

Elevation of Hub 688.5

688.5	to	688.0	Loose dry brown silt
688.0	"	687.0	Med. moist brown silt
687.0	"	684.0	Very stiff moist brown silty clay
684.0	"	681.0	Hard moist brown silty clay
681.0	"	681.1	Very stiff moist brown silty clay
681.0	"	675.2	Gray limestone
"		"	
"		"	

C/L Ft. L4 (SB) T. STA. 1277+22

Elevation of Hub 687.5

687.5	to	686.0	Brown sand clay fill
686.0	"	684.0	Very stiff moist brown
"		"	silty clay
684.0	"	679.0	Hard moist brown silty clay
679.0	"	673.2	Gray limestone
"		"	
"		"	

M & T F-1 xxxx - 3 -

C/L Ft. Survey T. STA. 13+68

Elevation of Hub 680.9

680.9	to	679.0	Med. moist brown silt
679.0	"	672.0	Very stiff brown silty clay
672.0	"	671.1	Very stiff brown silty clay w/
"		"	small amount of chert
671.1	"	665.0	Med. gray shaley limestone
"		"	
"		"	
"		"	

C/L Ft. Survey T. STA. 14+02

Elevation of Hub 680.7

680.7	to	679.0	Med. moist brown silt
679.0	"	675.0	Very stiff brown silty clay
675.0	"	671.4	Very stiff brown cherty clay
671.4	"	"	Rock
"		"	
"		"	
"		"	
"		"	

Ft. T. STA.

Elevation of Hub

	to		
"		"	
"		"	
"		"	
"		"	
"		"	
"		"	
"		"	

M & T F-1 xxxx - 2 -

Ft. T. STA. 6/29/60

Elevation of Hub

	to		I-59-2(21)197
"		"	Overpass Ala. #68
"		"	DeKalb Co.
"		"	
"		"	
"		"	
"		"	
"		"	

C/L Ft. R4 (EB) T. STA. 1276+43

Elevation of Hub 683.7

683.7	to	682.0	Dry med. brown silt
682.0	"	674.0	Hard moist silty brown clay
674.0	"	673.0	Damp moist silty brown clay
673.0	"	"	Rock
"		"	
"		"	
"		"	
"		"	

R4 (EB) T. STA. 1277+00

Elevation of Hub 685.6

685.6	to	684.0	Med. moist brown silt
684.0	"	677.4	Very stiff moist yellow brown
"		"	silty clay
677.4	"	674.6	Hard damp brown silty clay
674.6	"	669.3	Gray limestone (hard)
"		"	
"		"	
"		"	

M & T F-1 xxxx - 1 -

Ft. T. STA.

Elevation of Hub

	to		I-59-2(21)197
"		"	Overpass Ala. #68
"		"	DeKalb Co.
"		"	
"		"	
"		"	
"		"	
"		"	

C/L Ft. L4 (SB) T. STA. 1276+10

Elevation of Hub 684.4

684.4	to	682.0	Dry med. brown silt
682.0	"	676.0	Very stiff to hard shaley brown
"		"	silty clay
676.0	"	675.3	Stiff damp brown silty clay
675.3	"	"	Rock
"		"	
"		"	
"		"	

C/L Ft. L4 (SB) T. STA. 1276+66

Elevation of Hub 686.5

686.5	to	687.0	Med. moist brown silt
687.0	"	684.0	Hard moist brown silty clay
684.0	"	677.9	Very stiff to hard
"		"	yellow brown silty clay
677.9	"	676.8	Hard brown shaley clay and
"		"	brown shale w/ thin layers of limestone
676.8	"	670.5	Gray limestone (hard)
"		"	

FED. RD. DIV. NO.	STATE	PROJ. NO.	FISCAL YEAR	SHEET NO.	TOTAL SHEETS
3	ALA.	I-59-2(21) Prop. "C"	1961	76	86

BRIDGE SHEET NO. 27 OF 30

REVISIONS

STATE OF ALABAMA
HIGHWAY DEPARTMENT

PROJECT NO. I-59-2(21)
CORE DRILLINGS FOR
STRUCTURES AND CHANNEL
CHANGE FOR LITTLE
WILLS CREEK (DEKALB CO.)

CORE DRILLINGS

APPROVED: J. H. Chambers
CHIEF BRIDGE DESIGN ENGINEER
BRIDGE ENGINEER

SCALE:

DESIGNED:
DRAWN:
TRACED:
CHECKED:

QUANTITIES

DATE JULY-6(

FED. RD. DIV. NO.	STATE	PROJ. NO.	FISCAL YEAR	SHEET NO.	TOTAL SHEETS
3	ALA.	I-59-2(21) Prop. "C"	1961	77	86

M&TF-1 — I-59-2(21)197 — Little Wills Creek + Ramp "A" — DeKalb Co. — xxxxxxxx - 1 - — 6/23/60

Elevation of Hub			B/L	Ft.
		677.5		
677.5	to	673.0		
673.0	"	672.0		
672.0	"	669.1		
669.1	"	658.0		

Survey T STA 10+00

Mod. moist brown silt

Mod. soft brown very silty clay

Loose wet gray sandy silt w/ small amount of shell

Mod. gray limestone

Elevation of Hub			B/L	Ft.
		678.0		
678.0	to	677.0		
677.0	"	676.0		
676.0	"	675.5		
675.5	"	669.5		
669.5	"	659.0		

Survey B STA 10+50

Slightly moist brown silt

Loose brown silt

Very stiff yellow silty clay

Stiff to mod. soft gray silty clay w/ sand

Mod. gray shaley limestone

Elevation of Hub			B/L	Ft.
		678.1		
678.1	to	677.0		
677.0	"	675.0		
675.0	"	672.0		
672.0	"	670.5		
670.5	"	669.5		
669.5	"	659.0		

Survey T STA 11+50

Mod. dry brown silt

Loose damp brown silt

Very stiff yellow damp silty clay

Stiff yellow silty chorty clay

Dark gray sandy silty clay

Mod. gray shaley limestone

M&TF-1 — (2) — 6/24/60

Elevation of Hub			B/L	Ft.
		678.0		
678.0	to	676.0		
676.0	"	675.0		
675.0	"	672.0		
672.0	"	671.0		
671.0	"	669.7		
669.7	"	659.3		

Survey T STA 11+00

Dry sand, brown silt

Moist sand, brown silt

Very stiff moist yellow silty clay

Stiff yellow brown chorty clay

Loose gray shaley sand w/ small amount gray clay

Mod. gray shaley limestone

Elevation of Hub			B/L	Ft.
		677.7		
677.7	to	677.0		
677.0	"	673.0		
673.0	"	669.5		
669.5	"	659.0		

Survey T STA 11+50

Mod. dry brown silt

Very stiff moist brown silty clay

Stiff deep gray brown slightly chorty clay

Mod. gray shaley limestone

Elevation of Hub			B/L	Ft.
		679.8		
679.8	to	678.0		
678.0	"	675.0		
675.0	"	671.0		
671.0	"	670.5		
670.5	"	659.0		

Survey T STA 12+00

Dry loose silt

Mod. moist brown silt

Very stiff moist yellow brown silty clay

Stiff deep gray-brown silty chorty clay

Mod. gray shaley limestone

M&TF-1 — xxxxxxxx - 2 - — 6/24/60

Elevation of Hub			B/L	Ft.
		677.2		
677.2	to	676.5		
676.5	"	672.0		
672.0	"	668.0		
668.0	"			

Ft. T STA 12+50

Mod. moist brown silt

Stiff deep dark brown very silty clay

Soft to mod. gray very silty clay

Mod. gray shaley limestone

Elevation of Hub			B/L	Ft.
		678.2		
678.2	to	678.0		
678.0	"	675.0		
675.0	"	671.0		
671.0	"	670.5		
670.5	"	659.0		

Ft. T STA 12+50

Dry loose silt

Mod. moist brown silt

Very stiff moist yellow brown silty clay

Stiff deep gray-brown silty chorty clay

Mod. gray shaley limestone

M&TF-1 — (2) — 6/24/60

Elevation of Hub			B/L	Ft.
		678.1		
678.1	to	677.0		
677.0	"	672.0		
672.0	"	669.2		
669.2	"	659.0		

1A (SB) T STA 12+25

Mod. moist brown silt

Stiff deep yellow brown silty clay

Stiff to mod. deep gray brown silty clay

Mod. gray shaley limestone

Elevation of Hub			B/L	Ft.
		678.0		
678.0	to	677.0		
677.0	"	672.0		
672.0	"	669.2		
669.2	"	659.0		

1A T STA 12+50

Mod. moist brown silt

Stiff deep brown silty clay

Stiff to mod. deep gray brown silty sand

Mod. gray shaley limestone

Elevation of Hub			B/L	Ft.
		679.0		
679.0	to	677.5		
677.5	"	673.0		
673.0	"	669.2		
669.2	"	659.0		

1A T STA 12+75

Moist mod. brown silt

Stiff deep yellow brown silty clay

Stiff to mod. deep gray brown silty clay w/ small amount of shell

Mod. gray shaley limestone

M&TF-1 — xxxxxxxx - 3 - — 6/24/60

Elevation of Hub			B/L	Ft.
		678.0		
678.0	to	676.0		
676.0	"	675.0		
675.0	"	671.0		
671.0	"	669.2		

Ft. T STA 12+52

Mod. soft brown silt

Mod. moist brown silt

Very stiff moist yellow-brown silty clay

Stiff gray-brown deep silty clay

Stiff deep brown chorty silty clay

Mod. gray shaley limestone

(All work on this sheet is horizontal control.)

(Bottom zones on drill holes to appear also. 675.0 = top approximate weathered shale elevation last eight holes.)

Elevation of Hub			B/L	Ft.
	to			
	"			
	"			
	"			
	"			
	"			
	"			
	"			

Ft. T STA

M&TF-1 — xxxxxxxx - 1 - — 6/24/60

Ft. T STA

Elevation of Hub

to

I-59-2(21)197

Little Wills Creek

Left or South Bound Lane

DeKalb County

Elevation of Hub			B/L	Ft.
		677.2		
677.2	to	676.5		
676.5	"	672.0		
672.0	"	668.0		
668.0	"			

1A T STA 12+50

Mod. moist brown silt

Stiff deep dark brown very silty clay

Soft to mod. gray very silty clay

Mod. gray shaley limestone

Elevation of Hub			B/L	Ft.
		678.2		
678.2	to	677.0		
677.0	"	671.0		
671.0	"	669.3		
669.3	"	659.0		

1A T STA 12+65

Mod. moist brown silt

Stiff deep brown very silty clay

Stiff deep gray silty clay w/ a few small limestone boulders

Mod. gray shaley limestone

M&TF-1 — (2) — 6/24/60

Elevation of Hub			B/L	Ft.
		678.4		
678.4	to	677.0		
677.0	"	672.0		
672.0	"	669.2		
669.2	"	659.0		

1A (SB) T STA 12+10

Mod. moist brown silt

Stiff deep yellow brown silty clay

Stiff to mod. deep gray brown silty clay

Mod. gray shaley limestone

Elevation of Hub			B/L	Ft.
		678.0		
678.0	to	677.0		
677.0	"	672.0		
672.0	"	669.2		
669.2	"	659.0		

1A T STA 12+53

Mod. moist brown silt

Stiff deep brown silty clay

Stiff to mod. deep gray brown silty sand

Mod. gray shaley limestone

Elevation of Hub			B/L	Ft.
		679.0		
679.0	to	677.5		
677.5	"	673.0		
673.0	"	669.5		
669.5	"	659.0		

1A T STA 12+93

Moist mod. brown silt

Stiff deep yellow brown silty clay

Stiff to mod. deep gray brown silty clay w/ small amount of shell

Mod. gray shaley limestone

BRIDGE SHEET NO. 28 OF 0

REVISIONS

APPROVED: J.M. Shamblin
CHIEF BRIDGE DESIGN ENGINEER
8/11/60
BRIDGE ENGINEER

STATE OF ALABAMA
HIGHWAY DEPARTMENT

PROJECT NO. I-59-2(21)
CORE DRILLINGS FOR STRUCTURES AND CHANNEL CHANGE FOR LITTLE WILLS CREEK (DEKALB CO.

CORE DRILLINGS

SCALE:	DESIGNED:	DRAWN:	TRACED:	CHECKED:	QUANTITIES	DATE
-						JULY-6

M & T F-1 (2) ALA 468 OVERPASS CONT'D

Rt (NB) T. STA 1277+56

Elevation of Hub	687.7	
687.7	to 685.5	Med. moist brown silt
685.5	" 681.0	Very stiff moist brown silty clay
681.0	" 675.2	Hard moist brown silty clay
675.2	" 669.4	Gray limestone (hard)

Rt (NB) T. STA 1278+12

Elevation of Hub	689.6	
689.6	to 688.0	Med. moist brown silt
688.0	" 687.0	Stiff moist dark brown silty clay
687.0	" 679.0	Very stiff to hard moist brown silty clay
679.0	" 673.4	Gray limestone

Rt (NB) T. STA 1278+69

Elevation of Hub	690.7	
690.7	to 689.0	Med. moist brown silt
689.0	" 681.0	Very stiff moist brown silty clay
681.0	" 678.8	Hard moist brown silty clay
678.8	" -	Rock

M & T F-1

Channel Change T. STA 9+00

Elevation of Hub	681.0	
681.0	to 678.0	Med. moist brown silt
678.0	" 672.0	Stiff moist brown silty clay
672.0	" 669.9	Med. damp gray sandy very silty chert clay
669.9	" 667.0	Med. gray shaley limerock

(all rock in this vicinity in horizontal strata)

T. STA

(Water rose in drill holes to approx. elev. 675.0 - no appreciable rainfall this vicinity last eight weeks.)

T. STA

M & T F-1

T. STA 6/22/60

I-59-2(21)197

Little Wills Creek - Channel Change

DeKalb County

Channel Ch. T. STA 1+00

Elevation of Hub	677.4	
677.4	to 676.5	Med. dry brown silt
676.5	" 675.0	Med. moist brown silt
675.0	" 670.0	Stiff deep brown very silty clay
670.0	" 668.1	Stiff deep gray sand clay
668.1	" -	Rock

Channel Ch. STA 2+08

Elevation of Hub	678.1	
678.1	to 676.5	Med. dry brown silt
676.5	" 674.5	Med. damp brown silt
674.5	" 668.7	Stiff yellow brown silty clay
668.7	" 667.3	Med. gray shaley limerock

M & T F-1

Channel Change T. STA 9+24

Elevation of Hub	679.3	
679.3	to 678.0	Med. dry brown silt
678.0	" 676.0	Med. moist brown silt
676.0	" 671.0	Stiff moist brown silty clay
671.0	" 669.8	Loose moist very silty sandy chert
669.8	" -	Rock

Channel Change T. STA 7+24

Elevation of Hub	680.9	
680.9	to 680.0	Med. dry brown silt
680.0	" 678.0	Med. moist brown silt
678.0	" 674.0	Stiff moist dark brown very silty clay
674.0	" 671.0	Med. moist dark brown very silty clay
671.0	" 670.3	Loose wet very silty sand chert
670.3	" -	Rock

Channel Change T. STA 7+95

Elevation of Hub	680.6	
680.6	to 680.0	Med. dry brown silt
680.0	" 677.0	Med. moist brown silt
677.0	" 671.0	Med. to stiff dark brown silty clay
671.0	" 668.6	Med. damp gray sandy silty clay w/ chert
668.6	" 668.0	Med. gray shaley limerock

M & T F-1 (2)

Channel Change T. STA 3+20

Elevation of Hub	678.6	
678.6	to 677.5	Med. dry brown silt
677.5	" 675.0	Med. moist brown silt
675.0	" 668.5	Stiff moist brown very silty clay
668.5	" 666.8	Med. gray shaley limerock

Channel Change T. STA 4+24

Elevation of Hub	679.4	
679.4	to 677.5	Med. dry brown silt
677.5	" 675.5	Med. moist brown silt
675.5	" 669.5	Stiff moist yellow brown silty clay
669.5	" 668.8	Med. wet gray silty sand clay
668.8	" -	Rock

Channel Change T. STA 5+35

Elevation of Hub	679.5	
679.5	to 678.5	Med. dry brown silt
678.5	" 676.0	Med. moist brown silt
676.0	" 672.0	Stiff deep dark brown very silty clay
672.0	" 668.0	Med. deep dark brown very silty clay
668.0	" 666.4	Med. deep dark brown very silty clay w/ limerock boulders
666.4	" -	Rock

FED. RD. DIV. NO.	STATE	PROJ. NO.	FISCAL YEAR	SHEET NO.	TOTAL SHEETS
3	ALA.	I-59-2(21) Prop. "C"	1961	78	84

BRIDGE SHEET NO. 29 OF 30

REVISIONS

STATE OF ALABAMA
HIGHWAY DEPARTMENT

PROJECT NO. I-59-2(21)
CORE DRILLINGS FOR STRUCTURES & CHANNEL CHANGE FOR LITTLE WILLS CREEK (DEKALB CO.)

CORE DRILLINGS

APPROVED: [signature]
CHIEF BRIDGE DESIGN ENGINEER
BRIDGE ENGINEER

SCALE:

DESIGNED:
DRAWN:
TRACED:
CHECKED:

QUANTITIES

DATE JULY-60

FED. RD. DIV. NO.	STATE	PROJ. NO.	FISCAL YEAR	SHEET NO.	TOTAL SHEETS
3	ALA.	I-59-2(20) Prop. "C"	1961	29	30

M & T F-1 — ~~XXXX~~ - 3 -

3' Lt Ft. C/L Lt T. STA. 1272+21

Elevation of Hub	678.8	
678.8	to 677.0	Med. moist brown silt
677.0	" 672.0	Stiff moist brown very silty clay
672.0	" 669.6	Stiff moist brown cherty clay
669.6	" 659.4	Med. gray shaley limestone
	"	
	"	
	"	
	"	

C/L Ft. Lt. T. STA. 1272+55

Elevation of Hub	678.7	
678.7	to 677.0	Med. moist brown silt
677.0	" 672.0	Stiff moist brown very silty clay
672.0	" 669.4	Stiff damp brown cherty clay
669.4	" 659.2	Med. gray shaley limestone
	"	(water rose in drill holes to approximately
	"	elev. 675.0; no appreciable rainfall this
	"	vicinity last eight weeks)
	"	

C/L Ft. Lt T. STA. 1272+89

Elevation of Hub	679.5	
679.5	to 676.0	Med. moist brown silt
676.0	" 673.0	Stiff moist brown very silty clay
673.0	" 669.4	Stiff damp brown cherty silty clay
669.4	" -	Med. gray shaley limestone
	"	(all rock in this vicinity is horizontal
	"	strata)
	"	
	"	

M & T F-1 — ~~XXXX~~ - 1 -

Ft. T. STA. 6/28/60

Elevation of Hub		
	to	I-59-2(21)197
	"	Little Wills Creek
	"	Right or Northbound Land
	"	DeKalb County
	"	
	"	
	"	
	"	

C/L Ft. Rt (NB) T. STA. 1271+60

Elevation of Hub	678.7	
678.7	to 678.0	Med. dry brown silt
678.0	" 675.5	Med. moist brown silt
675.5	" 673.0	Very stiff moist brown silty clay
673.0	" 669.5	Med. to stiff damp gray
	"	silty clay w/ a few small
	"	limerock boulders and float
669.5	" -	Med. gray shaley limerock
	"	

C/L Ft. Rt (NB) T. STA. 1271+94

Elevation of Hub	678.9	
678.9	to 676.0	Med. moist brown silt
676.0	" 674.0	Very stiff moist brown very
	"	silty clay
674.0	" 673.0	Stiff damp brown silty clay
673.0	" 668.4	Med. gray sandy silty clay
	"	w/ float gravel & small boulders
668.4	" 667.3	Med. gray shaley limestone
667.3	" 666.0	Stiff to very stiff gray shaley clay
666.0	656.4	Med. gray shaley limestone

M & T F-1 — (2)

C/L Ft. Rt (NB) T. STA. 1272+20

Elevation of Hub	679.3	
679.3	to 678.0	Med. moist brown silt
678.0	" 671.0	Stiff damp dark brown very silty clay
671.0	" 669.0	Med. to soft gray silty cherty clay
669.0	" 668.7	Med. gray shaley clay
668.7	" 668.5	Stiff gray clay
668.5	" 658.0	Grey limestone
	"	
	"	

C/L Ft. Rt (NB) T. STA. 1272+62

Elevation of Hub	678.2	
678.2	to 677.5	Med. damp brown silt
677.5	" 672.0	Stiff damp dark brown very silty clay
672.0	" 668.2	Med. gray silty cherty clay
668.2	" 667.0	Med. gray shaley limestone
667.0	" 665.7	Stiff grey clay
665.7	" 656.0	Med. gray shaley limestone
	"	
	"	

C/L Ft. Rt (NB) T. STA. 1272+96

Elevation of Hub	680.1	
680.1	to 678.5	Med. moist brown silt
678.5	" 673.0	Stiff damp dark brown very
	"	silty clay
673.0	" 669.3	Med. damp gray brown very
	"	silty w/ small amount of chert
669.3	" 669.0	Med. gray shaley limestone
	"	
	"	

M & T F-1 — ~~XXXX~~ - 3 -

4' Lt Ft. C/L Rt T. STA. 1273+30

Elevation of Hub	680.5	
680.5	to 679.0	Med. damp brown silt
679.0	" 675.0	Very stiff damp brown very
	"	silty clay
675.0	" 672.0	Stiff damp yellow brown
	"	silty clay w/ small amount of chert
672.0	" 670.8	Med. damp brown silty clay
670.8	" 664.3	Med. gray shaley limestone
	"	

C/L Rt Lane Ft. (NB) T. STA. 1273+43

Elevation of Hub	680.3	
680.3	to 679.0	Med. moist brown silt
679.0	" 673.0	Stiff damp yellow brown
	"	silty clay
673.0	" 671.5	Stiff damp brown cherty clay
671.5	" 670.5	Med. brown gray cherty silty clay
670.5	" 664.2	Med. gray shaley limestone
	"	
	"	
	"	

C/L Rt Lane Ft. (NB) T. STA. 1273+56

Elevation of Hub	680.2	
680.2	to 678.5	Med. moist brown silt
678.5	" 673.0	Very stiff damp brown silty clay
673.0	" 670.7	Stiff damp brown cherty
	"	silty clay
670.7	" -	Med. gray shaley limestone
	"	
	"	

M & T F-1 — ~~XXXX~~ - 1 -

Ft. T. STA. 6/29/60

Elevation of Hub		
	to	I-59-2(21)197
	"	Little Wills Creek - Ramp "G"
	"	DeKalb County
	"	
	"	
	"	
	"	
	"	

C/L Ft. Survey T. STA. 11+98

Elevation of Hub	679.4	
679.4	to 678.0	Med. moist brown silt
678.0	" 673.0	Stiff moist brown clay
673.0	" 670.0	Stiff damp brown clay w/
	"	small chert boulders
670.0	" -	Rock
	"	
	"	
	"	

C/L Ft. Survey T. STA. 12+32

Elevation of Hub	679.5	
679.5	to 679.0	Med. dry brown silt
679.0	" 670.0	Stiff brown silty clay
	"	w/ small amount of chert
670.0	" 664.2	Med. gray shaley limestone
	"	
	"	
	"	

BRIDGE SHEET NO. 30 OF 30

REVISIONS

STATE OF ALABAMA
HIGHWAY DEPARTMENT

PROJECT NO. I-59-2(21)
CORE DRILLINGS FOR
STRUCTURES & CHANNEL
CHANGE FOR LITTLE
WILLS CREEK (DEKALB CO.

CORE DRILLINGS

APPROVED: W. A. Lambert
CHIEF BRIDGE DESIGN ENGINEER
B. S. Higgins
BRIDGE ENGINEER

SCALE:

DESIGNED:
DRAWN:
TRACED:
CHECKED:

QUANTITIES

DATE JULY-6

FED. RD. DIV. NO.	STATE	PROJ. NO.	FISCAL YEAR	SHEET NO.	TOTAL SHEETS
3	ALA.				

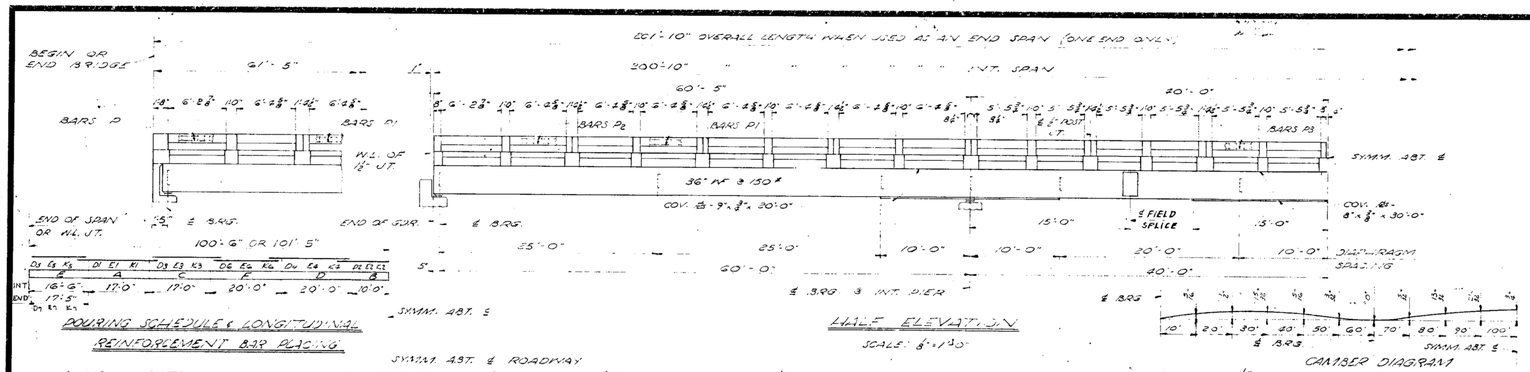

DOUBLING SCHEDULE & LONGITUDINAL REINFORCEMENT BAR PLACING

WALL ELEVATION

SCALE: 3/8" = 1'-0"

CAMBER DIAGRAM

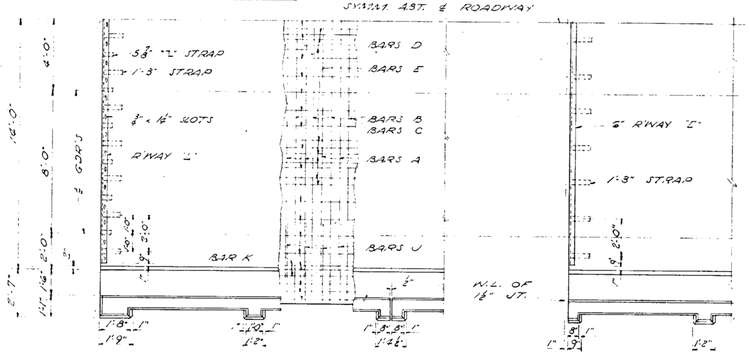

END SPAN

INT. SPAN

PART PLAN

SCALE: 1/4" = 1'-0"

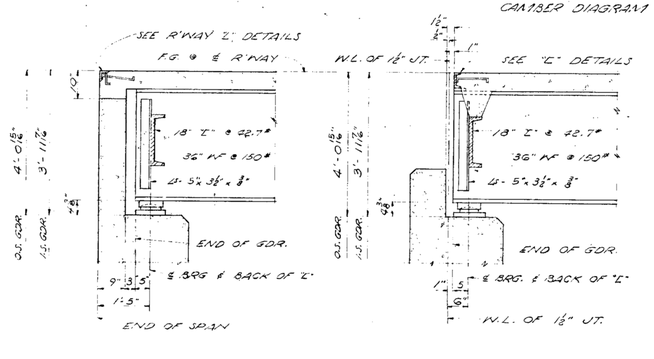

SECTION AT END

SECTION AT END OF END SPAN

SECTION AT EXPANSION JOINT

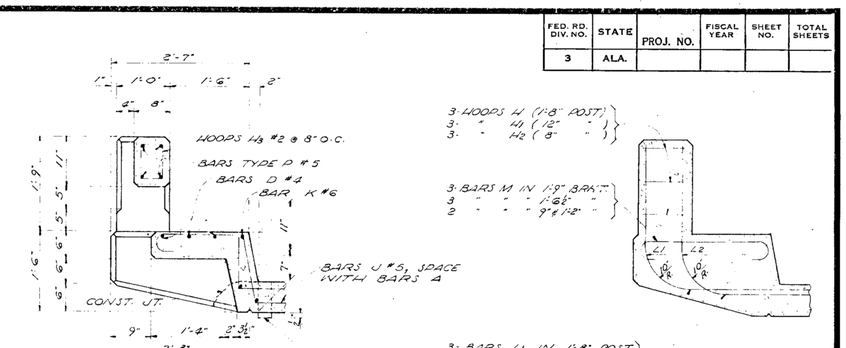

℄ 6" DRIP BEAD, CONT.

3" ℄ G.I. DRAIN, 16 GA. OR 3" ℄ TRANSITE, SPACE MIDWAY BETWEEN POSTS, OMIT OVER SLOPE FILLS & HIGH SIDE IF SUPERELEVATED.

SECTION THRU HANDRAIL & CURB

SECTION THRU POST & BRACKET

SCALE: 3/8" = 1'-0"

NOTE! ALL STRAPS TO BE HOT BENT. FILLET WELD (6") TO SIDES ONLY.

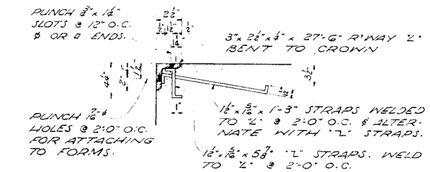

ROADWAY "L" DETAILS

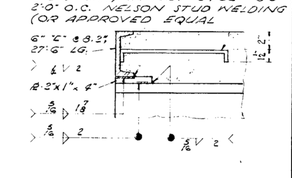

ROADWAY "E" DETAILS

GENERAL NOTES

1...ROADWAY.....28'-0" ROADWAY WITH 1'-6" SAFETY CURB
2...SPECIFICATIONS.....ALABAMA STATE HIGHWAY DEPT. (JULY 1, 1950)
3...DESIGN LOADING.....H20-S16-44 AASHO
4...CONCRETE.....SHALL BE BRIDGE CONCRETE CL. A.
5...STRUCTURAL STEEL.....BEAMS & COVER PL. THAT ARE TO BE WELDED SHALL CONFORM TO ASTM A-373-547 SPECIFICATIONS. USE EXX 15 OR 16 ELECTRODES OR 200° F PREHEAT AND INTERPASS TEMPERATURE. LOW HYDROGEN ELECTRODES SHALL CONFORM TO THE REQUIREMENTS OF THE MILITARY SPECIFICATIONS FOR ELECTRODES (MILITARY COATED, LOW HYDROGEN) FOR WELDING MEDIUM ALLOY STEEL, MIL. E-986 (SHIPS), GRADE 180, DATED NOV. 1, 1949. ALL OTHER STEEL SHALL CONFORM WITH SECTION 836 OF THE STANDARD SPECIFICATIONS.
6...PAINT.....ALL STRUCTURAL STEEL SURFACES NOT IN CONTACT WITH CONC. SHALL BE PAINTED 3 COATS IN THE FOLLOWING ORDER;* PRIMER OR SHOP COAT; YELLOW ZINC CHROMATE (10); SECOND COAT; YELLOW ZINC CHROMATE (10); THIRD COAT; ALUMINUM (35).
7...STEEL REINFORCEMENT.....ALL NEW REINFORCEMENT SHALL HAVE DEFORMATIONS IN ACCORDANCE WITH ASTM A-305-49 AND SHALL BE INTERMEDIATE GRADE VEN BILLET OR RAIL STEEL AS PERMITTED IN THE SPECIFICATIONS. (0.00008 P. TO 0.0025)
8...BEARINGS.....STANDARD BRONZE ALLOY "LUBRITE EXPANSION PLATES" OR EQUAL

*--- SEE OTHER EXCEPTION TO LEFT ABOVE.

BILL OF STELL REINFORCEMENT (SPLICE BARS TYPE D, E & K EQ DIA.)

	MARK	A	B	C	D1	D2	D3	D4	D5	D6	D7	E1	E2	E3	E4	E5	E6	E7	H	H1	H2	J	K	L1	L2	M	P	S1	S2
END	SIZE	5	5	5	4	4	4	4	4	4	4	4	4	4	4	4	4	4	4	4	4	4	4	4	4	4	4	4	4
	NO.	185	186	186	64	32	64	64	64	64	64	30	15	30	30	30	30	30	3	3	3	370	6	6	6	6	6	6	6
	LGTH	30'-0"	30'-0"	29'-11"	18'-10"	18'-10"	18'-10"	18'-10"	18'-10"	18'-10"	6'-2"	9'-10"	9'-10"	9'-10"	9'-10"	9'-10"	9'-10"	9'-10"	11'-8"	11'-8"	11'-8"	5'-3"	5'-1"	11'-8"	11'-8"	11'-8"	11'-8"	11'-8"	11'-8"	11'-8"
	D																												
INT	SIZE	5	5	5	4	4	4	4	4	4	4	4	4	4	4	4	4	4	4	4	4	4	4	4	4	4	4	4	4
	NO.	176	181	181	68	36	68	68	68	68	68	30	15	30	30	30	30	30	3	3	3	370	6	6	6	6	6	6	6
	LGTH	30'-0"	30'-0"	29'-11"	18'-10"	18'-10"	18'-10"	18'-10"	18'-10"	18'-10"	6'-2"	9'-10"	9'-10"	9'-10"	9'-10"	9'-10"	9'-10"	9'-10"	11'-8"	11'-8"	11'-8"	5'-3"	5'-1"	11'-8"	11'-8"	11'-8"	11'-8"	11'-8"	11'-8"	11'-8"
	D																												

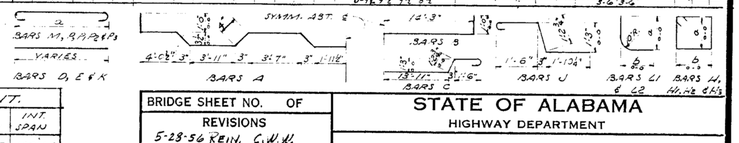

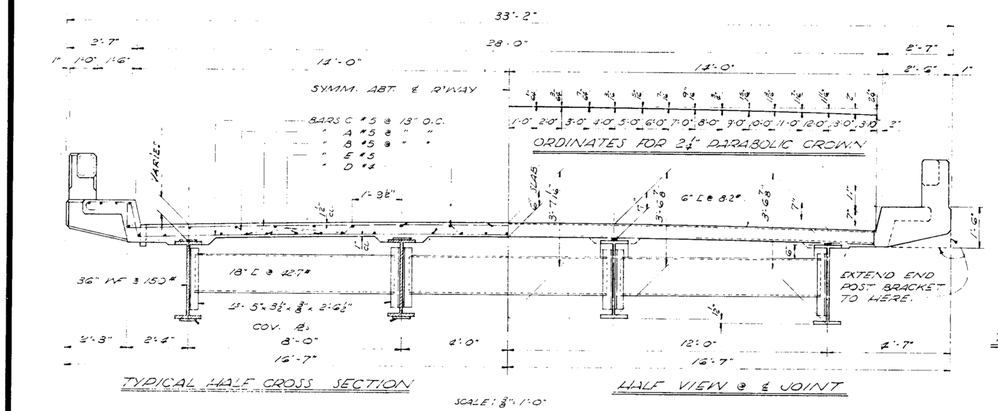

TYPICAL HALF CROSS SECTION

HALF VIEW @ ℄ JOINT

SCALE: 3/8" = 1'-0"

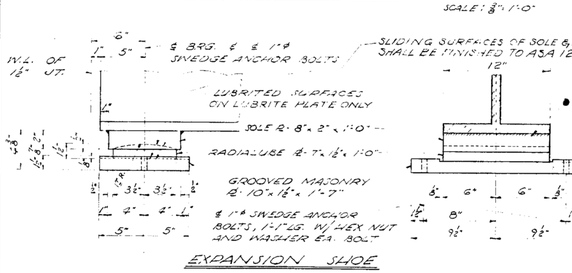

EXPANSION SHOE

NOTE! MACHINED SLIDING SURFACES OF MASS. & SOLE PL. SHALL BE COATED AT TIME OF ASSEMBLY WITH LIQUID OR STICK LUBRITE LUBRICANT WHICH IS FURNISHED WITH THE LUBRITE @. ALL PAINT SHALL BE REMOVED FROM THESE SURFACES BEFORE COATING.

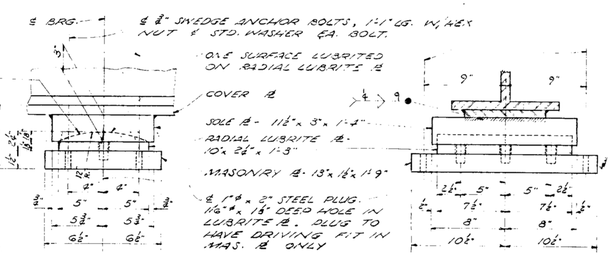

FIXED SHOE

NOTE:
HIGH TENSILE STRENGTH BOLTS, CONFORMING TO A.S.T.M. DESIGNATION A-325, MAY BE USED IN LIEU OF RIVETS. CONTACT SURFACES OF JOINTS SHALL NOT BE PAINTED. SEE SPECIAL PROVISION No. 121

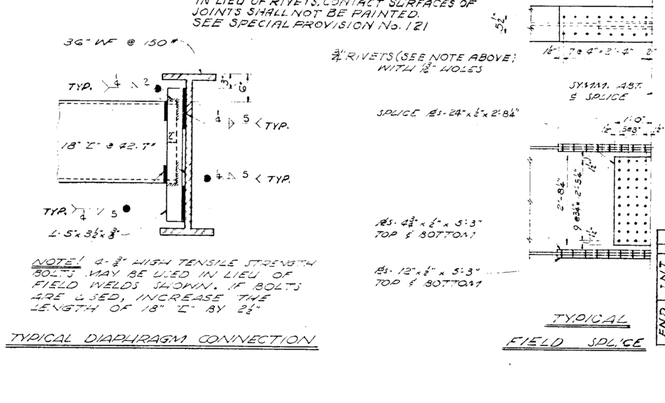

NOTE! 4 - 7/8" HIGH TENSILE STRENGTH BOLTS MAY BE USED IN LIEU OF FIELD WELDS SHOWN. IF BOLTS ARE USED, INCREASE THE LENGTH OF 18" "E" BY 2".

TYPICAL DIAPHRAGM CONNECTION

TYPICAL FIELD SPLICE

EST. QUANT.	END SPAN	INT. SPAN
CU. YDS. CONC.	143.67	192.68
LBS. STEEL REINF	34756	33713
LBS. STR. STEEL	163064	162565

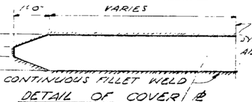

DETAIL OF COVER PL. @

FOR SIZE & LOCATION SEE HALF ELEVATION

BRIDGE SHEET NO. OF
REVISIONS
5-28-56 REIN. C.W.H.
Splice Removed G-7-56 END
11-16-56 Rev. Reinf. B.N.B.C.G.E.
Welds 12/14/56 J.M.S.

APPROVED:
CHIEF BRIDGE DESIGNER
BRIDGE ENGINEER

STATE OF ALABAMA
HIGHWAY DEPARTMENT

STANDARD
60'-80'-60' STEEL I BEAM SPAN WITH REINFORCED CONCRETE DECK 28'-0" ROADWAY
H20-S16-44 LOADING ⇒ 0° SKEW

60'+80'+60' CONTINUOUS SPAN

SCALE:	DESIGNED: D.M.P.D.	QUANTITIES	STATE
AS SHOWN	DRAWN: BMW Rev'd SS	COMP'D G.N.B.	B-2807
	TRACED:	CHECKED	
	CHECKED: L.S.O. 3/30/56		

OLD RDWY WIDTH - SEE B-2807-1

VOID

B-2807-1

FED. RD. DIV. NO.	STATE	PROJ. NO.	FISCAL YEAR	SHEET NO.	TOTAL SHEETS
3	ALA.				

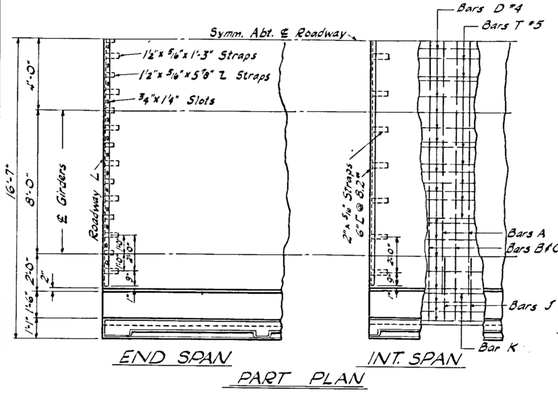

END SPAN — INT. SPAN

PART PLAN

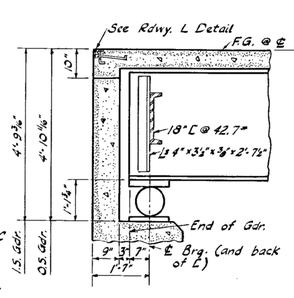

SECTION AT BEGINNING (OR END) OF SPAN

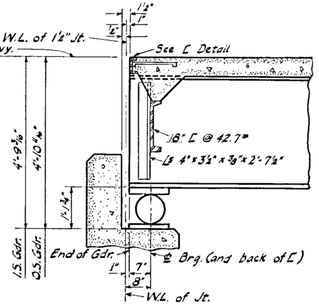

SECTION AT EXPANSION JOINT

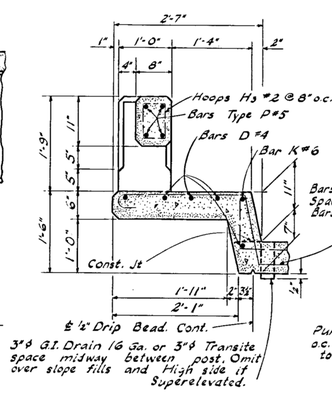

3"ϕ G.I. Drain 16 Ga. or 3"ϕ Transite space midway between post. Omit over slope fills and High side if Superelevated.

SECTION THRU HANDRAIL ℄ CURB

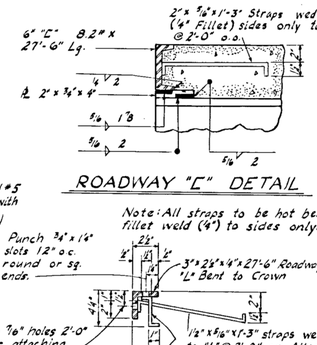

ROADWAY "L" DETAIL

Note: All straps to be hot bent fillet weld (4") to sides only.

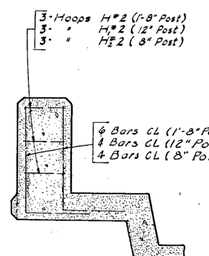

SECTION THRU POST

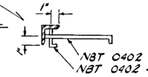

Nelson Stud Welding or approved equal.

ALTERNATE FOR STUD WELDING (OTHER DETAILS SAME AS REGULAR ANGLE)

REINFORCING INT. SPANS					
BAR	SIZE	NO	A	B	LENGTH
A	5	241			31'-0⅛"
B	5	241	1'-0"	28'-6"	30'-4⅛"
C	5	241	6"	1'-6"	34'-3⅛"
D_1	4	68			26'-0"
D_2	4	36			28'-6"
D_3	4	68			24'-2"
D_4	4	68			26'-9"
D_5	4	68			22'-9"
D_6	4	68			24'-10"
K_1	6	4			27'-8½"
K_2	6	2			30'-2"
K_3	6	4			25'-0"
K_4	6	4			27'-6"
K_5	6	4			22'-2"
K_6	6	4			24'-10"
J	5	482	6"	1'-6"	5'-1"
L_1	6	192		3'-6"	5'-9"
L_2	6	192		3'-6"	5'-11"
M	5	162	6"	2½"	3'-3"
P_1	5	80	6"	2½"	16'-9"
P_2	5	38	6"	2½"	17'-3⅜"
T_1	5	30			23'-10⅝"
T_2	5	15			23'-4"
T_3	5	30			24'-7"
T_4	5	30			27'-1"
T_5	5	30			22'-9"
T_6	5	30			24'-10"
H_1	2	96	9½"	9½"	3'-11"
H_2	2	192	9½"	5½"	3'-3"
H_3	2	704	5½"	8½"	3'-1"
A	5	1			31'-0⅛"
B	5	1			30'-4⅛"
C	5	1			34'-3⅛"
D_1	4	34			23'-9"
K_1	6	2			28'-9"
T_1	5	15			23'-9"
H	2	6	9½"	1'-5½"	5'-3"
L_1	6	2			5'-9"
L_2	6	2			5'-11"
P	5	8	16'-9"		17'-9"
M1	5	2	2'-3"		3'-3"
J	5	2	6"	1'-6"	3'-1"

When used as End Span substitute 34 Bars A, 2 Bars C, 1 Bar D, 2 Bars K, 2 Bars L & 8 Bars P

When used as End Span (1 End Only) load to above.

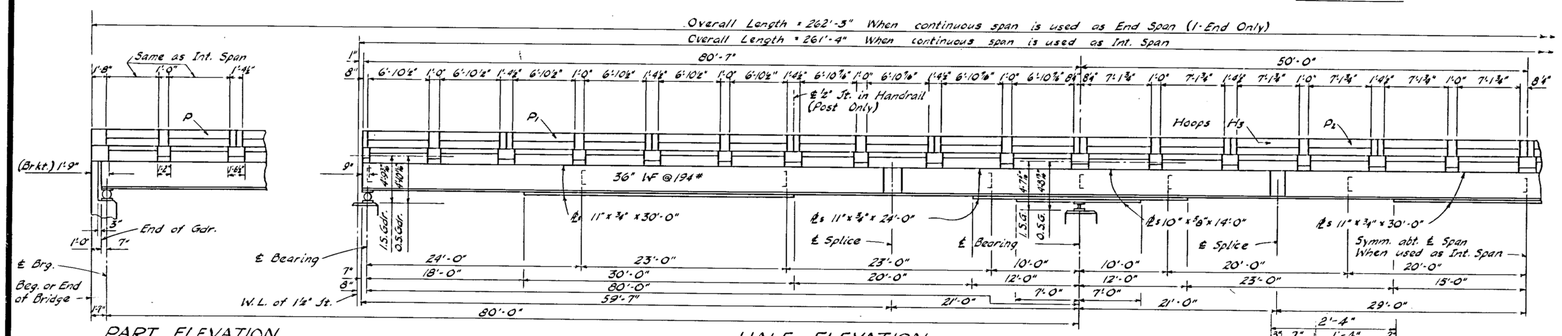

PART ELEVATION END SPAN

HALF ELEVATION

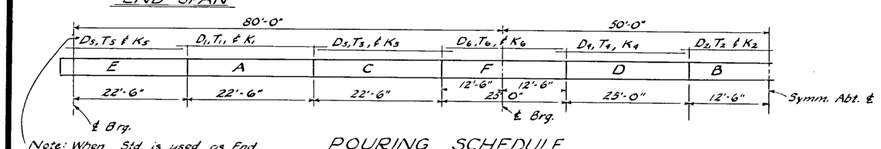

Note: When Std. is used as End Span substitute Bars D1, T1 & K1 for Ds, Ts & Ks.

POURING SCHEDULE

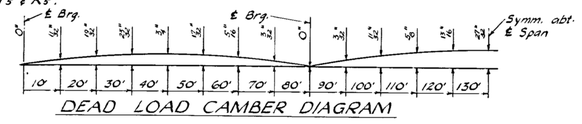

DEAD LOAD CAMBER DIAGRAM

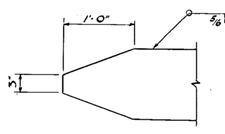

COVER PLATE DETAIL

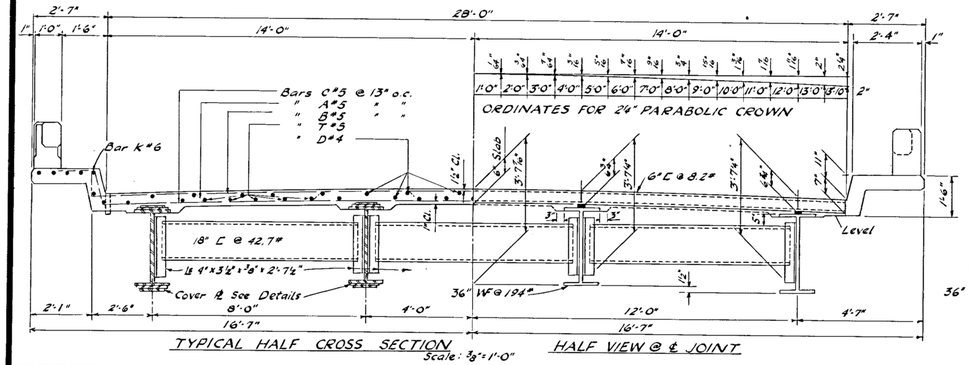

TYPICAL HALF CROSS SECTION Scale: ⅜"=1'-0"

HALF VIEW @ ℄ JOINT

PINTLE DETAIL

Grind pintle for full expansion movement of roller. Pintle to have driving fit.

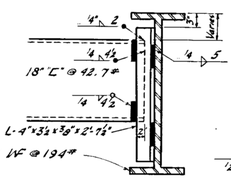

DIAPHRAM CONNECTION

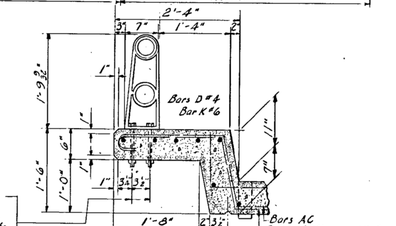

SECTION THRU CURB FOR ALUMINUM RAIL ALT. (For details not shown see Std. Dwg. No. AR-2)

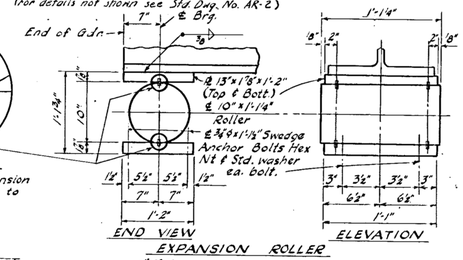

END VIEW — EXPANSION ROLLER — ELEVATION

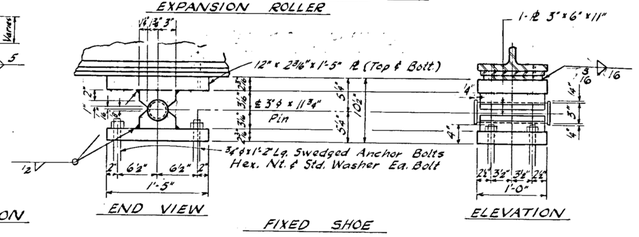

END VIEW — FIXED SHOE — ELEVATION

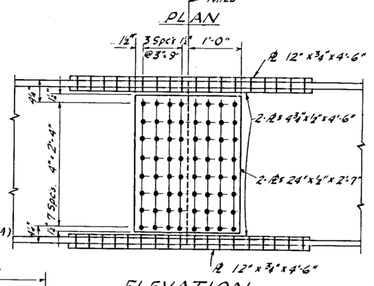

PLAN — ELEVATION

FIELD SPLICE

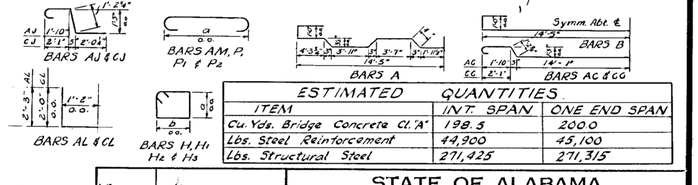

ESTIMATED QUANTITIES		
ITEM	INT. SPAN	ONE END SPAN
Cu. Yds. Bridge Concrete Cl. "A"	198.5	200.0
Lbs. Steel Reinforcement	44,900	45,100
Lbs. Structural Steel	271,425	271,315

GENERAL NOTES

ROADWAY : 28'-0" Roadway 1'-6" Safety Curb.
SPECIFICATIONS : Ala. State Highway Dept. (July 1, 1950)
DESIGN LOADING : H-20 -S-16-44 A.A.S.H.O.
CONCRETE : Shall be Bridge Concrete Class "A".
STRUCTURAL STEEL : Beams and Cover Plates that are to be welded shall conform to A.S.T.M.A.-373 -54 T Specifications.
Use Exx 15 or 16 Electrodes or 200° F Preheat and Interpass Temperature. Low Hydrogen Electrodes shall conform to the requirements of the Military specifications for Electrodes (Mineral Covered, Low Hydrogen) for welding medium alloy steel, Mill E-986 (Ships) Grade 180, dated Nov. 1, 1949.
All other steel with Section 936 of the Std. Specification
High Tensile Strength Bolts, conforming to A.S.T.M. Designation A-325, may be used in lieu of rivets.
Contact surfaces of joints shall not be painted.
See Special Provision No. 121.
PAINT : All structural steel surfaces, not in contact with concrete shall be painted three (3) coats in the following manner.*
Primer or Shop Coat ---- Yellow Zinc Chromate (1C)
Second Coat ---------- Yellow Zinc Chromate (1C)
Third Coat ---------- Alluminum (3C)
STEEL REINFORCEMENT : All reinforcement shall have deformations in accordance with A.S.T.M.-A-305-49 and shall be intermediate grade new billet or rail steel as permitted in the specifications. f_s = 20,000 p.s.i. & f_c = 1,200 p.s.i.

*See other exception above.

THIS STANDARD USED WITH ANY OF THE FOLLOWING STANDARDS

REVISIONS
Fixed Shoe 12-31-57 AHS

APPROVED:
CHIEF BRIDGE DESIGNER
BRIDGE ENGINEER

DESIGNED COOK QUANT. COMP. AHS
DRAWN STINSON QUANT. CHKD. JRM
TRACED J.D.Y. DATE JULY 13, 1956
CHECKED SCALE

STATE OF ALABAMA
HIGHWAY DEPARTMENT

STANDARD
CONTINUOUS STEEL BEAM SPAN WITH CONCRETE SLAB
28' ROADWAY H-20-S16 LOADING
80'-100'-80' CONT. SPAN

STANDARD DWG. NO. B 2806

VOID

OLD ROADWAY WIDTH